

Preparation, Characterization and Conformational Variability of η^6 -Hexaethylbenzene and Other Arene Complexes of Ruthenium

A thesis submitted for the degree of Doctor of Philosophy at the
Australian National University

By

Richard Kimo Baldwin

Research School Chemistry
Australian National University
Canberra
AUSTRALIA

June 1998

The work described in this thesis, except where otherwise stated, is the candidate's own. It was carried out at the Australian National University, from 1994 - 1998.

Richard Baldwin

R. Baldwin

Acknowledgements

The number of people I have to thank for helping me complete this thesis is large and difficult to compile, mainly for fear of omissions.

To start with I would like to thank Professor Bennett for taking me on as a PhD student in the first place, for his interest in, and discussions about my project and what seems to me an epic undertaking in reading and correcting this thesis through a number of drafts. In fact anyone who had a go at reading any of this deserves thanks; Nick, Fiona, Matt and Matt, Lee, Mark, Eric and Chris being the main people on whom it was inflicted.

I have to thank all the people I have shared the lab with in my time in the group: Horst and Lee the lab technicians for their help with technique and good humour despite the vertical filing system on my desk and bench, the postdoctoral research fellows who have passed through the group, especially Mark and Eric both of whom were always willing to offer advice and help with just about anything and later on Maria and Chris, the other PhD students who have been in the group, Ivan, the two Matts, Joanne and Lu, as well as all the other people who have passed through the group, especially Anja.

The crystallographers Tony and Dave also deserve a big vote of thanks, having to regularly deal with imaginary crystals and endless requests for help with diagrams. The NMR staff, especially Peta, Tin and Chris should also be acknowledged for dealing with things like crashed spinners and setting up unusual experiments on short notice without complaining too much. The people of the mass spectrometry service should be thanked, in particular Carl, who was willing to try just about anything once.

I also have to thank all the people who have been part of my life in Canberra, who are too numerous to list but who made a move to what was initially an unfamiliar place good fun for most of the time, especially those who have had the dubious pleasure of sharing a house with me.

Finally, I have to thank the Australian Government for the award of an APA scholarship, supplying the cold hard cash that makes such an undertaking possible.

Abbreviations

benzotris(cyclooctene) = benzo(1',2':3',4':5',6')tri(1,2,3,4,5,6-hexahydro) cyclooctene

br = broad

Bu = butyl

Bu^t = tertiarybutyl

C₆Et₆ = hexaethylbenzene

C₆Me₆ = hexamethylbenzene

Cl^b = bridging chloro ligand

Cl^t = terminal chloro ligand

COD = 1,5-cyclooctadiene

δ = chemical shift

d = doublet

EI = Electron impact

Et = Ethyl

FAB = Fast atom bombardment

m = multiplet

Me = Methyl

naphth = naphthalene

NMR = Nuclear magnetic resonance

p-cym = paracymene (1,4-MeC₆H₄CHMe₂)

ppm = parts per million

Pr = propyl

Prⁱ = isopropyl

q = quartet

s = singlet

t = triplet

THF = tetrahydrofuran

trindane = benzo(1,2:3,4:5,6)-1,2,3-trihydrocyclopentene

Table of contents

Acknowledgments.....	III
Abbreviations.....	I
Abstract.....	V I I
 Chapter 1 : Introduction.....	 1
Arene metal complexes.....	2
Arene ruthenium complexes.....	7
Conformational properties of the hexaethylbenzene ligand.....	17
 Chapter 2 : New η^6-arene ruthenium complexes.....	 29
Preparation and characterization of new $\text{Ru}(\eta^6\text{-arene})(\eta^4\text{-COD})$ complexes.....	30
Preparation and characterization of dimeric ruthenium(II) complexes of the type $[\text{Ru}(\eta^6\text{-arene})\text{Cl}_2]_2$ [arene= $\text{C}_6\text{H}_3\text{Pr}^i_3$, C_6Et_6 and benzotris(cyclooctene)].....	42
Preparation and characterization of triply-bridged dimeric $\text{Ru}(\text{II})$ complexes of the type $[\text{Ru}_2(\eta^6\text{-arene})_2\text{Cl}_3]^+\text{PF}_6^-$ (where arene = C_6Et_6 , $\text{C}_6\text{H}_4\text{-1,2-Et}_2$ and $\text{C}_6\text{H}_4\text{-1,2-Pr}^i_2$).....	50
Solution behaviour of $\text{Ru}(\eta^6\text{-C}_6\text{Et}_6)\text{Cl}_2]_2$	66
 Chapter 3 : Hexaethylbenzene piano stool complexes.....	 81
Preparation and characterization of complexes of the type $\text{Ru}(\eta^6\text{-C}_6\text{Et}_6)(\text{L})\text{Cl}_2$ ($\text{L}=\text{CO}$, Bu^tNC , PMe_3 , PPh_3).....	88
Complexes of the type $\text{Ru}(\eta^6\text{-arene})(\text{PMe}_3)(\text{X})_m\text{Cl}_{(2-m)}$ ($\text{X}=\text{Me}$, $m=1,2$; $\text{X}=\text{H}$, $m=2$).....	90
Monomeric cationic ruthenium(II) complexes.....	92
Crystallographic determinations of the solid state structures of ruthenium complexes of hexaethylbenzene.....	94
X-ray structures of complexes of the type $\text{Ru}(\eta^6\text{-C}_6\text{Et}_6)(\text{L})\text{Cl}_2$ ($\text{L}=\text{CO}$, Bu^tNC , PMe_3 , PPh_3).....	100
X-ray structures of complexes of the type $\text{Ru}(\eta^6\text{-arene})(\text{PMe}_3)(\text{X})_m\text{Cl}_{(2-m)}$ ($\text{X}=\text{Me}$, $m=1,2$; $\text{X}=\text{H}$, $m=1$).....	109
X-ray structures of monomeric cationic ruthenium(II) complexes.....	118
The X-ray structures in general.....	130
 Chapter 4 : Variable temperature NMR spectroscopy.....	 133
Room temperature NMR spectra of hexaethylbenzene complexes.....	134
Low temperature NMR spectra.....	137
Complexes with one sort of ethyl group at the limiting temperature.....	141
The complexes $[\text{Ru}(\eta^6\text{-C}_6\text{Et}_6)\text{Cl}_2]_2$ and $[\text{Ru}_2(\eta^6\text{-C}_6\text{Et}_6)_2\text{Cl}_3]^+\text{PF}_6^-$	143

Complexes with three small cylindrical ligands making up the tripod.....	151
$Ru(\eta^6-C_6Et_6)(PMe_3)(H)_2$	168
Other arenes	173
Summary.....	173
Chapter 5 : Experimental.....	175
Preparation of $Ru(\eta^6-C_6Et_6)(\eta^4-COD)$	178
Preparation of $Ru[\eta^6-benzo(1,2:3,4:5,6)$ 1,2,3,4,5,6-hexahydrocyclooctene] (η^4-COD)	179
Preparation of $Ru(\eta^6-tri-isopropylbenzene)(\eta^4-COD)$	180
Preparation of $Ru[\eta^6-tris(trimethylsilyl)benzene](\eta^4-COD)$	181
Preparation of $Ru(\eta^6-C_6H_3Bu^t_3)(\eta^4-COD)$	182
Preparation of $[Ru(\eta^6-C_6Et_6)Cl_2]_2$	183
Preparation of $[Ru\{\eta^6-benzotris(cyclooctene)\}Cl_2]_2$	184
Preparation of $[Ru_2(\eta^6-C_6Et_6)_2Cl_3]^+PF_6^-$	185
Preparation of $[Ru_2(\eta^6-C_6H_4-1,2-Pr^i_2)_2Cl_3]^+PF_6^-$ and $[Ru_2(\eta^6-C_6H_4-1,2-Et_2)_2Cl_3]^+PF_6^-$	186
Preparation of $Ru(\eta^6-C_6Et_6)(PPh_3)Cl_2$	187
Preparation of $Ru(\eta^6-C_6Et_6)(PMe_3)Cl_2$	188
Preparation of $Ru[\eta^6-benzotris(cyclooctene)](PMe_3)Cl_2$	189
Preparation of $Ru(\eta^6-C_6Et_6)(PMe_3)(Me)Cl$	190
Preparation of $Ru(\eta^6-C_6Et_6)(PMe_3)(Me)_2$	191
Preparation of $Ru(\eta^6-C_6Et_6)(PMe_3)(H)_2$	192
Preparation of $Ru(\eta^6-C_6Et_6)(CO)Cl_2$	193
Preparation of $Ru[\eta^6-benzotris(cyclooctene)](CO)Cl_2$	194
Preparation of $Ru(\eta^6-tri-isopropylbenzene)(CO)Cl_2$	195
Preparation of $Ru(\eta^6-C_6Et_6)(Bu^tNC)Cl_2$	196
Preparation of $[Ru(\eta^6-C_6Et_6)(CH_3CN)_2Cl]^+PF_6^-$	197
Preparation of $[Ru(\eta^6-C_6Et_6)(CH_3CN)_3]_2^+(CF_3SO_3^-)_2$	198
Preparation of $[Ru(\eta^6-C_6Et_6)(Bu^tNC)_2Cl]^+PF_6^-$	199
Preparation of $[Ru(\eta^6-C_6Et_6)(CO)_2Cl]^+PF_6^-$	200
Preparation of $[Ru(\eta^6-C_6Et_6)(Bu^tNC)(CO)Cl]^+PF_6^-$	201
Experimental details for the collection of X-ray data and solution of structures.....	203
Chapter 6 : Conclusions.....	209
Bibliography.....	216

Abstract

The preparation and characterization of new arene ruthenium complexes, obtained by cyclotrimerization of acetylenes on $\text{Ru}(\eta^6\text{-naphth})(\eta^4\text{-COD})$ (naphth = naphthalene; COD = cyclooctadiene) to give $\text{Ru}(0)$ complexes of the type $\text{Ru}(\eta^6\text{-arene})(\eta^4\text{-COD})$ (arene = C_6Et_6 , benzotris(cyclooctene), $\text{C}_6\text{H}_3\text{Pr}^i_3$, $\text{C}_6\text{H}_3\text{Bu}^t_3$, and $\text{C}_6\text{H}_3(\text{SiMe}_3)_3$) are described. This method provides a route to arene ruthenium complexes previously inaccessible in reasonable yield by literature methods.

Treatment of the $\text{Ru}(\eta^6\text{-arene})(\eta^4\text{-COD})$ complexes with HCl gave the synthetically useful Ru(II) arene dichloride dimers of the type $[\text{Ru}(\eta^6\text{-arene})\text{Cl}_2]_2$ (arene = C_6Et_6 , benzotris(cyclooctene) and $\text{C}_6\text{H}_3\text{Pr}^i_3$). For arene = C_6Et_6 the reaction chemistry and dynamic behaviour in solution were investigated in detail, in particular, the relationship between the solid state structure and solution behaviour. It was found by single crystal X-ray crystallography that this complex has a bioctahedral edge-sharing structure with two bridging and two terminal chlorine ligands and two planar and parallel $\eta^6\text{-arene}$ ligands.

It was found by vapour pressure osmometry, conductance measurements, far infrared spectroscopy, ^{35}Cl , ^1H and $^{13}\text{C}\{^1\text{H}\}$ NMR spectroscopy that while $[\text{Ru}(\eta^6\text{-C}_6\text{Et}_6)\text{Cl}_2]_2$ is the predominant species in solution, the equilibrium mixture contains some $[\text{Ru}_2(\eta^6\text{-C}_6\text{Et}_6)_2\text{Cl}_3]^+\text{Cl}^-$, formed by dissociation of chloride ion..

The complex $[\text{Ru}(\eta^6\text{-C}_6\text{Et}_6)\text{Cl}_2]_2$, when treated with NH_4PF_6 , gives the triply chloro-bridged cationic Ru(II) complex, $[\text{Ru}_2(\eta^6\text{-C}_6\text{Et}_6)_2\text{Cl}_3]^+\text{PF}_6^-$, which in the solid state has a bioctahedral face-sharing structure with symmetrically coordinated arene ligands at each end of the Ru_2 unit.

When treated with a number of neutral two-electron ligands the chloride bridges in the complex $[\text{Ru}(\eta^6\text{-C}_6\text{Et}_6)\text{Cl}_2]_2$ are cleaved to give monomeric neutral Ru(II) ligand adducts of the type $\text{Ru}(\eta^6\text{-C}_6\text{Et}_6)(\text{L})\text{Cl}_2$ ($\text{L} = \text{PMe}_3$, PPh_3 , CO and Bu^tNC). Similar carbonyl complexes were made for arene = benzotris(cyclooctene) and $\text{C}_6\text{H}_3\text{Pr}^i_3$, and a PMe_3 complex was also made when the arene = benzotris(cyclooctene). The hydrido complex $\text{Ru}(\eta^6\text{-C}_6\text{Et}_6)(\text{PMe}_3)(\text{H})_2$ and the methyl complexes $\text{Ru}(\eta^6\text{-C}_6\text{Et}_6)(\text{PMe}_3)(\text{Me})\text{X}$ ($\text{X} = \text{Cl}, \text{Me}$) were made by treatment of $\text{Ru}(\eta^6\text{-C}_6\text{Et}_6)(\text{PMe}_3)\text{Cl}_2$ with, respectively, sodium borohydride and methyllithium.

Reaction of $\text{Ru}(\eta^6\text{-C}_6\text{Et}_6)(\text{L})\text{Cl}_2$ ($\text{L} = \text{CO}, \text{Bu}^t\text{NC}$) with AgPF_6 followed by treatment with L gave cationic Ru(II) complexes of the type $[\text{Ru}(\eta^6\text{-C}_6\text{Et}_6)(\text{L}')(\text{L}'')\text{Cl}]^+\text{PF}_6^-$ ($\text{L}' = \text{L}'' = \text{CO}, = \text{Bu}^t\text{NC}$; $\text{L}' = \text{CO}, \text{L}'' = \text{Bu}^t\text{NC}$).

The cationic complex, $[\text{Ru}(\eta^6\text{-C}_6\text{Et}_6)(\text{CH}_3\text{CN})_2\text{Cl}]^+\text{PF}_6^-$ was obtained by direct treatment of $[\text{Ru}(\eta^6\text{-C}_6\text{Et}_6)\text{Cl}_2]_2$ with NH_4PF_6 in acetonitrile. Reaction of $[\text{Ru}(\eta^6\text{-C}_6\text{Et}_6)\text{Cl}_2]_2$ with the stronger chloride abstractor AgCF_3SO_3 in CH_2Cl_2 and subsequent treatment with CH_3CN gave the dicationic Ru(II) complex $[\text{Ru}(\eta^6\text{-C}_6\text{Et}_6)(\text{CH}_3\text{CN})_3]^{2+}(\text{CF}_3\text{SO}_3^-)_2$.

The structures of all complexes containing C_6Et_6 , except the two cationic acetonitrile complexes, were determined by single crystal X-ray analyses. All have the expected half-sandwich piano-stool structure. The arene is essentially planar and all carbon atoms of the arene ring are equidistant from the metal atom. In the complexes studied, the following conformations of the ethyl groups of the C_6Et_6 relative to Ru are observed: all distal, 1,3,5-proximal-2,4,6-distal, 1,3-proximal-2,4,5,6-distal and 1,4-proximal-2,3,5,6-distal.

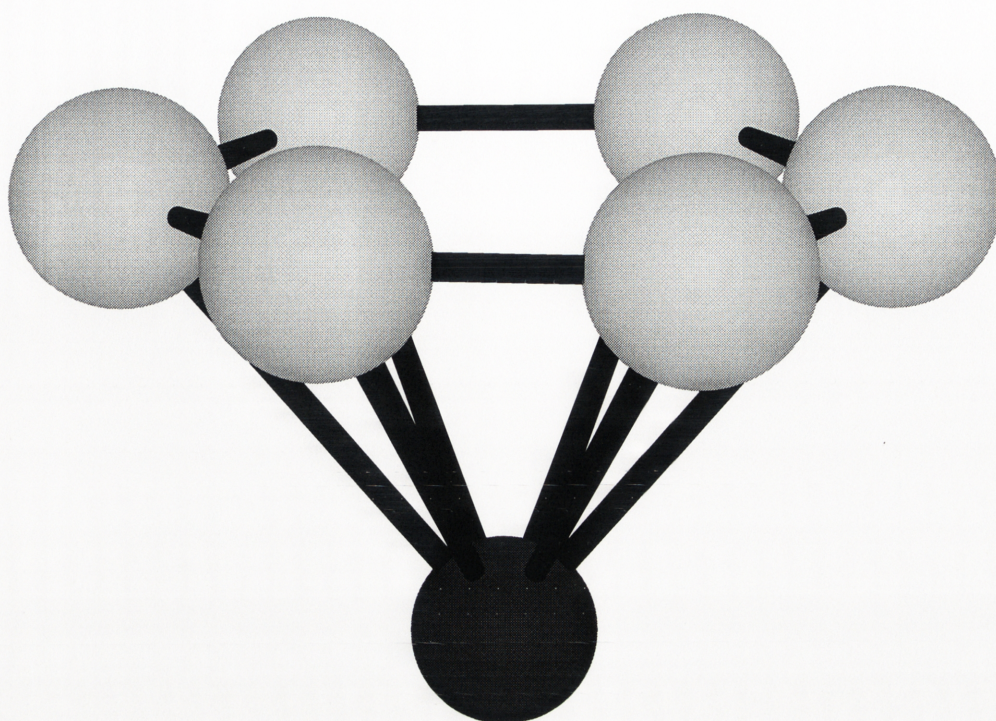
There is a correlation between the steric bulk of the auxiliary ligands and the conformation of the ethyl groups of the arene observed in the solid state. Bulky ligands, such as tertiary phosphines, favour the all distal conformation while smaller auxiliary ligands allow some of the ethyl groups to become proximal, as steric interactions within the arene are reduced.

At room temperature in solution all the ethyl groups in each complex are equivalent by ^1H and $^{13}\text{C}\{^1\text{H}\}$ NMR spectroscopy, probably because of rapid rotations on the NMR timescale about the arene-ruthenium bond axis and the arene methylene bonds. In some cases, these processes can be slowed at low temperature, so that inequivalent ethyl groups and carbons atoms are observed.

In general the low temperature spectra are consistent with the solid state conformation, presumably because one or both of the rotational motions have slowed on an NMR timescale. The most persuasive evidence for this comes from the complex $[\text{Ru}(\eta^6\text{-C}_6\text{Et}_6)(\text{CO})(\text{Bu}^t\text{NC})\text{Cl}]^+\text{PF}_6^-$ which, at -97°C in CD_2Cl_2 , displays six different resonances of equal intensity for the aromatic carbon atoms in the $^{13}\text{C}\{^1\text{H}\}$ NMR spectrum. However, it has not been possible to prove unequivocally whether restricted rotations about the metal-arene bond or about the arene-methylene bonds are responsible for this behaviour.

The results are compared with those reported in the literature for the other metal complexes of bulky arenes, especially the tricarbonylchromium complexes.

Chapter 1: *Introduction*



Chem 3D representation of a η^6 -coordinated arene

<i>Arene metal complexes</i>	2
<i>Arene ruthenium complexes</i>	7
<i>Conformational properties of the hexaethylbenzene ligand</i>	17

The study of η^6 -arene ruthenium complexes has attracted much interest. There are several review articles on the subject, including that of Bozec, Touchard and Dixneuf¹ and that of Bennett². This thesis is concerned with an investigation of a new route to arene ruthenium complexes, namely, the cyclotrimerization of acetylenes on $\text{Ru}(\eta^6\text{-naphthalene})(\eta^4\text{-COD})$ and an investigation of the reaction chemistry and the solid and solution conformational preferences of the complexes obtained. Thus, this introduction is intended to cover two areas. Firstly, it gives an introduction to arene ruthenium complexes and secondly, as the bulk of the complexes made contain hexaethylbenzene as the arene ligand, it gives a discussion of the literature relevant to the special stereodynamic properties of this ligand.

Arene metal complexes

The first η^6 -arene metal complex was prepared, but not recognised as such, by Hein³ in 1919. When CrCl_3 was reacted with $\text{C}_6\text{H}_5\text{MgBr}$ a dark brown solid was obtained. Hein formulated this as a mixture of polyphenylchromium complexes of the type $(\text{Ph})_n\text{Cr}^{0,1+}$, $n=2,3,4$. The true nature of this complex was not discovered until 1955 when Zeiss and Tsutsui repeated this preparation and concluded, in light of the sandwich structure of the recently discovered ferrocene, that the brown solid was a mixture of the η^6 -arene sandwich complexes shown in Figure 1.1.⁴

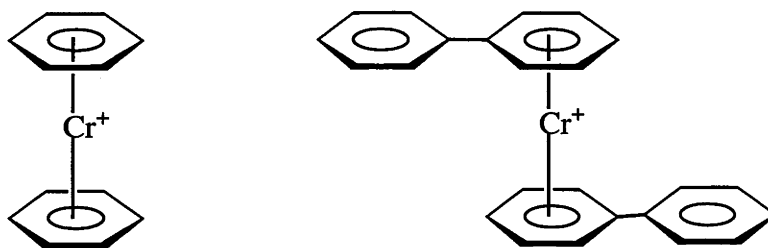


Figure 1.1. η^6 -Arene complexes of chromium as originally prepared by Hein³.

Zeiss and Tsutsui's η^6 -arene sandwich formulation was established unequivocally by Weiss and Fischer's X-ray crystallographic study of $\text{Cr}(\eta^6\text{-C}_6\text{H}_6)_2$.⁵ This complex was prepared by Fischer and Hafner^{6,7} by heating aluminium powder, anhydrous aluminium chloride, chromium chloride and benzene to give $[\text{Cr}(\eta^6\text{-C}_6\text{H}_6)_2]^+$, a method which now bears their name and which has been extended to include most of the transition metals. The cation thus obtained was then reduced to the neutral species by treatment with

dithionite (Figure 1.2).

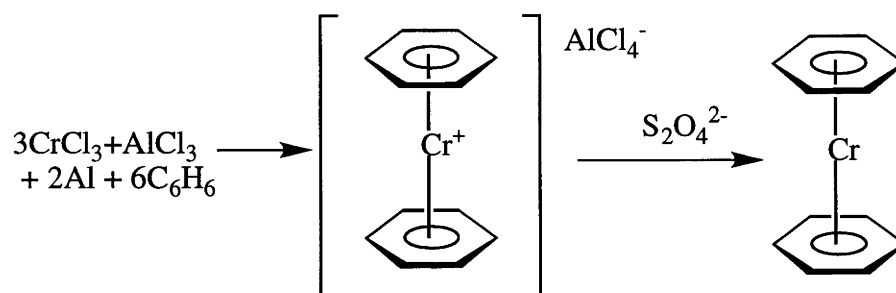


Figure 1.2. Fischer/Hafner synthesis of the arene sandwich complex $\text{Cr}(\eta^6\text{-C}_6\text{H}_6)_2$

The methods used to prepare arene metal complexes today can be divided into two groups; those that involve replacement of other ligands with an arene, or the transformation of another organic compound into an arene on the metal. The first class includes the Fischer Hafner method itself, metal vapour synthesis, treatment of metal carbonyls with an arene, while in the second come such methods as cyclotrimerization of acetylenes and dehydrogenation of cyclohexadienes.⁸

In metal vapour synthesis metal atoms and arenes are co-condensed on a surface at liquid nitrogen temperatures. This method is useful for the preparation of zero valent $\text{M}(\eta^6\text{-arene})_2$ complexes which are not accessible using the Fischer/Hafner procedure, either because the substituents of the arene are not stable under the conditions employed or because polymeric half sandwich complexes are preferentially formed.^{9,10} An example is given in Figure 1.3.

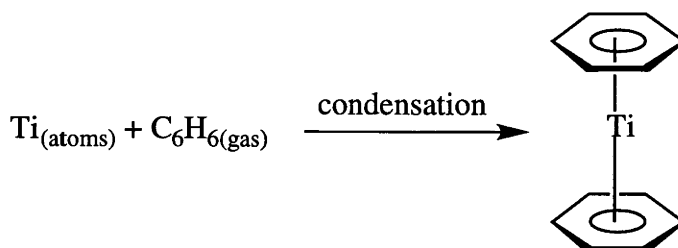


Figure 1.3. Metal vapour synthesis of $\text{Ti}(\eta^6\text{-C}_6\text{H}_6)_2$

Half sandwich arene complexes are commonly prepared by the displacement of labile

ligands by an arene. One very commonly used example of this is the preparation of complexes of the type $\text{Cr}(\eta^6\text{-arene})(\text{CO})_3$.¹¹⁻¹⁴ (Figure 1.4)

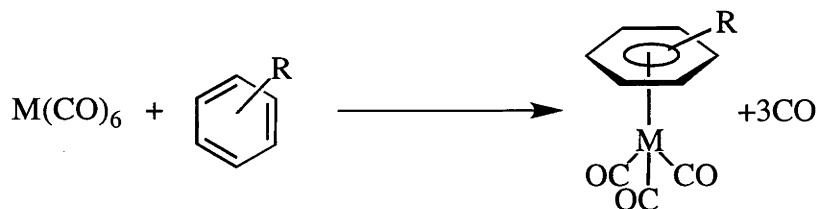


Figure 1.4. Ligand displacement by an arene (M = Cr, Mo, W)

Cyclotrimerization of acetylenes on certain transition metal complexes may also yield arene metal complexes. This method can be employed in the preparation of $\text{Cr}(\eta^6\text{-C}_6\text{Me}_6)_2$, (Figure 1.5).¹⁵

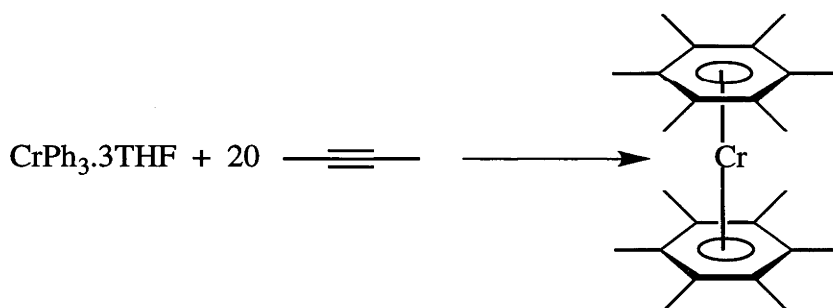


Figure 1.5. Cyclotrimerization of 2-butyne to give $\text{Cr}(\eta^6\text{-C}_6\text{Me}_6)_2$

Reactions of transition metal salts with cyclohexadienes may also give rise to arene metal complexes. Indeed this is the most commonly used method for the preparation of arene ruthenium complexes, as discussed below.

In general, in arene metal complexes, the arene acts as a six-electron donor, the ring is planar, all the arene carbon atoms are equally displaced from the metal and the arene carbon-carbon distances are equivalent, or nearly so. There are exceptions to this, the

most obvious being η^4 - and η^2 -arene complexes, the former being a much better represented class than the latter. In η^4 -arene complexes the arene is strongly distorted from planarity. In $\text{Ru}(\eta^6\text{-C}_6\text{Me}_6)(\eta^4\text{-C}_6\text{Me}_6)$, for example, the second arene is bent through 43° degrees away from the metal centre. It is thought that the need for only four electrons from the second arene to make up the stable 18-electron configuration leads to the diene-like coordination of the η^4 -hexamethylbenzene.¹⁶⁻¹⁸

Complexation of an arene to a metal changes the reactivity of the arene. These changes in reactivity, which are summarised in Figure 1.6, have all been used in organic synthesis. The most commonly utilized systems for this are based on arene chromium tricarbonyl complexes. Reasons for this include the wide range of arenes which can easily be coordinated to the chromium tricarbonyl fragment and the air- and temperature-stability of these complexes.

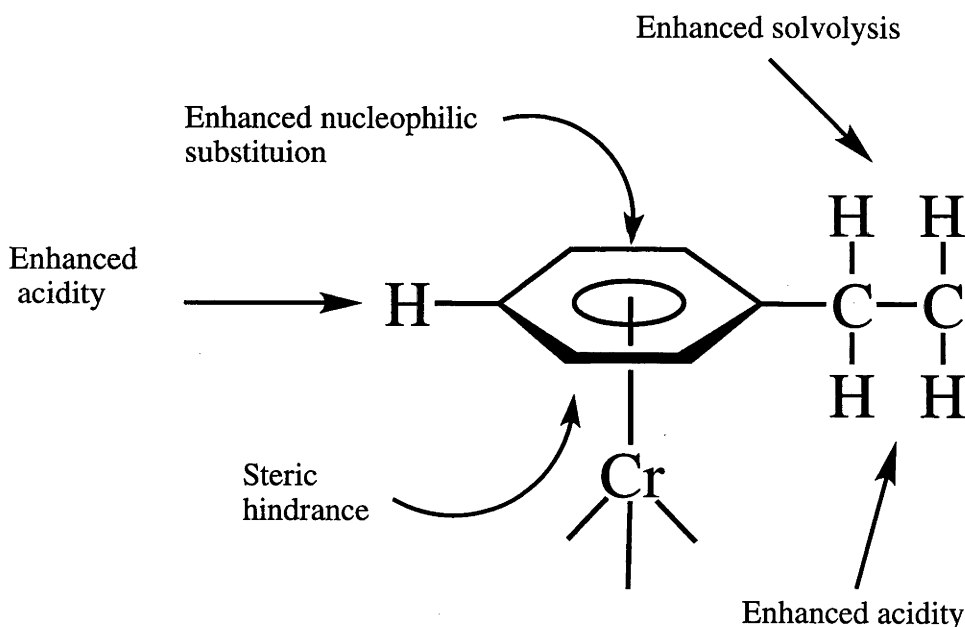


Figure 1.6. Changes in reactivity of arenes upon coordination (figure adapted from Collman, Hegedus, Norton and Finke¹⁹)

In bonding an arene to a metal the electron density of the arene is displaced towards the metal orbitals. The resulting electron deficiency of the ring can account for the reactivity changes encountered on coordination. This change in electron density is also reflected in the ^{13}C and ^1H NMR shifts for the arene carbons and protons. These are usually at a

lower frequency than in the free arene due to the reduction in aromatic ring current anisotropic shielding with reduction in electron density at the arene ring.¹⁹

Arene ruthenium complexes

The normal points of entry into arene ruthenium complexes are ruthenium dichloride dimers of the type $[\text{Ru}(\eta^6\text{-arene})\text{Cl}_2]_2$, which are made by reaction of cyclohexa-1,3-dienes or cyclohexa-1,4-dienes with $\text{RuCl}_3 \cdot x\text{H}_2\text{O}$ in refluxing ethanol as shown in Figure 1.7.

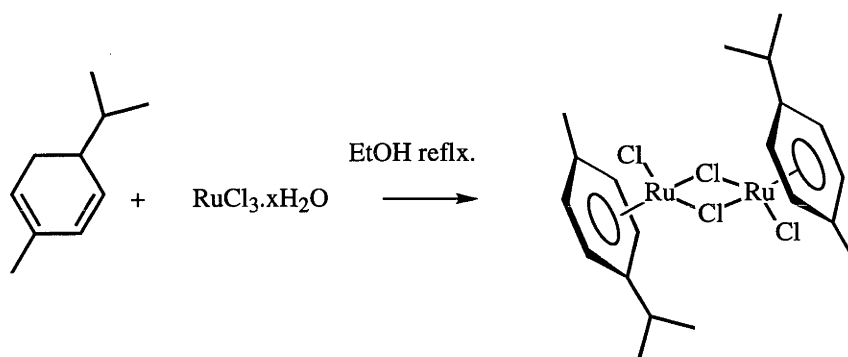


Figure 1.7. Reaction of a cyclohexadiene with $\text{RuCl}_3 \cdot x\text{H}_2\text{O}$

The reaction of $\text{RuCl}_3 \cdot x\text{H}_2\text{O}$ with cyclohexadiene to give a compound originally formulated as $[\text{Ru}(\eta^4\text{-C}_6\text{H}_6)\text{Cl}_2]_x$ was first reported by Winkhaus and Singer.²⁰ This method was used by Zelonka and Baird for the preparation of η^6 -benzene ruthenium dichloride dimer, $[\text{Ru}(\eta^6\text{-C}_6\text{H}_6)\text{Cl}_2]_2$ ^{21,22} and by Bennett and coworkers for the preparation of the *p*-cymene dichloride dimer and other substituted arene dichloride dimers with arenes such as xylene and mesitylene.^{23,24,25} This method is very convenient for arenes which can be reduced to the corresponding cyclohexadiene by a Birch reduction. The precise structure of some of the products referred to as 'arene dichloride dimers' is not clear, especially for the parent benzene compound (see below).

Unfortunately, the technique of dehydrogenation of cyclohexadienes has proven ineffective for the introduction of some arene ligands into the coordination sphere of ruthenium. If it is difficult to obtain the appropriate cyclohexadiene, as in the case of hexamethylbenzene, then a different strategy has to be employed, taking advantage of the

relative lability of the *p*-cymene ligand. If the *p*-cymene dichloride dimer $[\text{Ru}(\eta^6\text{-}p\text{-cymene})\text{Cl}_2]_2$ is fused with a large excess of a peralkylated arene, such as hexamethylbenzene, which has a higher boiling point than *p*-cymene, then the corresponding η^6 -arene ruthenium dichloride dimer is obtained (Figure 1.8).²⁵ This technique has also been used to make the corresponding complexes of such arenes as 1,2,3,4-tetramethylbenzene, 1,3,5-triethylbenzene and 1,3,5-tri-isopropylbenzene.²⁶

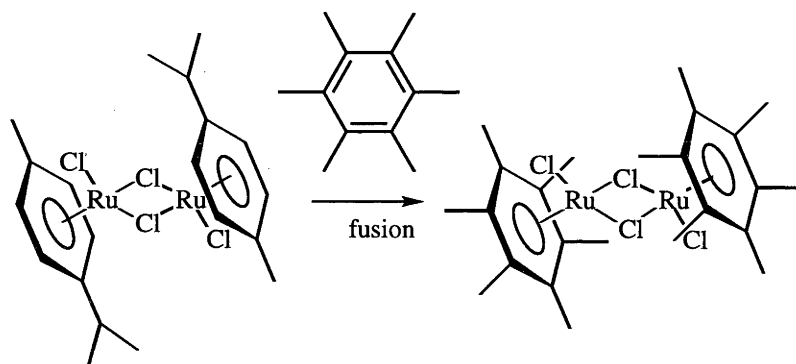


Figure 1.8. Fusion of *p*-cymene dichloride dimer with hexamethylbenzene

It is also possible to exchange ligands for arenes in certain $\text{Ru}(0)$ complexes. Treatment of $\text{Ru}(\eta^4\text{-COD})(\eta^6\text{-COT})$ ($\text{COT}=\text{cycloocta-1,3,5-triene}$), (prepared by the reaction of $\text{RuCl}_3 \cdot x\text{H}_2\text{O}$ and cycloocta-1,5,-diene in the presence of zinc dust),²⁷ with an arene under a hydrogen atmosphere gives rise to $\text{Ru}(\eta^6\text{-arene})(\eta^4\text{-COD})$ complexes. Subsequent treatment of the $\text{Ru}(\eta^6\text{-arene})(\eta^4\text{-COD})$ complexes with HCl gives dichloride dimers.²⁸

One of the arenes which has been exchanged with COT is naphthalene. The naphthalene in the resulting complex, $\text{Ru}(\eta^6\text{-naphth})(\eta^4\text{-COD})$, can be replaced by an another arene when the compound is treated with an excess of the arene in the presence of acetonitrile (Figure 1.9).²⁹ It has subsequently been found that $\text{Ru}(\eta^6\text{-naphth})(\eta^4\text{-COD})$ can be more easily prepared from the reaction of $\text{Ru}(\text{COD})(\text{acac})_2$ with sodium naphthalide in THF.³⁰

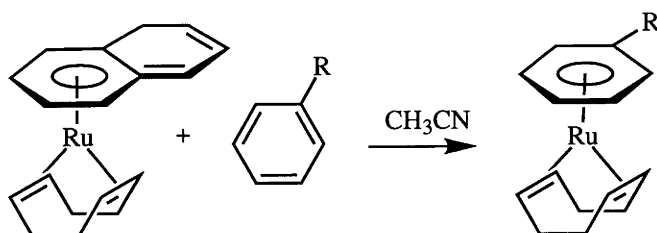


Figure 1.9. Arene exchange reaction of $\text{Ru}(\eta^6\text{-naphthalene})(\eta^4\text{-COD})$

It is thought that the arene exchange reaction is facilitated by the partial dissociation of the naphthalene so that it becomes η^4 -coordinated upon introduction of acetonitrile into the coordination sphere, making the naphthalene an easier target for displacement.³⁰ The η^4 -coordination is stabilised by the attainment of aromaticity in the non-coordinated ring. The $\text{Ru}(\eta^6\text{-arene})(\eta^4\text{-COD})$ complexes thus formed can then be treated with a source of HCl to give the synthetically useful dichloride dimers.

It has been found that some complexes of ruthenium cyclotrimerize acetylenes to give arenes which remain coordinated. For instance, when $\text{Ru}(\eta^6\text{-C}_6\text{H}_6)(\eta^4\text{-cyclohexa-1,3-diene})$ is irradiated by UV light in the presence of an excess of alkyne, RC_2R , ($\text{R}=\text{phenyl, COOCH}_3, \text{CH}_3$), zerovalent ruthenium complexes of the type $\text{Ru}(\eta^6\text{-C}_6\text{H}_6)(\eta^4\text{-C}_6\text{R}_6)$ can be obtained.³¹

When $[\text{Ru}(\text{CO})_2(\eta^5\text{-C}_5\text{H}_5)]_2$ is reacted with diphenylacetylene in the presence of AgBF_4 in dichloromethane, the tetraphenylcyclobutadiene complex $[\text{Ru}(\eta^4\text{-C}_4\text{Ph}_4)(\eta^5\text{-C}_5\text{H}_5)\text{CO}]^+\text{BF}_4^-$ is obtained. This complex reacts with an excess of various acetylenes under UV irradiation to give cationic ruthenium(II) complexes of the type $[\text{Ru}(\eta^6\text{-arene})(\eta^5\text{-C}_5\text{H}_5)]^+\text{BF}_4^-$. $[\text{Ru}(\text{CO})_2(\eta^5\text{-C}_5\text{H}_5)]_2$ reacts with an excess of 3-hexyne in the presence of AgBF_4 to give, in 9% yield, $[\text{Ru}(\eta^6\text{-C}_6\text{Et}_6)(\eta^5\text{-C}_5\text{H}_5)]^+\text{BF}_4^-$ (Figure 1.10).^{32,33} The stereodynamics of this molecule will be discussed later.

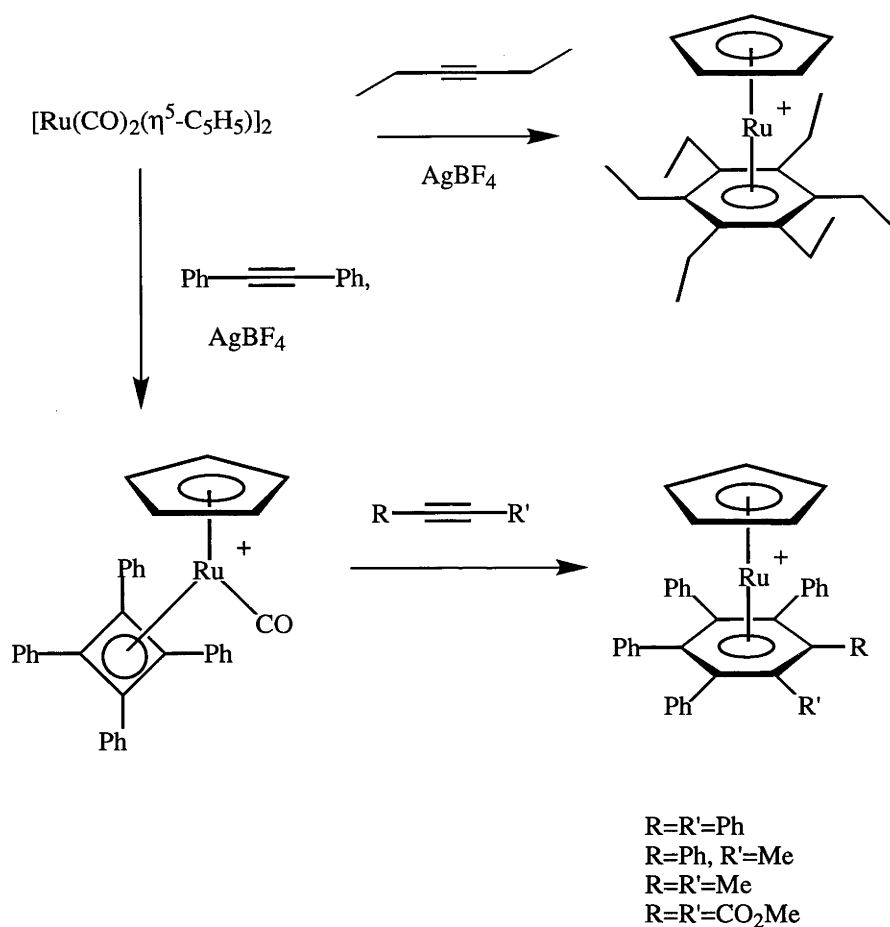


Figure 1.10. Cyclotrimerization of alkynes leading to arene ruthenium complexes

Certain ruthenium diene complexes also react with alkynes to give rise to arene ruthenium complexes. For instance $\text{Ru}(\eta^5\text{-C}_5\text{Me}_5)(\eta^4\text{-diene})$, (diene = butadiene, or 1,3-pentadiene) react with excess alkyne in the presence of silver triflate to give, amongst other products, arene ruthenium(II) complexes of the type $[\text{Ru}(\eta^5\text{-C}_5\text{Me}_5)(\eta^6\text{-arene})]^+\text{CF}_3\text{SO}_3^-$.³⁴

Recently Pertici *et al.*³⁵ discovered that $\text{Ru}(\eta^6\text{-naphth})(\eta^4\text{-COD})$ also reacts with alkynes, $\text{RC}_2\text{R'}$, to give $\text{Ru}(\eta^6\text{-C}_6\text{R}_3\text{R'}_3)(\eta^4\text{-COD})$ in 20-90% yield, the alkyne being cyclotrimerized to give the coordinated arene (see Chapter 2). One of the alkynes investigated in this study was 3-hexyne. To date, the cyclotrimerization of 3-hexyne by $\text{Ru}(\eta^6\text{-naphthalene})(\eta^4\text{-COD})$ to give $[\text{Ru}(\eta^6\text{-C}_6\text{Et}_6)(\text{COD})]$ is the only way to introduce the hexaethylbenzene moiety into the coordination sphere of ruthenium in reasonable yield (Figure 1.11).

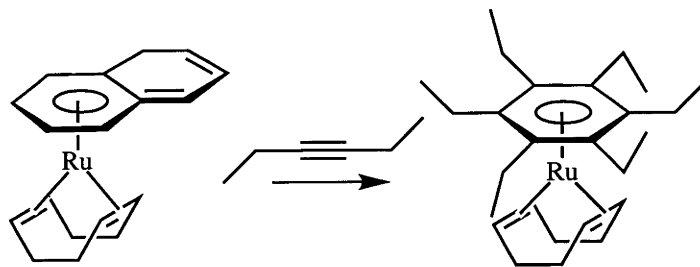
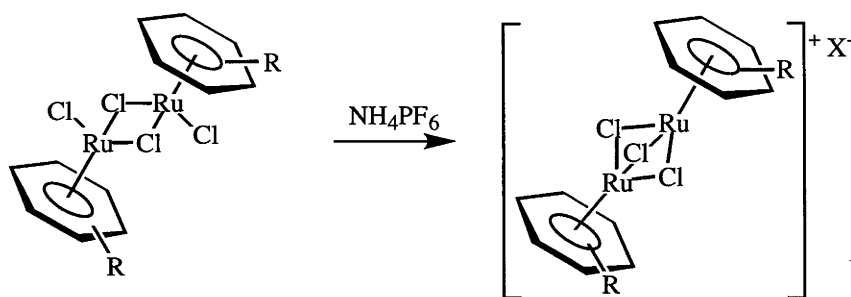


Figure 1.11. Reaction of $\text{Ru}(\eta^6\text{-naphth})(\eta^4\text{-COD})$ with 3-hexyne

Hexaethylbenzene, like hexamethylbenzene, cannot be reduced to the corresponding diene by Birch reduction, thus the cyclohexadiene dehydrogenation route to arene ruthenium complexes is not available. It does not displace *p*-cymene from $[\text{Ru}(\eta^6\text{-}p\text{-cymene})\text{Cl}_2]_2$ or the naphthalene from $\text{Ru}(\eta^6\text{-naphthalene})(\eta^4\text{-COD})$, presumably due to the steric hindrance of the six ethyl groups.

The synthetic utility of the dichloride dimers stems from the lability of the chloride ligands.^{1,2} * Removal of a single chloride ion from $[\text{Ru}(\eta^6\text{-arene})\text{Cl}_2]_2$ gives rise to a tri- μ -chloro salt of the type $[\text{Ru}_2(\eta^6\text{-arene})_2(\mu\text{-Cl})_3]^+\text{X}^-$ (Figure 1.12). Many methods have been employed to prepare these complexes, including treatment of a hot water solution of $[\text{Ru}(\eta^6\text{-arene})\text{Cl}_2]_2$ with NH_4PF_6 (arene = C_6H_6 , $\text{X} = \text{PF}_6^-$)²⁴ and treatment of methanolic solutions of $[\text{Ru}(\eta^6\text{-arene})\text{Cl}_2]_2$ with NH_4PF_6 (arene = C_6Me_6 , C_6H_6 ; $\text{X} = \text{PF}_6^-$).³⁶⁻³⁸ Stephenson and coworkers have treated an equimolar mixture of $\text{Ru}(\eta^6\text{-arene})(\text{Py})\text{Cl}_2$ and $[\text{Ru}(\eta^6\text{-arene})(\text{Py})_2\text{Cl}]^+$ in methanol with HBF_4 or HPF_6 to give $[\text{Ru}_2(\eta^6\text{-arene})_2\text{Cl}_3]^+\text{X}^-$ complexes (arene = C_6H_6 , $\text{C}_6\text{H}_3\text{Me}_3$ and *p*-cymene and $\text{X} = \text{BF}_4^-$ and PF_6^-).^{39,40}

* It should be noted that many of the complexes described here are also accessible for osmium and halogens other than chlorine.

Figure 1.12. Preparation of $[\text{Ru}_2(\eta^6\text{-arene})_2\text{Cl}_3]^+\text{X}^-$

These complexes were originally ascribed the cationic triply bridged face sharing bioctahedral structure on the basis of their far infrared spectra, which contains a only a broad band ($\text{ca } 260 \text{ cm}^{-1}$) for the bridging chloride atoms, and conductance measurements in nitromethane from which they were determined to be 1:1 electrolytes.²⁴ Single crystal X-ray structural determinations on $[\text{Ru}_2(\eta^6\text{-C}_6\text{H}_6)_2\text{Cl}_3]^+\text{AsF}_6^-$,⁴¹ $[\text{Ru}_2(\eta^6\text{-}p\text{-cymene})_2\text{Cl}_3]^+\text{BPh}_4^-$,⁴² $[\text{Ru}_2(\eta^6\text{-mesitylene})_2\text{Cl}_3]^+\text{BF}_4^-$,⁴³ $[\text{Ru}_2(\eta^6\text{-C}_6\text{H}_6)_2\text{Cl}_3]^+\text{BF}_4^-$ ⁴⁴ and $[\text{Ru}_2(\eta^6\text{-C}_6\text{H}_5\text{Me})_2\text{Cl}_3]^+\text{BF}_4^-$ ⁴⁴ confirm this molecular structure.

The chloride bridges can also be easily cleaved by a wide range of neutral two-electron ligands to give monomeric neutral Ru(II) complexes of the type $\text{Ru}(\eta^6\text{-arene})(\text{L})\text{Cl}_2$ (Figure 1.13). The ligands for which this is possible include RNC ⁴⁵, CO , PR_3 , and nitrogen, oxygen and sulphur donors.^{1,2}

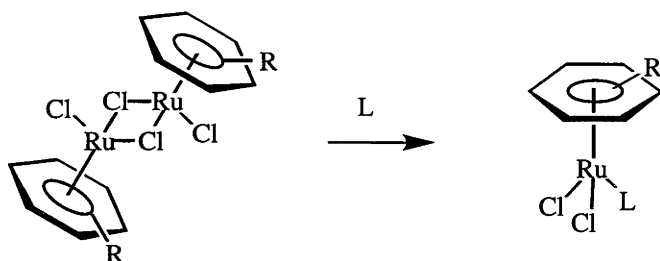


Figure 1.13. Formation of monomeric ligand adducts

The anionic ligands in tertiary phosphine complexes of the type $\text{Ru}(\eta^6\text{-arene})(\text{PR}_3)\text{Y}_2$ ($\text{Y} = \text{Cl}, \text{CF}_3\text{CO}_2$) undergo stepwise replacement of the chloro ligands by either hydride or methyl. Figure 1.14 gives an example.

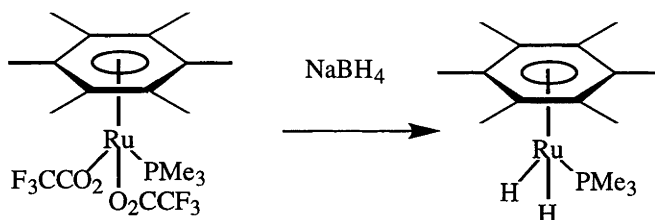


Figure 1.14. Preparation of $\text{Ru}(\eta^6\text{-C}_6\text{Me}_6)(\text{PMe}_3)(\text{H})_2$ ⁴⁶

Complexes of the type $\text{Ru}(\eta^6\text{-arene})(\text{PR}_3)(\text{H})\text{Cl}$ can be obtained from the reaction of $\text{Ru}(\eta^6\text{-arene})(\text{PR}_3)\text{Cl}_2$ with zinc dust in methanol at room temperature⁴⁷⁻⁵⁰ or by refluxing with sodium carbonate in isopropanol.⁵¹⁻⁵³ Dihydride complexes of the type $\text{Ru}(\eta^6\text{-arene})(\text{PR}_3)(\text{H})_2$ can be obtained from the reaction of reducing agents such as NaBH_4 , LiAlH_4 or $\text{RedAl} [\text{NaAlH}_2(\text{OCH}_2\text{CH}_2\text{OCH}_3)_2]$ in THF or benzene with $\text{Ru}(\eta^6\text{-arene})(\text{PR}_3)\text{Cl}_2$ or the corresponding trifluoroacetates.^{46,50,53-55}

Methyl ruthenium arene complexes of the type $\text{Ru}(\eta^6\text{-arene})(\text{PR}_3)(\text{Me})\text{Cl}$ and $\text{Ru}(\eta^6\text{-arene})(\text{PR}_3)\text{Me}_2$ can be obtained by the treatment of $\text{Ru}(\eta^6\text{-arene})(\text{PR}_3)\text{Cl}_2$ with an appropriate amount of methyl lithium, the dimethyl complex being obtained from an excess of methyl lithium^{24,46} and the (methyl)chloro complex being obtained from a single equivalent of methyl lithium.⁵⁶ The (methyl)chloro complexes may be better obtained through the action of a milder methylating reagent, such as HgMe_2 or SnMe_4 on $[\text{Ru}(\eta^6\text{-arene})\text{Cl}_2]_2$ in CH_3CN followed by treatment of the labile solvento species, $[\text{Ru}(\eta^6\text{-arene})(\text{MeCN})(\text{Me})\text{Cl}]$, thus generated with a phosphine.^{21,57}

It is possible to introduce a second and in some cases even a third ligand, replacing Cl in the ligand adduct complexes to give cationic ruthenium complexes. A general reaction scheme is given below in Figure 1.15.

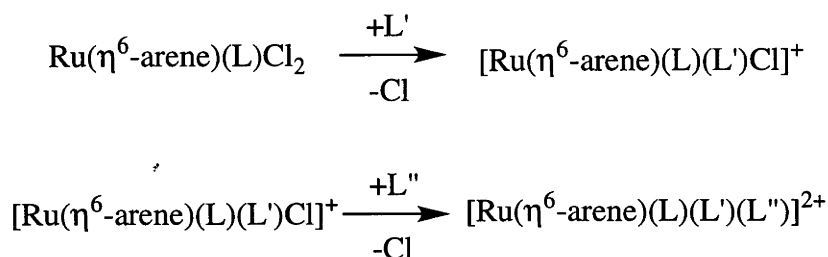


Figure 1.15. Preparation of cationic ruthenium arene complexes

For example, treatment of $[\text{Ru}(\eta^6\text{-C}_6\text{H}_6)\text{Cl}_2]_2$ with AgPF_6 in MeCN gives rise to the tris(acetonitrile) salt $[\text{Ru}(\eta^6\text{-C}_6\text{H}_6)(\text{CH}_3\text{CN})_3]^{2+}(\text{PF}_6^-)_2$.⁵⁸ If $[\text{Ru}(\eta^6\text{-C}_6\text{H}_6)\text{Cl}_2]_2$ is reacted with a milder reagent such as TiPF_6 , NH_4PF_6 , LiBF_4 or KAsF_6 in MeCN then the bis(acetonitrile) salt $[\text{Ru}(\eta^6\text{-C}_6\text{H}_6)(\text{CH}_3\text{CN})_2\text{Cl}]^+\text{PF}_6^-$ is obtained.⁵⁹ The acetonitrile ligands in these complexes are labile, exchange with free acetonitrile and are easily replaced by other ligands. Bis(tertiary-phosphine) complexes can be obtained by the stepwise treatment of $\text{Ru}(\eta^6\text{-arene})(\text{PR}_3)\text{Cl}_2$ complexes with chloride abstractors and subsequent treatment with a second phosphine. Repetition of this procedure on the bis(tertiary-phosphine) complexes gives the tris(tertiary-phosphine) complexes $[\text{Ru}(\eta^6\text{-arene})(\text{PR}_3)_3]^{2+}$.⁵⁰ The cationic bis(carbonyl) complex, $[\text{Ru}(\eta^6\text{-C}_6\text{Me}_6)(\text{CO})_2\text{Cl}]^+\text{PF}_6^-$, can be prepared from the reaction of the mono(carbonyl) adduct, $\text{Ru}(\eta^6\text{-C}_6\text{Me}_6)(\text{CO})\text{Cl}_2$, with one equivalent of AgPF_6 and CO.⁵⁰ This general scheme of removal of chloride followed by treatment with a replacement ligand has also been used to form mixed bis arene complexes, for example, $[\text{Ru}(\eta^6\text{-arene})(\eta^6\text{-arene}')]^{2+}$ from treatment of $[\text{Ru}(\eta^6\text{-arene})\text{Cl}_2]_2$ with AgBF_4 , $\text{CF}_3\text{CO}_2\text{H}$ and arene⁶⁰ with AgNO_3 and arene' in water,⁶¹ and arene Cp complexes, such as $[\text{Ru}(\eta^6\text{-C}_6\text{H}_6)(\eta^5\text{-C}_5\text{H}_5)]^+$, obtained from the treatment of $[\text{Ru}(\eta^6\text{-C}_6\text{H}_6)\text{Cl}_2]_2$ with TiC_5H_5 ^{22,62} or with AgBF_4 and cyclopentadiene in ethanol.⁶³

Ru(II) arene complexes are beginning to find use as catalysts. For example, complexes of the type $\text{Ru}(\eta^6\text{-p-cymene})(\text{L})\text{Cl}_2$ (where $\text{L}=\text{PCy}_3$, PPr^i_3 and PPhCy_2), activated by the addition of trimethylsilyldiazomethane, have been found to be good precursors to an active ring opening metathesis polymerization catalyst for norbornenes and cyclooctene.⁶⁴ Noyori *et al.* have used chelating diamine ruthenium arene complexes as hydrogenation transfer catalysts for high yielding enantioselective hydrogenation of ketones to alcohols.⁶⁵ Ruthenium arene BINAP complexes have been used for the asymmetric

hydrogenation of various unsaturated organic compounds.⁶⁶

X-ray crystallographic studies of $[\text{Ru}(\eta^6\text{-hexamethylbenzene})\text{Cl}_2]_2$,⁶⁷ $[\text{Os}(\eta^6\text{-}p\text{-cymene})\text{Cl}_2]_2$,⁶⁸ $[\text{Ru}(\eta^6\text{-trindane})\text{Cl}_2]_2$ ⁶⁹ (trindane = benzo(1,2:3,4:5,6)-1,2,3-trihydrocyclopentene), and $[\text{Ru}(\eta^6\text{-C}_6\text{H}_5\text{CO}_2\text{Et})\text{Cl}_2]_2$ ⁷⁰ have shown that, in the solid state, these complexes have each metal atom in a pseudooctahedral geometry with the arene taking up three coordination sites and the remaining three being occupied by two edge-sharing bridging chlorine atoms and one terminal chlorine atom (Figure 1.8). For the simplest member of the series, the benzene dichloride dimer, $[\text{Ru}(\eta^6\text{-C}_6\text{H}_6)\text{Cl}_2]_2$, the exact nature of the species in the solid state is not well defined. It has been suggested that it may be polymeric on the basis of its insolubility,²⁰ although the presence of a band assignable to a terminal Cl ligand in the far infrared spectrum is also consistent with the dimeric structure.^{21,22,24} It has even been suggested that there is not just one form of this complex. Iwata *et al.*⁷¹ found that the elemental analysis of their $[\text{Ru}(\eta^6\text{-C}_6\text{H}_6)\text{Cl}_2]_2$ prepared from the dehydrogenation of cyclohexadiene by RuCl_3 in EtOH was consistent with a polymer of formula $[\text{Ru}(\eta^6\text{-C}_6\text{H}_6)\text{Cl}_2]_m[\text{RuCl}_2]_n$ ($n/m=0.2\text{-}0.4$), that is, some of the polymer chain is lacking a $\eta^6\text{-C}_6\text{H}_6$ ligand. The triphenylbenzene complex $[\text{Ru}(\eta^6\text{-C}_6\text{H}_3\text{-}1,3,5\text{-Ph}_3)\text{Cl}_2]_m[\text{RuCl}_2]_n$ was also prepared and in this complex the ratio of n/m was found to be 0.4-0.5.

The nature of the species present in solutions of these dichloride dimers is also poorly defined. The most extensively studied is $[\text{Ru}(\eta^6\text{-C}_6\text{H}_6)\text{Cl}_2]_2$. Unfortunately this complex is essentially insoluble in poorly coordinating solvents. In solvents such as $d^6\text{-DMSO}$ and D_2O , however, the ^1H NMR spectrum displays two resonances for the coordinated arene protons.³⁷ It is thought that a proportion of the dichloride dimer is cleaved by the solvent to give monomeric solvento species of the type $\text{Ru}(\eta^6\text{-C}_6\text{H}_6)\text{Cl}_{(3-x)}(\text{solvent})_x$ ($x=1,2,3$), one of these species accounting for the second peak. The recombination of these monomeric species in the presence of an appropriate cation is thought to be the method of formation of the triply bridged cation $[\text{Ru}_2(\eta^6\text{-C}_6\text{H}_6)_2(\mu\text{-Cl})_3]^+$.³⁷ In Arthur and Stephenson's paper³⁹ on the formation of triply halide bridged arene complexes of osmium and ruthenium a reaction mechanism was proposed for the scrambling of the halogens in mixed solutions of $[\text{Ru}(\eta^6\text{-arene})_2(\mu\text{-Cl})_3]^+$ and $[\text{Ru}(\eta^6\text{-arene})_2(\mu\text{-Br})_3]^+$. Intermediates of the type $[\text{Ru}_2(\eta^6\text{-arene})_2(\mu\text{-X})_2\text{X}(\text{solvent})]^+$ were proposed along with a tetrameric transition state for the halide exchange. It was also found that the coordinated halides in complexes of this type were very labile in solution.

It has been generally assumed that in non-coordinating solvents the dimeric halogen bridged dimer is the species present in solution. Recently McGlinchey *et al.*⁶⁹ reported

the variable temperature ^1H and $^{13}\text{C}\{^1\text{H}\}$ NMR spectra of $[\text{Ru}(\eta^6\text{-trindane})\text{Cl}_2]_2$. In CD_2Cl_2 the room temperature ^1H NMR spectrum contained, not the expected four methylene proton environments, but eight in a 4:4:2:2:1:1 ratio. This pattern was also reflected in the ^{13}C NMR spectrum, where two aromatic ring carbon resonances were observed and the methylene carbons gave rise to a four peak pattern. As the solution was cooled the relative intensities of these peaks changed and it was proposed that an equilibrium between the doubly bridged neutral species and the triply bridged cationic species existed (Figure 1.16). This proposal was also supported by the observation that in CD_3NO_2 , a more polar solvent that should favour the formation of the ionized species, the ratio of the two different structural isomers was 1:10.

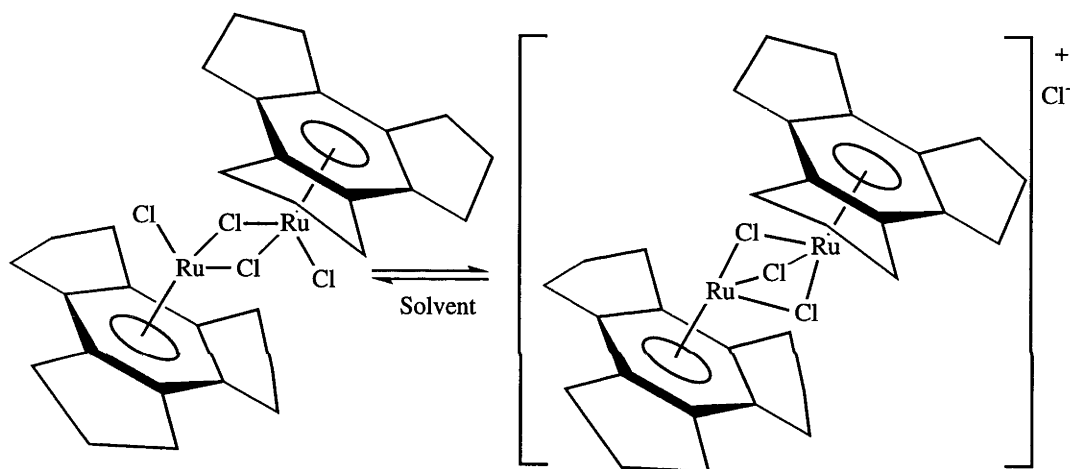


Figure 1.16. Proposed dissociation of $[\text{Ru}(\eta^6\text{-trindane})\text{Cl}_2]$

Conformational properties of η^6 -arene metal complexes.

As mentioned at the start of this introduction, most of the complexes prepared in the course of this study contain hexaethylbenzene. An investigation of the conformational properties of this ligand in its complexes, both in the solution and solid state forms a large part of this thesis. In the case of $\text{Cr}(\eta^6\text{-C}_6\text{Et}_6)(\text{CO})_3$ and its derivatives, these properties have been studied in great detail. In the solid state it has been found by single crystal X-ray crystallography that the six ethyl groups of free hexaethylbenzene take on a staggered conformation about the ring, that is, each ethyl group points in a direction opposite to those adjacent to it^{72,73}(Figure 1.17). Of the eight different possible conformations of ethyl groups, Iverson *et al.* have shown by calculations that this is the most sterically favoured conformation.⁷²

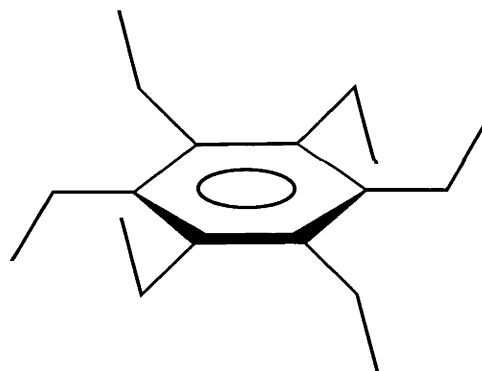


Figure 1.17. Solid state conformation of free hexaethylbenzene

Once the hexaethylbenzene is coordinated to a metal the two faces of the arene become inequivalent. The ethyl groups can either point towards the metal atom, designated proximal, or away from it, designated distal. In principle, there are thirteen different conformations for the coordinated hexaethylbenzene ligand in the solid state, with differing proportions and placements of proximal and distal ethyl groups. Some of these possibilities are shown in Figure 1.18.

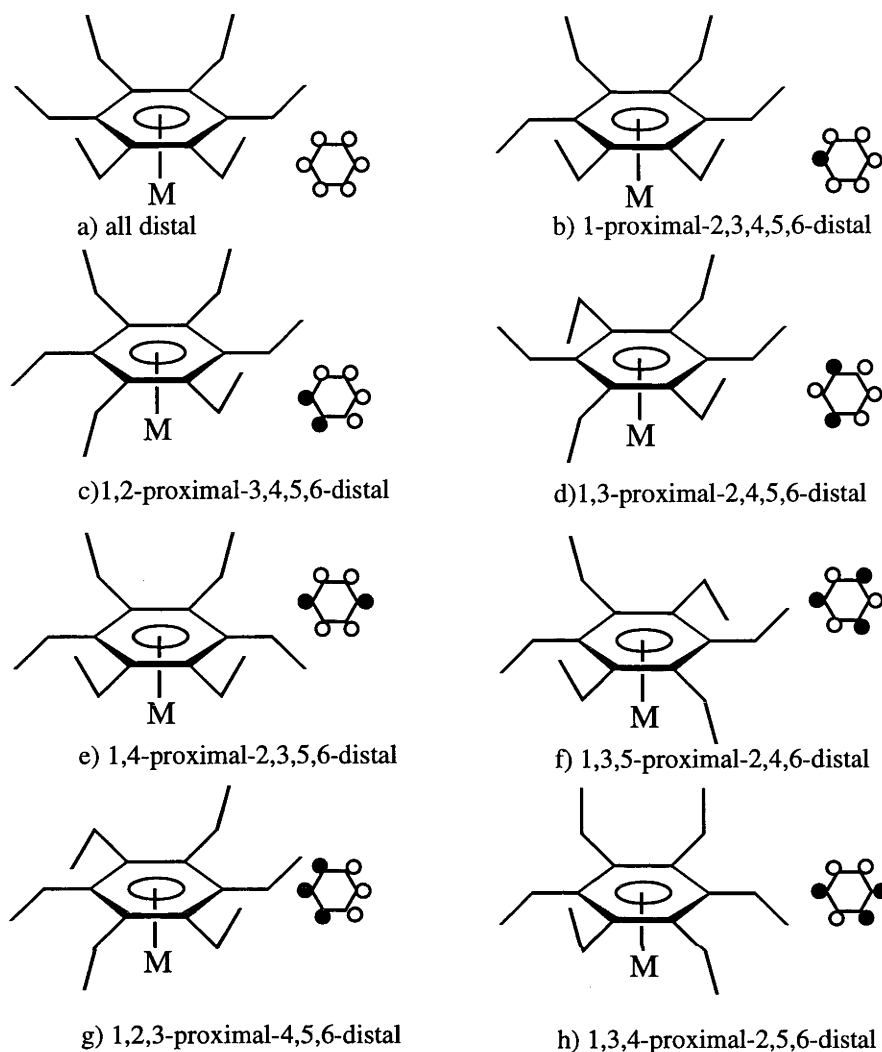


Figure 1.18. Some of the possible conformations of coordinated hexaethylbenzene. A filled circle represents a proximal ethyl group while a hollow circle represents a distal ethyl group

Two dynamic processes are believed to occur in complexes of this type; rotation of the arene about the arene-metal bond and rotation of the ethyl groups about the arene methylene bond, both depicted in Figure 1.19. The first motion can also be described as rotation of the metal-ligand tripod relative to the arene. Mislow *et al.*⁷⁴ refer to the second process as 'uncorrelated ethyl group rotation', *ie.* rotation of one ethyl group does not depend on the rotation of others. In the following discussion these motions are often described as 'stopped' or having 'ceased'. This is intended to mean that motions have slowed on an NMR timescale and not to imply that all molecular motions have come to a

complete halt.

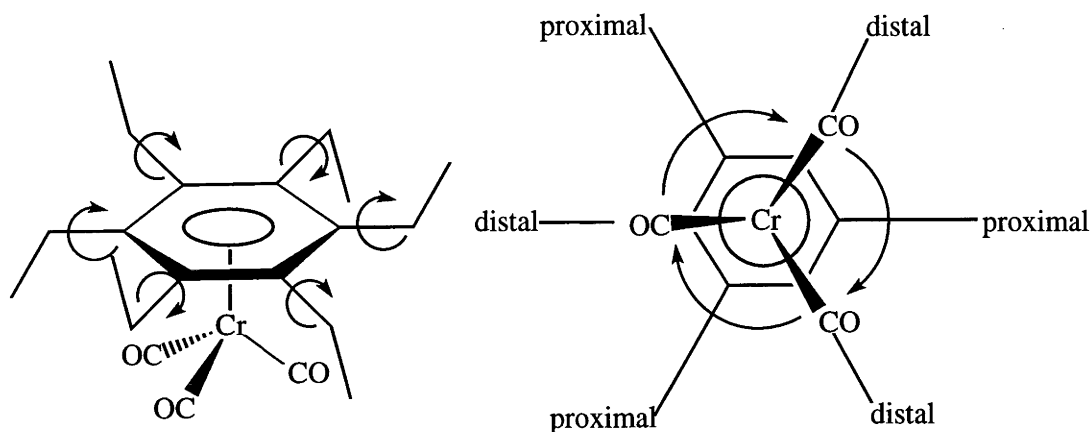


Figure 1.19. Two possible rotational motions in η^6 -hexaethylbenzene metal complexes

These processes are rapid at room temperature in solution but, because of the steric bulk of hexaethylbenzene, it may be possible to ‘freeze out’ these processes at low temperature in solution, that is, to slow them such that they become observable by NMR spectroscopy. The ability of the hexaethylbenzene to take on a number of conformations complicates study of these processes and the interpretation of the observed spectra has been contentious. A review by McGlinchey discusses the issue of fluxional behaviour in complexes of this type in some detail.⁷⁵

The starting point is the observation that, at room temperature in solution, $\text{Cr}(\eta^6\text{-C}_6\text{Et}_6)(\text{CO})_3$ displays only one resonance for each of the arene carbon methyl and methylene carbon atoms in the $^{13}\text{C}\{^1\text{H}\}$ NMR spectrum and the hydrogen atoms of the methyl and methylene groups give only one set of ethyl resonances in the ^1H NMR spectrum. At low temperature in solution the complex displays two resonances for the arene carbon atoms and methyl and methylene carbon and hydrogen atoms. A single crystal X-ray crystallographic investigation of $\text{Cr}(\eta^6\text{-C}_6\text{Et}_6)(\text{CO})_3$ showed that in the solid state hexaethylbenzene takes on a 1,3,5-proximal-2,4,6-distal conformation, similar to that of the free ligand and that, in projection, the distal ethyl groups eclipse the three carbonyl groups making up the tripod (Figure 1.20).⁷⁶ That this is the most energetically favourable conformation for the hexaethylbenzene ligand when interactions with other substituents are not taken into account is supported by the calculations of Iverson *et al.*⁷²

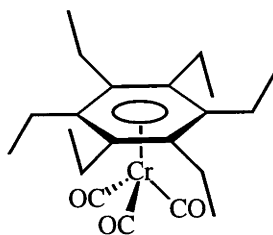


Figure 1.20. Solid state structure of $\text{Cr}(\eta^6\text{-C}_6\text{Et}_6)(\text{CO})_3$ showing 1,3,5-proximal-2,4,6-distal ethyl group conformations for the hexaethylbenzene

At room temperature it is thought that free rotation about both the arene-methylene and arene-metal bonds make the ethyl groups equivalent on an NMR timescale.⁷⁵ There are three possible explanations for the low temperature behaviour observed for $\text{Cr}(\eta^6\text{-C}_6\text{Et}_6)(\text{CO})_3$:

- (1) The arene has stopped rotating about the arene metal axis, leaving the ethyl groups freely rotating but positioned either over a CO group or in the gap between CO groups
- (2) The ethyl groups have stopped spinning leaving the arene in the 1,3,5-proximal-2,4,6-distal conformation while the arene continues freely rotating
- (3) All the motions have ceased.

In all these cases the symmetry of the molecule is such that two inequivalent ethyl groups should be observed in the NMR spectra.

The barriers to rotation of π -bonded arenes about the arene metal bond are generally thought to be too low to detect by conventional variable temperature NMR spectroscopy unless there are special steric or electronic constraints. They have, however, been measured for complexes in the solid state. In $\text{Cr}(\eta^6\text{-C}_6\text{H}_6)(\text{CO})_3$, where such constraints are absent, the activation energy of the rotation has been measured by quasielastic neutron scattering to be as low as 16 kJmol^{-1} .⁷⁷ This is to be compared with the 27.5 kJmol^{-1} measured by inelastic neutron scattering,⁷⁸ 19.5 kJmol^{-1} from Raman spectra,⁷⁹ 17.6 kJmol^{-1} from solid state NMR measurements⁸⁰ and 19.2 kJmol^{-1} from potential energy calculations.⁸⁰ In the ruthenium complexes $[\text{Ru}_2(\eta^6\text{-arene})_2\text{Cl}_3]^+\text{BF}_4^-$ (arene = C_6H_6 , $\text{C}_6\text{H}_5\text{Me}$), thermal motion analysis of the solid state structures determined by single crystal X-ray crystallography gave, for the benzene complex at 150 K, a barrier to

rotation of the arene ring about the arene-ruthenium axis of 21 and 27 kJmol⁻¹ for each of the two arene rings present, while for the toluene case it was found that free rotation about the arene ruthenium bond did not occur, but rather what was described as a 'swinging' motion about the arene ruthenium axis was observed.⁴⁴

As the substituents on the ring become bulkier, the activation energy for ring rotation increases to the point where this process is observable and activation barriers can be derived by standard NMR spectroscopy line broadening techniques. Some examples are:

Mo[η⁶-C₆{1,3,5-Et₃-2,4,6-(SiMe₃)₃}] (CO)₃, (35 kJmol⁻¹),⁸¹
 Cr(η⁶-1,4-C₆H₄Bu^{*t*}₂)(CO)₂(PPh₃), (31.6 kJmol⁻¹),⁸² Ru(η⁶-C₆H₄Bu^{*t*}₂)(CO)(SiCl₃)₂,
 (51 kJmol⁻¹)⁸³ and Fe(η⁶-1,4-C₆H₄R₂)(CO)(SiCl₃)₂, (R=Me, Et, ^{*i*}Pr), (40-45 kJmol⁻¹)⁸⁴.

Ru(η⁶-C₆H₄Bu^{*t*}₂)(CO)(SiCl₃)₂ was the first complex in which restricted rotation about the arene metal bond was conclusively observed. It was found that when a solution of this complex was cooled to -60°C both the ¹³C{¹H} and ¹H NMR spectra were consistent only with rotation about the arene metal bond having ceased on an NMR timescale.⁸³

Subsequently, in a study of nearly forty different arene complexes⁸⁵ it was found that several half sandwich complexes of the type M(η⁶-C₆H₄Bu^{*t*}₂)(ERCl₂)₂ (where M=Ru, E=Si, R= Me; M=Ru, E=Ge, R=Cl; M=Os, E= Si, R=Cl) display this same variable temperature NMR behaviour. Much of the discussion in this publication was devoted to an explanation of why many similar complexes studied, such as the *p*-di-isopropylbenzene complex, Ru(η⁶-C₆H₄Pr^{*i*}₂)(CO)(SiCl₃) and tri-*t*-butylbenzene complex Ru(η⁶-C₆H₃1,3,5-Bu^{*t*}₃)(CO)(SiCl₃)₂, had much lower barriers to arene ring rotation than Ru(η⁶-C₆H₄Bu^{*t*}₂)(CO)(SiCl₃)₂. Two mechanisms were invoked to explain these anomalies. For the *p*-di-isopropylbenzene complex it was proposed that, with a gear like mechanism, the isopropyl groups rotated in such a manner that the hydrogen atom was orientated towards the bulky ligands of the tripod as the rotation of the arene ring carried the isopropyl groups past the ligands. For the 1,3,5-tri-*t*-butylbenzene complex ring tilting was invoked to explain the lower barrier to rotation; the arene ring was suggested to tilt in such a manner as to reduce the steric interaction between the substituents on the arene and the bulky ligands of the tripod. This was not considered possible in the case of the *p*-di-*t*-butylbenzene complex as the placement of the two para substituents are such that when one is trying to tilt away from one of the bulky ligands of the tripod the other substituent is being forced towards a bulky ligand

This ring tilting explanation was later revoked⁸⁴ in a paper on restricted rotation in related complexes of the type $\text{Fe}(\eta^6\text{-arene})(\text{CO})(\text{SiCl}_3)_2$. It was proposed that the effect arose from the relative stabilities of the ground and transition states in the arene ring rotation of these complexes. It was thought that while the transition state for complexes of greater steric bulk such as the tri-*t*-butylbenzene complex was of higher energy than that of the di-*t*-butylbenzene complex the ground state of the tri-*t*-butylbenzene complex was far less stable than that of the di-*t*-butylbenzene complex, thus the rotational barrier to be overcome to rotate was much lower.

Localization of the double bond character in the ring as in $\text{Cr}(\text{endo-}\eta^6\text{-starphenylene})(\text{CO})_3$ and derivatives can also raise the barrier to ring rotation (*ca.* 48 kJmol⁻¹).⁸⁶ Starphenylene is depicted in Figure 1.21. In this arene the central ring is more cyclohexatriene-like than benzenoid, whereas the outer six membered rings are more aromatic in nature.

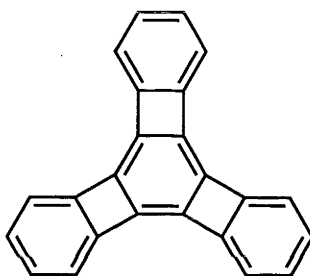


Figure 1.21. Starphenylene

In complexes of the type $[\text{Cr}(\eta^6\text{-MeC}_6\text{H}_4\text{R})(\text{CO})_3]$, ($\text{R}=\text{CHMe}^+$, CHPh^+) localization of the double bond character in the coordinated ring raises the barrier to ring rotation such that the process is observable by NMR line broadening techniques.⁸⁷ It is also possible to raise the barrier to ring rotation by the substitution of a heteroatom in the aromatic ring, for example in the 2,5-dimethylthiophene complex, $\text{Cr}(\eta^5\text{-2,5-C}_5\text{H}_2\text{Me}_2\text{S})(\text{CO})_3$.⁸⁸

The question of whether, in complexes of η^6 -hexaethylbenzene, the slowing of rotation about the arene metal bond could be observed at the temperatures accessible with NMR line broadening techniques has been contentious. Table 1.1 gives a list of hexaethylbenzene complexes whose solid state structures have been determined crystallographically, their solid state conformations, as per Figure 1.18, a summary of pertinent NMR spectral behaviour at low temperature in solution, and suggested rationalizations.

Table 1.1. Properties and complexes of η^6 -hexaethylbenzene

Complex	Conformation	Low temperature solution behaviour and explanation
$\text{Cr}(\eta^6\text{-C}_6\text{Et}_6)(\text{CO})_2\text{-}\mu\text{-N}_2\text{-Cr}(\eta^6\text{-C}_6\text{Et}_6)(\text{CO})_2$ ⁸⁹		-2 different arene carbon resonances in the ¹³ C NMR spectrum -caused by slowed ethyl rotation ⁸⁹
$\text{Cr}(\eta^6\text{-C}_6\text{Et}_6)(\text{CO})_3$ ⁹⁰		-2 different arene carbon atom resonances in the ¹³ C NMR spectrum, 1:1 ratio -Two explanations: a) caused by slowed ethyl rotation ⁹⁰ b) hindered rotation about the arene metal bond axis ⁷⁵
$\text{Cr}(\eta^6\text{-C}_6\text{Et}_6)(\text{CO})_2\text{PPh}_3$ ⁹⁰		-only one resonance in the ¹³ C NMR spectrum -all distal conformation present with free arene-metal bond axis rotation ⁹⁰
$[\text{Mo}(\eta^6\text{-C}_6\text{Et}_6)(\text{CO})_3\text{Cl}]^+(\text{MoCl}_6^-)$ ⁹¹		low temperature solution behaviour not discussed
$[\text{Cr}(\eta^6\text{-C}_6\text{Et}_6)(\text{CO})_2(\text{NO})]^+(\text{BF}_4^-)$ ⁹²		-four different arene carbon atom 2:1:2:1 ratio -slowed rotation about the arene-metal bond axis, C ₆ Et ₆ has taken on solid state conformation ⁹²
$[\text{Cr}(\eta^6\text{-C}_6\text{Et}_6)(\text{CO})(\text{CS})(\text{NO})]^+(\text{BF}_4^-)$ ⁹²		-six different arene carbon atom resonances in the ¹³ C NMR spectrum -slowed rotation about the arene-metal bond axis, C ₆ Et ₆ has taken on solid state conformation ⁹²
$\text{Ir}(\eta^6\text{-C}_6\text{Et}_6)(\eta^1, \eta^3\text{-cyclooct-1-en-5-yl})$ ⁹³		low temperature solution behaviour not discussed
$\text{Ta}(\eta^6\text{-C}_6\text{Et}_6)(\text{C}_6\text{H}_4\text{-1-O-2-Pr}^i)_2$ ⁹⁴		low temperature solution behaviour not discussed
$[\text{Fe}(\eta^6\text{-C}_6\text{Et}_6)(\eta^5\text{-C}_5\text{H}_5)]^+(\text{BPh}_4^-)$ ⁹⁵		low temperature solution behaviour not discussed

Table 1.1. continued

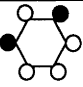
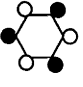
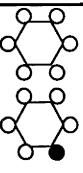
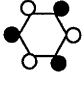
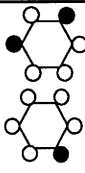
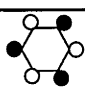
Complex	Conformation	Low temperature solution behaviour and explanation
$[\text{Fe}(\eta^6\text{-C}_6\text{Et}_6)(\eta^5\text{-C}_5\text{H}_5)]^+$ (PF_6^-) ⁹⁶		-three different carbon atom resonances observed in the ^{13}C NMR spectrum for the C_5H_5 ligand -rapid rotation about the arene-metal bond axis, slowed rotation about the arene-methylene bond axis giving three different stereoisomers in solution ⁷⁴
$\text{Mo}(\eta^6\text{-C}_6\text{Et}_6)(\text{CO})_3$ ⁷²		-two different arene carbon atom resonances observed in the ^{13}C NMR spectrum -slowing of rotation about the arene-methylene bond ⁷²
$\text{Cr}(\eta^6\text{-C}_6\text{Et}_6)(\text{CO})_2\text{PEt}_3$ ⁹⁷		-two different resonances in the ^{31}P NMR spectrum, assignable to the triethylphosphine -slowed rotation about the arene-methylene bond, rapid rotation about the arene-metal bond axis, two different stereoisomers present in solution ⁷⁴
$\text{Cr}(\eta^6\text{-C}_6\text{Et}_6)(\text{CO})_2(\text{CS})$ ⁹⁸		-four different resonances observed for the arene carbon atoms in a 2:1:2:1 ratio in the ^{13}C NMR spectrum -two explanations: a) slowed rotation about the arene-methylene bond, rapid rotation about the arene-metal bond axis, two stereoisomers present in solution ⁷⁴ b) slowed rotation about both the arene-metal bond axis and the arene-methylene bond leading to a static conformation the same as the solid state at low temperature in solution ⁹⁸

Table 1.1. continued

Complex	Conformation	Low temperature solution behaviour and explanation
$\text{Cr}(\eta^6\text{-C}_6\text{Et}_6)(\text{CO})_2\text{PMe}_3^{99}$		-four different resonances in the ^{31}P NMR spectrum -slowed rotation about the arene-methylene bond, four different stereoisomers present ^{74,99}
$\text{Mo}(\eta^6\text{-C}_6\text{Et}_6)(\text{CO})_2$ (η^2 -maleic anhydride) ⁷⁴		-two or more stereoisomers present ⁷⁴

To gain some insight into the question of slowed rotation about the arene-ruthenium bond, McGlinchey *et al.*⁹⁸ exchanged one of the carbonyl ligands in $\text{Cr}(\eta^6\text{-C}_6\text{Et}_6)(\text{CO})_3$ for a thiocarbonyl group to give $\text{Cr}(\eta^6\text{-C}_6\text{Et}_6)(\text{CO})_2\text{CS}$, thus reducing the symmetry of the tripodal set of ligands. The x-ray structure of this molecule was found to be similar to that for $\text{Cr}(\eta^6\text{-C}_6\text{Et}_6)(\text{CO})_3$ in that the ethyl groups of the hexaethylbenzene have taken on a 1,3,5-proximal-2,4,6-distal conformation with respect to the metal and the three distal ethyl groups eclipse the tripodal ligand system.

At 163 K in CD_2Cl_2 , this molecule displays a 1:2:2:1 ratio in the $^{13}\text{C}\{^1\text{H}\}$ NMR spectrum for each of the arene, methylene and methyl carbons. At 308 K only a single resonance for each group is observed. This behaviour can be rationalized in two ways. It has been proposed by McGlinchey⁹⁸ that the arene has the same conformation as in the solid state and rotation about the arene-metal bond has ceased on an NMR timescale at 163K. The activation barrier to the process was calculated to be 48 kJmol^{-1} .⁹⁸

Unfortunately, the assumption that the arene has the same conformation in solution as in the solid state is not necessarily valid because of the small energy differences between conformations. Merely changing the counter ion from PF_6^- ⁹⁶ to BPh_4^- ⁹⁵ in $[\text{Fe}(\eta^6\text{-C}_6\text{Et}_6)(\eta^5\text{-C}_5\text{H}_5)]^+$ changes the conformation of the ethyl groups from 1,3-proximal-2,4,5,6-distal to 1-proximal-2,3,4,5,6-distal. In fact, the relative difference in energies between conformations is so small, at least in the case of complexes of the type $\text{Cr}(\eta^6\text{-C}_6\text{Et}_6)(\text{CO})_2\text{PR}_3$ ($\text{R}=\text{Ph}^{90}$, Me^{99} , Et^{97}), that the X-ray structures contain two different ethyl group conformations for each complex. For $\text{Cr}(\eta^6\text{-C}_6\text{Et}_6)(\text{CO})_2(\text{PMe}_3)$ the $^{31}\text{P}\{^1\text{H}\}$ NMR spectrum at low temperature in CD_2Cl_2 showed the presence of four resonances that were assigned to hexaethylbenzene conformers. The most abundant stereoisomer in the crystal (1,3,5-proximal-2,4,6-distal) is apparently the least abundant

in CD_2Cl_2 solution at low temperature.⁹⁹

Hunter and Mislow preferred to explain the low temperature behaviour of $\text{Cr}(\eta^6\text{-C}_6\text{Et}_6)(\text{CO})_2\text{CS}$ in solution purely in terms of slowed ethyl group rotation, leaving the arene in a 1,3-proximal-2,4,5,6-distal conformation while rotation about the arene-metal bond axis remains rapid.⁷⁴ They postulated that in the absence of special steric or electronic character in the arene, the rotation of the arene about the arene metal bond would never slow enough in solution to be observed by NMR spectroscopy.¹⁰⁰

A second approach to lowering the symmetry of the system was the replacement of the hexaethylbenzene ligand with pentaethylacetophenone.¹⁰¹ The X-ray structure of $\text{Cr}(\eta^6\text{-C}_6\text{Et}_5\text{COMe})(\text{CO})_3$ shows that the arene ligand has a very similar conformation to that displayed by $\text{Cr}(\eta^6\text{-C}_6\text{Et}_6)(\text{CO})_3$ (Figure 1.22).

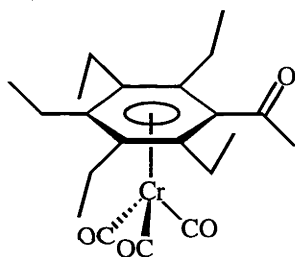


Figure 1.22. Solid state structure of $\text{Cr}(\eta^6\text{-pentaethylacetophenone})(\text{CO})_3$ showing the similarity between the conformation of the pentaethylbenzophenone and the coordinated hexaethylbenzene in $\text{Cr}(\eta^6\text{-C}_6\text{Et}_6)(\text{CO})_3$

In this molecule the spinning rate of the arene ligand should not affect the resonances for methyl, methylene and arene carbons and methyl and methylene hydrogens in the $^{13}\text{C}\{^1\text{H}\}$ and ^1H NMR spectra. There will always be three different sorts of ethyl groups. For the CO groups in the tripod, however, the reduction of symmetry of the arene to a single mirror plane means that if the arene stops rotating about the arene metal bond then more than one sort of CO resonance will be observed. Thus the 2:1 splitting of the $\text{Cr}(^{13}\text{CO})_3$ signal seen at -100°C in solution demonstrates with certainty that rotation about the arene metal bond has ceased on an NMR timescale. It was calculated that the barrier for this process was 36-40 kJmol^{-1} .⁹⁹ A second useful result that came out of this study is the ability to unequivocally assign the ^{13}C NMR resonances of proximal and

distal ethyl groups.

While this experiment demonstrates that arene rotation can cease on an NMR timescale in chromium carbonyl complexes, it does not resolve unambiguously whether arene rotation continues in complexes of hexaethylbenzene. This question was finally solved using a molecule containing three different ligands geometrically similar to CO in the tripod, namely, $[\text{Cr}(\eta^6\text{-C}_6\text{Et}_6)(\text{CO})(\text{CS})(\text{NO})]^+\text{BF}_4^-$.⁹² In the solid state an X-ray crystallographic study showed that the hexaethylbenzene in this complex adopts the same staggered proximal distal conformation as observed in $\text{Cr}(\eta^6\text{-C}_6\text{Et}_6)(\text{CO})_3$, with the distal groups positioned such that they eclipse the ligands forming the tripod. At low temperature in solution, the $^{13}\text{C}\{^1\text{H}\}$ NMR spectrum displays eighteen different signals, six for each of the methyl, methylene and arene carbons. Unfortunately, even this information, if taken alone, is not enough to prove that rotation about the arene metal bond has slowed on an NMR timescale, since it is still necessary to assume that the arene conformation in the solid state and solution are the same. Thus, if at low temperature in solution the arene had taken on a 1,3-proximal-2,4,5,6-distal conformation, then the 1,3-distal and 2,4-proximal ethyl groups would become diastereotopic. This would give rise to six different ethyl resonances, even if the arene were still rotating rapidly on an NMR timescale about the arene metal bond. However, the compilation of a large amount of chemical shift data on complexes of hexaethylbenzene¹⁰² and of pentaethylacetophenone (see above) allowed the assignment of proximal and distal ethyl groups and it was concluded that there were three ethyl groups of each type present. The only other necessary assumption is that the hexaethylbenzene has not taken on the high energy 1,2,3-proximal-4,5,6-distal conformation, which is regarded as highly unlikely.⁷² Thus it can be concluded that the process responsible for the observed NMR behaviour is slowing of rotation of the arene about the metal arene bond. The activation energy for the observed process was found to be 46 kJmol^{-1} .⁹²

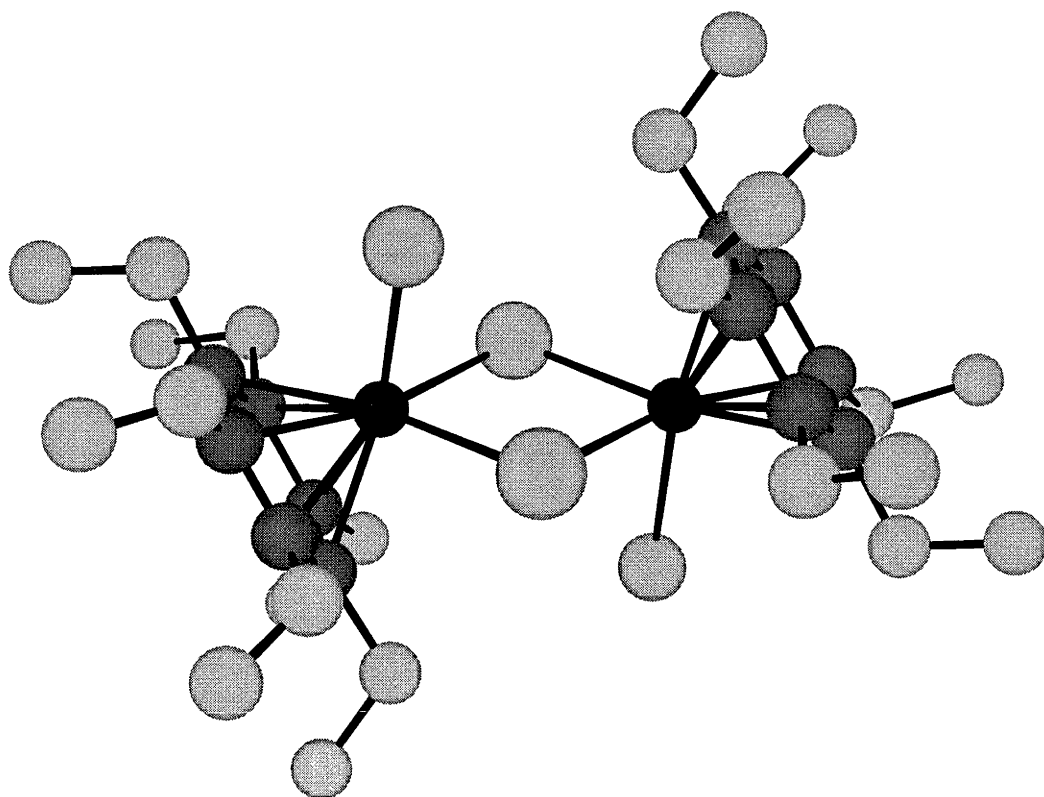
There is one case in the literature where the variable temperature NMR behaviour of a ruthenium complex of hexaethylbenzene has been studied, namely, $[\text{Ru}(\eta^6\text{-C}_6\text{Et}_6)(\eta^5\text{-C}_5\text{H}_5)]^+\text{BF}_4^-$.^{32,33} While at room temperature in CH_2Cl_2 solution only one ethyl and arene carbon resonance was present in the $^{13}\text{C}\{^1\text{H}\}$ NMR spectrum, below 183 K two singlets are observed for each of the methyl, methylene and arene carbons. The process producing this behaviour was calculated to have an activation barrier of *ca.* 39 kJmol^{-1} . It was proposed that this was evidence for the presence of more than one conformer due to slowing of the rotation about the arene-methylene bonds. As the resonances for the Cp ring were temperature invariant, it was thought that rotation of the arene about the arene ring axis continued unhindered. The fact that the linewidths for the different arene carbon

resonances observable below 183 K differed was put forward as supporting evidence for the presence of different stereoisomers. This is in contrast to the analogous iron compound, namely, $[\text{Fe}(\eta^6\text{-C}_6\text{Et}_6)(\eta^5\text{-C}_5\text{H}_5)]^+\text{BF}_4^-$ ⁷⁴, in which the three Cp resonances in the $^{13}\text{C}\{^1\text{H}\}$ NMR spectrum at low temperature in CH_2Cl_2 could only be simulated effectively on the basis of three different stereoisomers, arising from different ethyl conformations.

Pertici *et al.*¹⁰³ have conducted a preliminary study of the stereodynamics of the complex $\text{Ru}(\eta^6\text{-C}_6\text{Et}_6)(\text{COD})$ in solution. The single crystal x-ray structure shows that in the solid state the ethyl groups take on a 1,4-proximal-2,3,5,6-distal conformation (Figure 4). The two proximal ethyl 'legs' sit in the gaps formed by the boat shaped cyclooctadiene ligand. At room temperature in solution both the ^1H and $^{13}\text{C}\{^1\text{H}\}$ NMR spectra have only one resonance for each of the nuclei associated with an ethyl group. However, at low temperature, each of these resonances is split in two in a 2:1 ratio. These results suggest that hexaethylbenzene in $\text{Ru}(\eta^6\text{-C}_6\text{Et}_6)(\eta^4\text{-COD})$ has the same conformation at low temperature in solution as in the solid state, that is, 1,4-proximal-2,3,5,6-distal. The variable temperature NMR behaviour is also consistent with slowing of rotation about the arene-metal bond.

Cyclotrimerization of acetylenes on $\text{Ru}(\eta^6\text{-naphthalene})(\eta^4\text{-COD})$ has enabled the preparation new arene ruthenium starting materials. Chapter Two of this thesis deals with the preparation and characterization of these complexes. The number of half sandwich $\text{Ru}(\text{II})$ complexes easily accessible from the versatile starting materials of the type $[\text{Ru}(\eta^6\text{-arene})\text{Cl}_2]_2$ is very large. Thus, hexaethylbenzene complexes of ruthenium should be ideal for following the conformational variability of the hexaethylbenzene ligand in the solution and solid state. Chapter Three deals the preparation and characterization of new arene ruthenium (II) half sandwich complexes, mainly of hexaethylbenzene while Chapter Four is concerned with the dynamic NMR behaviour of these complexes in solution and the relationship to their solid state structure.

Chapter 2: *New η^6 -arene ruthenium complexes*



Chem 3D representation of the molecular structure of $[\text{Ru}(\eta^6\text{-C}_6\text{Et}_6)\text{Cl}_2]_2$

<i>Preparation and characterization of new $\text{Ru}(\eta^6\text{-arene})(\eta^4\text{-COD})$ complexes</i>	30
<i>Preparation and characterization of dimeric ruthenium(II) complexes of the type $[\text{Ru}(\eta^6\text{-arene})\text{Cl}_2]_2$ [arene=$\text{C}_6\text{H}_3\text{Pr}^i_3$, C_6Et_6 and benzotris(cyclooctene)]</i>	42
<i>Preparation and characterization of triply-bridged dimeric $\text{Ru}(\text{II})$ complexes of the type $[\text{Ru}_2(\eta^6\text{-arene})_2\text{Cl}_3]^+\text{PF}_6^-$ (where arene = C_6Et_6, $\text{C}_6\text{H}_4\text{-1,2-Et}_2$ and $\text{C}_6\text{H}_4\text{-1,2-Pr}^i_2$)</i>	50
<i>Solution behaviour of $\text{Ru}(\eta^6\text{-C}_6\text{Et}_6)\text{Cl}_2]_2$</i>	66

In the course of this study the synthetic utility of the reaction between $\text{Ru}(\eta^6\text{-naphth})(\eta^4\text{-COD})$ and 3-hexyne and other acetylenes containing bulky groups to give $\text{Ru}(0)$ complexes of the type $\text{Ru}(\eta^6\text{-arene})(\eta^4\text{-COD})$ will be shown. This reaction provides a route into complexes of ruthenium containing η^6 -hexaethylbenzene or other sterically demanding arenes. Indeed, there are a number of arenes which it would be difficult to coordinate to ruthenium using any other previously existing method.

For example, neither hexaethylbenzene nor benzo(1',2':3',4':5',6') tri(1,2,3,4,5,6-hexahydro) cyclooctene [benzotris(cyclooctene)] exchange with the *p*-cymene in $[\text{Ru}(\eta^6\text{-}p\text{-cymene})\text{Cl}_2]_2$ when the arene and the dichloride dimer are fused together. Neither arene will replace naphthalene when $\text{Ru}(\eta^6\text{-naphth})(\eta^4\text{-COD})$ is treated with the arene in the presence of acetonitrile. Although the Birch reduction of benzotris(cyclooctene) was not attempted, it proved to be impossible to effectively reduce hexaethylbenzene to the corresponding cyclohexadiene. Thus the reaction of this cyclohexadiene with $\text{RuCl}_3 \cdot x\text{H}_2\text{O}$ in refluxing ethanol in a dehydrogenation reaction analogous to that used to obtain $[\text{Ru}(\eta^6\text{-benzene})\text{Cl}_2]_2$ and $[\text{Ru}(\eta^6\text{-}p\text{-cymene})\text{Cl}_2]_2$ (see Chapter 1) was not available.

Hexaphenylbenzene is another example of an arene which would not be possible to coordinate to ruthenium in any other way, at least to the central ring. In any exchange reaction, the proportion of hexaphenylbenzene coordinated through the central ring could, at most, be only one seventh of the total, in the absence of steric or electronic effects. Further, selective Birch reduction of the central ring of hexaphenylbenzene to a hexaphenyl-1,4-cyclohexadiene is unlikely.

This chapter is concerned with the preparation and characterization of $\text{Ru}(\eta^6\text{-arene})(\eta^4\text{-COD})$ complexes and of derived ruthenium(II) complexes, $[\text{Ru}(\eta^6\text{-arene})\text{Cl}_2]_2$, and cationic tri- μ -chloro salts, $[\text{Ru}_2(\eta^6\text{-arene})_2\text{Cl}_3]^+\text{PF}_6^-$.

Preparation and characterization of new $\text{Ru}(\eta^6\text{-arene})(\eta^4\text{-COD})$ complexes

Pertici *et al.*³⁵ reacted a number of acetylenes with $\text{Ru}(\eta^6\text{-naphth})(\eta^4\text{-COD})$ in a *ca.* 6:1 mol ratio in THF at room temperature to give complexes of the type $\text{Ru}(\eta^6\text{-arene})(\eta^4\text{-COD})$, as outlined in Figure 2.1. The results of this group's work are listed in Table 2.1a below. All of these $\text{Ru}(\eta^6\text{-arene})(\eta^4\text{-COD})$ complexes have been characterized by ^1H NMR, EI or FAB mass spectrometry, and microanalysis.

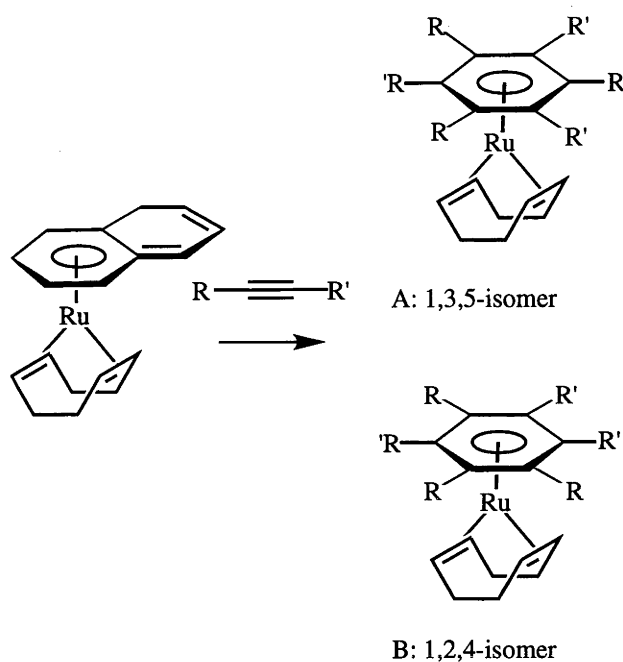


Figure 2.1. Reaction of $Ru(\eta^6\text{-naphth})(\eta^4\text{-COD})$ with acetylenes showing two possible isomers obtained.

In the course of this PhD study, the work of Pertici *et al.* was extended. Several new acetylenes were reacted with $Ru(\eta^6\text{-naphth})(\eta^4\text{-COD})$, under the same conditions as used by Pertici *et al.*. The results of this study are listed in Table 2.1b. Characterizing data for the new complexes of the type $Ru(\eta^6\text{-arene})(\eta^4\text{-COD})$, prepared as part of this thesis, are contained in Table 2.2 discussed below; the preparative details are given in the Experimental chapter.

Table 2.1a. Reactions of $\text{Ru}(\eta^6\text{-naphth})(\eta^4\text{-COD})$ with acetylenes in THF at room temperature studied by Pertici *et al.*

Alkyne	Time (h)	Yield (%)	Products	Isomeric ratio, A:B
1-hexyne, $\text{Bu}^n\text{C}_2\text{H}$	1	95	$\text{Ru}(\eta^6\text{-C}_6\text{H}_3\text{Bu}^n_3)(\eta^4\text{-COD})$	70:30
4-methyl-1-hexyne, $(\text{Me})(\text{Et})\text{CHCH}_2\text{C}_2\text{H}$	2	95	$\text{Ru}(\eta^6\text{-1,2,4-}((\text{Me})(\text{Et})\text{CHCH}_2)_3)(\eta^4\text{-COD})$	75:25
phenylacetylene, PhC_2H	5	95	$\text{Ru}(\eta^6\text{-C}_6\text{H}_3\text{Ph}_3)(\eta^4\text{-COD})$	20:80
1,8-nonadiyne, $\text{HC}_2(\text{CH}_2)_5\text{C}_2\text{H}$	3	90	$\text{Ru}(\eta^6\text{-C}_6\text{H}_3((\text{CH}_2)_5\text{C}_2\text{H})(\eta^4\text{-COD})$	70:30
2-butyne, MeC_2Me	2	95	$\text{Ru}(\eta^6\text{-C}_6\text{Me}_6)(\eta^4\text{-COD})$	
4-octyne, $\text{Pr}^n\text{C}_2\text{Pr}^n$	4	90	$\text{Ru}(\eta^6\text{-C}_6\text{Pr}^n_6)(\eta^4\text{-COD})$	
diphenylacetylene, PhC_2Ph	10	50	$\text{Ru}(\eta^6\text{-C}_6\text{Ph}_6)(\eta^4\text{-COD})$	
2-hexyne, MeC_2Pr^n	3	95	$\text{Ru}(\eta^6\text{-C}_6\text{Me}_3\text{Pr}^n_3)(\eta^4\text{-COD})$	30:70

Table 2.1b. Reactions of $\text{Ru}(\eta^6\text{-naphth})(\eta^4\text{-COD})$ with acetylenes in THF at room temperature carried out as part of this study

Alkyne	Time (h)	Yield (%)	Products	Isomeric ratio, A:B
isopropylacetylene, $\text{Pr}^i\text{C}_2\text{H}$	15	28	$\text{Ru}(\eta^6\text{-C}_6\text{H}_3\text{Pr}^i_3)(\eta^4\text{-COD})$	88:12
<i>t</i> -butylacetylene, $\text{Bu}^t\text{C}_2\text{H}$	15	33	$\text{Ru}(\eta^6\text{-C}_6\text{H}_3\text{Bu}^t_3)(\eta^4\text{-COD})$	>95%A
trimethylsilylacetylene, $\text{Me}_3\text{SiC}_2\text{H}$	3.5	23	$\text{Ru}(\eta^6\text{-C}_6\text{H}_3(\text{SiMe}_3)_3)(\eta^4\text{-COD})$	40:60
3-hexyne, EtC_2Et	3	95	$\text{Ru}(\eta^6\text{-C}_6\text{Et}_6)(\eta^4\text{-COD})$	
cyclooctyne	12	22	$\text{Ru}(\eta^6\text{-benzotris(cyclooctene)})(\eta^4\text{-COD})$	
di-isopropylacetylene, $\text{Pr}^i\text{C}_2\text{Pr}^i$			no characterizable products	
bis(trimethylsilyl)acetylene $\text{Me}_3\text{SiC}_2\text{SiMe}_3$			no reaction	

Table 2.2 Characterizing data for Ru(η^6 -arene)(η^4 -COD) complexes

Complex	NMR Data	Other Data
Ru(η^6 -C ₆ Et ₆)(η^4 -COD)	¹ H NMR (C ₆ D ₆ , 200 MHz) δ 2.76 [br s, 4H, CH(COD)], 2.36 (br s, 8H, CH ₂ (COD)), 2.1 (q, 12H, ³ J(HH) 7.5 Hz, CH ₂), 1.82 ppm (t, ³ J(HH) 7.5 Hz, CH ₃) ¹³ C{ ¹ H} NMR (C ₆ D ₆ , 75.42 MHz) δ 103.4 (s, Caromatic), 64.3 [s, CH(COD)], 34.6 [s, CH ₂ (COD)], 21.1 (s, CH ₂), 18.8 ppm (s, CH ₃)	Anal. calcd for C ₂₆ H ₄₂ Ru: C 68.56; H 9.23. Found: C 68.72; H 8.97. <i>m/z</i> = 456 (M ⁺)
Ru(η^6 -C ₂₄ H ₃₆)(η^4 -COD ¹)	¹ H NMR (C ₆ D ₆ , 300 MHz) δ 1-3 ppm [m, 48H, COD and C ₂₄ H ₃₆] ¹³ C{ ¹ H} NMR (C ₆ D ₆ , 75.42 MHz) δ 101.4 (s, Caromatic), 64.1 [s, CH(COD)], 34.5 [s, CH ₂ (COD)], 32.0 [s, CH ₂ C ₂₄ H ₃₆], 27.6 [s, CH ₂ (C ₂₄ H ₃₆)], 27.3 ppm [s, CH ₂ (C ₂₄ H ₃₆)]	Anal. calcd. for C ₃₂ H ₆₀ Ru: C 72.00; H 9.06. Found: C 71.67; H 8.60. <i>m/z</i> = 533 (M ⁺)
Ru(η^6 -C ₆ H ₃ Pr ^{<i>i</i>} ₃)(η^4 -COD)	¹ H NMR [C ₆ D ₆ , 300 MHz (for a mixture of both isomers)] δ 1.25 [d, ³ J(HH) 6.8 Hz, 9H, CH ₃ (symmetrical isopropyl)], 1.8-2.2 [m, 8H, CH ₂ (η^4 -COD)], 2.38 [septet, 3H, ³ J (HH) 6.8 Hz, 3H, CH (symmetrical isopropyl)], 2.9-3.0 [m, 4H, CH (η^4 -COD)], 4.60-4.75 [m, 3H, CH _{aromatic} (unsymmetrical)] ^b , 5.10 ppm [s, 3H, CH _{aromatic} (symmetrical)] ^b . ¹³ C{ ¹ H} NMR [C ₆ D ₆ , 75.42 MHz (data for symmetrical isomer)] δ 109.8 (s, CH _{aromatic}), 84.6 [CH(COD)], 61.5 [s, CH ₂ (COD)], 34.0 [s, CH(isopropyl)], 23.8 ppm [s, CH ₃ (isopropyl)] ^c	High resolution FAB ⁺ mass spectrum gave a peak at 412.185914 amu which is less than 0.1 ppm different from the calculated mass for ¹² C ₂₃ H ₃₆ ¹⁰¹ Ru of 412.185919 amu.

¹C₂₄H₃₆ = benzotris(cyclooctene)^b resonances integrated to determine ratio of isomers^c tertiary aromatic carbons not seen.

Table 2.2 continued

Complex	NMR Data	Other data
$\text{Ru}(\eta^6\text{-C}_6\text{H}_3\text{Bu}^t_3)(\eta^4\text{-COD})$	<p>^1H NMR [CD_2Cl_2, 300 MHz (symmetrical isomer)] δ 1.29 [s, 9H, $\text{CH}_3(\text{Bu}^t)$], 1.8-2.1 [m, 8H, $\text{CH}_2(\text{COD})$], 3.15-3.25 [m, 4H, $\text{CH}(\text{COD})$], 5.46 ppm [s, 3H, $\text{CH}_{\text{aromatic}}$]</p> <p>$^{13}\text{C}\{^1\text{H}\}$ NMR [CD_2Cl_2, 75.42 MHz (symmetrical isomer)] δ 113.2 (s, $\text{CH}_{\text{aromatic}}$), 81.6 [s, $\text{CH}(\text{COD})$], 58.6 [s, $\text{CH}_2(\text{COD})$], 33.2 [s, $\text{C}(\text{Bu}^t)$], 31.5 ppm [s, $\text{CH}_3(\text{Bu}^t)$]</p>	High res FAB ⁺ mass spec gave a peak at 455.234426 amu which is within 0.4 ppm of the calculated peak for $^{12}\text{C}_{26}^{1}\text{H}_{42}^{102}\text{Ru}$ of 455.234232 amu.
$\text{Ru}[\eta^6\text{-C}_6\text{H}_3(\text{SiMe}_3)_3](\eta^4\text{-COD})$	<p>^1H NMR [CD_2Cl_2, 300 MHz (symmetrical and unsymmetrical isomers)] δ 0.22 [s, 27H, TMS (symmetrical)], 0.22 [s, 9H, TMS (unsymmetrical)], 0.33 [s, 9H, TMS (unsymmetrical)], 0.425 [s, 9H, TMS (unsymmetrical)], 2.33-2.14 [m, 8H, $\text{CH}_2(\text{COD})$, both isomers], 3.54-3.46 [m, 4H $\text{CH}(\text{COD})$, both isomers], 4.48 [m, H, $\text{CH}_{\text{aromatic}}$ (unsymmetrical)], 4.75 (m, H, $\text{CH}_{\text{aromatic}}$ (unsymmetrical)], 4.82 [m, H, $\text{CH}_{\text{aromatic}}$ (unsymmetrical)], 5.36 ppm [s, 3H, CH (symmetrical)]</p>	The EI high resolution mass spec gave an M^+ peak at 504.1643 amu which is within 1 ppm of the calculated peak for $^{12}\text{C}_{23}^{1}\text{H}_{42}^{102}\text{Ru}^{28}\text{Si}_3$ of 504.1638 amu.

The three unsymmetrical acetylenes, *t*-butylacetylene, trimethylsilylacetylene and isopropylacetylene, reacted with $\text{Ru}(\eta^6\text{-naphth})(\eta^4\text{-COD})$ to give mixtures of arene complexes containing the 1,3,5 and 1,2,4 isomers, although in the case of the *t*-butylacetylene the amount of the unsymmetrical arene complex formed was very small. All were air-sensitive yellow oils, hence microanalysis was not attempted, and accurate mass determination by mass spectrometry in combination with NMR spectroscopy was used instead for characterization. The proportion of different isomers formed was determined by integration of various resonances of the ^1H NMR spectrum as described in Chapter 5. The symmetrical isomers gave a singlet between δ 5.0 and 5.5 ppm for the protons of the aromatic ring while the unsymmetrical isomers gave a series of multiplets in the region δ 4.5 to 5.4 ppm.

Cyclooctyne is a somewhat strained molecule, being the smallest unsubstituted cyclic acetylene that is stable at room temperature.^{104,105} When cyclooctyne is reacted with $\text{Ru}(\eta^6\text{-naphth})(\eta^4\text{-COD})$ the complex $\text{Ru}[\eta^6\text{-benzotris(cyclooctene)}](\eta^4\text{-COD})$ [benzotris(cyclooctene) = benzo (1,2:3,4:5,6) 1,2,3,4,5,6-hexahydrocyclooctene] is isolated in 22% yield as a pale yellow solid. The dynamic inversion of the three eight membered rings of the arene thus formed is such that, at room temperature in solution, only four different carbon resonances for the coordinated arene are observable in the $^{13}\text{C}\{^1\text{H}\}$ NMR spectrum, one at δ 101.4 ppm for the coordinated arene carbon atoms and three resonances in the range δ 31.9-27.3 ppm for the carbon atoms of CH_2 groups of the eight membered rings. The methylene region of the ^1H NMR spectrum of this complex, and indeed all benzotris(cyclooctene) complexes studied, contained a series of complex multiplets

All of the $\text{Ru}(\eta^6\text{-arene})(\eta^4\text{-COD})$ complexes prepared had similar NMR resonances for the cyclooctadiene portion of the molecules. Taking $\text{Ru}(\eta^6\text{-C}_6\text{Et}_6)(\eta^4\text{-COD})$ as a representative example, there are two broad singlets in the ^1H NMR spectrum at δ 2.76 and 2.36 ppm for the protons of the CH and CH_2 groups of the cyclooctadiene and two singlets in the $^{13}\text{C}\{^1\text{H}\}$ NMR spectrum at δ 64.3 and 34.6 ppm from the CH and CH_2 carbons respectively. At room temperature the coordinated hexaethylbenzene gives rise to a quartet at δ 2.10 ppm and a triplet at δ 1.82 ppm, assignable to the methylene and methyl protons of the ethyl groups and singlets at δ 103.4, 21.1 and 18.9 ppm in the $^{13}\text{C}\{^1\text{H}\}$ NMR spectrum, assignable to the aromatic, methylene and methyl carbon atoms respectively of the coordinated hexaethylbenzene.

Neither di-isopropylacetylene nor bis(trimethylsilyl)acetylene gave any characterizable products on attempted reaction with $\text{Ru}(\eta^6\text{-naphth})(\eta^4\text{-COD})$ under similar reaction conditions to those employed for the other acetylenes. In both cases much decomposition

was observed and no new η^6 -arene products could be isolated. In the case of the di-isopropylacetylene, however, an electron impact mass spectrum of the crude reaction mixture showed a peak corresponding to $\text{Ru}(\eta^6\text{-C}_6\text{Pr}_6)(\eta^4\text{-COD})$ as well as a peak for free hexakis(isopropylbenzene). The difficulties encountered in the preparation and purification of di-isopropylacetylene prevented further attempts at this promising reaction. It is thought that, while both the hexakis(trimethylsilyl)benzene¹⁰⁶ and hexakis(isopropyl)benzene¹⁰⁷ have been isolated previously as free arenes, the steric interactions that must be overcome to form and coordinate these arenes to the ruthenium metal are too great. A previous attempt to coordinate hexakis(isopropylbenzene) to a chromium tricarbonyl fragment has also failed.¹⁰⁷

Pertici *et al.*¹⁰⁸ were able to obtain crystals of $\text{Ru}(\eta^6\text{-C}_6\text{Et}_6)(\eta^4\text{-COD})$ suitable for single crystal X-ray crystallography, which was carried out at the University of Pisa. Fig 2.2 shows a diagram of the structure, and Table 2.3 contains pertinent distances and angles for this complex. The complex has the classic piano stool structure, the arene being η^6 -coordinated to the ruthenium metal and the cyclooctadiene η^4 -coordinated on the opposite face. The arene is essentially planar with each carbon bonded in an equivalent manner to the ruthenium atom. The ethyl 'arms' of the arene adopt a 1,4-proximal-2,3,5,6-distal conformation with respect to the metal atom. The proximal ethyl groups are orientated such that they occupy the space created by the boat shaped conformation of the COD ligand, thus minimizing any steric interactions between proximal ethyl groups and the COD ligand.¹⁰⁸ The structure of $\text{Ru}(\eta^6\text{-C}_6\text{H}_6)(\eta^4\text{-COD})$ has been determined previously.¹⁰⁹ The overall geometry of the benzene and hexaethylbenzene complexes is the same. The coordinated COD carbon atoms are displaced the same distance from the ruthenium atom (2.127 - 2.136(4) Å and 2.133-2.138(5) Å for the benzene and hexaethylbenzene complexes respectively). The carbon atoms of the benzene ring are slightly further away in the case of the hexaethylbenzene complex (2.250 - 2.265(4) Å as against 2.195 - 2.256(7) Å), which is in keeping with the extra steric bulk of the hexaethylbenzene ligand. In the case of the benzene complex the aromatic ring is not absolutely planar, having a shallow boat conformation. This can be seen in the large range of ruthenium atom to arene ring carbon atom bond lengths. This is not observed in the case of the hexaethylbenzene complex, where all of these distances are essentially the same.

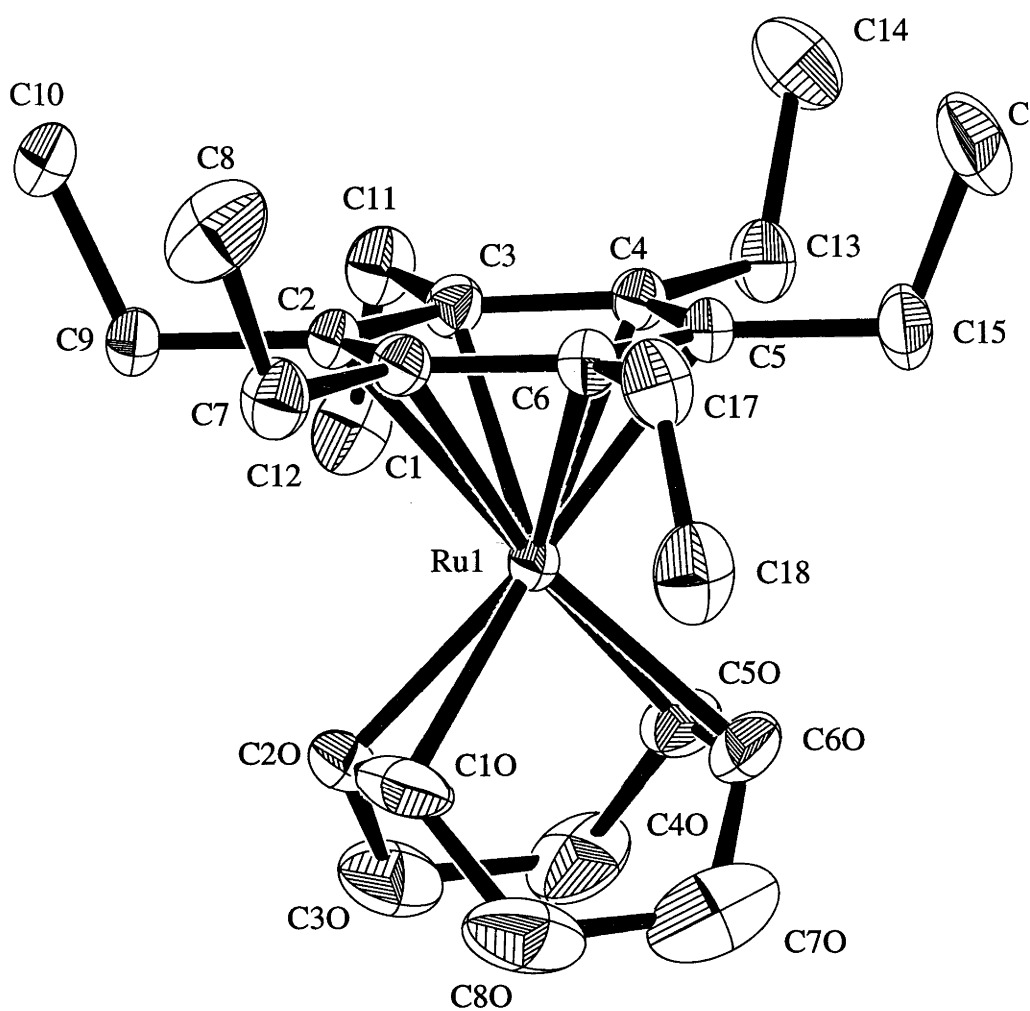


Figure 2.2. ORTEP diagram of the molecular structure of $\text{Ru}(\eta^6\text{-C}_6\text{Et}_6)(\eta^4\text{-COD})$

Table 2.3. Selected bond lengths (Å) and angles (°) for Ru(η^6 -C₆Et₆)(η^4 -COD)

Ru-C(10)	2.127(4)	C(4)-C(13)	1.516(5)
Ru-C(60)	2.130(4)	C(5)-C(6)	1.424(5)
Ru-C(50)	2.133(4)	C(5)-C(15)	1.525(5)
Ru-C(20)	2.136(4)	C(6)-C(17)	1.523(5)
Ru-C(5)	2.250(3)	C(7)-C(8)	1.519(6)
Ru-C(3)	2.253(4)	C(9)-C(10)	1.528(5)
Ru-C(2)	2.254(3)	C(11)-C(12)	1.518(6)
Ru-C(6)	2.259(4)	C(13)-C(14)	1.525(6)
Ru-C(4)	2.260(4)	C(15)-C(16)	1.524(6)
Ru-C(1)	2.265(3)	C(17)-C(18)	1.514(7)
Ru-Cph ^a	1.750(1)	C(10)-C(20)	1.379(7)
C(1)-C(2)	1.419(5)	C(10)-C(80)	1.490(8)
C(1)-C(6)	1.431(5)	C(20)-C(30)	1.505(7)
C(1)-C(7)	1.520(5)	C(30)-C(40)	1.501(9)
C(2)-C(3)	1.425(5)	C(40)-C(50)	1.494(8)
C(2)-C(9)	1.518(5)	C(50)-C(60)	1.401(7)
C(3)-C(4)	1.431(5)	C(60)-C(70)	1.518(9)
C(3)-C(1)	1.530(5)	C(70)-C(80)	1.509(10)
C(4)-C(5)	1.419(5)	Cph-Ru-Cco ^b	79.9(2)
C(2)-C(1)-C(6)	120.5(3)	C(5)-C(6)-C(17)	120.7(3)
C(2)-C(1)-C(7)	121.1(3)	C(1)-C(6)-C(17)	120.1(3)
C(6)-C(1)-C(7)	118.4(3)	C(8)-C(7)-C(1)	114.3(4)
C(1)-C(2)-C(3)	120.3(3)	C(2)-C(9)-C(10)	113.7(3)
C(1)-C(2)-C(9)	120.6(3)	C(12)-C(11)-C(3)	115.2(3)
C(3)-C(2)-C(9)	119.0(3)	C(4)-C(13)-C(14)	114.3(4)
C(2)-C(3)-C(4)	119.3(3)	C(16)-C(15)-C(5)	113.4(4)
C(2)-C(3)-C(11)	120.2(3)	C(18)-C(17)-C(6)	115.5(4)
C(4)-C(3)-C(11)	120.3(3)	C(20)-C(10)-C(80)	123.0(5)
C(5)-C(4)-C(3)	120.2(3)	C(10)-C(20)-C(30)	123.7(5)
C(5)-C(4)-C(13)	121.1(3)	C(40)-C(30)-C(20)	112.9(4)
C(3)-C(4)-C(13)	118.7(3)	C(50)-C(40)-C(30)	114.9(4)
C(4)-C(5)-C(6)	120.6(3)	C(60)-C(50)-C(40)	123.0(5)
C(4)-C(5)-C(15)	120.8(3)	C(50)-C(60)-C(70)	122.6(5)
C(6)-C(5)-C(15)	118.6(3)	C(80)-C(70)-C(60)	114.2(5)
C(5)-C(6)-C(1)	119.1(3)	C(10)-C(80)-C(70)	113.9(5)

^aCph is the centroid of the phenyl ring^bCco is the centroid of the cyclooctadiene

When the data from both the work done here and Pertici's work are considered together there appears to be a trend in both the time taken to form and in the yields of these products, the new Ru(η^6 -arene)(η^4 -COD) complexes. Bulky alkynes like *t*-butylacetylene and isopropylacetylene take longer to react (15 h as against 1 h for 1-hexyne) and give lower yields (*ca.* 30% as against 95% for acetylenes like 3-hexyne). In general a mixture of the two possible isomers is obtained. For terminal aliphatic alkynes

the 1,3,5-isomer is preferentially formed, being the more thermodynamically favourable for steric reasons. This steric effect is most noticeable in the case of the very bulky *t*-butylacetylene, where the presence of the sterically unfavoured unsymmetrical isomer is only just detectable by ^1H NMR spectroscopy.

In the case of phenylacetylene and trimethylsilylacetylene the trend is reversed and the more sterically hindered isomer is preferentially formed. From these two cases it can be seen that substituent electronic effects also play a role, presumably in the intermediate steps of the reaction.

In an attempt to gain some insight into the mechanism of the cyclotrimerization, Pertici *et al.* mixed $\text{Ru}(\eta^6\text{-naphth})(\eta^4\text{-COD})$ with 2-butyne at -80°C in $\text{d}^8\text{-THF}$ and the reaction mixture was slowly warmed to -5°C in the NMR spectrometer, whereupon a reaction was observed to start. It was found that a dinuclear intermediate of the form $\text{Ru}_2(\eta^4\text{-COD})_2(\mu\text{-naphth})$ as well as free naphthalene, the expected product, $\text{Ru}(\eta^6\text{-C}_6\text{Me}_6)(\eta^4\text{-COD})$, and starting material, were present. The dinuclear compound has been observed before in the reaction of $\text{Ru}(\eta^6\text{-naphth})(\eta^4\text{-COD})$ with mononuclear arenes in the presence of acetonitrile.³⁰ It is believed that in this case the acetonitrile displaces the naphthalene from the monomeric COD complex to create a very reactive solvento species which then reacts with the arene to give $\text{Ru}(\eta^6\text{-arene})(\eta^4\text{-COD})$ or with unreacted $\text{Ru}(\eta^6\text{-naphth})(\eta^4\text{-COD})$ to give $\text{Ru}_2(\eta^4\text{-COD})_2(\mu\text{-naphth})$.

In the reaction with 2-butyne the acetylene may behave similarly to acetonitrile, firstly displacing the naphthalene and forming some sort of reactive $\text{Ru}(\eta^4\text{-COD})$ fragment, the presence of which is inferred from its reversible reaction with $\text{Ru}(\eta^6\text{-naphth})(\eta^4\text{-COD})$ to give the dimeric $\text{Ru}_2(\eta^4\text{-COD})_2(\mu\text{-naphth})$ species. It is this reactive $\text{Ru}(\eta^4\text{-COD})$ fragment that is thought to be the species upon which the acetylene cyclotrimerizes. A possible reaction sequence for the reaction of $\text{Ru}(\eta^6\text{-arene})(\eta^4\text{-COD})$ with 2-butyne as a representative alkyne is given in Figure 2.3.

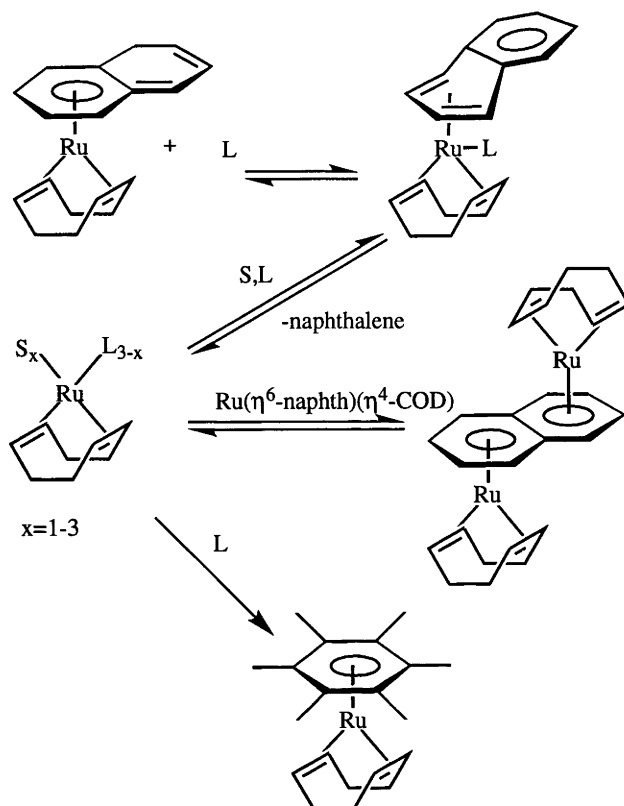


Figure 2.3. Proposed mechanism for the formation of $\text{Ru}(\eta^6\text{-C}_6\text{Me}_6)(\eta^4\text{-COD})$, where s = solvent and L = 2-butyne

Evidence for a η^4 -naphthalene precursor to the reactive solvento species comes from recent work^{110,111} in which complexes of the type $\text{Ru}(\eta^4\text{-naphth})(\eta^4\text{-COD})\text{PR}_3$ ($R=\text{OMe, Me, Et}$) have been obtained by the reaction of $\text{Ru}(\eta^6\text{-naphth})(\eta^4\text{-COD})$ with the described ligands and structurally characterized. Complexes of the type $[\text{Ru}_2(\eta^6, \eta^4\text{-naphth})(\eta^4\text{-COD})_2\text{PR}_3]$, which could be considered derivatives of the bridging naphthalene complex observed as an intermediate, have also been prepared and characterized crystallographically.^{110,111} In these complexes one ruthenium is η^6 -bound to the bridging naphthalene while the other is η^4 -bound. The η^4 -bound ruthenium is also coordinated to the PR_3 group. Both ruthenium atoms are η^4 -coordinated to COD.

In only one case, the reaction of $\text{Ru}(\eta^6\text{-naphth})(\eta^4\text{-COD})$ with trimethylsilylacetylene, can intermediates be observed by ^1H NMR spectroscopy neither of which appear to be the bridging naphthalene complex. After ten minutes in C_6D_6 at room temperature all of the starting material has gone and, as well peaks due to the final product, two AB quartets are observed in the ^1H NMR spectrum in the region between δ 5.5 ppm and 6.6 ppm ($J_{\text{AB}} = ca. 20 \text{ Hz}$, $J_{\text{AB}} = ca. 4 \text{ Hz}$). These do not correspond either with the starting

complex, the final product or the proposed bridging naphthalene complex. These two AB quartets disappear after 1hr, seemingly converted into the final product. These AB quartets could be due to ruthenacyclopentadienes as displayed in Figure 2.4.

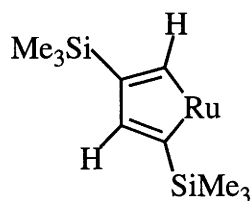


Figure 2.4. Proposed ruthenacyclopentadiene

Similar complexes have been isolated and characterized crystallographically for the reaction of alkynes with transition metals previously. For example, when $\text{Co}(\eta^5\text{-C}_5\text{H}_4\text{R})(\text{PPh}_3)_2$ ($\text{R}=\text{COOMe}$, H) is reacted with acetylene the complex $(\eta^5\text{-C}_5\text{H}_5)(\text{CoCH}=\text{CH}-\text{CH}=\text{CH})(\text{PPh}_3)$ is obtained which contains a metallacyclopentadiene. The structure of this complex was determined by X-ray crystallography.¹¹²

Preparation and characterization of dimeric ruthenium(II) complexes of the type $[\text{Ru}(\eta^6\text{-arene})\text{Cl}_2]_2$ [arene= $\text{C}_6\text{H}_3\text{Pr}^i$, C_6Et_6 and benzotris(cyclooctene)]

The $\text{Ru}(\eta^6\text{-arene})(\eta^4\text{-COD})$ complexes (arene = benzotris(cyclooctene), triisopropylbenzene and hexaethylbenzene) reacted with HCl to give dichloride dimers of the type $[\text{Ru}(\eta^6\text{-arene})\text{Cl}_2]_2$ in 28 to 87 % yield based on $\text{Ru}(\eta^6\text{-naphthalene})(\eta^4\text{-COD})$. It was not necessary to isolate the ruthenium(0) complexes for this purpose. The hexane solution of the cyclooctadiene complex obtained from chromatography of the reaction mixture was treated immediately with concentrated aqueous HCl. The triisopropylbenzene dichloride dimer was not fully characterized, but was used after recrystallization from $\text{CH}_2\text{Cl}_2/\text{Et}_2\text{O}$ directly for the preparation of $\text{Ru}(\eta^6\text{-C}_6\text{H}_3\text{Pr}^i_3)(\text{CO})\text{Cl}_2$ (see Chapter 3).

The complexes $[\text{Ru}\{\eta^6\text{-benzotris(cyclooctene)}\}\text{Cl}_2]_2$ and $[\text{Ru}(\eta^6\text{-C}_6\text{Et}_6)\text{Cl}_2]_2$ could be recrystallised from dichloromethane/ether or dichloromethane/pentane by vapour diffusion to give air-stable, red crystalline solids. Because of the high level of alkyl substitution of the aromatic ring, these complexes are much more soluble in less polar solvents than other arene dichloride dimers such as $[\text{Ru}(\eta^6\text{-benzene})\text{Cl}_2]_2$, which is almost completely insoluble in solvents such as dichloromethane, alcohols and acetone. The complex $[\text{Ru}(\eta^6\text{-C}_6\text{Et}_6)\text{Cl}_2]_2$ also proved to be substantially more soluble than $[\text{Ru}(\eta^6\text{-C}_6\text{Me}_6)\text{Cl}_2]_2$, which was an advantage in further reactions and attempts at crystallization. If dichloromethane solutions of either $[\text{Ru}(\eta^6\text{-C}_6\text{Et}_6)\text{Cl}_2]_2$ or $[\text{Ru}\{\eta^6\text{-benzotris(cyclooctene)}\}\text{Cl}_2]_2$ were allowed to stand for several weeks partial decomposition occurred.

Both $[\text{Ru}(\eta^6\text{-C}_6\text{Et}_6)\text{Cl}_2]_2$ and $[\text{Ru}\{\eta^6\text{-benzotris(cyclooctene)}\}\text{Cl}_2]_2$ were characterized completely by ^1H and ^{13}C NMR spectroscopy, as well as mass spectrometry and microanalysis. Characterizing data for $[\text{Ru}(\eta^6\text{-C}_6\text{Et}_6)\text{Cl}_2]_2$ and $[\text{Ru}\{\eta^6\text{-benzotris(cyclooctene)}\}\text{Cl}_2]_2$ are listed in Table 2.4. For the hexaethylbenzene complex [obtained in 87% yield from $\text{Ru}(\eta^6\text{-naphthalene})(\eta^4\text{-COD})$], the ^1H NMR spectrum in CD_2Cl_2 at room temperature consists of just a triplet at δ 1.3 ppm, and a quartet at δ 2.4 ppm, assignable to the methyl and methylene protons of the ethyl groups respectively. The $^{13}\text{C}\{^1\text{H}\}$ NMR spectrum has three resonances; δ 14.7, 21.1 and 94 ppm corresponding to the methyl, methylene and coordinated aromatic carbons respectively. As a result of coordination the aromatic carbon atoms of the hexaethylbenzene are shifted

by *ca.* 40 ppm upfield from those of the free arene. All of the arene ruthenium complexes studied showed this behaviour, this being typical of arene metal complexes in general (see Chapter 1). The EI mass spectrum of the hexaethylbenzene complex did not contain an M^+ peak but rather the peak corresponding to the complex having lost one chloride ($m/z = 800$). This is interesting in light of the behaviour of the dichloride dimer in solution, discussed below.

The ^1H NMR spectrum of $[\text{Ru}\{\eta^6\text{-benzotris(cyclooctene)}\}\text{Cl}_2]_2$, [obtained in 28% yield based on $\text{Ru}(\eta^6\text{-naphth})(\eta^4\text{-COD})$, without isolation of the intermediate $\text{Ru}[\eta^6\text{-benzotris(cyclooctene)}](\eta^4\text{-COD})$ complex], was difficult to interpret, since even at 500MHz it consisted of a series of poorly resolved, overlapping multiplets between δ 1 and 3 ppm. The ^{13}C NMR spectrum, however, was much simpler, consisting of only four resonances at δ 93.7, 30.6, 28.5 and 27.3 ppm which are assignable to the coordinated aromatic and three different methylene carbons respectively. Again the mass spectrum (FAB) lacked an M^+ peak; instead, the peak with the highest m/z ratio was observed at 957 amu, also consistent with loss of a chloride ion.

Crystals of $[\text{Ru}(\eta^6\text{-C}_6\text{Et}_6)\text{Cl}_2]_2$ and $[\text{Ru}\{\eta^6\text{-benzotris(cyclooctene)}\}\text{Cl}_2]_2$ suitable for single crystal X-ray crystallography were grown from solutions in dichloromethane/hexane into which ether vapour was allowed to diffuse. The X-ray structures of both these complexes were determined. ORTEP diagrams and tables of pertinent bond lengths and angles are given in Figures 2.5 and 2.6 and Tables 2.5 and 2.6.

Table 2.4. Characterizing Data for $[\text{Ru}(\eta^6\text{-arene})\text{Cl}_2]_2$ complexes

Complex	NMR Data	Other data
$[\text{Ru}(\eta^6\text{-C}_6\text{Et}_6)\text{Cl}_2]_2$	^1H NMR (CD_2Cl_2 , 300 MHz): δ 2.40 (q, 12H, $^3J(\text{HH})$ 8Hz, CH_2), 1.30 ppm (t, 18H, $^3J(\text{HH})$ 8Hz, CH_3) $^{13}\text{C}\{^1\text{H}\}$ NMR (CD_2Cl_2 , 75.42 MHz): δ 94-95 (s, Caromatic), 21.1 (s, CH_2), 14.7 ppm (s, CH_3).	Anal. calcd for $\text{C}_{36}\text{H}_{60}\text{Cl}_4\text{Ru}_2$: C 51.67; H 7.23. Found: C 50.01; H 7.1. $m/z=800$ (M^+-Cl)
$[\text{Ru}(\eta^6\text{-C}_{24}\text{H}_{36})\text{Cl}_2]_2$	^1H NMR (CD_2Cl_2 , 500 MHz) δ 2.6 - 2.9 (m, $\text{C}_{24}\text{H}_{36}$), 1.9 - 2.0 [m, $\text{C}_{24}\text{H}_{36}$] 1.5 - 1.3 ppm [m $\text{C}_{24}\text{H}_{36}$] $^{13}\text{C}\{^1\text{H}\}$ NMR (CD_2Cl_2 , 75.42 MHz) δ 93.7 (s, Caromatic), 30.6 [s, $\text{CH}_2(\text{C}_{24}\text{H}_{36})$], 28.5 [s, $\text{CH}_2(\text{C}_{24}\text{H}_{36})$], 27.3 ppm [s, $\text{CH}_2(\text{C}_{24}\text{H}_{36})$]	Anal. calcd. for $\text{C}_{48}\text{H}_{72}\text{Cl}_4\text{Ru}_2$: C 58.06; H 57.67. Found C 57.67; H 7.64. $m/z = 957$ (M^+-Cl)

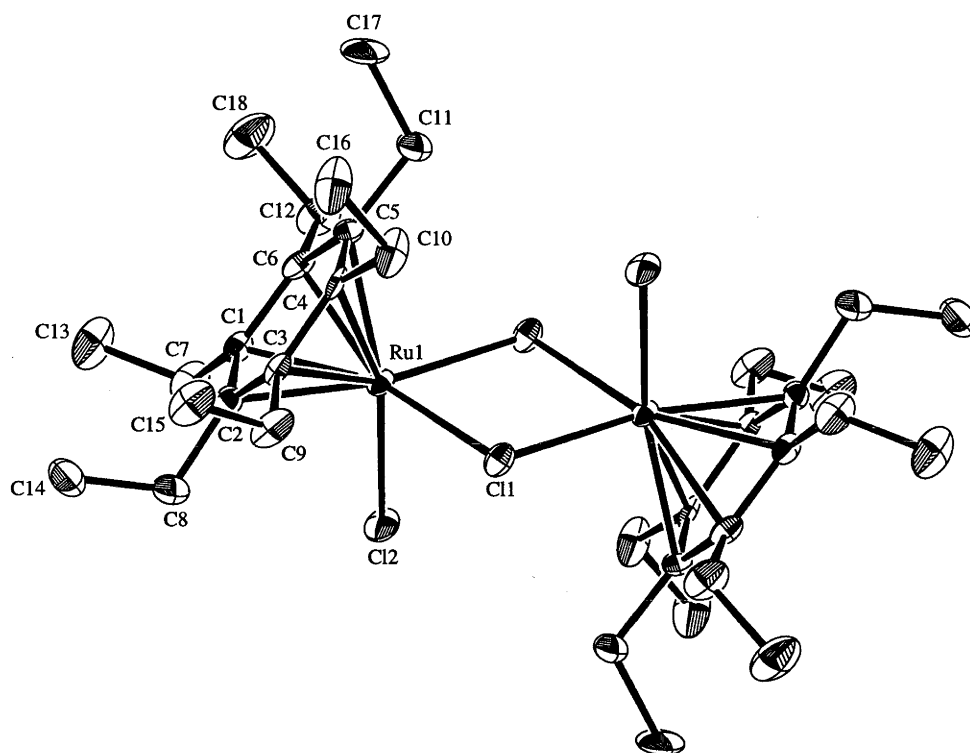


Figure 2.5. ORTEP diagram of solid state structure of $[\text{Ru}(\eta^6\text{-C}_6\text{Et}_6)\text{Cl}_2]_2$

Table 2.5. Selected distances (Å) and angles (°) for $[\text{Ru}(\eta^6\text{-C}_6\text{Et}_6)\text{Cl}_2]_2$

Ru(1)-Cl(1)	2.454(2)	Ru(1)-Cl(1)	2.460(2)
Ru(1)-Cl(2)	2.402(2)	Ru(1)-C(1)	2.163(7)
Ru(1)-C(2)	2.158(7)	Ru(1)-C(3)	2.170(7)
Ru(1)-C(4)	2.193(7)	Ru(1)-C(5)	2.190(7)
Ru(1)-C(6)	2.159(7)	C(1)-C(2)	1.43(1)
C(1)-C(6)	1.42(1)	C(2)-C(7)	1.524(10)
C(2)-C(3)	1.405(10)	C(3)-C(8)	1.50(1)
C(3)-C(4)	1.44(1)	C(4)-C(9)	1.51(1)
C(4)-C(5)	1.40(1)	C(5)-C(10)	1.529(9)
C(5)-C(6)	1.466(10)	C(6)-C(11)	1.51(1)
C(6)-C(12)	1.52(1)	C(7)-C(13)	1.48(1)
C(8)-C(14)	1.50(1)	C(9)-C(15)	1.50(1)
C(10)-C(16)	1.52(1)	C(11)-C(17)	1.52(1)
C(12)-C(18)	1.51(1)	Ru-centroid	1.638(3)
Cl(1) Ru(1) Cl(2)	86.97(7)	C(6) C(1) C(2)	120.9(7)
Cl(1) Ru(1) Cl(1)	80.23(7)	C(6) C(12) C(18)	115.6(9)
Ru(1) Cl(1) Ru(1)	99.77(7)	C(1) C(2) C(3)	119.6(7)
C(1) C(7) C(13)	115.1(7)	C(2) C(3) C(4)	120.2(7)
C(2) C(8) C(14)	115.5(8)	C(3) C(4) C(5)	121.0(6)
C(3) C(9) C(15)	115.7(7)	C(4) C(5) C(6)	118.7(7)
C(4) C(10) C(16)	112.1(7)	C(5) C(6) C(1)	119.4(7)
C(5) C(11) C(17)	113.2(8)		

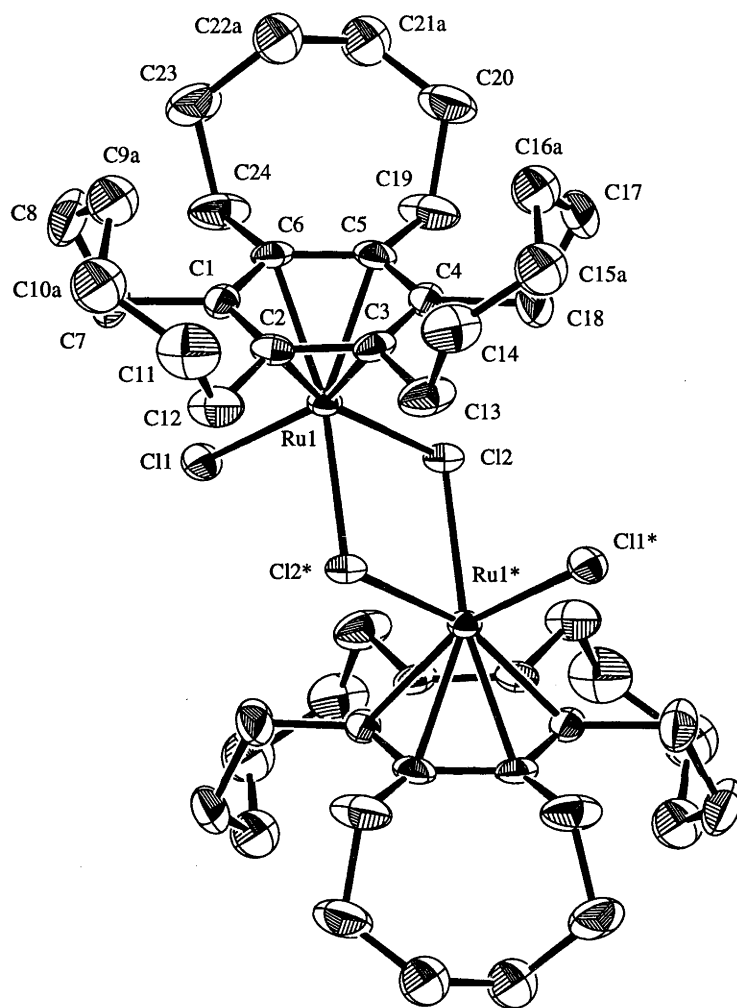


Figure 2.6. ORTEP diagram of $[\text{Ru}\{\eta^6\text{-benzotris(cyclooctene)}\}\text{Cl}_2]_2$

Table 2.6. Selected bond lengths (Å) and angles(°) for
 $[\text{Ru}\{\eta^6\text{-benzotris(cyclooctene)}\}\text{Cl}_2]_2^\ddagger$

Ru(1)-Cl(1)	2.405(2)	Ru(1)-Cl(2)	2.470(2)
Ru(1)-Cl(2)	2.463(2)	Ru(1)-C(1)	2.179(5)
Ru(1)-C(2)	2.162(5)	Ru(1)-C(3)	2.198(5)
Ru(1)-C(4)	2.204(7)	Ru(1)-C(5)	2.161(6)
Ru(1)-C(6)	2.174(5)	Cl(3)-C(25)	1.73(1)
Cl(4)-C(25)	1.70(1)	Cl(5)-C(26)	1.71(1)
Cl(6)-C(26)	1.71(1)	C(1)-C(2)	1.408(8)
C(1)-C(6)	1.429(9)	C(1)-C(7)	1.53(1)
C(2)-C(3)	1.42(1)	C(2)-C(12)	1.524(9)
C(3)-C(4)	1.407(9)	C(3)-C(13)	1.529(9)
C(4)-C(5)	1.457(8)	C(4)-C(18)	1.51(1)
C(5)-C(6)	1.43(1)	C(5)-C(19)	1.501(9)
C(6)-C(24)	1.51(1)	C(7)-C(8)	1.525(9)
C(8)-C(9a)	1.52(1)	C(8)-C(9b)	1.54(1)
C(9a)-C(10a)	1.53(2)	C(9b)-C(10b)	1.52(2)
C(10a)-C(11)	1.55(2)	C(10b)-C(11)	1.52(1)
C(11)-C(12)	1.518(9)	C(13)-C(14)	1.521(9)
C(14)-C(15a)	1.51(1)	C(14)-C(15b)	1.55(2)
C(15a)-C(16a)	1.51(1)	C(15b)-C(16b)	1.53(3)
C(16a)-C(17)	1.57(1)	C(16b)-C(17)	1.52(2)
C(17)-C(18)	1.56(1)	C(19)-C(20)	1.52(1)
C(20)-C(21a)	1.50(1)	C(20)-C(21b)	1.55(2)
C(21a)-C(22a)	1.53(1)	C(21b)-C(22b)	1.53(3)
C(22a)-C(23)	1.54(2)	C(22b)-C(23)	1.53(2)
C(23)-C(24)	1.52(1)	Ru-centroid	3.756
Ru(1) Cl(2) Ru(1*)	98.95(7)	C(3) C(4) C(5)	119.8(5)
Cl(1) Ru(1) Cl(2)	87.33(6)	C(4) C(5) C(6)	118.9(5)
Cl(2) Ru(1) Cl(2*)	81.05(7)	C(5) C(6) C(1)	119.9(5)
C(1) C(2) C(3)	120.2(5)	C(6) C(1) C(2)	120.4(6)
C(2) C(3) C(4)	120.5(5)		

‡ atoms designated a or b have been restrained during refinement such that all C-C bonds are 1.54(1) Å and all bond angles C-C-C are 114(1)° for any bonds or angles containing an atom so designated

* indicate atoms generated by crystallographic symmetry operators

From Figures 2.5 and 2.6 it can be seen that in the solid state both $[\text{Ru}(\eta^6\text{-C}_6\text{Et}_6)\text{Cl}_2]_2$ and $[\text{Ru}\{\eta^6\text{-benzotris(cyclooctene)}\}\text{Cl}_2]_2$ have the same edge sharing bioctahedral structure as that previously determined for $[\text{Os}(\eta^6\text{-p-cymene})\text{Cl}_2]_2^{68}$, $[\text{Ru}(\eta^6\text{-trindane})\text{Cl}_2]_2^{69}$ (where trindane = benzo(1,2:3,4:5,6)-1,2,3-trihydrocyclopentene), $[\text{Ru}(\eta^6\text{-C}_6\text{Me}_6)\text{Cl}_2]_2^{67}$, and $[\text{Ru}(\eta^6\text{-C}_6\text{H}_5\text{CO}_2\text{Et})\text{Cl}_2]_2^{70}$. The aromatic carbon atoms of each arene ligand are in the same plane within experimental error and these planes at each end of the molecule are parallel. The two ruthenium atoms and two bridging chlorine atoms are coplanar and each of the terminal chlorine atoms are almost orthogonal to this plane, with one above and one below it. An important feature

of the hexaethylbenzene complex is that all the ethyl groups are distal with respect to the ruthenium. The alkyl rings of the benzotris(cyclooctene) are also orientated such that they are distal with respect to the ruthenium. A comparison of metal-ligand bond lengths and angles for complexes of this type (Table 2.7) shows that they differ very little among the various complexes.

Table 2.7. Selected bond lengths (Å) and angles (°) for various arene ruthenium and osmium dichloride dimers^{a-d}

Quantity	benzotris (cyclooctene)	trindane	C ₆ Et ₆	C ₆ Me ₆	<i>p</i> -cymene	C ₆ H ₅ CO ₂ Et
M-M	3.756	3.715	3.7583(8)	3.743(1)	3.742(1)	3.718(1)
M-Arene	1.6475(1)	1.640	1.638(3)	1.654	1.637(2)	1.648(3)
M-Cl ^t	2.405(2)	2.389(2)	2.402(2)	2.394(1)	2.389(2)	2.3871(9)
M-Cl ^b	2.470(2)	2.451(2)	2.460(2)	2.460(1)	2.450(2)	2.4440(8)
Cl ^b -M- Cl ^b	81.05(7)	81.44(7)	80.23(7)	80.90(2)	80.44(4)	80.82(3)
Cl ^t -M-Cl ^b	87.33(6)		86.97(7)	87.53(2)	85.66(6)	87.26(3)
M-Cl ^b -M	98.95(7)	98.56(7)	99.77(7)	99.09(2)	99.53(4)	99.18(3)

^a M=Os for arene=*p*-cymene, otherwise M=Ru

^b Cl^t=terminal chloride

^c Cl^b=bridging chloride

^d M-Arene = distance either to the arene ring centroid or the arene plane

To gain a qualitative idea about the relative labilities of η^6 -hexaethylbenzene and η^6 -hexamethylbenzene, [Ru(η^6 -C₆Et₆)Cl₂]₂ was fused with hexamethylbenzene at the melting point of hexamethylbenzene in an open test-tube for *ca.* 2h. A FAB⁺ mass spectrum of the resulting ether insoluble solids contained peaks for [Ru₂(C₆Me₆)₂Cl₃]⁺ and [Ru₂(C₆Me₆)(C₆Et₆)Cl₃]⁺. When [Ru(η^6 -C₆Me₆)Cl₂]₂ was fused with hexaethylbenzene there was no evidence of arene exchange; only a peak for [Ru₂(η^6 -C₆Me₆)₂Cl₃]⁺ is observed in the FAB mass spectrum. These observations suggest that η^6 -hexaethylbenzene is more labile than η^6 -hexamethylbenzene, at least when coordinated to ruthenium(II). In agreement, whereas [Ru(η^6 -C₆Me₆)Cl₂]₂ reacts with pyridine to cleave the chlorine bridges giving Ru(η^6 -C₆Me₆)(C₅H₅N)Cl₂, under similar conditions, pyridine displaces hexaethylbenzene from [Ru(η^6 -C₆Et₆)Cl₂]₂, to give trans-Ru(pyridine)₄Cl₂.

Preparation and characterization of triply-bridged dimeric Ru(II) complexes of the type $[\text{Ru}_2(\eta^6\text{-arene})_2\text{Cl}_3]^+\text{PF}_6^-$ (where arene= C_6Et_6 , $\text{C}_6\text{H}_4\text{-1,2-Et}_2$ and $\text{C}_6\text{H}_4\text{-1,2-Pr}^i_2$)

Treatment of $[\text{Ru}(\eta^6\text{-C}_6\text{Et}_6)\text{Cl}_2]_2$ with a saturated solution of NH_4PF_6 in methanol removed one chloride ion and gave the tri- μ -chloro salt, $[\text{Ru}_2(\eta^6\text{-C}_6\text{Et}_6)_2\text{Cl}_3]^+\text{PF}_6^-$. This complex precipitated out of the methanol solution as dark red, block like crystals suitable for single crystal X-ray crystallography (see below). The ^1H NMR spectrum in CD_3OD is much the same as that observed for the dichloride dimer, consisting of a quartet at δ 2.50 and triplet at 1.33 ppm in a 2:3 ratio, assignable to the methylene and methyl protons. The ^{31}P NMR spectrum showed the characteristic septet due to PF_6 .

Two other tri- μ -chloro salts, $[\text{Ru}_2(\eta^6\text{-C}_6\text{H}_4\text{-1,2-Et}_2)_2\text{Cl}_3]^+\text{PF}_6^-$ and $[\text{Ru}_2(\eta^6\text{-C}_6\text{H}_4\text{-1,2-Pr}^i_2)_2\text{Cl}_3]^+\text{PF}_6^-$, were prepared from the reactions of $[\text{Ru}(\eta^6\text{-C}_6\text{H}_4\text{-1,2-Et}_2)\text{Cl}_2]_2$ and $[\text{Ru}(\eta^6\text{-C}_6\text{H}_4\text{-1,2-Pr}^i_2)\text{Cl}_2]_2$ with NH_4PF_6 in methanol and characterized crystallographically.* These two complexes were originally prepared as simpler models for the variable temperature ^1H NMR behaviour of $[\text{Ru}_2(\eta^6\text{-C}_6\text{Et}_6)_2\text{Cl}_3]^+\text{PF}_6^-$. Unfortunately 'simpler' is not an appropriate word for describing the NMR spectra of these complexes. The ^1H and $^{13}\text{C}\{^1\text{H}\}$ NMR spectra of these complexes are given in Figures 2.8a, 2.8b, 2.9a and 2.9b. The characterizing data for these complexes is given in Table 2.8, along with that for $[\text{Ru}_2(\text{C}_6\text{Et}_6)_2\text{Cl}_3]^+\text{PF}_6^-$.

The ^1H NMR spectrum of $[\text{Ru}_2(\eta^6\text{-C}_6\text{H}_4\text{-1,2-Et}_2)_2\text{Cl}_3]^+\text{PF}_6^-$ has more than the expected multiplicity for the methylene protons of the two ethyl groups. Careful scrutiny of the molecular structure of this complex shows that the methylene protons have become magnetically inequivalent on coordination of the arene to ruthenium. Thus, instead of expected quartet, there is the complex multiplet of an ABX_3 system. A similar pattern has been observed in the ^1H NMR spectrum for the methylene protons of $\text{Cr}(\eta^6\text{-C}_6\text{H}_4\text{-1,2-Et}_2)(\text{CO})_3$, where the spin system was determined by matching with simulated spectra.¹¹³ The $^{13}\text{C}\{^1\text{H}\}$ NMR spectrum of $[\text{Ru}_2(\eta^6\text{-C}_6\text{H}_4\text{-1,2-Et}_2)_2\text{Cl}_3]^+\text{PF}_6^-$ contains the expected three resonances for the three different aromatic carbons at δ 98.0,

* The parent dichloride dimers were prepared by Dr Mark Bown. The complex $[\text{Ru}(\eta^6\text{-C}_6\text{H}_4\text{-1,2-Et}_2)\text{Cl}_2]_2$ was made via arene exchange with $\text{Ru}(\eta^6\text{-naphth})(\eta^4\text{-COD})$ followed by treatment with HCl while $[\text{Ru}(\eta^6\text{-C}_6\text{H}_4\text{-1,2-Pr}^i_2)\text{Cl}_2]_2$ was prepared via arene exchange with $[\text{Ru}(\eta^6\text{-p-cymene})\text{Cl}_2]_2$.

78.7 and 78.3 ppm and a resonance for the methylene and methyl carbons at δ 23.5 and 12.8 ppm respectively. This is the same behaviour as was observed for the corresponding dichloride dimer at low temperature in solution (see Chapter 4).

In the ^1H and $^{13}\text{C}\{^1\text{H}\}$ NMR spectra of $[\text{Ru}_2(\eta^6\text{-C}_6\text{H}_4\text{-1,2-Pr}^i_2)_2\text{Cl}_3]^+\text{PF}_6^-$, further complexity arises from the presence of more than one species in solution. Thus in the ^1H NMR spectrum between δ 5.8 and 5.3 ppm there are three different AA'BB' multiplets of different intensities for aromatic protons and between δ 1.4 and 1.0 ppm three different methyl resonances can be observed. The methyne protons give rise to a very complex multiplet at δ 3.15 ppm. In the $^{13}\text{C}\{^1\text{H}\}$ NMR spectrum two sets of aromatic carbons can be observed in about a 1:3 ratio, but only one set of resonances for the isopropyl groups is present. It is assumed that the different species present have coincident ^{13}C chemical shifts for the isopropyl groups.

If one just considers the most prevalent of the three species in solution it can be seen that the methyls of the isopropyl groups are magnetically inequivalent, with a pair of doublets in the ^1H NMR spectrum at δ 1.39 and 1.32 ppm and singlets at δ 24.8 and 21.3 ppm in the $^{13}\text{C}\{^1\text{H}\}$ NMR spectrum. These methyl groups could be considered equivalent to the methylene protons of $[\text{Ru}_2(\eta^6\text{-C}_6\text{H}_4\text{-1,2-Et}_2)_2\text{Cl}_3]^+\text{PF}_6^-$.

One possible explanation for the different species observed in these NMR spectra of $[\text{Ru}_2(\eta^6\text{-C}_6\text{H}_4\text{-1,2-Pr}^i_2)_2\text{Cl}_3]^+\text{PF}_6^-$ is that there is an equilibrium mixture of different rotational isomers of the complex. In the solid state structure of $[\text{Ru}_2(\eta^6\text{-C}_6\text{H}_4\text{-1,2-Pr}^i_2)_2\text{Cl}_3]^+\text{PF}_6^-$, the isopropyl groups of the arenes at either end of the molecule eclipse each other. It could be envisaged that in solution there is a rotational conformer in which the two arenes are orientated such that the isopropyl groups are staggered, that is, a 'trans' conformation is present as well as the solid state 'cis' conformation. This assumes a slowing of the rotation about the arene ruthenium bond axis on an NMR timescale at room temperature, which appears unlikely. A second possibility is the presence of different rotational isomers of the two isopropyl groups. The three signals could arise from the complexes in which the hydrogen atoms of the isopropyl groups point towards each other (Figure 2.7A), point away from each other (Figure 2.7B) or are orientated such that the hydrogen atom of one isopropyl group and the methyl groups of the adjacent isopropyl group are pointing towards each other (Figure 2.7C). Difficulties in the preparation of 1,2-di-isopropylbenzene and its coordination to ruthenium have prevented further studies of this interesting system.

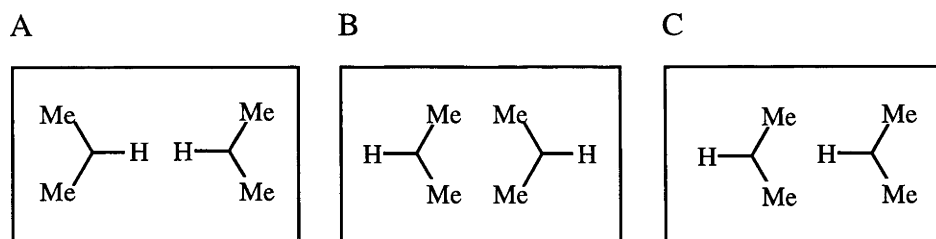
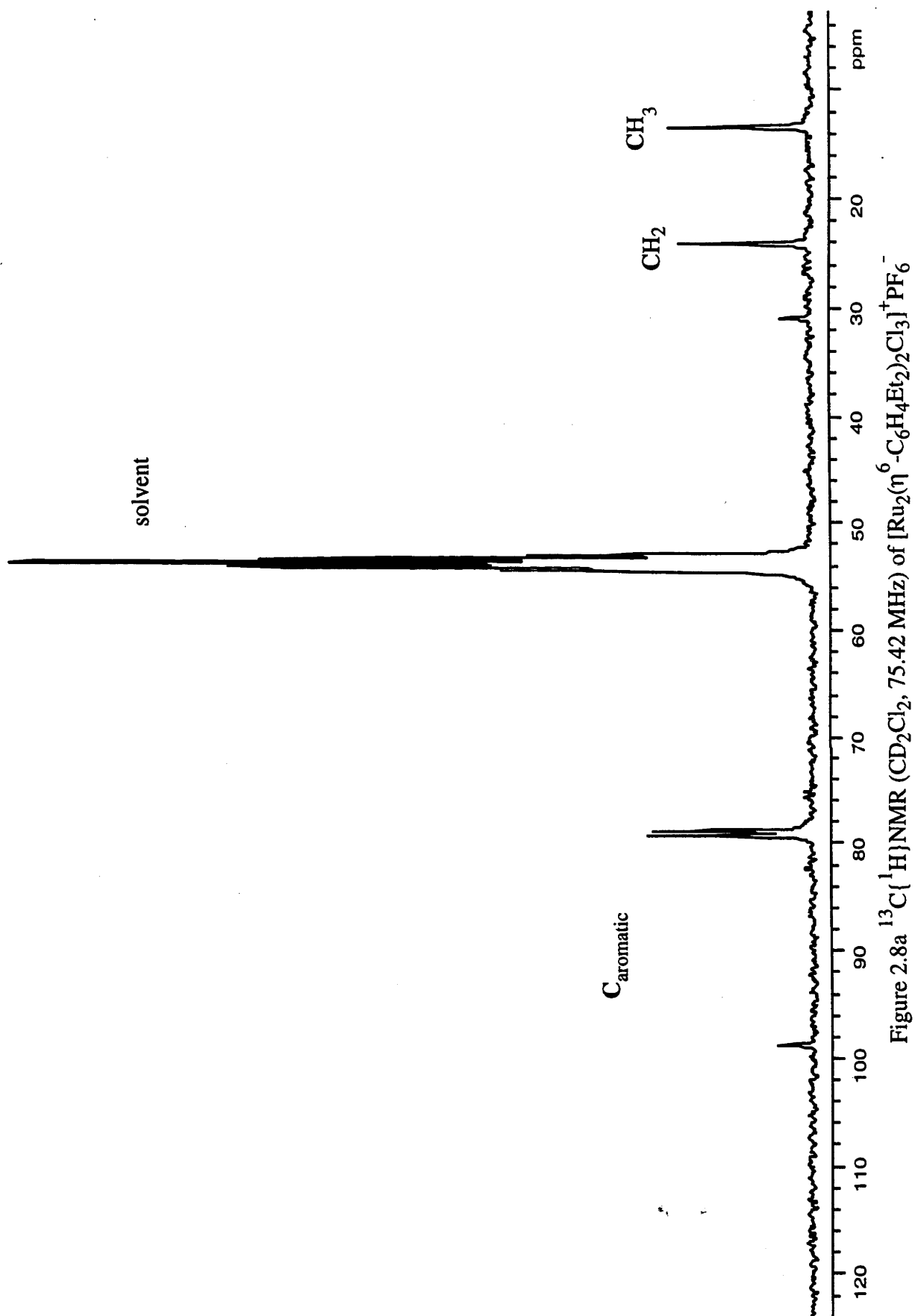
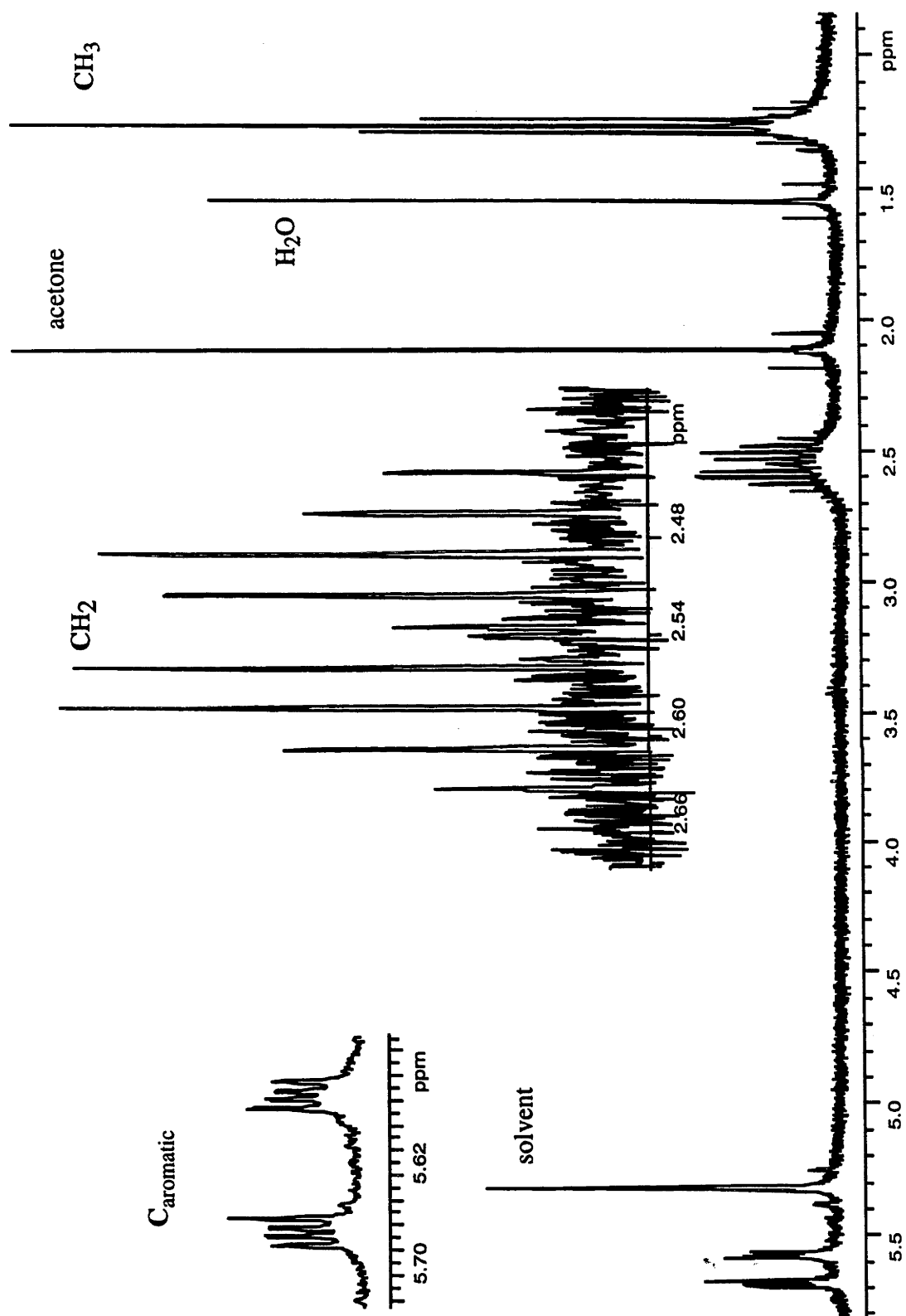


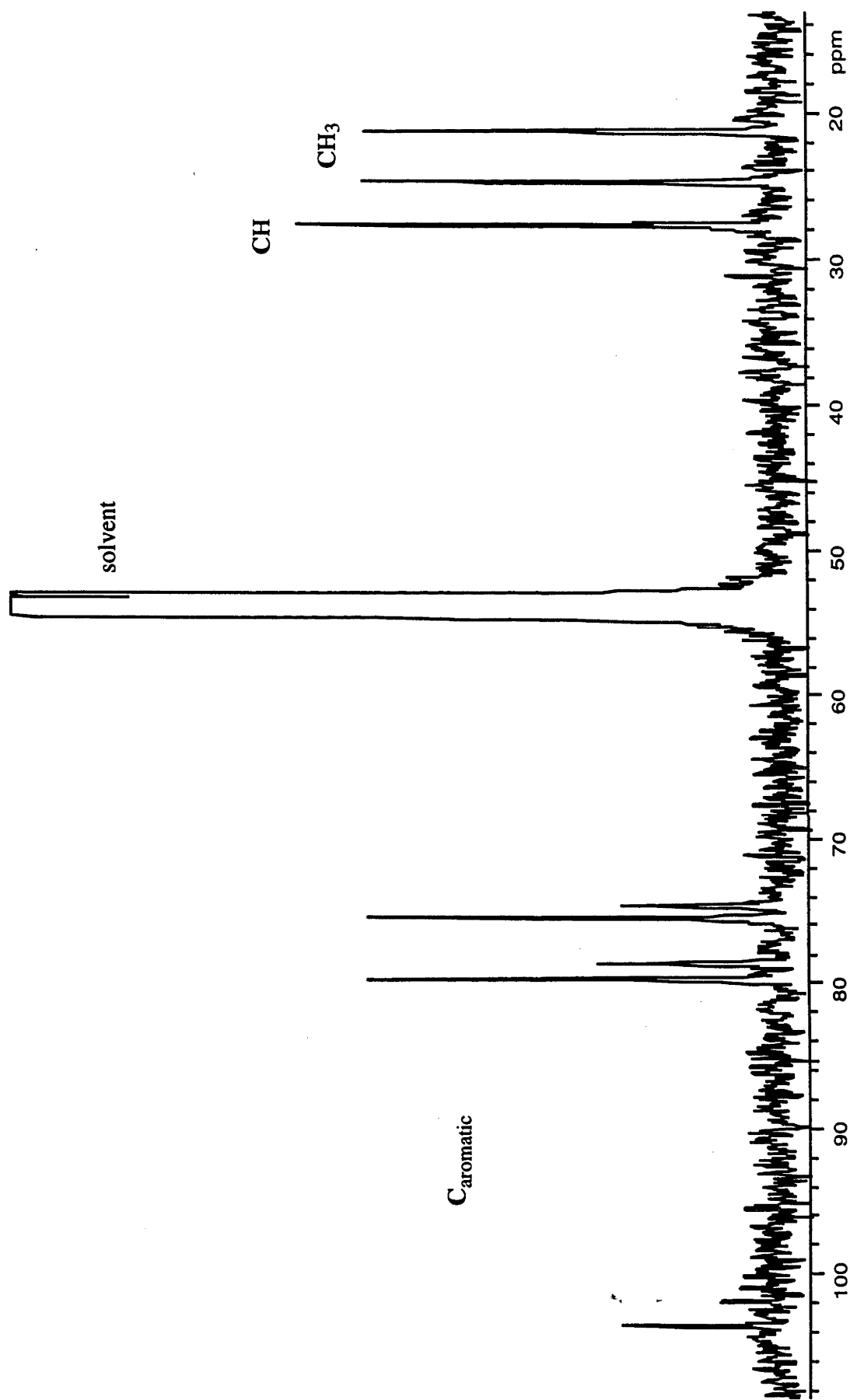
Figure 2.7. Three of the possible rotational isomers of the isopropyl groups of 1,2-di-isopropylbenzene

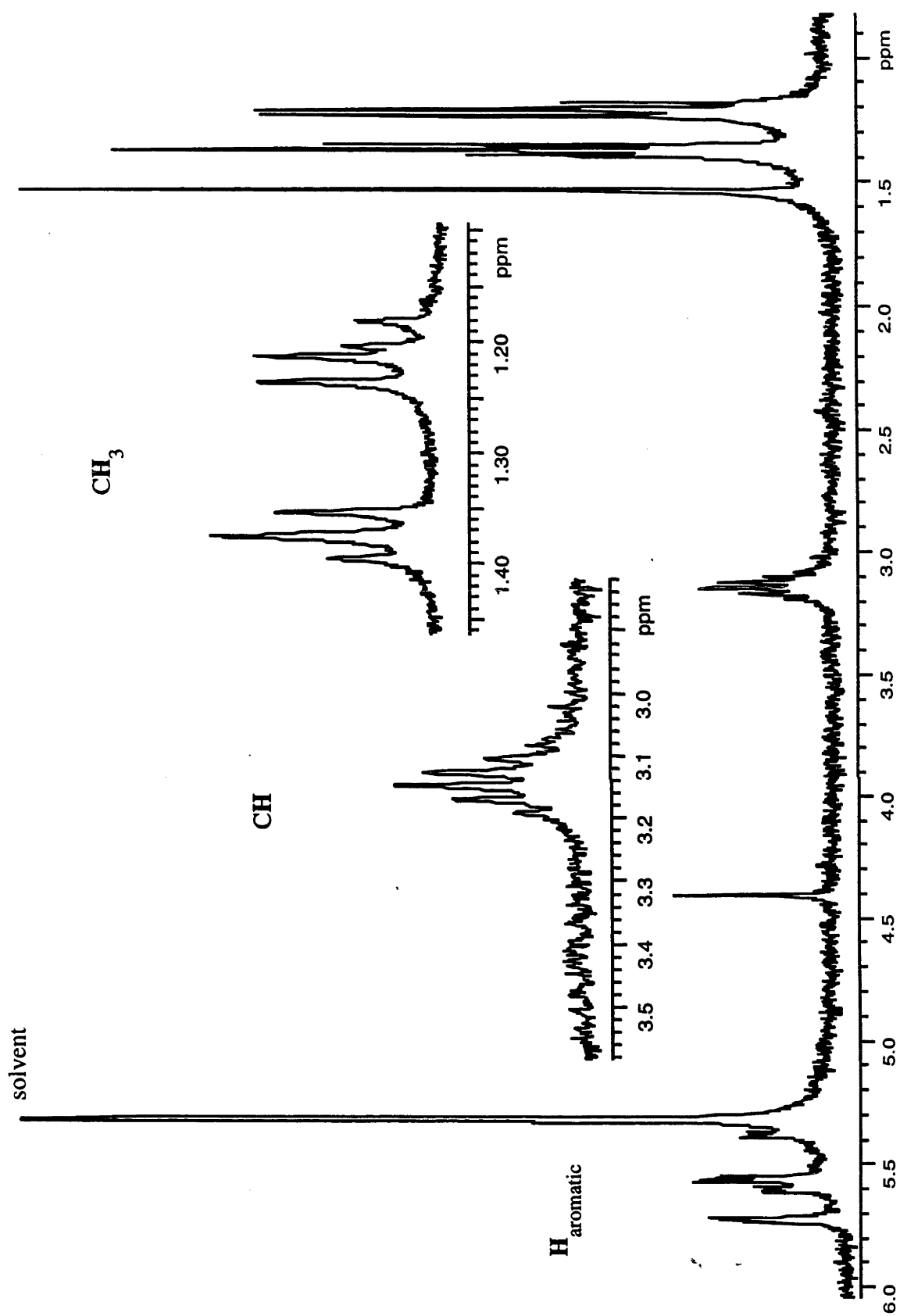
Table 2.8. Characterizing data for $[\text{Ru}_2(\eta^6\text{-arene})_2\text{Cl}_3]^+\text{PF}_6^-$ complexes

Complex	NMR Data	Other data
$[\text{Ru}_2(\eta^6\text{-C}_6\text{Et}_6\text{Cl}_3)^+\text{PF}_6^-]$	^1H NMR (CD_3OD , 200 MHz) δ 2.50 (q, 12H, $^3J(\text{HH})$ 7.6 Hz, CH_2), 1.33 ppm (t, 18H, $^3J(\text{HH})$ 7.6 Hz, CH_3). $^{13}\text{C}\{^1\text{H}\}$ NMR (CD_2Cl_2 , 75.42 MHz) δ 93–95 (br, Caromatic) 21.5 (s, CH_2), 15.0 ppm (s, CH_3) $^3\text{P}\{^1\text{H}\}$ NMR (CD_3OD , 81 MHz) δ -142.7 ppm (sept, $^1J(\text{PF})$ 708 Hz, PF_6).	Anal. calcd. for $\text{C}_{36}\text{H}_{60}\text{Cl}_3\text{F}_6\text{PRu}_2$: C 45.69; H 6.31. Found: C 44.31; H 6.50. m/z = 383 ($\text{RuCl}(\text{C}_6\text{Et}_6)^+$)
$[\text{Ru}_2(\eta^6\text{-C}_6\text{H}_4\text{-1,2-Pr}^i_2)_2\text{Cl}_3]^+\text{PF}_6^-$	For $\text{Ru}_2(\eta^6\text{-C}_6\text{H}_4\text{-1,2-Pr}^i_2)_2\text{Cl}_3]^+\text{PF}_6^-$ (most abundant species): ^1H NMR (CD_2Cl_2 , 300MHz) δ 5.64 (m(AA'BB')), 8H, Haromatic), 3.42 (m(ABX), 4H, CH), 1.39 (d, 12H, CH_3), 1.22 ppm (d, 12H, CH_3) $^{13}\text{C}\{^1\text{H}\}$ NMR (CD_2Cl_2 , 75.42MHz) δ 103.6 (s, Caromatic), 79.8 (s, Caromatic), 75.5 (s, Caromatic), 27.74 (s, CH), 24.8 (s, CH_3), 21.3 ppm (s, CH_3)	Comparison of the isotopic peak ratio found with that calculated gave an exact match m/z = 635 (M-PF_6) ⁺
$[\text{Ru}_2(\eta^6\text{-C}_6\text{H}_4\text{-1,2-Et}_2)_2\text{Cl}_3]^+\text{PF}_6^-$	For $[\text{Ru}_2(\eta^6\text{-C}_6\text{H}_4\text{-1,2-Et}_2)_2\text{Cl}_3]^+\text{PF}_6^-$: ^1H NMR (CD_2Cl_2 , 300MHz) δ 5.63 [m(AA'BB')], 8H, Haromatic], 2.54 [m(ABX), 8H, CH_2], 1.27 ppm (t, 12H, CH_3) $^{13}\text{C}\{^1\text{H}\}$ NMR (CD_2Cl_2 , 75.42MHz) δ 98.0 (s, Caromatic), 78.7 (s, Caromatic), 78.3 (s, Caromatic), 23.5 (s, CH_2), 12.8 ppm (s, CH_3).	Anal. calcd. for $\text{C}_{20}\text{H}_{28}\text{Cl}_3\text{F}_6\text{PRu}_2$: C 33.28; H 3.91. Found: C 32.56; H 3.41. m/z = 579 (M-PF_6) ⁺

Figure 2.8a $^{13}\text{C}\{^1\text{H}\}$ NMR (CD_2Cl_2 , 75.42 MHz) of $[\text{Ru}_2(\eta^6\text{-C}_6\text{H}_4\text{Et}_2)_2\text{Cl}_3]^+\text{PF}_6^-$

Figure 2.8b ^1H NMR (CD_2Cl_2 , 300MHz) of $[\text{Ru}_2(\eta^6\text{-C}_6\text{H}_4\text{-1,2-Et}_2)_2\text{Cl}_3]^+\text{PF}_6^-$

Figure 2.9a $^{13}\text{C}\{^1\text{H}\}$ NMR (CD_2Cl_2 , 70.43 MHz) of $[\text{Ru}_2(\eta^6\text{-C}_6\text{H}_4\text{-1,2-Pr}^i)_2\text{Cl}_3]^+\text{PF}_6^-$

Figure 2.9b ^1H NMR (CD_2Cl_2 , 300MHz) of $[\text{Ru}_2(\text{C}_6\text{H}_4\text{Pr}^i_2)_2\text{Cl}_3]^+\text{PF}_6^-$

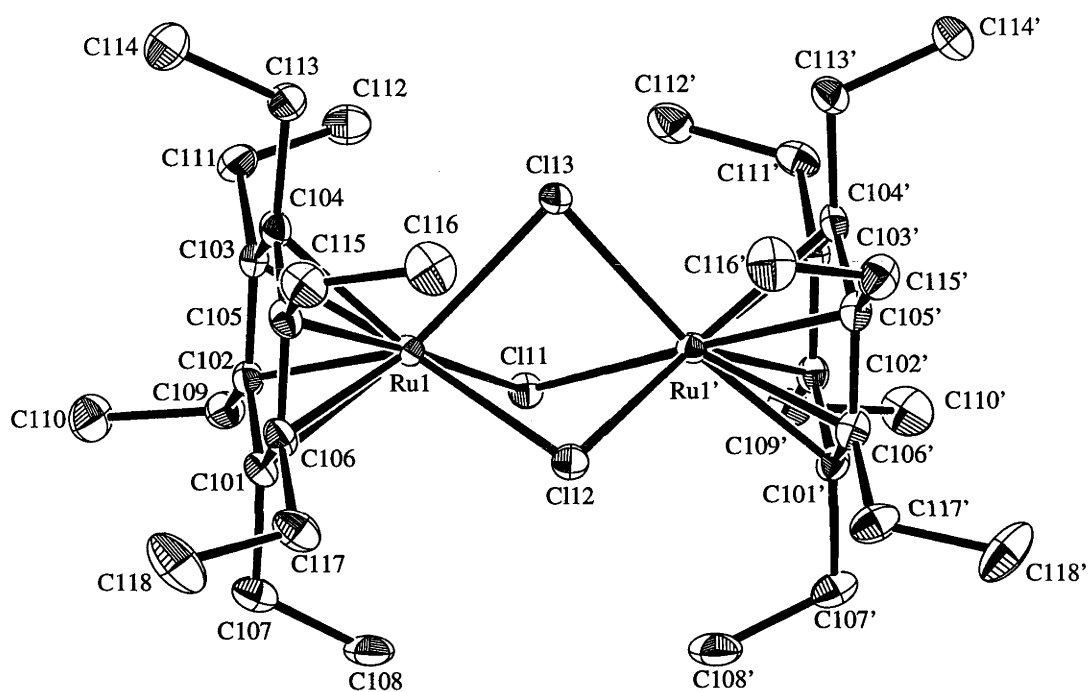


Figure 2.10. ORTEP diagram of $[\text{Ru}_2(\eta^6\text{-C}_6\text{Et}_6)_2\text{Cl}_3]^+\text{PF}_6^-$

Table 2.9. Selected bond distances(Å) and angles (°) for $[\text{Ru}_2(\eta^6\text{-C}_6\text{Et}_6)_2\text{Cl}_3]^+\text{PF}_6^-$

Ru(1)-Cl(11)	2.445(1)	C(103)-C(111)	1.536(6)
Ru(1)-Cl(12)	2.461(1)	C(104)-C(105)	1.420(6)
Ru(1)-Cl(13)	2.431(1)	C(104)-C(113)	1.513(6)
Ru(1)-C(101)	2.190(4)	C(105)-C(106)	1.426(6)
Ru(1)-C(102)	2.173(4)	C(105)-C(115)	1.538(7)
Ru(1)-C(103)	2.184(5)	C(106)-C(117)	1.523(7)
Ru(1)-C(104)	2.167(5)	C(107)-C(108)	1.525(7)
Ru(1)-C(105)	2.189(5)	C(109)-C(110)	1.532(7)
Ru(1)-C(106)	2.169(5)	C(111)-C(112)	1.523(7)
C(101)-C(102)	1.434(6)	C(113)-C(114)	1.541(7)
C(101)-C(106)	1.418(6)	C(115)-C(116)	1.525(7)
C(101)-C(107)	1.524(6)	C(117)-C(118)	1.540(8)
C(103)-C(104)	1.432(6)	Ru-centroid	1.649(2)
		Ru(1)-Ru(1)'	3.3023(6)
Ru(1) Cl(11) Ru(1')	84.19(4)	C(104) C(105) C(106)	119.4(4)
Ru(1) Cl(12) Ru(1')	84.38(4)	C(105) C(106) C(101)	121.7(5)
Ru(1) Cl(13) Ru(1')	85.60(4)	C(106) C(101) C(102)	117.9(4)
Cl(11) Ru(1) Cl(12)	79.11(4)	C(101) C(107) C(108)	115.9(4)
Cl(12) Ru(1) Cl(13)	79.52(4)	C(102) C(109) C(110)	108.2(4)
Cl(13) Ru(1) Cl(11)	79.47(4)	C(103) C(111) C(112)	115.9(4)
C(101) C(102) C(103)	121.4(4)	C(104) C(113) C(114)	112.0(4)
C(102) C(103) C(104)	119.4(4)	C(105) C(115) C(116)	115.9(4)
C(103) C(104) C(105)	120.1(4)	C(106) C(117) C(118)	110.4(5)

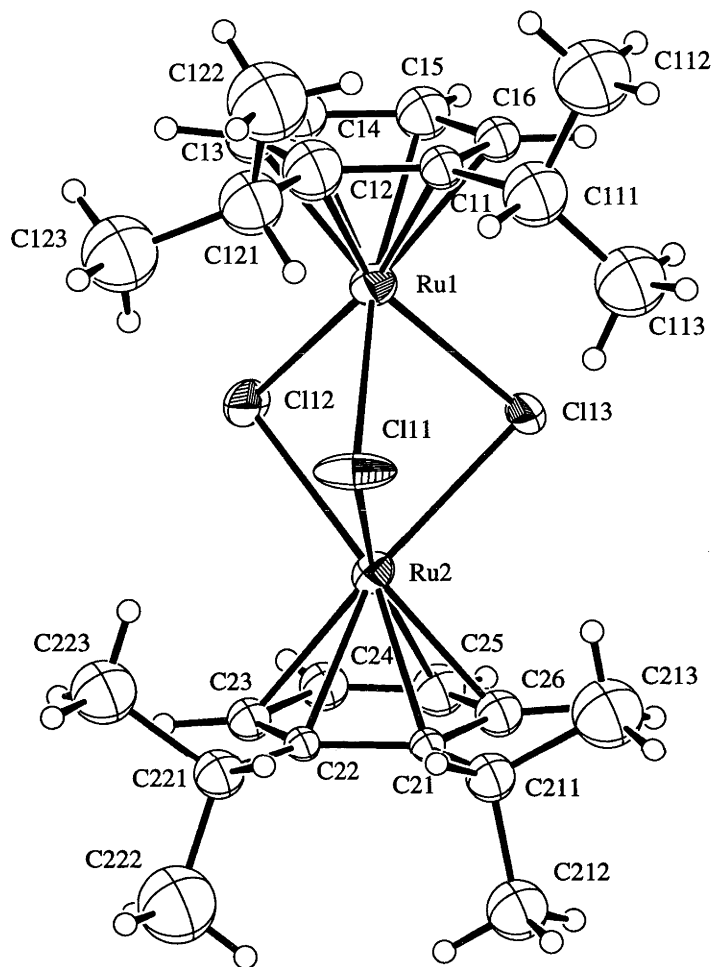


Figure 2.11. ORTEP diagram of $[\text{Ru}_2(\eta^6\text{-C}_6\text{H}_4\text{-1,2-Pr}^i_2)_2\text{Cl}_3]^+\text{PF}_6^-$

Table 2.10. Selected bond lengths (Å) and angles (°) for
 $[\text{Ru}(\eta^6\text{-C}_6\text{H}_4\text{-1,2-Pr}^i_2)_2\text{Cl}_3]^+\text{PF}_6^-$

Ru(1) Cl(11)	2.435(7)	Ru(1) Cl(12)	2.415(7)
Ru(1) Cl(13)	2.439(8)	Ru(1) C(11)	2.08(3)
Ru(1) C(12)	2.21(4)	Ru(1) C(13)	2.16(3)
Ru(1) C(14)	2.15(3)	Ru(1) C(15)	2.14(3)
Ru(1) C(16)	2.11(3)	Ru(2) Cl(11)	2.413(8)
Ru(2) Cl(12)	2.416(7)	Ru(2) Cl(13)	2.436(7)
Ru(2) C(21)	2.14(2)	Ru(2) C(22)	2.15(2)
Ru(2) C(23)	2.21(3)	Ru(2) C(24)	2.17(3)
Ru(2) C(25)	2.19(3)	Ru(2) C(26)	2.10(3)
C(11) C(12)	1.44(4)	C(11) C(16)	1.36(3)
C(11)C(111)	1.64(4)	C(12) C(13)	1.39(4)
C(12) C(121)	1.47(4)	C(13) C(14)	1.41(4)
C(14) C(15)	1.36(4)	C(15) C(16)	1.46(4)
C(21) C(22)	1.38(3)	C(21) C(26)	1.40(3)
C(21) C(211)	1.58(3)	C(22) C(23)	1.41(3)
C(22) C(221)	1.54(3)	C(23) C(24)	1.41(3)
C(24) C(25)	1.26(3)	C(25) C(26)	1.47(4)
C(111) C(112)	1.48(5)	C(111) C(113)	1.45(5)
C(121) C(122)	1.52(5)	C(121) C(123)	1.59(5)
C(211) C(212)	1.50(4)	C(211) C(213)	1.49(4)
C(221) C(222)	1.53(5)	C(221) C(223)	1.55(4)
Ru(1) Ru(2)	3.264(4)		
Cl(11) Ru(1) Cl(12)	80.0(3)	Cl(11)Ru(1)Cl(13)	79.0(3)
Cl(12)Ru(1)Cl(13)	79.3(3)	Cl(11)Ru(2)Cl(12)	80.5(3)
Cl(11)Ru(2)Cl(13)	79.5(3)	Cl(12)Ru(2)Cl(13)	79.3(3)
Ru(1)Cl(11)Ru(2)	84.7(2)	Ru(1)Cl(12)Ru(2)	85.1(2)
Ru(1)Cl(13)Ru(2)	84.2(2)	C(12)C(11)C(16)	126(2)
C(11)C(12)C(13)	109(3)	C(12)C(13)C(14)	128(3)
C(13)C(14)C(15)	117(2)	C(14)C(15)C(16)	118(2)
C(11)C(16)C(15)	118(2)	C(22)C(21)C(26)	118(2)
C(21)C(22)C(23)	119(2)	C(22)C(23)C(24)	119(2)
C(23)C(24)C(25)	121(2)	C(24)C(25)C(26)	120(2)
C(21)C(26)C(25)	118(2)	C(11)C(111)C(112)	109(3)
C(11)C(111)C(113)	112(3)	C(112)C(111)C(113)	109(3)
C(12)C(121)C(122)	110(3)	C(12)C(121)C(123)	106(3)
C(122)C(121)C(123)	121(3)	C(21)C(211)C(212)	101(2)
C(21)C(211)C(213)	111(2)	C(212)C(211)C(213)	108(2)
C(22)C(221)C(222)	109(2)	C(22)C(221)C(223)	113(2)
C(222)C(221)C(223)	108(2)		

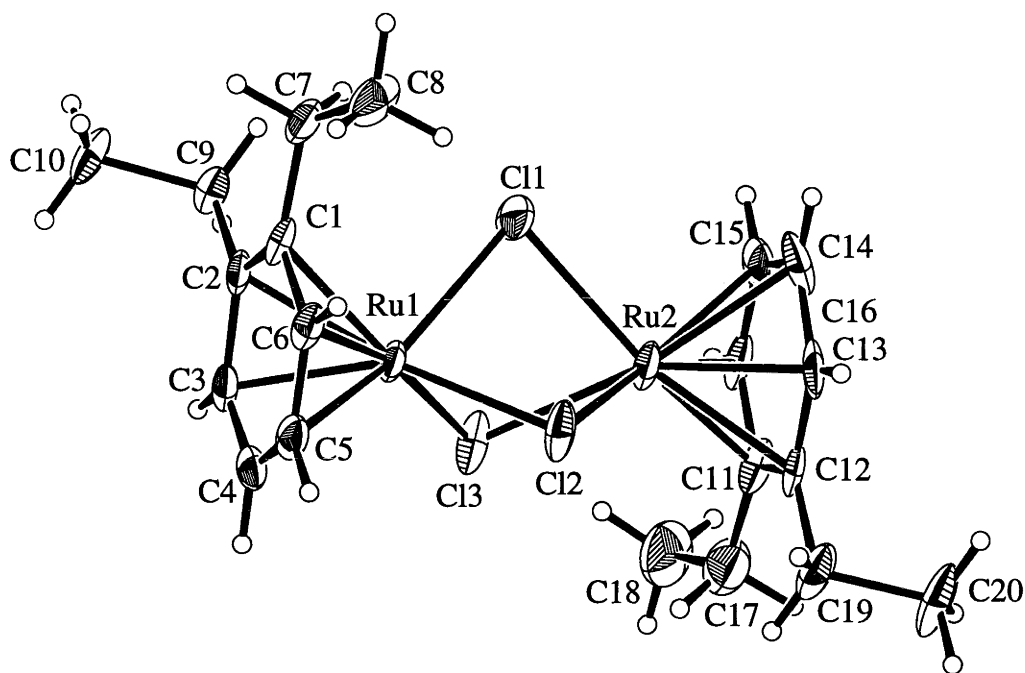


Figure 2.12. ORTEP diagram of $[\text{Ru}_2(\eta^6\text{-C}_6\text{H}_4\text{-1,2-Et}_2)_2\text{Cl}_3]^+\text{PF}_6^-$

Table 2.11. Selected bond lengths (Å) and angles (°) for $[\text{Ru}_2(\eta^6\text{-C}_6\text{H}_4\text{-1,2-Et}_2)_2\text{Cl}_3]^+\text{PF}_6^-$

Ru(1) Cl(1)	2.428(5)	Ru(1) Cl(1')	2.27(1)
Ru(1) Cl(2)	2.377(4)	Ru(1) Cl(2')	2.56(1)
Ru(1) Cl(3)	2.451(5)	Ru(1) Cl(3')	2.47(1)
Ru(1) C(2)	2.19(1)	Ru(1) C(1)	2.18(1)
Ru(1) C(4)	2.16(1)	Ru(1) C(3)	2.17(1)
Ru(1) C(6)	2.14(1)	Ru(1) C(5)	2.16(1)
Ru(2) Cl(1)	2.420(5)	Ru(2) Cl(1')	2.26(1)
Ru(2) Cl(2)	2.366(5)	Ru(2) Cl(2')	2.50(1)
Ru(2) Cl(3)	2.491(5)	Ru(2) Cl(3')	2.41(1)
Ru(2) C(12)	2.19(1)	Ru(2) C(11)	2.15(1)
Ru(2) C(14)	2.23(1)	Ru(2) C(13)	2.16(1)
Ru(2) C(16)	2.13(1)	Ru(2) C(15)	2.14(1)
C(1) C(2)	1.41(2)	C(1) C(6)	1.43(2)
C(1) C(7)	1.50(2)	C(2) C(3)	1.44(2)
C(2) C(9)	1.50(2)	C(3) C(4)	1.40(2)
C(4) C(5)	1.40(2)	C(5) C(6)	1.38(2)
C(7) C(8)	1.54(2)	C(9) C(10)	1.53(2)
C(11) C(12)	1.40(2)	C(11) C(16)	1.42(2)
C(11) C(17)	1.47(2)	C(12) C(13)	1.39(2)
C(12) C(19)	1.50(2)	C(13) C(14)	1.39(2)
C(14) C(15)	1.46(2)	C(15) C(16)	1.38(2)
C(17) C(18)	1.57(3)	C(19) C(20)	1.51(2)
		Ru - Ru	3.291(1)
Cl(1) Ru(1) Cl(2)	80.7(2)	Ru(1) Cl(1) Ru(2)	85.5(2)
Cl(1') Ru(1) Cl(2')	75.4(6)	Ru(1) Cl(1') Ru(2)	93.2(5)
Cl(1) Ru(1) Cl(3)	76.7(2)	Ru(1) Cl(2) Ru(2)	87.9(2)
Cl(1') Ru(1) Cl(3')	81.7(5)	Ru(1) Cl(2') Ru(2)	81.2(4)
Cl(2) Ru(1) Cl(3)	79.3(2)	Ru(1) Cl(3) Ru(2)	83.5(2)
Cl(2') Ru(1) Cl(3')	73.9(5)	Ru(1) Cl(3') Ru(2)	84.7(3)
C(1) C(2) C(3)	119(1)	C(4) C(5) C(6)	120(1)
C(2) C(3) C(4)	120(1)	C(5) C(6) C(1)	121(1)
C(3) C(4) C(5)	120(1)	C(6) C(1) C(2)	119(1)
C(11) C(12) C(13)	117(1)	C(16) C(11) C(12)	120(1)
C(12) C(13) C(14)	129(2)	C(1) C(7) C(8)	115(1)
C(13) C(14) C(15)	112(2)	C(11) C(17) C(18)	118(2)
C(14) C(15) C(16)	123(2)	C(2) C(9) C(10)	108(1)
C(15) C(16) C(11)	120(1)	C(12) C(19) C(20)	108(1)

' designates Cl atom of lower occupancy

ORTEP diagrams of the molecular structure of these three $[\text{Ru}_2(\eta^6\text{-arene})_2\text{Cl}_3]^+\text{PF}_6^-$ complexes are shown in Figures 2.10, 2.11 and 2.12. Tables 2.9, 2.10 and 2.11 contain selected bond lengths and angles. For $[\text{Ru}_2(\eta^6\text{-C}_6\text{Et}_6)_2\text{Cl}_3]^+\text{PF}_6^-$ there are two independent molecules in the unit cell whose bond lengths and angles do not differ greatly. The quoted metrical parameters refer to only one of the two molecules. For

$[\text{Ru}_2(\eta^6\text{-C}_6\text{H}_4\text{-1,2-Pr}^i_2)_2\text{Cl}_3]^+\text{PF}_6^-$ there are three molecules present in the unit cell, but again these do not differ greatly and the metrical parameters presented refer to only one of the three molecules. For $[\text{Ru}_2(\eta^6\text{-C}_6\text{H}_4\text{-1,2-Et}_2)_2\text{Cl}_3]^+\text{PF}_6^-$ there is only one molecule present in the unit cell but the chloride bridges are disordered.

It can be seen from the molecular structures in Figures 2.10, 2.11 and 2.12 that these dimeric molecule contain three bridging chloride atoms almost symmetrically orientated between the two ruthenium atoms, giving rise to a face-sharing bioctahedral structure. The ruthenium coordination sphere can still be considered essentially octahedral with the arene taking up three coordination sites and the remaining three being filled by the bridging chlorides. The two arenes are planar and parallel to each other, sandwiching the ruthenium μ -chloride backbone. For $[\text{Ru}_2(\eta^6\text{-C}_6\text{Et}_6)_2\text{Cl}_3]^+\text{PF}_6^-$ the ethyl groups of the arene are orientated in an alternating proximal/distal arrangement, that is, a 1,3,5-proximal-2,4,6-distal conformation, with the three proximal ethyl groups occupying the space between the bridging chloride ligands and the aromatic carbons connected to the distal ethyl groups eclipsing the chloride ligands. For $[\text{Ru}_2(\eta^6\text{-C}_6\text{H}_4\text{-1,2-Pr}^i_2)_2\text{Cl}_3]^+\text{PF}_6^-$ the isopropyl groups of the arene are orientated such that the two hydrogens of the isopropyl groups point towards each other, thus reducing the steric hindrance between the methyl groups. When viewed along the Ru-Ru axis the two arenes are orientated such that the isopropyl groups eclipse each other. In $[\text{Ru}_2(\eta^6\text{-C}_6\text{H}_4\text{-1,2-Et}_2)_2\text{Cl}_3]^+\text{PF}_6^-$ this is not the case and the alkyl substituents are not eclipsed, falling on opposite sides of the molecule. In this molecule one of the two ethyl groups of each arene lies roughly in the plane of the arene while the other is pointing away from the ruthenium.

Complexes of this type previously prepared and characterized by x-ray crystallography are $[\text{Ru}_2(\eta^6\text{-C}_6\text{H}_6)_2\text{Cl}_3]^+\text{AsF}_6^-$,⁴¹ $[\text{Ru}_2(\eta^6\text{-p-cymene})_2\text{Cl}_3]^+\text{BPh}_4^-$,⁴² $[\text{Ru}_2(\eta^6\text{-mesitylene})_2\text{Cl}_3]^+\text{BF}_4^-$,⁴³ $[\text{Ru}_2(\eta^6\text{-C}_6\text{H}_6)_2\text{Cl}_3]^+\text{BF}_4^-$,⁴⁴ and $[\text{Ru}_2(\eta^6\text{-C}_6\text{H}_5\text{Me})_2\text{Cl}_3]^+\text{BF}_4^-$.⁴⁴ All five of these complexes, as well as $[\text{Ru}_2(\eta^6\text{-C}_6\text{Et}_6)_2\text{Cl}_3]^+\text{PF}_6^-$, $[\text{Ru}_2(\eta^6\text{-C}_6\text{H}_4\text{-1,2-Pr}^i_2)_2\text{Cl}_3]^+\text{PF}_6^-$ and $[\text{Ru}_2(\eta^6\text{-C}_6\text{H}_4\text{-1,2-Et}_2)_2\text{Cl}_3]^+\text{PF}_6^-$ prepared in the course of this study, have the same gross structural features. However, the rotational orientation of the coordinated arenes with respect to the bridging chlorides and each other does differ. When viewed along the Ru-Ru axis, three of the arene carbon atoms in $[\text{Ru}_2(\eta^6\text{-C}_6\text{Et}_6)_2\text{Cl}_3]^+\text{PF}_6^-$ and $[\text{Ru}_2(\eta^6\text{-C}_6\text{H}_6)_2\text{Cl}_3]^+\text{BF}_4^-$ eclipse the bridging chlorine atoms (Fig 2.13b), whereas in $[\text{Ru}_2(\eta^6\text{-C}_6\text{H}_6)_2\text{Cl}_3]^+\text{AsF}_6^-$, $[\text{Ru}_2(\eta^6\text{-C}_6\text{H}_5\text{Me})_2\text{Cl}_3]^+\text{BF}_4^-$, $[\text{Ru}_2(\eta^6\text{-C}_6\text{H}_4\text{-1,2-Pr}^i_2)_2\text{Cl}_3]^+\text{PF}_6^-$, $[\text{Ru}_2(\eta^6\text{-C}_6\text{H}_4\text{-1,2-Et}_2)_2\text{Cl}_3]^+\text{PF}_6^-$ and $[\text{Ru}_2(\eta^6\text{-mesitylene})_2\text{Cl}_3]^+\text{BF}_4^-$ the Ru-Cl vectors bisect the aromatic C-C bonds to give a staggered conformation (Fig 2.13a). Just changing the counter ion

from BF_4^- to AsF_6^- for $[\text{Ru}_2(\eta^6\text{-C}_6\text{H}_6)_2\text{Cl}_3]^+$ changes the orientation of the ring. $[\text{Ru}_2(\eta^6\text{-}p\text{-cymene})_2\text{Cl}_3]^+\text{BPh}_4^-$ differs from all seven of these complexes in that, when viewed along the Ru-Ru axis, the aromatic carbons from the arene on each end of the molecule are mutually staggered rather than eclipsed. (Figure 2.13c). This structural variability shows that energy differences between different rotational isomers must be small.

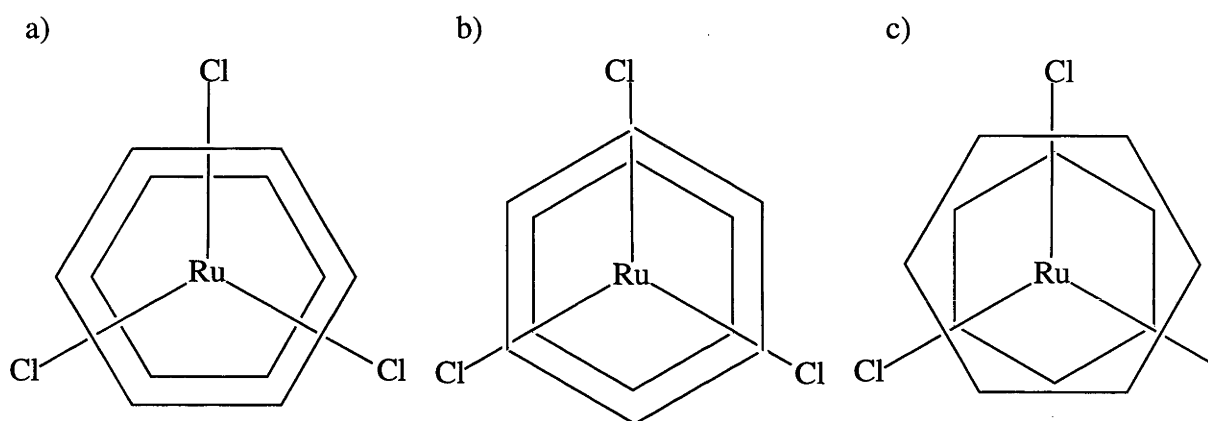


Figure 2.13. Rotational conformers for complexes of the type $[\text{Ru}_2(\eta^6\text{-arene})_2\text{Cl}_3]^+\text{PF}_6^-$

Solution behaviour of $[\text{Ru}(\eta^6\text{-C}_6\text{Et}_6)\text{Cl}_2]_2$

In order to attempt to account for the variable temperature NMR behaviour of $[\text{Ru}(\eta^6\text{-C}_6\text{Et}_6)\text{Cl}_2]_2$ and $[\text{Ru}_2(\eta^6\text{-C}_6\text{Et}_6)_2\text{Cl}_3]^+\text{PF}_6^-$, it was necessary to determine whether the structure of $[\text{Ru}(\eta^6\text{-C}_6\text{Et}_6)\text{Cl}_2]_2$ is maintained in dichloromethane and methanol solution or whether it dissociates with loss of a chloride ion to give $[\text{Ru}_2(\eta^6\text{-C}_6\text{Et}_6)_2\text{Cl}_3]^+\text{Cl}^-$ (Figure 2.14).

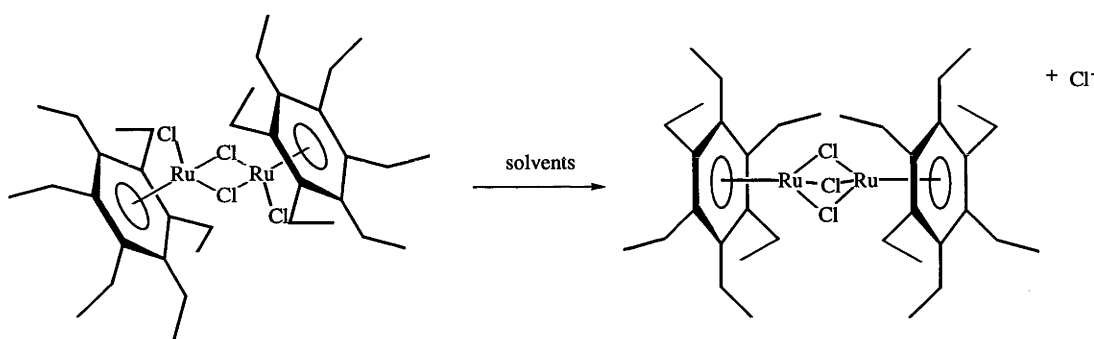


Figure 2.14 Possible dissociation of $[\text{Ru}(\eta^6\text{-C}_6\text{Et}_6)\text{Cl}_2]_2$ to $[\text{Ru}_2(\eta^6\text{-C}_6\text{Et}_6)_2\text{Cl}_3]^+\text{Cl}^-$

Four techniques were utilized: molecular weight determination by vapour pressure osmometry, far infrared spectroscopy of the dichloride dimer in solid state and in solution, conductance measurements, and ^{35}Cl NMR spectroscopy.

The molecular weight of $[\text{Ru}(\eta^6\text{-C}_6\text{Et}_6)\text{Cl}_2]_2$ in CH_2Cl_2 at a concentration of *ca.* 16 mgcm^{-3} at 37°C was determined by vapour pressure osmometry to be 670 amu, compared with the calculated value of 836 amu. This suggests that there is some degree of dissociation of the complex in solution, although it is assumed that there is no significant decomposition of the solution of the complex in air.

If $[\text{Ru}(\eta^6\text{-C}_6\text{Et}_6)\text{Cl}_2]_2$ dissociates in solution to give $[\text{Ru}_2(\eta^6\text{-C}_6\text{Et}_6)_2\text{Cl}_3]^+\text{Cl}^-$ then it should behave as a 1:1 electrolyte. Three quantities are commonly used to determine electrolyte type from conductivity measurements: molar conductivity at a given concentration (Λ_M), usually 10^{-3} or 10^{-4} M, the extrapolation of the straight portion of a

graph of Λ_M against the square root of concentration to infinite dilution to give the absolute conductance (Λ_0), and the gradient of the plot of $(\Lambda_0 - \Lambda_M)$ against the square root of concentration.¹¹⁴ These quantities do not give an absolute measure of electrolyte stoichiometry, rather, a comparison between the values obtained for the unknown and the values for similar compounds of known electrolyte type can sometimes allow electrolyte type to be assigned. The use of just Λ_M and Λ_0 values has at least one drawback, namely that the molecular weights of the species present in solution need to be known. For the calculations here the molecular masses used were those appropriate for the dissociation of $[\text{Ru}(\eta^6\text{-C}_6\text{Et}_6)\text{Cl}_2]_2$ to $[\text{Ru}_2(\eta^6\text{-C}_6\text{Et}_6)_2\text{Cl}_3]^+\text{Cl}^-$.

A collection of Λ_M and Λ_0 values for various complexes and various solvents is given in a review article by Geary¹¹⁵. In methanol, where the data for almost 100 complexes are available, it has been found that 1:1 electrolytes have Λ_M values between 85 and 115 $\text{ohm}^{-1}\text{cm}^2\text{mol}^{-1}$ while for 2:1 electrolytes the range has been found to be 160-220 $\text{ohm}^{-1}\text{cm}^2\text{mol}^{-1}$.¹¹⁵ Unfortunately a collection of gradients of $(\Lambda_0 - \Lambda_M)$ against the square root of concentration for complexes of the type being investigated is not available.

Much less is known about conductivities in dichloromethane. Rosenthal and Drago¹¹⁶ state that due to the extensive ion pairing even at low concentrations, conductance measurements in dichloromethane should only be used to determine whether or not a complex is ionic rather than trying to determine what type of ionic species is present. This raises an important point: conductivity measurement do not distinguish between ion pairs and covalently bound molecules. The technique depends on the presence of freely dissociated ions. Thus, for dichloromethane, only Λ_0 not Λ_M should be used because at infinite dilution there should be no ion pairing contribution. Uguagliati *et al.*¹¹⁷, however, successfully used Λ_M measurements in dichloromethane to determine electrolyte types for cationic rhodium complexes, with Λ_M values of between 22 and 26 $\text{ohm}^{-1}\text{cm}^2\text{mol}^{-1}$ for 1:1 electrolytes at 25°C and 10^{-3} M.

To gain at least a qualitative idea of the Λ_0 values expected in dichloromethane for 1:1 electrolytes, the conductance of $[\text{NEt}_4]^+\text{Cl}^-$ was measured at a range of concentrations and plotted against the square root of concentration. Λ_0 was found to be 120 $\text{ohm}^{-1}\text{cm}^2\text{mol}^{-1}$.

In the paper of Arthur and Stephenson³⁹ on the synthesis of triple halide bridged arene complexes of ruthenium, the conductance of several tri- μ -chloro BF_4 salts was measured in nitromethane, a more polar solvent than dichloromethane. It was found that the molar conductance of $[\text{Ru}_2(\eta^6\text{-C}_6\text{H}_3\text{Me}_3)_2\text{Cl}_3]^+\text{BF}_4^-$ was 90.5 $\text{ohm}^{-1}\text{cm}^2\text{mol}^{-1}$, falling in the range for 1:1 electrolytes in nitromethane (75-95 $\text{ohm}^{-1}\text{cm}^2\text{mol}^{-1}$). That of

$[\text{Ru}_2(\eta^6\text{-C}_6\text{H}_6)_2\text{Cl}_3]^+\text{PF}_6^-$ has also been measured previously and was found to be $82 \text{ ohm}^{-1}\text{cm}^2\text{mol}^{-1}$ in nitromethane,³⁷ again within the range of 1:1 electrolytes.

The conductances in methanol of $[\text{Ru}(\eta^6\text{-C}_6\text{Et}_6)\text{Cl}_2]_2$ and $[\text{Ru}_2(\eta^6\text{-C}_6\text{Et}_6)_2\text{Cl}_3]^+\text{PF}_6^-$ were measured over a range of concentrations. Plots of molar conductivity against the square root of concentration are shown in Figures 2.15a and 2.15b. For $[\text{Ru}(\eta^6\text{-C}_6\text{Et}_6)\text{Cl}_2]_2$, Λ_{M} at a concentration of 10^{-3} M was found to be $75 \text{ ohm}^{-1}\text{cm}^2\text{mol}^{-1}$ and Λ_0 was found to be $117 \text{ ohm}^{-1}\text{cm}^2\text{mol}^{-1}$. For $[\text{Ru}_2(\eta^6\text{-C}_6\text{Et}_6)_2\text{Cl}_3]^+\text{PF}_6^-$, Λ_{M} at 10^{-3} M was found to be $103 \text{ ohm}^{-1}\text{cm}^2\text{mol}^{-1}$ and Λ_0 was $112 \text{ ohm}^{-1}\text{cm}^2\text{mol}^{-1}$. Thus both $[\text{Ru}_2(\eta^6\text{-C}_6\text{Et}_6)_2\text{Cl}_3]^+\text{PF}_6^-$ and $[\text{Ru}(\eta^6\text{-C}_6\text{Et}_6)\text{Cl}_2]_2$ behave as 1:1 electrolytes in methanol.

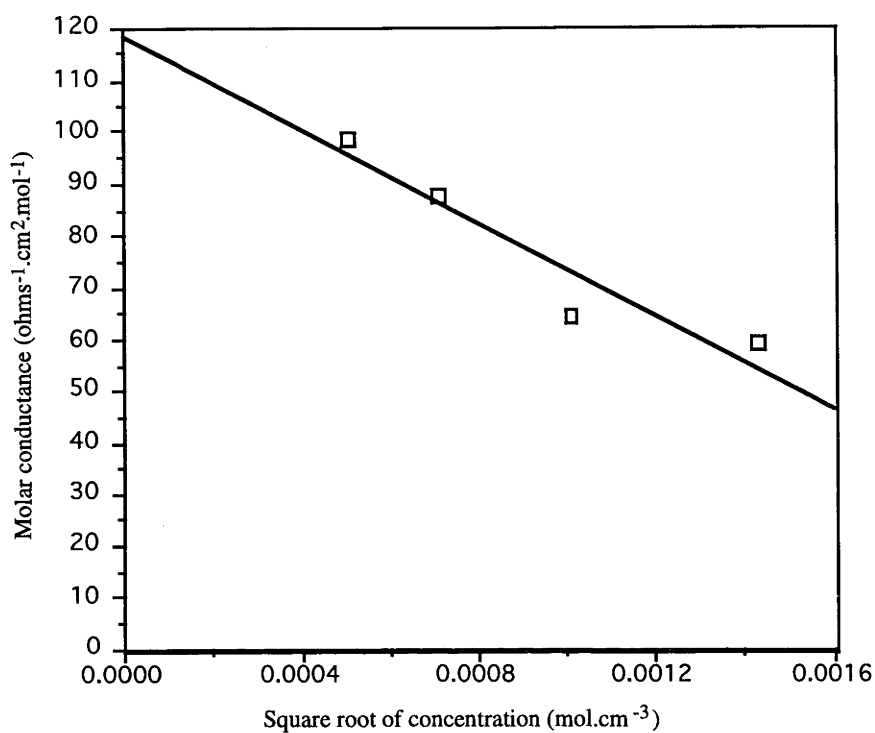


Figure 2.15a Conductivity plot for $[\text{Ru}(\eta^6\text{-C}_6\text{Et}_6)\text{Cl}_2]_2$ in MeOH.

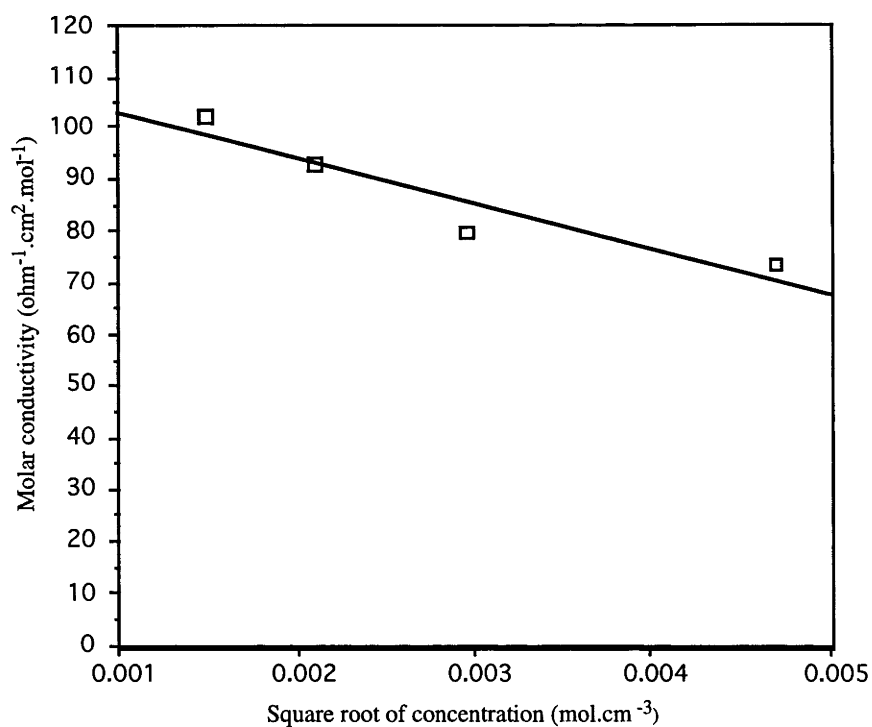
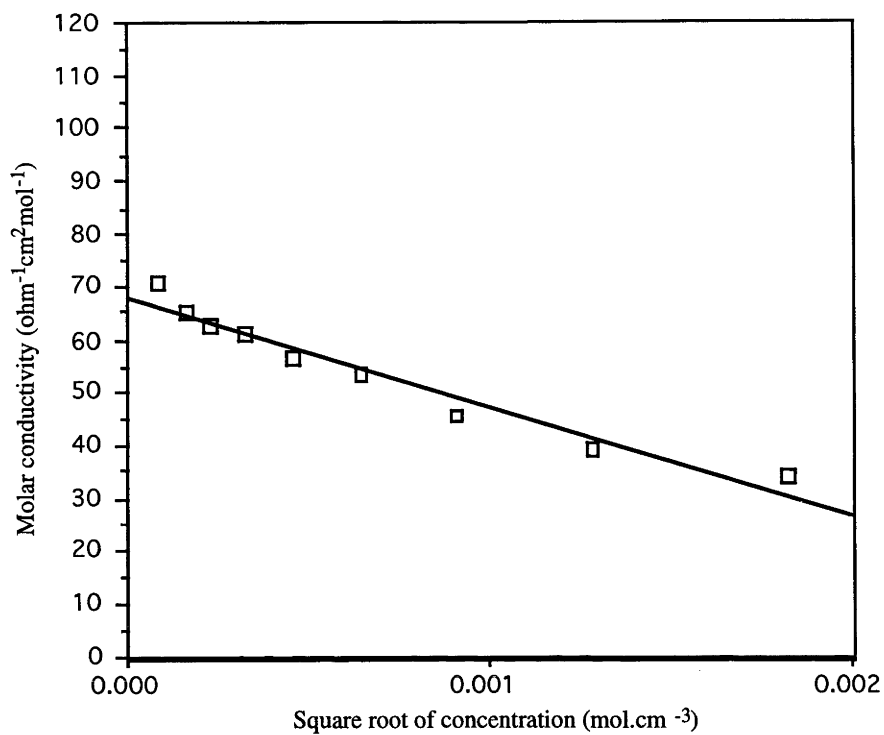
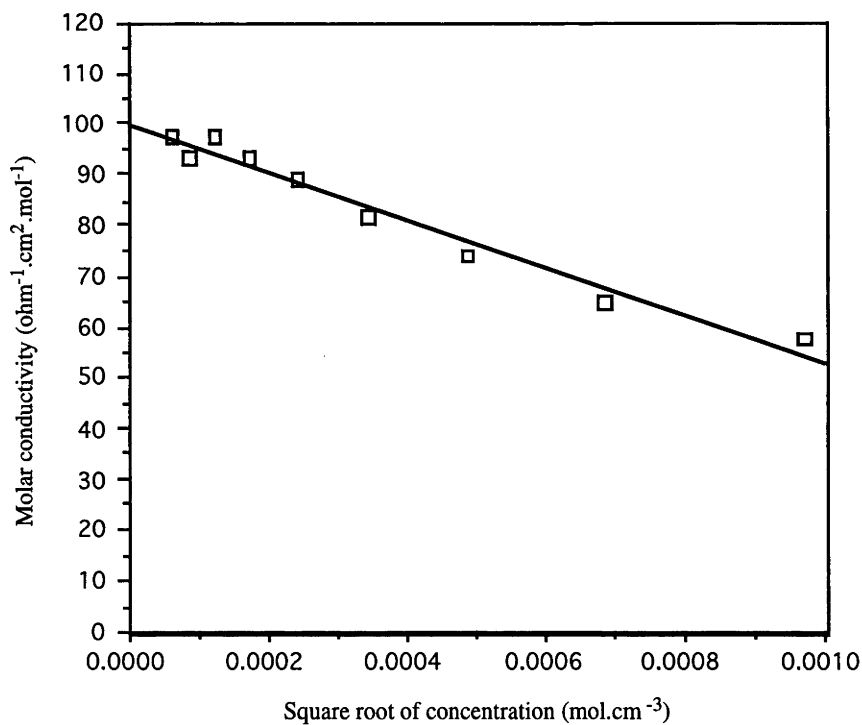


Figure 2.15b Conductivity plot for $[\text{Ru}_2(\eta^6\text{-C}_6\text{Et}_6)_2\text{Cl}_3]^+\text{PF}_6^-$ in MeOH

Figure 2.16a Conductivity plot for $[\text{Ru}(\eta^6\text{-C}_6\text{Et}_6)\text{Cl}_2]_2$ in CH_2Cl_2 Figure 2.16b Conductivity plot of $[\text{Ru}_2(\eta^6\text{-C}_6\text{Et}_6)_2\text{Cl}_3]^+\text{PF}_6^-$ in CH_2Cl_2

The conductivities of $[\text{Ru}(\eta^6\text{-C}_6\text{Et}_6)\text{Cl}_2]_2$ and $[\text{Ru}_2(\eta^6\text{-C}_6\text{Et}_6)_2\text{Cl}_3]^+\text{PF}_6^-$ were measured in dichloromethane over a range of concentrations. Plots of Λ_0 against the square root of concentration are shown in Figure 2.16a and Figure 2.16b. In dichloromethane Λ_0 for $[\text{Ru}_2(\eta^6\text{-C}_6\text{Et}_6)_2\text{Cl}_3]^+\text{PF}_6^-$ was found to be $100 \text{ ohm}^{-1}\text{cm}^2\text{mol}^{-1}$ while that for $[\text{Ru}(\eta^6\text{-C}_6\text{Et}_6)\text{Cl}_2]_2$ was found to be $68 \text{ ohm}^{-1}\text{cm}^2\text{mol}^{-1}$. The less reliable Λ_M values at 10^{-3} M were about $50 \text{ ohm}^{-1}\text{cm}^2\text{mol}^{-1}$ for both complexes, significantly higher than those determined by Uguagliati. These results imply that in dichloromethane $[\text{Ru}(\eta^6\text{-C}_6\text{Et}_6)\text{Cl}_2]_2$ does dissociate, but probably not to the same extent as $[\text{Ru}_2(\eta^6\text{-C}_6\text{Et}_6)_2\text{Cl}_3]^+\text{PF}_6^-$.

In both methanol and dichloromethane the plots of Λ_M against the square root of concentration give straight lines for both $[\text{Ru}(\eta^6\text{-C}_6\text{Et}_6)\text{Cl}_2]_2$ and $[\text{Ru}_2(\eta^6\text{-C}_6\text{Et}_6)_2\text{Cl}_3]^+\text{PF}_6^-$. From this it can be concluded that these complexes do not undergo multiple dissociations, at least over the concentration range observed. The dichloride dimer exists to some extent as an ionized species in solution, and the observed values of Λ_0 and Λ_M are consistent with its being a 1:1 electrolyte in methanol and dissociated to some extent in dichloromethane, presumably to an ionic species.

Perhaps the most information about the nature of the dichloride dimer in solution comes from ^{35}Cl NMR spectroscopy. The nucleus ^{35}Cl is quadrupolar^a and when covalently bound gives rise to very broad resonances, due to the very rapid quadrupolar relaxation processes; however, relatively narrow resonances are observed for ionic chloride, where these rapid relaxation processes play less of a role. It has been found that for Cl^- , where the chlorine is in a highly symmetrical electrical environment, line widths as low as 8 Hz can be observed in aqueous solution, while for covalent chlorine containing compounds, where the chlorine is not in a symmetrical electrical environment, line widths vary from 1000-22000 Hz.¹¹⁸

For $[\text{Ru}(\eta^6\text{-C}_6\text{Et}_6)\text{Cl}_2]_2$ in CD_3OD at room temperature, a broad resonance is observed. When the temperature is lowered to -50°C , however, a new, much sharper resonance assignable to the chloride ion appears. No such resonance was observed for $[\text{Ru}_2(\eta^6\text{-C}_6\text{Et}_6)_2\text{Cl}_3]^+\text{PF}_6^-$ under the same conditions. In CD_2Cl_2 the observation becomes more difficult due to the large amounts of covalently bound chlorine present in the solvent. The spectrum of $[\text{NEt}_4]\text{Cl}$ in CD_2Cl_2 displayed only the sharp resonance due to Cl^- . In the spectrum of $[\text{Ru}(\eta^6\text{-C}_6\text{Et}_6)\text{Cl}_2]_2$ in CD_2Cl_2 the ionic chloride resonance again was not

^a Quadrupolar moment, $Q = -8.2 \times 10^{-30} \text{ m}^2$

observed at room temperature but became apparent at -50°C . At -75°C the ionic chloride resonance sharpened to give a peak with a line width of approximately 200Hz, well outside the range expected for covalently bound chlorine (Figure 2.17). This peak was not present in the ^{35}Cl NMR spectrum of CD_2Cl_2 . It is not known whether ^{35}Cl NMR can distinguish between free and ion paired Cl^- .

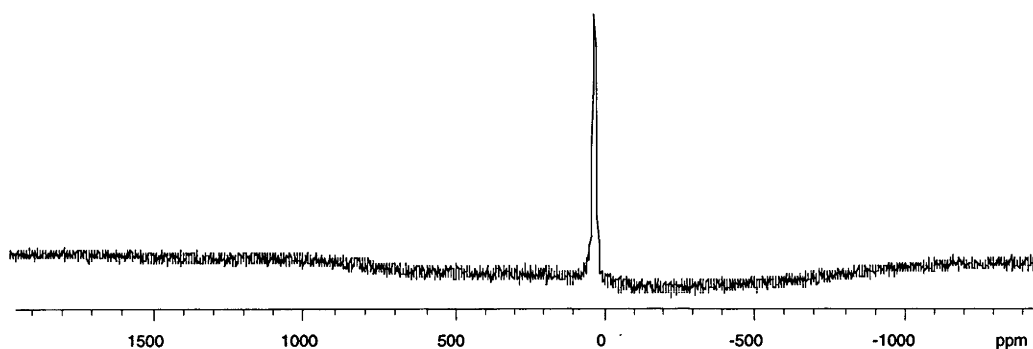


Figure 2.17. ^{35}Cl NMR spectrum of $[\text{Ru}(\eta^6\text{-C}_6\text{Et}_6)\text{Cl}_2]_2$ at -75°C (CD_2Cl_2 , 29.396MHz)

Several conclusions can be drawn from these NMR results. Firstly, in agreement with the conductivity data, the dichloride dimer does dissociate in both methanol and dichloromethane to give free chloride ion and, presumably, the bioctahedral face sharing dimer cation. The temperature dependence of the appearance of the free chloride resonance suggests that exchange, rapid on an NMR timescale at room temperature, prevents the observation of the resonance due to free chloride. Once this process is slowed on an NMR timescale by the reduction of temperature, it becomes possible to observe the resonance due to chloride. Thus the dissociation of chloride ion is a facile dynamic process. However, it is not possible from these results to determine the degree of dissociation of $[\text{Ru}(\eta^6\text{-C}_6\text{Et}_6)\text{Cl}_2]_2$.

The conclusions drawn from far infrared spectroscopic measurements are not inconsistent with the conclusions drawn from the ^{35}Cl NMR spectroscopy and conductance measurements. The solid state and solution far infrared spectra of $[\text{Ru}(\eta^6\text{-C}_6\text{Et}_6)\text{Cl}_2]_2$ and $[\text{Ru}_2(\eta^6\text{-C}_6\text{Et}_6)_2\text{Cl}_3]^+\text{PF}_6^-$ are given in Figures 2.18 and 2.19. In theory it should

be possible to observe bands assignable to the bridging and terminal Ru-Cl (Ru-Cl^b and Ru-Cl^t) vibrations in the far infrared spectra. Thus $[\text{Ru}(\eta^6\text{-C}_6\text{Et}_6)\text{Cl}_2]_2$ should have bands for both Ru-Cl^t and Ru-Cl^b stretching frequencies, while $[\text{Ru}_2(\eta^6\text{-C}_6\text{Et}_6)_2\text{Cl}_3]^+\text{PF}_6^-$ should contain only bands for Ru-Cl^b vibrations. If the dichloride dimer does dissociate completely in solution to give the triply bridged species, a band assignable to terminal Cl should not be present in the solution far infrared spectrum. The value of $\nu(\text{Ru-Cl}^b)$ for $[\text{Ru}_2(\eta^6\text{-C}_6\text{H}_6)_2\text{Cl}_3]^+\text{PF}_6^-$ has previously been found to be 260 cm^{-1} , while for $[\text{Ru}(\eta^6\text{-C}_6\text{H}_6)\text{Cl}_2]_2$ the bands due to $\nu(\text{RuCl}^t)$ appeared at 295 cm^{-1} and those due to $\nu(\text{Ru-Cl}^b)$ were at 259 and 248 cm^{-1} .²⁴ Table 2.12 gives the far infrared Ru-Cl stretching bands for previously measured species

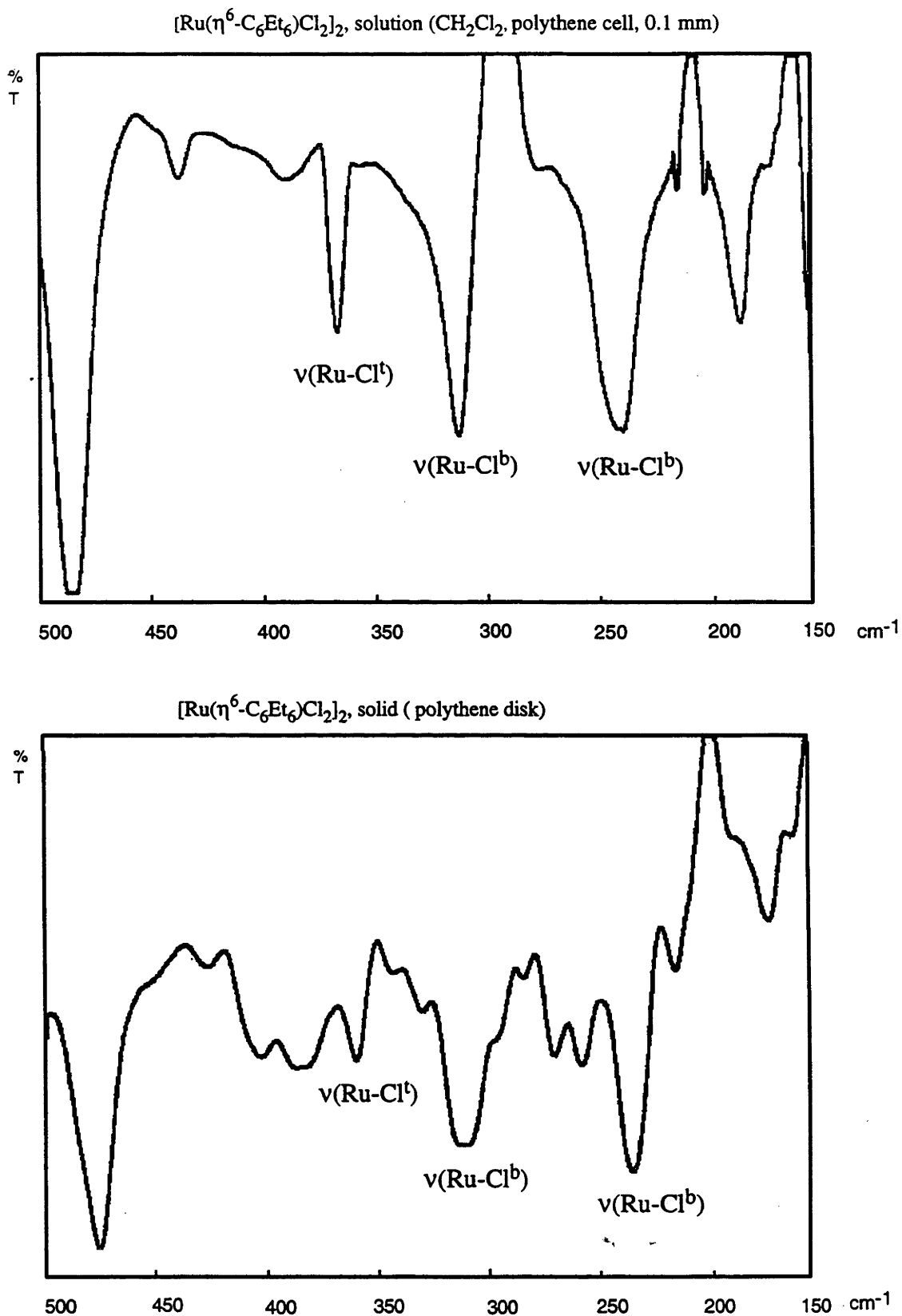
Table 2.12. Far infrared Ru-Cl stretching bands of $[\text{Ru}(\eta^6\text{-arene})\text{Cl}_2]_2$ complexes

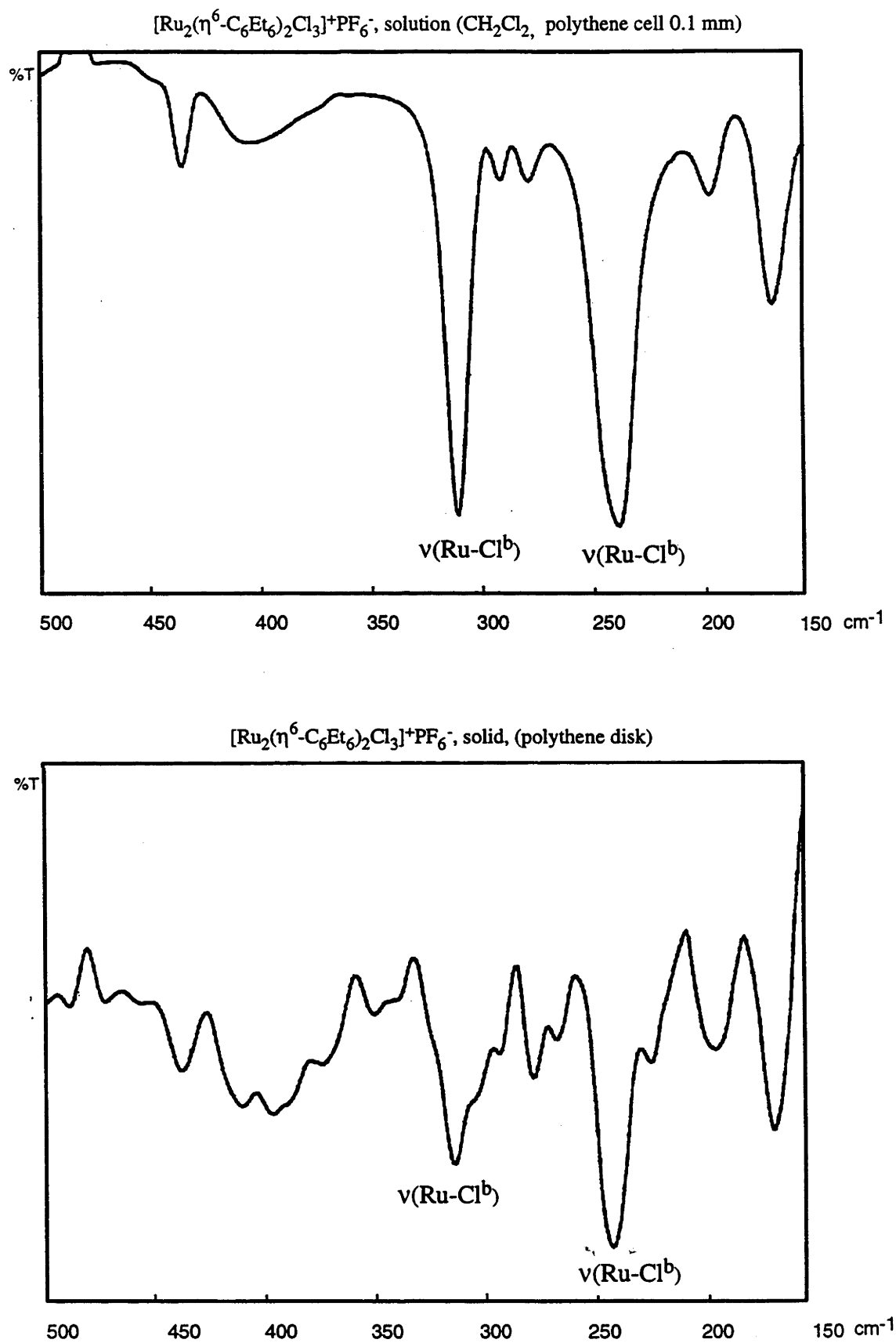
Complex	$\nu(\text{Ru-Cl})\text{ (cm}^{-1}\text{)}$
$[\text{Ru}(\eta^6\text{-C}_6\text{H}_6)\text{Cl}_2]_2$ ²¹	294, 256, 248
$[\text{Ru}(\eta^6\text{-C}_6\text{H}_5\text{Me})\text{Cl}_2]_2$ ²⁴	293, 250
$[\text{Ru}(\eta^6\text{-C}_6\text{H}_4\text{-1,4-Me}_2)\text{Cl}_2]_2$ ²⁴	292, 254, 247
$[\text{Ru}(\eta^6\text{-p-cymene})\text{Cl}_2]_2$ ²⁴	292, 260, 250
$[\text{Ru}(\eta^6\text{-C}_6\text{H}_3\text{-1,3,5-Me}_3)\text{Cl}_2]_2$ ²⁴	298, 270, 260, 248
$[\text{Ru}(\eta^6\text{-C}_6\text{H}_5\text{OMe})\text{Cl}_2]_2$ ²⁴	300, 255, 248
$[\text{Ru}(\eta^6\text{-C}_6\text{H}_6)\text{Cl}_2]_2$ ²⁵	299, 258

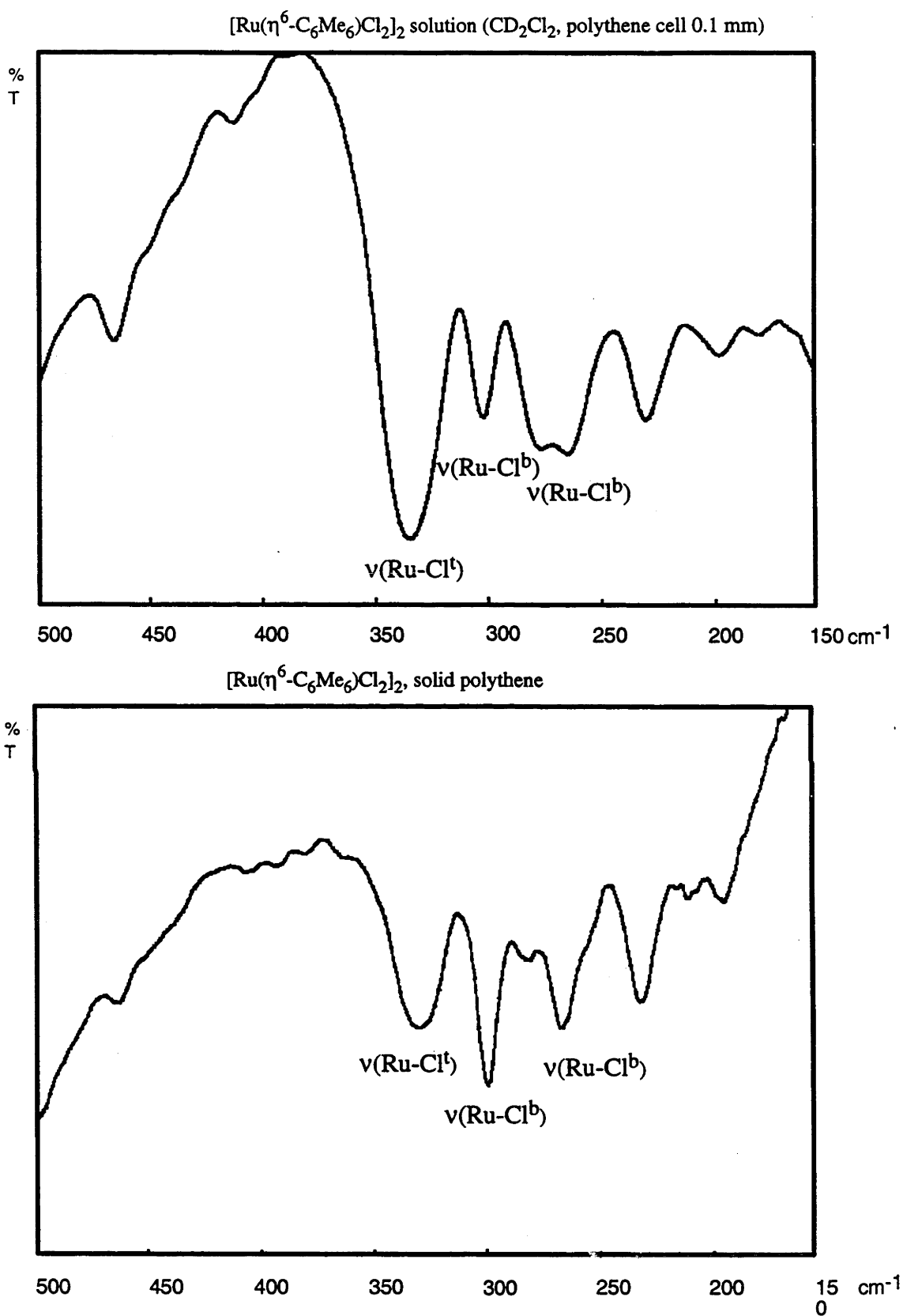
Both the solid state and CH_2Cl_2 solution far infrared spectra of $[\text{Ru}(\eta^6\text{-C}_6\text{Et}_6)\text{Cl}_2]_2$ contain three bands assignable to ruthenium-chloride stretching frequencies, *ca.* ν 240 (Ru-Cl^b), 310 (Ru-Cl^b) and 365 cm^{-1} (Ru-Cl^t). For the complex $[\text{Ru}_2(\eta^6\text{-C}_6\text{Et}_6)_2\text{Cl}_3]^+\text{PF}_6^-$ only two bands assignable Ru-Cl^b are present, at *ca.* ν 310 and 240 cm^{-1} . The presence of a band assignable to Ru-Cl^t stretching vibrations in the solution far infrared spectrum suggests that there is not complete dissociation of the dichloride dimer in solution to the triply bridged species, in fact, it suggests that the dissociation only occurs to a very small extent.

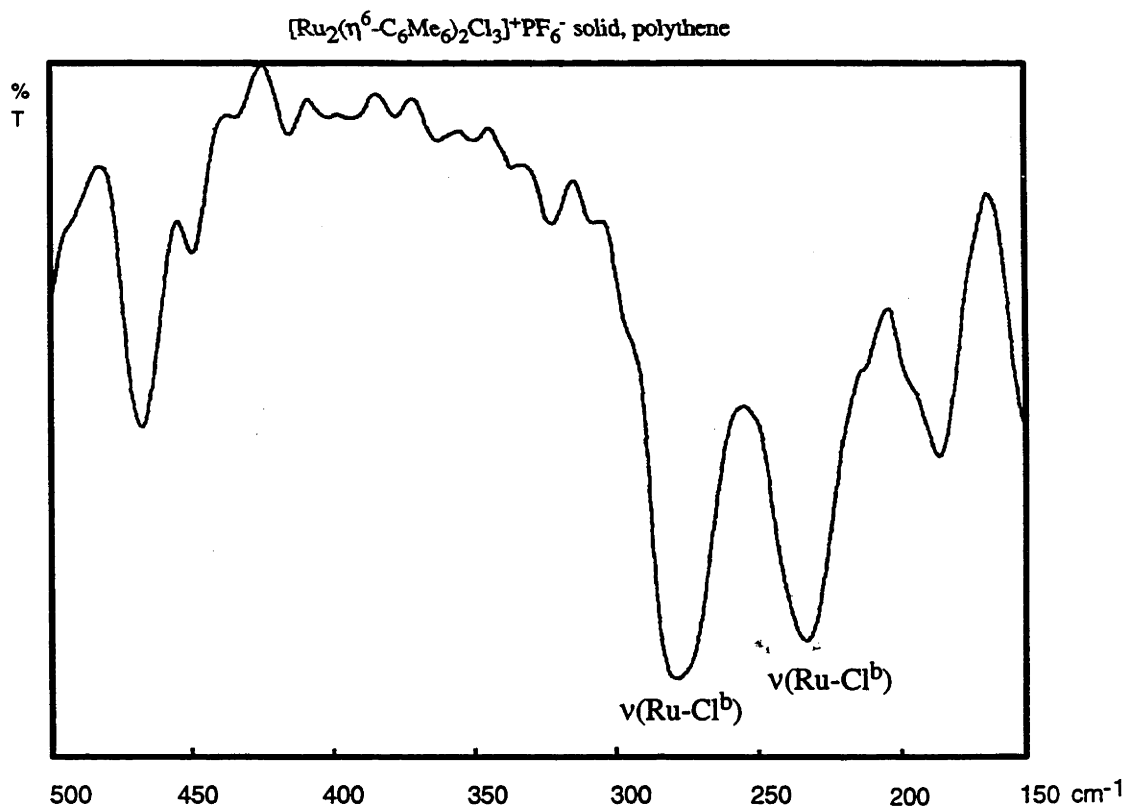
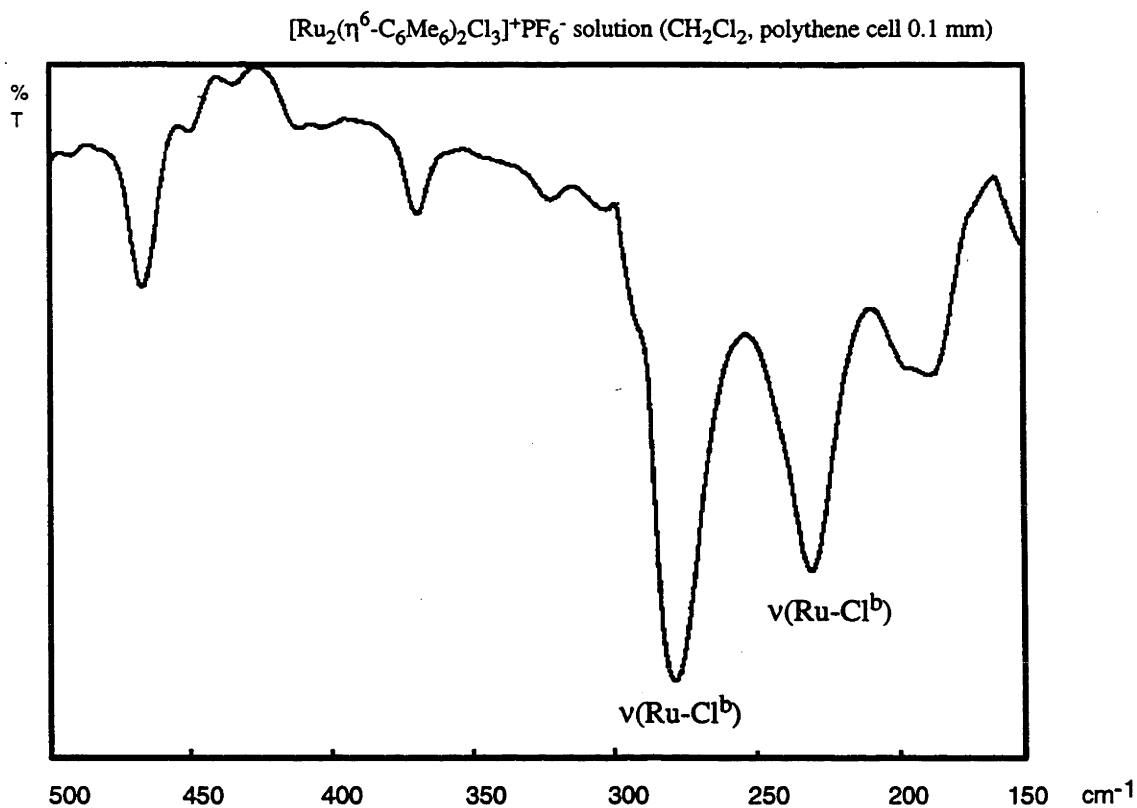
Equivalent results were obtained for $[\text{Ru}(\eta^6\text{-C}_6\text{Me}_6)\text{Cl}_2]_2$ and $[\text{Ru}_2(\eta^6\text{-C}_6\text{Me}_6)_2\text{Cl}_3]^+\text{PF}_6^-$. The far infrared spectra of these two complexes, in CH_2Cl_2 solution and the solid state, are displayed in Figures 2.20 and 2.21. For $[(\eta^6\text{-C}_6\text{Me}_6)\text{RuCl}_2]_2$ in both solution and solid state a Ru-Cl^t stretching band occurs at *ca.* ν 340 cm^{-1} while Ru-Cl^b bands can be observed at *ca.* ν 300 and 265 cm^{-1} . For $[\text{Ru}_2(\eta^6\text{-C}_6\text{Me}_6)_2\text{Cl}_3]^+\text{PF}_6^-$ there are only the two Ru-Cl^b bands present, at *ca.* ν 280 and 230 cm^{-1} . Thus it appears that in solutions of the dichloride dimer $[\text{Ru}(\eta^6\text{-C}_6\text{Me}_6)\text{Cl}_2]_2$ is the main species present.

In $[\text{Ru}(\eta^6\text{-C}_6\text{Me}_6)\text{Cl}_2]_2$ the two previously reported bands were found, but the literature does not report the higher band at 340 cm^{-1} , which has been assigned to Ru-Cl^t . The assignment of Ru-Cl^t in this study was made on the basis that it was the band that disappeared in the move from the dichloride dimer to the tri- μ -chloro salt. For both hexaethylbenzene and hexamethylbenzene this band was found to be anomalously high relative to the previously measured bands, being well over 300 cm^{-1} . It is assumed that this band is present in the previously studied complexes but was ignored due to its high frequency.

Figure 2.18. Solution and solid state infrared spectra of $[\text{Ru}(\eta^6\text{-C}_6\text{Et}_6)\text{Cl}_2]_2$

Figure 2.19. Solution and solid state infrared spectra of $[\text{Ru}_2(\eta^6\text{-C}_6\text{Et}_6)_2\text{Cl}_3]^+\text{PF}_6^-$

Figure 2.20. Solution and solid state infrared spectra of $[\text{Ru}(\eta^6\text{-C}_6\text{Me}_6)\text{Cl}_2]_2$

Figure 2.21. Solution and solid state infrared spectra of $[\text{Ru}_2(\eta^6\text{-C}_6\text{Me}_6)_2\text{Cl}_3]^+\text{PF}_6^-$

Taken together, observations from all the techniques employed suggest that $[\text{Ru}(\eta^6\text{-C}_6\text{Et}_6)\text{Cl}_2]_2$ only partially dissociates, especially in dichloromethane. This partial dissociation does not explain the anomalous variable temperature behaviour of the dichloride dimer discussed in Chapter 4.

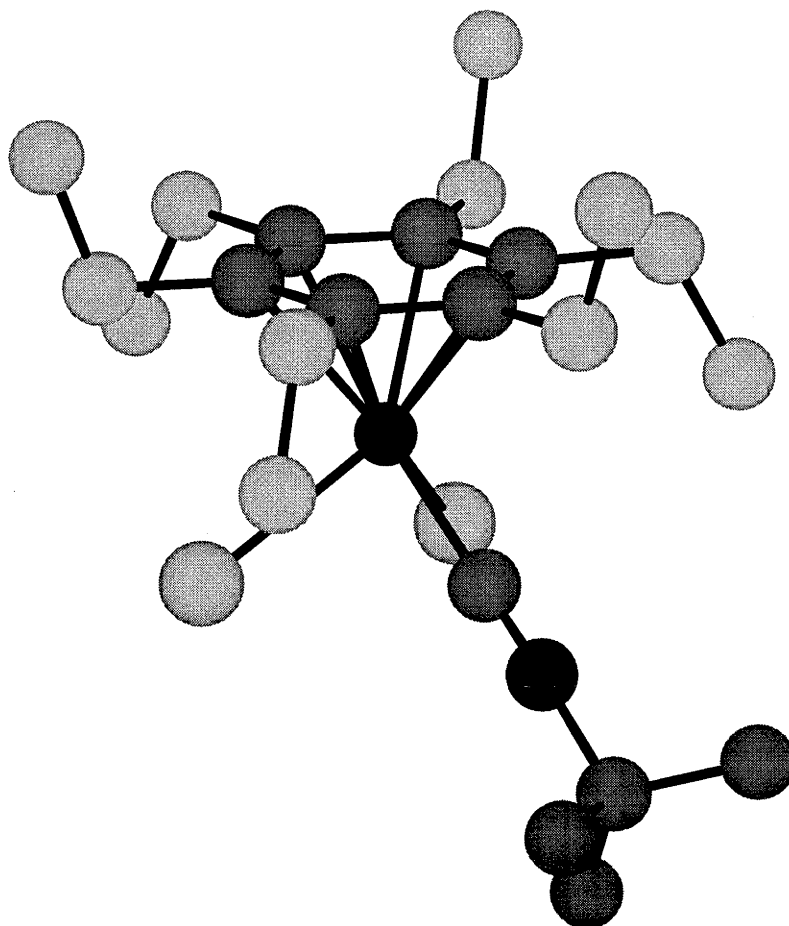
In the case of $[\text{Ru}(\eta^6\text{-trindane})\text{Cl}_2]_2$ in CD_2Cl_2 it has been found that at room temperature in solution there were twice as many ^1H and ^{13}C NMR resonances as expected⁶⁹ (see Chapter 1). The possibility that this was due to hindered rotation of the arene ring was summarily rejected and the results were explained in terms of partial ionization to give a solution containing both $[\text{Ru}_2(\eta^6\text{-trindane})_2\text{Cl}_3]^+\text{Cl}^-$ and the original dichloride dimer. This hypothesis was supported by the observation that the relative intensities of the peaks changed with change in temperature, as the proportion of dichloride dimer to tri- μ -chloro salt changed. Also the relative proportions of the peaks changed, with one species, presumed to be the salt, becoming far more abundant when a more polar solvent, CD_3NO_2 , was used. None of these effects were observed in the case of $[\text{Ru}(\eta^6\text{-C}_6\text{Et}_6)\text{Cl}_2]_2$. There was no appreciable difference in the NMR spectra in methanol, dichloromethane or CD_3NO_2 or a change of the nature described with change in temperature.

One other possible explanation for the ionic behaviour of $[\text{Ru}(\eta^6\text{-C}_6\text{Et}_6)\text{Cl}_2]_2$ in solution, suggested by Robertson, Stephenson and Arthur³⁹ for other arene ruthenium dichloride dimers, is that a monomeric solvento species is present to some extent. These authors studied complexes with less alkyl substituted arenes and thus, for reasons of solubility, were limited to more coordinating solvents, such as DMSO and water. These conditions would favour the formation of monomeric species, stabilized by the coordination of solvent, which is much less likely in dichloromethane.

However, when equimolar amounts of $[\text{Ru}(\eta^6\text{-C}_6\text{Me}_6)\text{Cl}_2]_2$ and $[\text{Os}(\eta^6\text{-C}_6\text{Me}_6)\text{Cl}_2]_2$ ^{119,120} are taken up in dichloromethane, the major peaks observed in the FAB^+ mass spectrum of this mixture were those for the mixed dimer, $[\text{RuOs}(\eta^6\text{-C}_6\text{Me}_6)_2\text{Cl}_3]$, as well as the equivalent diosmium and diruthenium complexes in the expected ratio for random scrambling of 2:1:1 respectively. While this is not conclusive evidence of the existence of a monomeric species in solution it does suggest that more dissociation than just to the tri- μ -chloro salt is occurring. Arthur and Stephenson³⁹ observed a similar scrambling when the cations $[\text{Ru}_2(\eta^6\text{-C}_6\text{H}_6)_2\text{Cl}_3]^+$ and $[\text{Os}_2(\eta^6\text{-C}_6\text{H}_6)_2\text{Cl}_3]^+$ mixed in solution. These authors postulate an associative mechanism for exchange of arene and halides

In summary, it has been found that cyclotrimerization of acetylenes on $\text{Ru}(\eta^6\text{-naphth})(\eta^4\text{-COD})$ is a good route to complexes of ruthenium containing arenes with bulky substituents. The treatment of the $\text{Ru}(0)$ complexes of the type $\text{Ru}(\eta^6\text{-arene})(\eta^4\text{-COD})$ thus obtained with HCl gives dichloride dimers of the type $[\text{Ru}(\eta^6\text{-arene})\text{Cl}_2]_2$ which are well defined in the solid state but, in the case of arene = C_6Et_6 , appear to exist in solution as a mixture of species, one of which is $[\text{Ru}_2(\eta^6\text{-C}_6\text{Et}_6)_2\text{Cl}_3]^+\text{Cl}^-$. The complex $[\text{Ru}(\eta^6\text{-C}_6\text{Et}_6)\text{Cl}_2]_2$ is a useful synthetic precursor, as will be shown in the next chapter.

Chapter 3: *Hexaethylbenzene piano stool complexes*



Chem 3D representation of $\text{Ru}(\eta^6\text{-C}_6\text{Et}_6)(\text{Bu}^i\text{NC})\text{Cl}_2$

Preparation and characterization of complexes of the type $\text{Ru}(\eta^6\text{-C}_6\text{Et}_6)(\text{L})\text{Cl}_2$ ($\text{L}=\text{CO}$, Bu^iNC , PMe_3 , PPh_3)	88
Complexes of the type $\text{Ru}(\eta^6\text{-arene})(\text{PMe}_3)(\text{X})_m\text{Cl}_{(2-m)}$ ($\text{X} = \text{Me}$, $m = 1, 2$; $\text{X} = \text{H}$, $m = 2$)	90
Monomeric cationic ruthenium(II) complexes	92
Crystallographic determinations of the solid state structures of ruthenium complexes of hexaethylbenzene.	94
X-ray structures of complexes of the type $\text{Ru}(\eta^6\text{-C}_6\text{Et}_6)(\text{L})\text{Cl}_2$ ($\text{L}=\text{CO}$, Bu^iNC , PMe_3 , PPh_3).....	100
X-ray structures of complexes of the type $\text{Ru}(\eta^6\text{-arene})(\text{PMe}_3)(\text{X})_m\text{Cl}_{(2-m)}$ ($\text{X}=\text{Me}$, $m = 1, 2$; $\text{X} = \text{H}$, $m = 1$).....	109
X-ray structures of monomeric cationic ruthenium(II) complexes	118
The X-ray structures in general.....	130

A reaction scheme for the compounds described in this chapter is given in Figure 3.1. The Ru(II) compounds investigated fall into four categories. There are neutral ligand adducts of the type $\text{Ru}(\eta^6\text{-C}_6\text{Et}_6)(\text{L})\text{Cl}_2$ ($\text{L}=\text{CO}$, Bu^tNC , PMe_3 , PPh_3), neutral Ru(II) alkyl and hydride complexes of the type $\text{Ru}(\eta^6\text{-arene})(\text{PMe}_3)(\text{X})_m\text{Cl}_{(2-m)}$ (where $\text{X}=\text{Me}$, H ; $m=2$; $\text{X}=\text{Me}$ $m=1$), cationic complexes of the type $[\text{Ru}(\eta^6\text{-C}_6\text{Et}_6)(\text{L})(\text{L}')\text{Cl}]^+\text{PF}_6^-$ ($\text{L}=\text{CO}$, Bu^tNC ; $\text{L}'=\text{CO}$, Bu^tNC , all combinations; $\text{L}=\text{L}'=\text{CH}_3\text{CN}$), and lastly the dicationic complex $[\text{Ru}(\eta^6\text{-C}_6\text{Et}_6)(\text{CH}_3\text{CN})_3]^{2+}(\text{CF}_3\text{SO}_3^-)_2$. Some of these complexes were also prepared with trisbenzo(cyclooctene) and 1,3,5-tri-isopropylbenzene as the arene. All of these complexes were fully characterized by ^1H and $^{13}\text{C}\{^1\text{H}\}$ and, where applicable, $^{31}\text{P}\{^1\text{H}\}$ NMR spectroscopy, mass spectrometry, microanalysis or accurate mass determination, and single crystal X-ray crystallography where possible. Table 3.1 gives the characterizing data for these complexes.

In the room temperature ^1H and $^{13}\text{C}\{^1\text{H}\}$ NMR spectra for all these complexes the hexaethylbenzene ligand gave rise to a series of common features. In the ^1H NMR spectra a triplet (δ 1.12-1.80 ppm) and quartet (δ 2.10-2.59 ppm) were observed for the methylene and methyl protons respectively. The $^{13}\text{C}\{^1\text{H}\}$ NMR spectra for all complexes contained single resonances for the methyl (δ 14.2-22.3 ppm), methylene (δ 21.1-30.2 ppm) and aromatic carbon atoms (δ 101.1-118.9 ppm) of hexaethylbenzene. (see Table 4.1)

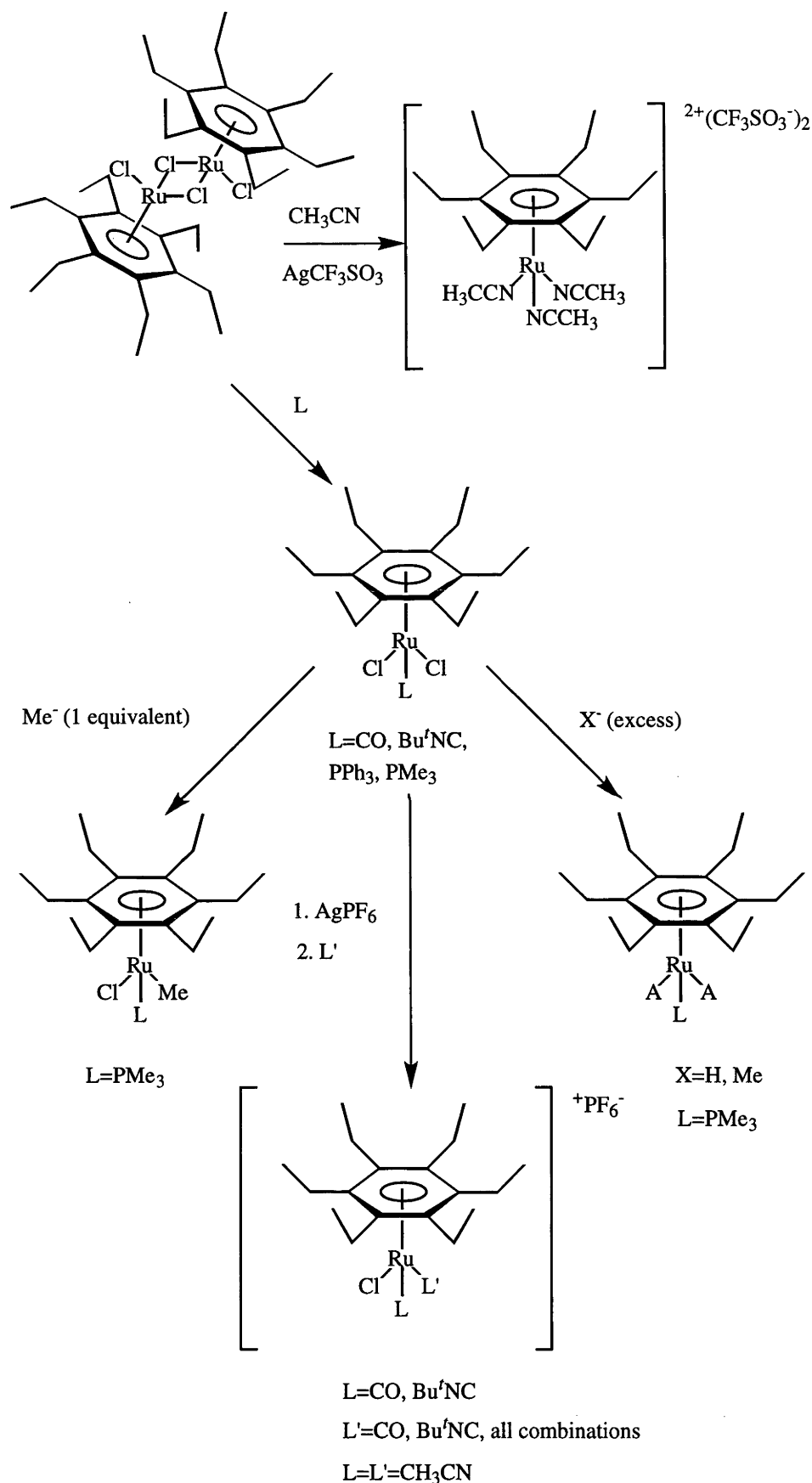


Figure 3.1. Reaction scheme for the compounds described in this chapter

Table 3.1. Characterizing data for new arene ruthenium complexes within this chapter

Complex	NMR data	Other Data
$\text{Ru}(\eta^6\text{-C}_6\text{Et}_6)(\text{PMe}_3)\text{Cl}_2$	^1H NMR (CD_2Cl_2 , 200 MHz) δ 2.40 (q, 12H, $^3J(\text{HH})$ 7.6 Hz, CH_2), 1.26 (d, 9H, $^2J(\text{PH})$ 10.4 Hz, PMe_3), 1.08 ppm (t, 18H, $^3J(\text{HH})$ 7.6 Hz, CH_3). $^{13}\text{C}\{^1\text{H}\}$ NMR (CD_2Cl_2 , 75.42 MHz) δ 100.5 (s, Caromatic), 22.6 (s, CH_2), 15.2 (d, $^1J(\text{PC})$ 34 Hz, PMe_3), 14.9 ppm (s, CH_3) $^3\text{P}\{^1\text{H}\}$ NMR (CD_2Cl_2 , 81.0 MHz) δ 3.1 ppm (s, PMe_3).	Anal. calcd. for $\text{C}_{21}\text{H}_{39}\text{Cl}_2\text{PRu}$: C 51.01; H 7.95. Found: C 50.98; H 7.80. m/z = 494 (M^+), m/z = 459 (M^+-Cl)
$\text{Ru}(\eta^6\text{-C}_{24}\text{H}_{36})(\text{PMe}_3)\text{Cl}_2$ ¹	^1H NMR (C_6D_6 , 300 MHz) δ 2.8-2.4 [m, $\text{CH}_2(\text{C}_{24}\text{H}_{36})$], 1.7-1.1 [m, $\text{CH}_2(\text{C}_{24}\text{H}_{36})$], 1.31 ppm (d, $J(\text{HP})$ 10.5 Hz, PMe_3) $^{13}\text{P}\{^1\text{H}\}$ NMR (C_6D_6 , 121.4 MHz) δ -1.7 ppm (s, PMe_3)	Anal. calcd. for $\text{C}_{27}\text{H}_{45}\text{Cl}_2\text{PRu}$: C 56.64; H 7.92; Cl 12.38. Found: C 56.74; H 7.83; Cl 12.56. m/z = 572 (M^+)
$\text{Ru}(\eta^6\text{-C}_6\text{Et}_6)(\text{PPh}_3)\text{Cl}_2$	^1H NMR (CD_2Cl_2 , 300 MHz) δ 7.3-8.1 (m, 15H, PPh_3), 2.26 (q, 12H, $^3J(\text{HH})$ 7.5 Hz, CH_2) 1.19 ppm (t, 18H, $^3J(\text{HH})$ 7.5 Hz, CH_3). $^{13}\text{C}\{^1\text{H}\}$ NMR (CD_2Cl_2 , 75.42 MHz) δ 136-128 (m, PPh_3), 101.9 (s, coord C), 22.2 (s, CH_2), 15.0 ppm (s, CH_3) $^3\text{P}\{^1\text{H}\}$ NMR (CD_2Cl_2 , 121.4 MHz) δ 24.0 ppm (s, PPh_3).	Anal. calcd. for $\text{C}_{36}\text{H}_{45}\text{Cl}_2\text{PRu}$: C 63.52; H 6.66. Found: C 61.97; H 6.67. m/z = 645, (M^+-PPh_3)
$\text{Ru}(\eta^6\text{-C}_6\text{Et}_6)(\text{CO})\text{Cl}_2$	^1H NMR (CD_2Cl_2 , 300 MHz) δ 2.52 (q, 12H, $^3J(\text{HH})$ 7.5 Hz, CH_2), 1.36 ppm (t, 18H, $^3J(\text{HH})$ 7.5 Hz, CH_3) $^{13}\text{C}\{^1\text{H}\}$ NMR (CD_2Cl_2 , 75.42 MHz) δ 193.4 (s, CO), 110.1 (s, Caromatic), 21.8 (s, CH_2), 14.6 ppm (s, CH_3)	Anal. calcd. for $\text{C}_{19}\text{H}_{30}\text{Cl}_2\text{ORu}$: C 51.12; H 6.77. Found: C 51.08; H 7.02. m/z = 418 (M^+-CO)

¹ $\text{C}_{24}\text{H}_{36}$ = benzotris(cyclooctene)

Table 3.1 continued

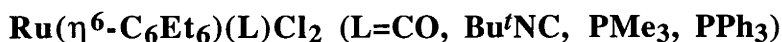
Complex	NMR data	Other data
$\text{Ru}(\eta^6\text{-C}_{24}\text{H}_{36})(\text{CO})\text{Cl}_2$	^1H NMR (CD_2Cl_2 , 300 MHz) δ 3.0-2.6 [m, $\text{CH}_2(\text{C}_{24}\text{H}_{36})$], 2.1-1.9 [m, $\text{C}_{24}\text{H}_{36}$], 1.8-1.3 [m, $\text{CH}_2(\text{C}_{24}\text{H}_{36})$]. $^{13}\text{C}\{^1\text{H}\}$ NMR (CD_2Cl_2 , 75.42 MHz) δ 109.1 (s, Aromatic), 31.1 [s, $\text{CH}_2(\text{C}_{24}\text{H}_{36})$], 28.8 [s, $\text{CH}_2(\text{C}_{24}\text{H}_{36})$], 27.19 ppm [s, $\text{CH}_2(\text{C}_{24}\text{H}_{36})$]	$m/z = 524 (\text{M}^+)$
$\text{Ru}(\eta^6\text{-C}_6\text{H}_3\text{Pr}^t_3)(\text{CO})\text{Cl}_2$	^1H NMR (CD_2Cl_2 , 300 MHz) δ 5.57 (s, $\text{CH}_{\text{aromatic}}$), 2.92 (d, $^3J(\text{HH})$ 7.2 Hz, $\text{CH}(\text{Pr}^t)$), 1.31 ppm [d, $^3J(\text{HH})$ 7.2 Hz, $\text{CH}_3(\text{Pr}^t)$] $^{13}\text{C}\{^1\text{H}\}$ NMR (CD_2Cl_2 , 125.74 MHz) δ 191.6 (s, CO), 121.5 (s, quaternary Aromatic), d 86.7 (s, $\text{CH}_{\text{aromatic}}$), 31.8 [s, $\text{CH}(\text{Pr}^t)$], 21.8 ppm [s, $\text{CH}_3(\text{Pr}^t)$]	Anal. calcd. for $\text{C}_{16}\text{H}_{24}\text{Cl}_2\text{ORu}$: C 47.53; H 5.98 Found: C 47.25; H 5.66. No fragments that could be related to this structure were observed in the EI mass spectrum
$\text{Ru}(\eta^6\text{-C}_6\text{Et}_6)(\text{Bu}^t\text{NC})\text{Cl}_2$	^1H NMR (CD_2Cl_2 , 300 MHz) δ 2.45 (q, 12H, $^3J(\text{HH})$ 7.5 Hz, CH_2), 1.53 (s, 9H, Bu^t), 1.34 ppm (t, 18H, $^3J(\text{HH})$ 7.5 Hz, CH_3) $^{13}\text{C}\{^1\text{H}\}$ NMR, δ 103.1 (s, $\text{C}_{\text{aromatic}}$), 30.7 [s, $\text{CH}_3 \text{Bu}^t$], 22.0 (s, CH_3), 15.0 ppm (s, CH_2)	Anal calcd. for $\text{C}_{22}\text{H}_{39}\text{Cl}_2\text{NRu}$: C 53.98; H 8.03; N 2.86. Found C 54.87; H 7.69; N 2.45. $m/z = 501 (\text{M}^+)$

Table 3.1 continued

Complex	NMR data	Other data
$\text{Ru}(\eta^6\text{-C}_6\text{Et}_6)(\text{PMe}_3)\text{ClMe}$	^1H NMR (CD_2Cl_2 , 300 MHz) δ 2.42 (q, 12H, $^3J(\text{HH})$ 7.5 Hz, CH_2), 1.26 (t, 18H, $^3J(\text{HH})$ 7.5 Hz, CH_3), 1.23 (d, $^2J(\text{HP})$ 9.2 Hz, PMe_3), 0.27 ppm [d, $^2J(\text{HP})$ 9.2 Hz, CH_3 (coordinated methyl group)] $^{13}\text{C}\{^1\text{H}\}$ NMR (CD_2Cl_2 , 75.42 MHz) δ 103.2 (s, Caromatic), 22.6 (s, CH_2), 15.9 (d, $^3J(\text{PC})$ 48 Hz, PMe_3), 15.7 (s, CH_3), 10.0 ppm [d, $^3J(\text{PC})$ 35 Hz, CH_3 (coordinated methyl group)] $^{31}\text{P}\{^1\text{H}\}$ NMR (CD_2Cl_2 , 121.24 MHz) δ 2.9 ppm (s, PMe_3)	Mass spectrum (EI, accurate mass with apparent resolution 1×10^4) Calcd. for $^{12}\text{C}_{22}^{1}\text{H}_{42}^{37}\text{Cl}^{31}\text{P}^{102}\text{Ru}$: 474.175615 amu Found : 474.176254 amu (1.3 ppm deviation)
$\text{Ru}(\eta^6\text{-C}_6\text{Et}_6)(\text{PMe}_3)\text{H}_2$	^1H NMR (C_6D_6 , 300 MHz) δ 2.34 (q, 12H, $^3J(\text{HH})$ 7.5 Hz, CH_2), 1.23 (t, 18H, $^3J(\text{HH})$ 7.5 Hz, CH_3), 1.20 (d, 9H, $^2J(\text{HP})$ 8.0 Hz, PMe_3), -10.84 ppm (d, 2H, $^2J(\text{PH})$ 50 Hz, coordinated hydride) $^{31}\text{P}\{^1\text{H}\}$ NMR δ 4.4 ppm (s, PMe_3) $^{13}\text{C}\{^1\text{H}\}$ (C_6D_6 , 75.42 MHz) δ 102.6 (s, Caromatic), 26.6 (d, $^1J(\text{CP})$ 48.5 Hz, PMe_3), 22.9 (s, CH_2), 19.7 ppm (s, CH_3)	Anal. calcd. for $\text{C}_{21}\text{H}_{41}\text{PRu}$: C 59.26; H 9.71. Found: C 59.08; H 9.50. $m/z = 424 (\text{M}^+)$
$[\text{Ru}(\eta^6\text{-C}_6\text{Et}_6)(\text{CH}_3\text{CN})_2\text{Cl}]^+\text{PF}_6^-$	^1H NMR ($\text{CD}_2\text{Cl}_2/\text{CH}_3\text{CN}$, 300 MHz) δ 2.46 (q, 12H, $^3J(\text{HH})$ 7.6 Hz, CH_2), 1.90 [br s, 3H, CH_3 (acetonitrile)], 1.31 ppm (t, 18H, $^3J(\text{HH})$ 7.5 Hz, CH_3) $^{13}\text{C}\{^1\text{H}\}$ NMR ($\text{CD}_2\text{Cl}_2/\text{CH}_3\text{CN}$, 75.42 MHz) δ 117.0 (s, CN), 100.3 (s, Caromatic), 21.4 (s, CH_2), 14.3 (s, CH_3), 1.0 ppm [m, CH_3 (acetonitrile)]	Anal. calcd. for $\text{C}_{22}\text{H}_{36}\text{N}_2\text{ClF}_6\text{PRu}$: C 43.32; H 5.95; N 4.59. Found: C 42.88; H 5.57; N 5.01. $m/z = 424 (\text{M}^+ - \text{CH}_3\text{CN})$

Table 3.1 continued

Complex	NMR data	Other data
$[\text{Ru}(\eta^6\text{-C}_6\text{Et}_6)(\text{CH}_3\text{CN})_3]^{2+}(\text{CF}_3\text{SO}_3^-)_2$	^1H NMR (CD_3CN , 300 MHz) δ 2.66 [br s, 9H, $\text{CH}_3(\text{acetonitrile})$], 2.50 (q, 12H, $^3J(\text{HH})$ 7.7 Hz, CH_2), 1.32 ppm (t, 18H, $^3J(\text{HH})$ 7.6 Hz, CH_3) ^{13}C (^1H) NMR ($\text{CD}_2\text{Cl}_2/\text{CD}_3\text{CN}$, 75.42 MHz) δ 116.9 (s, Caromatic), 21.4 (s, CH_2), 14.2 ppm (s, CH_3)	Anal calcd. for $\text{C}_{26}\text{H}_{39}\text{N}_3\text{F}_6\text{O}_6\text{S}_2\text{Ru}$: C 40.6; H 5.08; N 5.46. Found: C 40.51; H 4.87; N 5.60. m/z = 620 ($\text{M}^+ - \text{CF}_3\text{SO}_3$)
$[\text{Ru}(\eta^6\text{-C}_6\text{Et}_6)(\text{CO})_2\text{Cl}]^+\text{PF}_6^-$	^1H NMR (CD_2Cl_2 , 300 MHz) δ 2.67 (q, 12H, $^3J(\text{HH})$ 7.4 Hz, CH_2), 1.42 ppm (t, 18H, $^3J(\text{HH})$ 7.4 Hz, CH_3) ^{13}C (^1H) NMR (CD_2Cl_2 , 75.42 MHz) δ 160.1 (s, CO), 95.3 (s, Caromatic), 21.4 (s, CH_2), 15.0 (s, CH_3)	Anal calcd. for $\text{C}_{20}\text{H}_{30}\text{ClF}_6\text{O}_2\text{PRu}$: C 41.14; H 5.18 Found: C 40.83; H 4.89
$[\text{Ru}(\eta^6\text{-C}_6\text{Et}_6)(\text{Bu}^t\text{NC})_2\text{Cl}]^+\text{PF}_6^-$	^1H NMR (CD_2Cl_2 , 200 MHz) δ 2.49 (q, 12H, $^3J(\text{HH})$ 7.4 Hz, CH_2), 2.12 (s, 18H, $\text{CH}_3(\text{Bu}^t)$), 1.32 ppm (t, 18H, $^3J(\text{HH})$ 7.4 Hz, CH_3) ^{13}C (^1H) NMR (CD_2Cl_2 , 75.42 MHz) δ 138.3 (s, CN), 109.8 (s, Caromatic), 30.2 (s, $\text{CH}_3(\text{Bu}^t\text{NC})$), 22.3 (s, CH_2), 16.2 ppm (s, CH_3)	Anal calcd. for $\text{C}_{28}\text{H}_{48}\text{ClF}_6\text{N}_2\text{PRu}$: C 48.45; H 6.97; N 4.04. Found: C 47.73; H 6.77; N 4.28. m/z = 549 ($\text{M}^+ - \text{PF}_6$)
$[\text{Ru}(\eta^6\text{-C}_6\text{Et}_6)(\text{Bu}^t\text{NC})(\text{CO})\text{Cl}]^+\text{PF}_6^-$	^1H NMR (CD_2Cl_2 , 300 MHz) δ 2.59 (q, 12H, $^3J(\text{HH})$ 7.65 Hz, CH_2), 1.59 [s, $\text{CH}_3(\text{Bu}^t\text{NC})$], 1.37 ppm (t, 18H, $^3J(\text{HH})$ 7.65 Hz, CH_3) ^{13}C (^1H) NMR (CD_2Cl_2 , 75.42 MHz) δ 191.1 (s, CO), 118.9 (s, Caromatic), 30.2 (s, CH_2), 22.3 (s, CH_3), 16.2 ppm [s, $\text{CH}_3(\text{Bu}^t\text{NC})]$	Anal calcd. for $\text{C}_{24}\text{H}_{39}\text{ClF}_6\text{NOPRu}$: C 45.11; H 6.15; N 2.19. Found: C 44.65; H 6.14; N 2.11. m/z = 494 ($\text{M}^+ - \text{PF}_6$)

Preparation and characterization of complexes of the type

It has been known for some time that treatment of an arene dichloride dimer with many two electron ligands cleaves the two chloride bridges and gives rise to the mononuclear neutral ruthenium (II) adducts (see Chapter 1). In the course of this study the adducts between a number of different ligands and $[\text{Ru}(\eta^6\text{-arene})\text{Cl}_2]_2$ were prepared. These include complexes of the type $\text{Ru}(\eta^6\text{-arene})(\text{L})\text{Cl}_2$ (L=PMe₃, PPh₃, CO and Bu'NC).

The first complexes to be discussed are the simple trimethylphosphine and triphenylphosphine adducts. The trimethylphosphine adduct, $\text{Ru}(\eta^6\text{-C}_6\text{Et}_6)(\text{PMe}_3)\text{Cl}_2$, was prepared in a manner similar to that described in the literature for the preparation of $\text{Ru}(\eta^6\text{-C}_6\text{Me}_6)(\text{PMe}_3)\text{Cl}_2$.¹²¹ $[\text{Ru}(\eta^6\text{-C}_6\text{Et}_6)\text{Cl}_2]_2$ was heated in toluene for 2h to which a stoichiometric amount of trimethylphosphine had been added to give, after removal of solvent, 78% yield of a bright red air stable solid. Recrystallization from a mixture of dichloromethane layered with hexane gave red air stable needles overnight which were suitable for single crystal X-ray analysis. The corresponding benzotris(cyclooctene) complex, $\text{Ru}[\eta^6\text{-benzotris(cyclooctene)}](\text{PMe}_3)\text{Cl}_2$, could be prepared from $[\text{Ru}\{\eta^6\text{-benzotris(cyclooctene)}\}\text{Cl}_2]_2$ under the same reaction conditions. In CD_2Cl_2 at room temperature the ¹H NMR spectrum of both complexes contains a doublet for the phosphorus coupled PMe₃ protons at *ca.* δ 1.3 ppm. The ¹H NMR spectrum for the benzotris(cyclooctene) also contains a series of complex, poorly resolved overlapping multiplets for the protons of the alkyl rings in the benzotris(cyclooctene) complex. The ³¹P{¹H} NMR spectrum of both complexes contain a singlet, at δ 3.1 ppm for $\text{Ru}(\eta^6\text{-C}_6\text{Et}_6)(\text{PMe}_3)\text{Cl}_2$ and at δ -1.7 ppm for $\text{Ru}[\eta^6\text{-benzotris(cyclooctene)}](\text{PMe}_3)\text{Cl}_2$. These NMR data show no substantive differences from those reported for $\text{Ru}(\eta^6\text{-C}_6\text{Me}_6)(\text{PMe}_3)\text{Cl}_2$.¹²¹

The triphenylphosphine complex, $\text{Ru}(\eta^6\text{-C}_6\text{Et}_6)(\text{PPh}_3)\text{Cl}_2$, was prepared in a manner analogous to the PMe₃ complexes, except that a slight excess of the phosphine was used and the solvent employed was refluxing dichloromethane. It proved harder to separate this phosphine adduct from unwanted side products. The phosphine adduct was crystallized from dichloromethane layered with n-hexane and dark red needle-like crystals which were suitable for single crystal X-ray crystallography were obtained in 60% yield overnight. The ³¹P{¹H} NMR spectrum contained a single peak at δ 24.0 ppm for the coordinated PPh₃.

Following a procedure similar to that used to prepare the analogous complex, $\text{Ru}(\eta^6\text{-C}_6\text{Me}_6)(\text{CO})\text{Cl}_2$ ¹²² it is possible to prepare $\text{Ru}(\eta^6\text{-C}_6\text{Et}_6)(\text{CO})\text{Cl}_2$, $\text{Ru}[\eta^6\text{-}$

benzotris(cyclooctene)](CO)Cl₂ and Ru(η^6 -C₆H₃Pr^{*i*}₃)(CO)Cl₂. When a dichloromethane solution of the corresponding arene dichloride dimer is stirred under an atmosphere of CO for *ca.* 1h, the CO adducts, Ru(η^6 -arene)(CO)Cl₂, can be obtained in high yields (*ca.* 70%). It was also possible to prepare Ru(η^6 -C₆Et₆)(¹³CO)Cl₂ under the same conditions. After recrystallization from dichloromethane/ether, Ru(η^6 -C₆Et₆)(CO)Cl₂ is obtained as small dark red crystals suitable for single crystal X-ray analysis.

When the arene is hexaethylbenzene, if the reaction is left on too long (12 h), or too vigorous a stream of CO is used, the hexaethylbenzene is displaced and the resulting red solid contains Ru₃(CO)₁₂, as shown by the electron impact mass spectrum, as well as Ru(η^6 -C₆Et₆)(CO)Cl₂. This was not observed in the case of the hexamethylbenzene dichloride dimer and again suggests that the hexaethylbenzene may not be as strongly bonded to ruthenium as hexamethylbenzene.¹²²

In the ¹³C{¹H} NMR spectrum of Ru(η^6 -C₆Et₆)(CO)Cl₂ the resonance for the coordinated CO ligand appears at δ 193.4 ppm, in the expected region. The triisopropylbenzene complex has a ¹³C{¹H} NMR resonance at δ 191.6 ppm for the quaternary CO carbon atom, whereas the corresponding resonance was not visible in the spectrum of Ru(η^6 -tricyclooctene)(CO)Cl₂. The infrared spectra of Ru(η^6 -C₆Et₆)(CO)Cl₂, Ru(η^6 -tricyclooctene)(CO)Cl₂ and Ru(η^6 -C₆H₃Pr^{*i*}₃)(CO)Cl₂ (nujol mull) each contain a peak at 2010, 2005 and 2007 cm⁻¹ respectively due to C \equiv O stretching (*cf.* 2015cm⁻¹ observed for ν (CO) in the hexamethylbenzene complex¹²²).

When [Ru(η^6 -C₆Et₆)Cl₂]₂ is stirred with a stoichiometric amount of *t*-butylisocyanide in dichloromethane for 3h, the adduct, Ru(η^6 -C₆Et₆)(Bu^{*t*}NC)Cl₂ is obtained as a red solid in 37% yield. This complex is much more soluble than the corresponding CO complex in organic solvents, possibly due to the lipophilic nature of the Bu^{*t*} group. The complex can be recrystallized from dichloromethane/ether to give dark red crystals suitable for X-ray analysis. The ¹H NMR spectrum of this compound has a singlet at δ 1.53 ppm for the protons of the coordinated *t*-butylisocyanide. The ¹³C{¹H} NMR spectrum only had resonances for the ethyl, Bu^{*t*} methyl and coordinated aromatic carbons; resonances for the coordinated isocyanide carbon atoms and central carbon atoms of the *t*-butyl group were not visible. The infrared spectrum (KCl disk) of this complex displays a peak at 2168 cm⁻¹, which can be assigned to the CN stretching vibration of the isocyanide ligand. The spectroscopic data are similar to those for the previously prepared complex Ru(η^6 -C₆Me₆)(Bu^{*t*}NC)Cl₂.⁴⁵

Complexes of the type $\text{Ru}(\eta^6\text{-arene})(\text{PMe}_3)(\text{X})_m\text{Cl}_{(2-m)}$ (where $\text{X}=\text{Me}$, H ; $m=2$; $\text{X}=\text{Me}$ $m=1$)

The complex $\text{Ru}(\eta^6\text{-C}_6\text{Et}_6)(\text{PMe}_3)\text{MeCl}$ was prepared in a manner similar to that employed for $\text{Ru}(\eta^6\text{-C}_6\text{Me}_6)(\text{PMe}_3)(\text{Me})\text{Cl}^{56}$ and $\text{Ru}(\eta^6\text{-C}_6\text{Et}_6)(\text{PMe}_3)\text{Me}_2$ was prepared similarly to $\text{Ru}(\eta^6\text{-C}_6\text{Me}_6)(\text{PMe}_3)(\text{Me})_2$.⁴⁶ Treatment of $\text{Ru}(\eta^6\text{-C}_6\text{Et}_6)(\text{PMe}_3)\text{Cl}_2$ with methyl lithium for 1h at room temperature in toluene gives rise to a mixture of both $\text{Ru}(\eta^6\text{-C}_6\text{Et}_6)(\text{PMe}_3)\text{Me}_2$ and $\text{Ru}(\eta^6\text{-C}_6\text{Et}_6)(\text{PMe}_3)\text{MeCl}$. These two complexes can be separated by careful chromatography on an alumina column. A $^{31}\text{P}\{^1\text{H}\}$ NMR spectrum of the reaction mixture resulting from the use of a single equivalent of MeLi contained resonances for $\text{Ru}(\eta^6\text{-C}_6\text{Et}_6)(\text{PMe}_3)\text{Cl}_2$ and $\text{Ru}(\eta^6\text{-C}_6\text{Et}_6)(\text{PMe}_3)\text{Me}_2$ as well as the desired product, $\text{Ru}(\eta^6\text{-C}_6\text{Et}_6)(\text{PMe}_3)\text{MeCl}$. This suggests that the chloro(methyl) complex is not the favoured product. This could be a contributing factor in the poor yield of 27% of pale yellow crystals suitable for single crystal X-ray analysis obtained after chromatography and recrystallization from pentane.

Use of slightly more than two equivalents of MeLi under the same conditions as above favours formation of $\text{Ru}(\eta^6\text{-C}_6\text{Et}_6)(\text{PMe}_3)\text{Me}_2$. The green colour of the crude reaction mixture for the hexaethylbenzene complex suggests that some decomposition also occurs. The substance giving rise to the green colour does not run with toluene on an alumina column; thus it is possible after chromatography to obtain the dimethyl complex as pale yellow crystals suitable for single crystal X-ray analysis in 17% yield after recrystallization from a minimum amount of pentane. The high solubility of this complex in pentane may considerably lower the yield after recrystallization.

Microanalyses were not attempted of these complexes due to their air-sensitivity. Instead, FAB^+ accurate mass determinations were carried out.

The ^1H NMR spectrum for both complexes contain, as well as the resonances for the hexaethylbenzene ligand, two doublets assignable to the protons of PMe_3 and coordinated methyl groups, at δ 0.99 and -0.04 ppm respectively for $\text{Ru}(\eta^6\text{-C}_6\text{Et}_6)(\text{PMe}_3)\text{Me}_2$ and δ 1.23 and 0.27 ppm for $\text{Ru}(\eta^6\text{-C}_6\text{Et}_6)(\text{PMe}_3)(\text{Me})\text{Cl}$. The coordinated methyl groups give doublets at δ -4.4 and 10.0 ppm for the dimethyl and chloro(methyl) complexes respectively in the $^{13}\text{C}\{^1\text{H}\}$ NMR spectra. The $^{31}\text{P}\{^1\text{H}\}$ NMR spectra have single resonances at δ 6.0 and 10.00 ppm for the dimethyl and chloro(methyl) complexes respectively. The ^1H NMR data for the two hexaethylbenzene complexes are similar to

that for the analogous hexamethylbenzene complexes $\text{Ru}(\eta^6\text{-C}_6\text{Me}_6)(\text{PMe}_3)\text{Me}_2$ [^{31}P NMR(C_6D_6) δ 7.97 ppm; ^1H NMR δ 0.10 (Me), 1.09 ppm (PMe_3)] and $\text{Ru}(\eta^6\text{-C}_6\text{Me}_6)(\text{PMe}_3)\text{MeCl}$ [^{31}P NMR (C_6D_6) δ 5.07 ppm; ^1H NMR δ 1.23 (PMe_3), 0.83 ppm (Me)].^{46,56}

Reaction of $\text{Ru}(\eta^6\text{-C}_6\text{Et}_6)(\text{PMe}_3)\text{Cl}_2$ with a slight excess of NaBH_4 in refluxing dry degassed isopropanol for 1hr gives, upon removal of solvent, a pale grey solid from which it is possible to sublime the dihydride complex, $\text{Ru}(\eta^6\text{-C}_6\text{Et}_6)(\text{PMe}_3)(\text{H})_2$, at 10^{-2} mmHg and 100°C onto a probe cooled to -15°C . This colourless solid can be recrystallized from pentane, in which it is exceedingly soluble, to obtain colourless crystals of the pure compound in 59% yield. It is very reactive to both air and water. It abstracts chloride from dichloromethane to form both the dichloride complex and what is thought to be the (hydrido)chloro complex quite rapidly. Slow evaporation of a cooled pentane solution gave colourless plate-like crystals suitable for single crystal X-ray crystallography.

The ^1H NMR spectrum of this complex contains a resonance for the hydride ligand at δ -10.84 ppm as a doublet, almost identical with that observed for $\text{Ru}(\eta^6\text{-C}_6\text{Me}_6)(\text{PMe}_2\text{Ph})(\text{H})_2$ at δ -10.77 ppm,⁵³ and $\text{Ru}(\eta^6\text{-C}_6\text{Me}_6)(\text{PMe}_3)(\text{H})_2$ at δ -10.80 ppm⁵⁴, and a doublet at δ 1.20 ppm for the protons of the trimethylphosphine ligand.

There are several different literature preparations for (hydrido)chloro complexes of the type $\text{Ru}(\eta^6\text{-arene})(\text{PR}_3)(\text{H})\text{Cl}$, including the reaction of the dihalo complex with Zn dust in methanol at room temperature⁴⁷⁻⁵⁰ or with anhydrous Na_2CO_3 isopropanol.⁵¹⁻⁵³ Unfortunately neither of these methods was an effective way to prepare a pure sample of the (hydrido)chloro complex $\text{Ru}(\eta^6\text{-C}_6\text{Et}_6)(\text{PMe}_3)(\text{H})\text{Cl}$; inseparable mixtures of the dihydride, dichloride and what was thought to be the (hydrido)chloro complex were obtained. The ^1H NMR spectra of reaction mixtures characteristically contained a doublet at δ -9.7 ppm which was assigned to the (hydrido)chloro complex, *cf.* $\text{Ru}(\eta^6\text{-C}_6\text{Me}_6)(\text{PMe}_3)(\text{H})\text{Cl}$ δ -9.44 ppm.⁵³

Monomeric cationic ruthenium(II) complexes

Treatment of $[\text{Ru}(\eta^6\text{-C}_6\text{Et}_6)\text{Cl}_2]_2$ with a stoichiometric amount of NH_4PF_6 in acetonitrile gives rise to the cationic ruthenium(II) species $[\text{Ru}(\eta^6\text{-C}_6\text{Et}_6)(\text{CH}_3\text{CN})_2\text{Cl}]^+\text{PF}_6^-$ which is obtained in 47% yield as yellow plate-like crystals. Unfortunately it was not possible to obtain crystals of this compound suitable for single crystal X-ray analysis.

If a stronger chloride abstractor than NH_4PF_6 is used, it is possible to remove all the chloride ligands. When $[\text{Ru}(\eta^6\text{-C}_6\text{Et}_6)\text{Cl}_2]_2$ is treated with AgSO_3CF_3 in dichloromethane over a period of fifteen hours a grey solid (AgCl) precipitates. The colour of the solution is initially intensely orange but becomes very pale at the end of the reaction. Careful decanting after centrifugation, followed by removal of solvent under vacuum, gives a pale yellow solid, which is thought to be the Ru(II) complex $\text{Ru}(\eta^6\text{-C}_6\text{Et}_6)(\text{SO}_3\text{CF}_3)_2$. No characterization was undertaken as this complex is exceedingly moisture sensitive. When this compound is taken up in CH_3CN , a very pale yellow solution is obtained from which a pale yellow solid can be precipitated by the addition of pentane. This complex is the triflate salt of the Ru(II) dication, $[\text{Ru}(\eta^6\text{-C}_6\text{Et}_6)(\text{CH}_3\text{CN})_3]^{2+}(\text{CF}_3\text{SO}_3^-)_2$. Again it was not possible to obtain crystals suitable for single crystal X-ray crystallography.

Unless an excess of acetonitrile is present in solutions of either the bis- or tris-acetonitrile complexes decomposition occurs, to give either $[\text{Ru}(\eta^6\text{-C}_6\text{Et}_6)\text{Cl}_2]_2$ or $[\text{Ru}_2(\eta^6\text{-C}_6\text{Et}_6)_2\text{Cl}_3]^+\text{PF}_6^-$ in the case of chlorinated solvents, or an unknown species in the case of acetone. The acetonitrile ligands in these complexes are clearly exceedingly labile. This was also the case with the analogous benzene complexes, $[\text{Ru}(\eta^6\text{-C}_6\text{H}_6)(\text{CH}_3\text{CN})_3]^+\text{PF}_6^-$ ⁵⁹ and $\text{Ru}(\eta^6\text{-C}_6\text{H}_6)(\text{CH}_3\text{CN})_2\text{Cl}]^+\text{PF}_6^-$ ⁵⁸.

If the CO adduct, $\text{Ru}(\eta^6\text{-C}_6\text{Et}_6)(\text{CO})\text{Cl}_2$, is treated with a stoichiometric amount of AgPF_6 in the dark in a dichloromethane solution for ten minutes and then stirred under an atmosphere of CO for two hours the cationic ruthenium(II) half sandwich complex, $[\text{Ru}(\eta^6\text{-C}_6\text{Et}_6)(\text{CO})_2\text{Cl}]^+\text{PF}_6^-$ is formed. The analogous hexamethylbenzene complex has been prepared by a similar method.⁵⁰ The complex $[\text{Ru}(\eta^6\text{-C}_6\text{Et}_6)(\text{CO})_2\text{Cl}]^+\text{PF}_6^-$ can be recrystallized from $\text{CH}_2\text{Cl}_2/\text{Et}_2\text{O}$ to give pale yellow needle-like crystals. Two bands were observed for $\nu(\text{CO})$ in the solid state spectrum of this complex; 2064 and 2000 cm^{-1} .

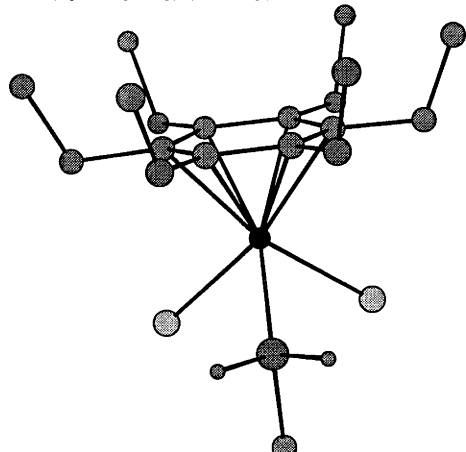
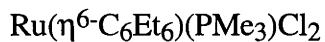
If the *t*-butylisocyanide adduct, $\text{Ru}(\eta^6\text{-C}_6\text{Et}_6)(\text{Bu}^t\text{NC})\text{Cl}_2$ is treated the same way, $[\text{Ru}(\eta^6\text{-C}_6\text{Et}_6)(\text{CO})(\text{Bu}^t\text{NC})\text{Cl}]^+\text{PF}_6^-$ can be obtained, after repeated recrystallization from $\text{CH}_2\text{Cl}_2/\text{Et}_2\text{O}$, as yellow plate-like crystals suitable for single crystal X-ray crystallography. This complex, having three different sterically undemanding ligands in the tripod, was prepared specifically as a probe for arene ruthenium rotation (Chapter 4). The solid state infrared spectrum of this complex has bands assignable to $\nu(\text{CN})$ and $\nu(\text{CO})$ at 2207 and 2035 cm^{-1} respectively. An attempt to prepare this complex by treatment of the CO adduct with AgPF_6 followed by the addition of a stoichiometric amount of *t*-butylisocyanide did not give the same product. Rather, the CO is preferentially displaced by the isocyanide ligand to yield $[\text{Ru}(\eta^6\text{-C}_6\text{Et}_6)(\text{Bu}^t\text{NC})_2\text{Cl}]^+\text{PF}_6^-$ and $\text{Ru}(\eta^6\text{-C}_6\text{Et}_6)(\text{Bu}^t\text{NC})\text{Cl}_2$.

The complex $[\text{Ru}(\eta^6\text{-C}_6\text{Et}_6)(\text{Bu}^t\text{NC})_2\text{Cl}]^+\text{PF}_6^-$ can be obtained, as expected, from treatment of the monoisocyanide adduct, $\text{Ru}(\eta^6\text{-C}_6\text{Et}_6)(\text{Bu}^t\text{NC})\text{Cl}_2$, with AgPF_6 in CH_2Cl_2 followed by addition of one equivalent of *t*-butylisocyanide. This complex too can be recrystallized from $\text{CH}_2\text{Cl}_2/\text{Et}_2\text{O}$ to give a yellow solid, again as yellow needles. Bands assignable to $\nu(\text{CN})$ were found at 2202 and 2186 cm^{-1} in the infrared spectrum. All the cationic species tended to be yellower in colour than the neutral species, which were red or orange.

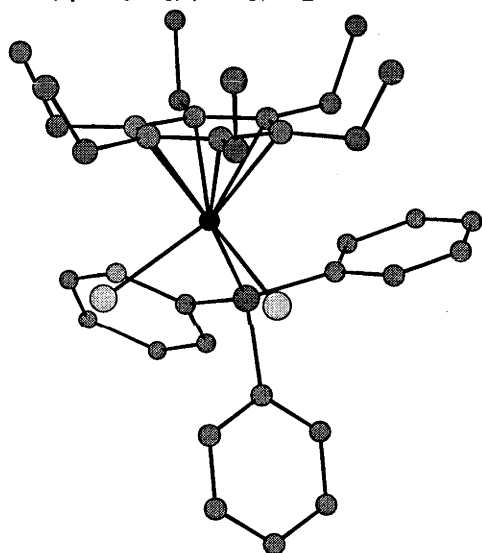
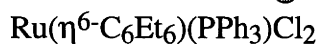
Crystallographic determinations of the solid state structures of ruthenium complexes of hexaethylbenzene.

All the half sandwich η^6 -hexaethylbenzene complexes studied by single crystal X-ray crystallography have the classical piano stool structure, with the arene forming the seat of the piano stool and the three monodentate ligands forming the legs which, with the ruthenium atom, form a tripod. Within each complex the six arene carbon atoms are displaced approximately the same distance from the ruthenium atom and are almost coplanar. In general, the C-C bond distances within the arene ring do not vary greatly between complexes (*ca.* 1.44 Å) or within each ring. The ruthenium-arene carbon atoms bond lengths range from 2.172 to 2.303 Å while the ruthenium-chlorine atom bond lengths range from 2.375 to 2.461 Å for those compounds containing chlorine ligands. There are two different rotational orientations of the arene with respect to the ligands when viewed along the arene ruthenium bond axis: either the ligands eclipse alternating arene carbon atoms or the ligands are between the aromatic carbon atoms. Four different conformations of ethyl groups are observed in the solid state structures of these complexes: the all distal conformation, the 1,3,5-proximal-2,4,6-distal conformation, the 1,4-proximal-2,4,5,6-distal conformation and the 1,3 proximal-2,4,5,6-distal conformation. A summary of the pertinent data for each complex along with a Chem 3D representation of the solid state structure is contained in Table 3.2 below. The conditions under which the data for the X-ray structures were collected and solved is at the end of Chapter 5.

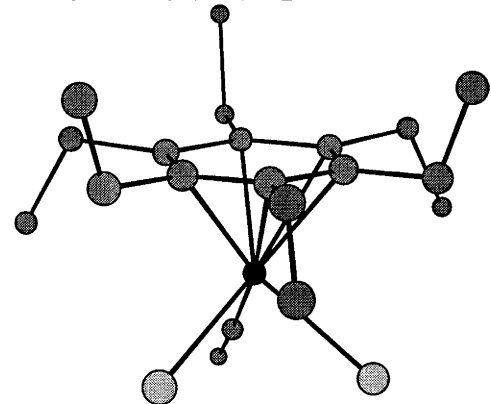
Table 3.2. Selected properties of tripodal arene ruthenium complexes



Ethyl conformation: All distal
 Ring orientation: not eclipsed
 Arene metal distance: 1.696(1) Å
 Average Ru-C_{aromatic} distance:
 2.22 Å
 Ru-Cl distance: 2.4181(9)

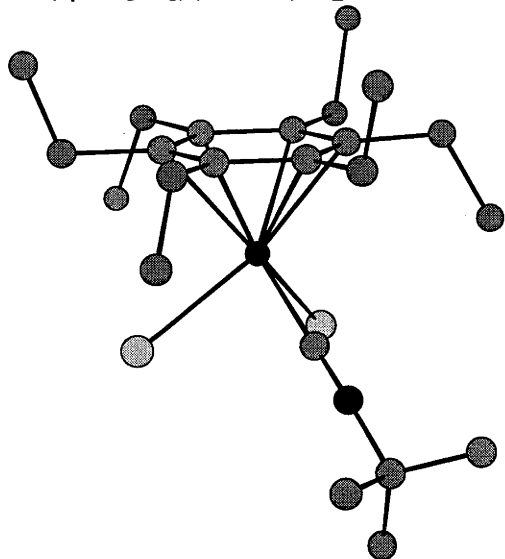
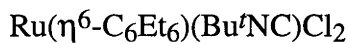


Ethyl conformation: All distal
 Ring orientation: not eclipsed
 Arene metal distance: 1.720(2) Å
 Average Ru-C_{aromatic} distance:
 2.31 Å
 Ru-Cl distance: 2.423(1), 2.412(1) Å

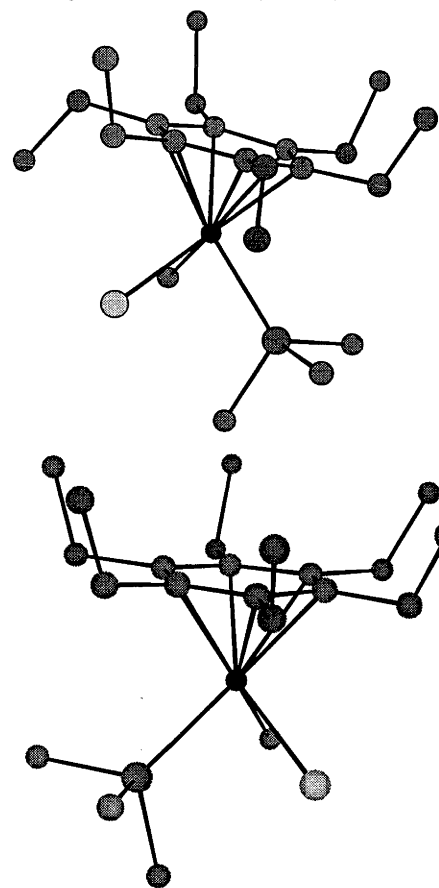
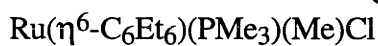


Ethyl conformation:
 1,3,5-proximal-2,4,6-distal
 Ring orientation: eclipsed
 Arene metal distance: 1.736(3) Å
 Average Ru-C_{aromatic} distance:
 2.24 Å
 Ru-Cl distance: 2.383(2) Å

Table 3.2. continued

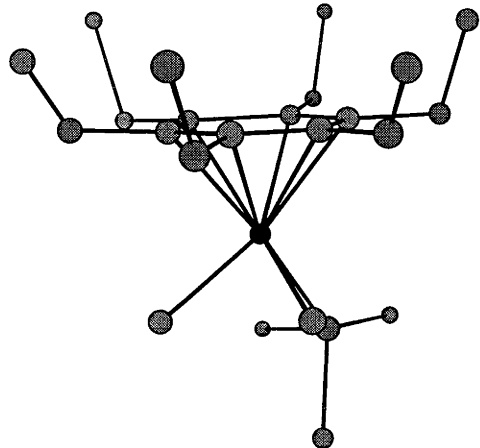
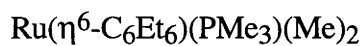


Ethyl conformation:
 1,3,5-proximal-2,4,6-distal
 Ring orientation: eclipsed
 Arene metal distance: 1.699(3) Å
 Average Ru-C_{aromatic} distance:
 2.22 Å
 Ru-Cl distance: 2.410(2) Å

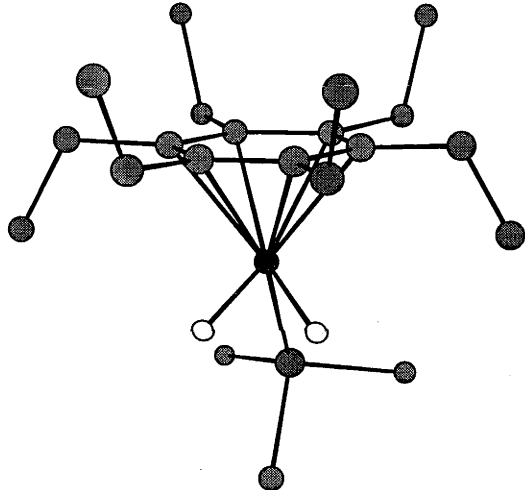
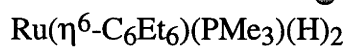


Ethyl conformation:
 1,3-proximal-2,4,5,6-distal
 1,3,5-proximal-2,4,6-distal
 Ring orientation: not eclipsed
 Arene metal distance:
 1.731(3), 1.725(3) Å
 Average Ru-C_{aromatic} distance:
 2.24, 2.24 Å
 Ru-Cl distance: 2.400(1), 2.426(1) Å

Table 3.2. continued

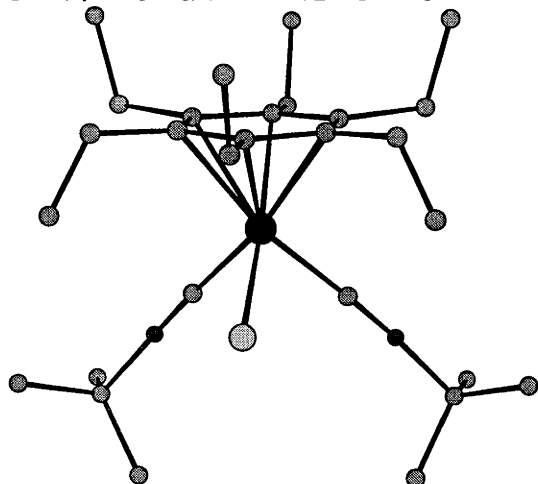
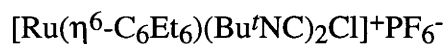


Ethyl conformation: all distal
Ring orientation: not eclipsed
Arene metal distance: 1.745(16) Å
Average Ru-C_{aromatic} distance:
2.25 Å

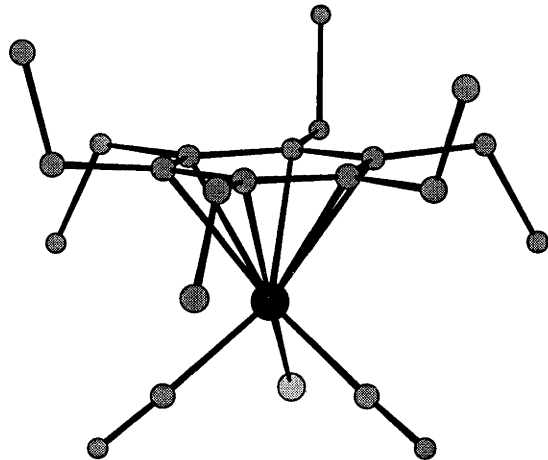
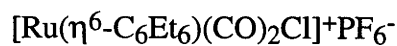
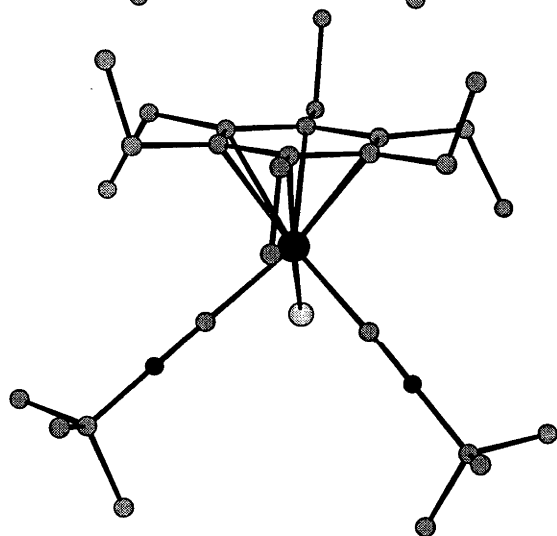


Ethyl conformation:
1,4-proximal-2,3,5,6-distal
Ring orientation:
not eclipsed
Arene metal distance: 1.7398(4) Å
Average Ru-C_{aromatic} distance:
2.26 Å

Table 3.2. continued

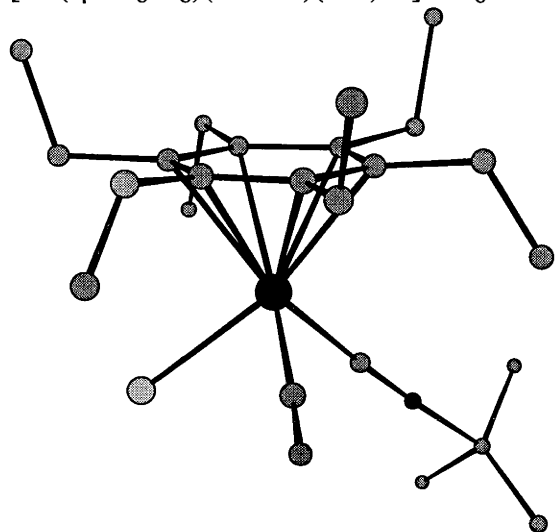


Ethyl conformation:
 1,3-proximal-2,4,5,6-distal
 1,3,5-proximal-2,4,6-distal
 Ring orientation: eclipsed
 Arene metal distance: 1.7532(14) Å
 Average Ru-C_{aromatic} distance:
 2.28, 2.26 Å
 Ru-Cl distance: 2.397(1), 2.405(1) Å



Ethyl conformation:
 1,3,5-proximal-2,4,6-distal
 Ring orientation: eclipsed
 Arene metal distance: 1.808(2) Å
 Average Ru-C_{aromatic} distance:
 2.30 Å
 Ru-Cl distance: 2.3755(8) Å

Table 3.2. continued



Ethyl conformation:
1,3,5-proximal-2,4,6-distal
Ring orientation: eclipsed
Arene metal distance: 1.793(2) Å
Average Ru-C_{aromatic} distance:
2.29 Å
Ru-Cl distance: 2.385(2) Å
¹³C{¹H} NMR δ C_{aromatic} 118.9 ppm

X-ray structures of complexes of the type $\text{Ru}(\eta^6\text{-C}_6\text{Et}_6)(\text{L})\text{Cl}_2$ ($\text{L}=\text{CO}$, Bu^tNC , PMe_3 , PPh_3)

The two tertiary phosphine adducts, $\text{Ru}(\eta^6\text{-C}_6\text{Et}_6)(\text{PMe}_3)\text{Cl}_2$ and $\text{Ru}(\eta^6\text{-C}_6\text{Et}_6)(\text{PPh}_3)\text{Cl}_2$, have the same gross structural features. ORTEP diagrams and tables of selected bond lengths and angles are listed in Figures 3.2 and 3.3 and Tables 3.3 and 3.4.

The few minor differences between these two structures are consistent with the relative steric bulks of triphenylphosphine and trimethylphosphine. For the triphenylphosphine complex, the arene is further from the ruthenium (Ru-arene ring centroid = 1.720(2) Å as against 1.696(1) Å), the chloride-ruthenium-chloride angle is smaller (*ca.* 88° as against 90°) and the ruthenium-phosphorus distance is longer (2.388(1) Å as against 2.343(1) Å). This could be explained by the greater steric bulk of the triphenylphosphine ligand pushing the arene away, forcing the two chloride ligands closer together and preventing the phosphine ligand approaching the ruthenium atom as closely. The $(\text{PPh}_3)\text{Cl}_2$ tripod is slightly asymmetric ($\text{P}(1)\text{-Ru}(1)\text{-Cl}(1) = \text{ca. } 87^\circ$ while $\text{P}(1)\text{-Ru}(1)\text{-Cl}(2) = \text{ca. } 82^\circ$) again probably because of steric demands of the triphenylphosphine ligand. In both these complexes the ethyl groups of the coordinated arene are all distal with respect to the ruthenium centre, possibly because the relative steric bulk of the ligand substituents interferes with the ethyl groups of the hexaethylbenzene. Another feature of these two complexes is that, when viewed along the arene-ruthenium bond axis the ligand tripod does not eclipse the arene carbon atoms.

The molecular structures of many complexes of the type $\text{Ru}(\eta^6\text{-arene})(\text{PR}_3)\text{Cl}_2$ have been determined by X-ray crystallography. A comparison of some of these complexes containing similar phosphines and those complexes prepared here shows no substantive differences. In some cases, eg. $\text{Ru}(\eta^6\text{-C}_6\text{H}_6)(\text{PPh}_2\text{Me})\text{Cl}_2$, $\text{Ru}(\eta^6\text{-}p\text{-cymene})(\text{PPh}_2\text{Me})\text{Cl}_2$ ¹²³ and $\text{Ru}(\eta^6\text{-C}_6\text{H}_6)(\text{PPh}_3)\text{Cl}_2$ ¹²⁴ the Ru-C bond distances opposite the P-ligand are greater than those opposite the chloride ligands, i.e. the ring is slightly non-planar. While there is some asymmetry of ruthenium to arene carbon ring distances, [Ru-C = 2.196-2.251(3) Å in $\text{Ru}(\eta^6\text{-C}_6\text{Et}_6)(\text{PMe}_3)\text{Cl}_2$ and 2.207-2.252(5) Å for $\text{Ru}(\eta^6\text{-C}_6\text{Et}_6)(\text{PPh}_3)\text{Cl}_2$] there is no systematic lengthening trans to the phosphine ligand.

Comparison of the molecular structures of $\text{Ru}(\eta^6\text{-C}_6\text{H}_6)(\text{PPh}_3)\text{Cl}_2$ ¹²⁴ and $\text{Ru}(\eta^6\text{-C}_6\text{Et}_6)(\text{PPh}_3)\text{Cl}_2$ gives insight into the nature of hexaethylbenzene as a ligand relative to benzene. For the hexaethylbenzene complex the Ru-P distance is slightly longer

(2.388(1) Å compared with 2.3637(2) Å for the benzene complex) and the Ru-arene carbon distances are on average slightly longer (2.312 Å as against 2.238 Å). The Ru-Cl distances are almost equal (*ca.* 2.41 Å), and the benzene complex displays the same asymmetry of P-Ru-Cl angles. One can easily ascribe these differences to the relative steric bulk of the two arenes. The two complexes also have a different rotational orientation of the arene with respect to the tripod; the tripod eclipses three of the arene carbon atoms in the benzene case, but does not in the hexaethylbenzene case.

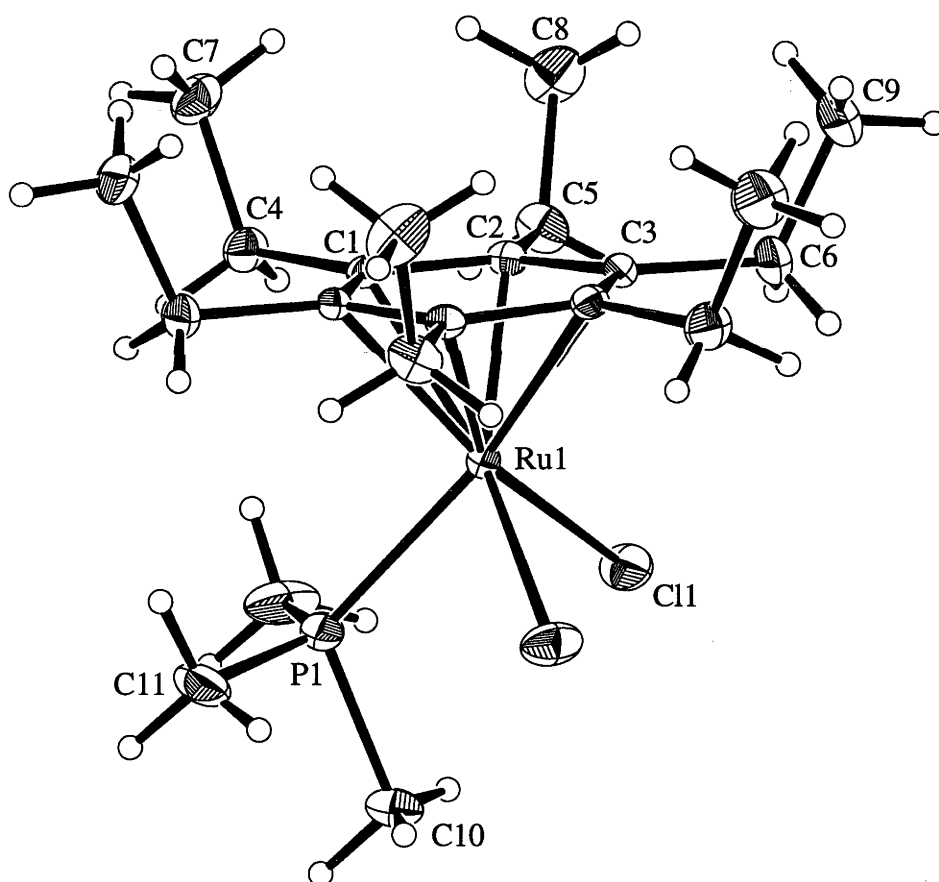


Figure 3.2. ORTEP plot of the solid state structure of
 $\text{Ru}(\eta^6\text{-C}_6\text{Et}_6)(\text{PMe}_3)\text{Cl}_2$

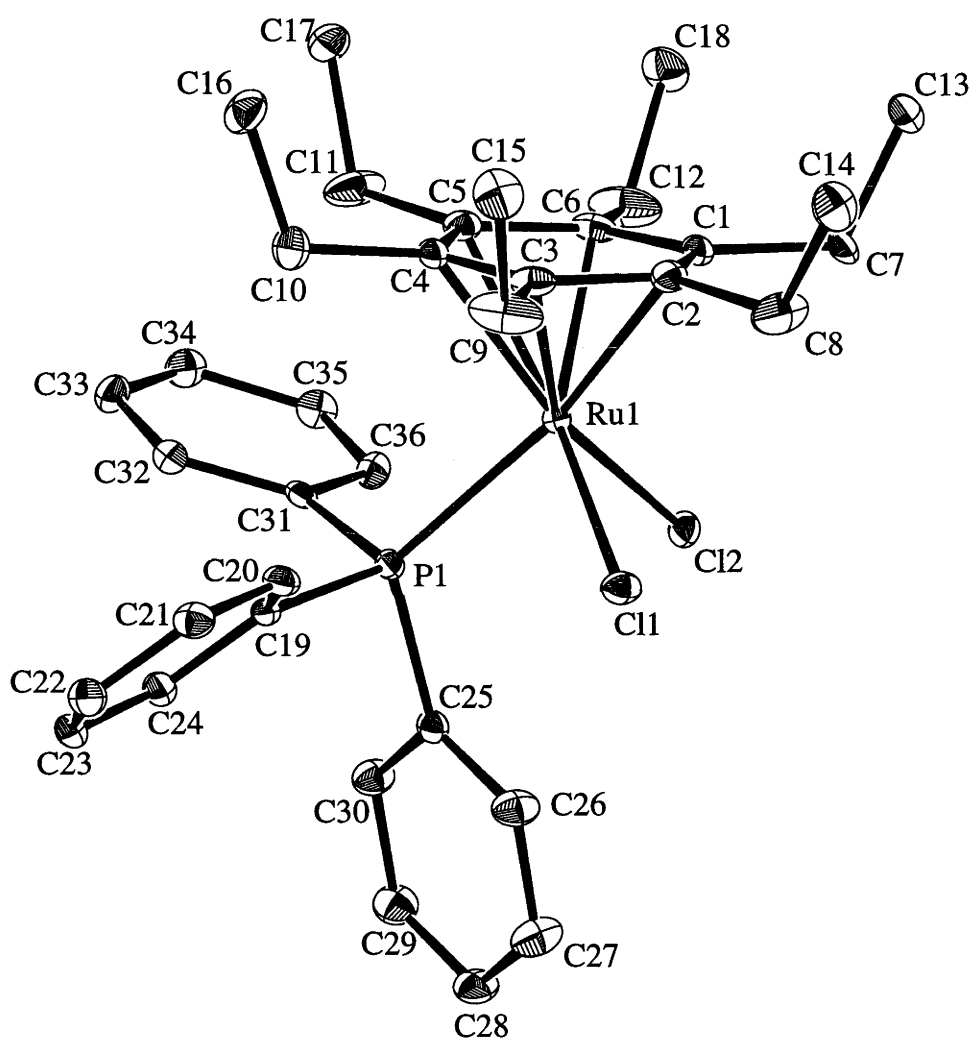


Figure 3.3. ORTEP plot of the solid state structure of $\text{Ru}(\eta^6\text{-C}_6\text{Et}_6)(\text{PPh}_3)\text{Cl}_2$

Table 3.3. Selected distances(Å) and angles (°) for Ru(η^6 -C₆Et₆)(PMe₃)Cl₂

Ru(1)-Cl(1)	2.4181(9)	Ru(1)-Cl(1)	2.4181(9)
Ru(1)-P(1)	2.343(1)	Ru(1)-C(1)	2.200(3)
Ru(1)-C(1')	2.200(3)	Ru(1)-C(2)	2.196(3)
Ru(1)-C(2')	2.196(3)	Ru(1)-C(3)	2.251(3)
Ru(1)-C(3')	2.251(3)	P(1)-C(10)	1.810(5)
P(1)-C(11)	1.98(1)	P(1)-C(11)	1.98(1)
P(1)-C(11')	1.69(1)	P(1)-C(11')	1.69(1)
C(1)-C(1')	1.431(6)	C(1)-C(2)	1.416(4)
C(1)-C(4)	1.526(4)	C(2)-C(3)	1.440(4)
C(2)-C(5)	1.521(4)	C(3)-C(3')	1.416(6)
C(3)-C(6)	1.516(4)	C(4)-C(7)	1.512(4)
C(5)-C(8)	1.498(4)	C(6)-C(9)	1.490(4)
C(11)-C(11')	1.12(1)	Ru(1)-centroid	1.696(1)
Cl(1) Ru(1) Cl(1)	90.35(5)	C(3) C(6) C(9)	115.9(3)
Cl(1) Ru(1) P(1)	82.11(3)	C(1) C(2) C(3)	120.5(3)
C(1) C(4) C(7)	114.2(3)	C(2) C(3) C(3')	119.6(2)
C(2) C(5) C(8)	114.6(3)	C(1') C(1) C(2)	119.8(2)

Table 3.4. Selected distances(Å) and angles (°) for Ru(η^6 -C₆Et₆)(PPh₃)Cl₂

Ru(1)-Cl(1)	2.423(1)	Ru(1)-Cl(2)	2.412(1)
Ru(1)-P(1)	2.388(1)	Ru(1)-C(1)	2.235(5)
Ru(1)-C(2)	2.242(5)	Ru(1)-C(3)	2.207(5)
Ru(1)-C(4)	2.234(5)	Ru(1)-C(5)	2.252(5)
Ru(1)-C(6)	2.217(5)	C(1)-C(6)	1.437(8)
C(1)-C(2)	1.403(7)	C(2)-C(3)	1.454(8)
C(1)-C(7)	1.523(7)	C(3)-C(4)	1.395(7)
C(2)-C(8)	1.513(8)	C(4)-C(5)	1.423(7)
C(3)-C(9)	1.512(7)	C(5)-C(6)	1.414(7)
C(4)-C(10)	1.533(7)	C(6)-C(12)	1.502(7)
C(5)-C(11)	1.511(7)	C(8)-C(14)	1.493(8)
C(7)-C(13)	1.506(7)	C(10)-C(16)	1.511(8)
C(9)-C(15)	1.519(8)	C(12)-C(18)	1.512(8)
C(11)-C(17)	1.505(8)	Ru(1)-centroid	1.720(2)
Cl(1) Ru(1) Cl(2)	87.99(4)	C(6) C(1) C(2)	120.7(4)
Cl(1) Ru(1) P(1)	86.83(5)	C(6) C(12) C(18)	117.4(6)
Cl(2) Ru(1) P(1)	82.63(4)	C(1) C(2) C(3)	118.9(5)
C(1) C(7) C(13)	113.7(4)	C(2) C(3) C(4)	120.0(5)
C(2) C(8) C(14)	117.9(5)	C(3) C(4) C(5)	120.9(4)
C(3) C(9) C(15)	115.6(5)	C(4) C(5) C(6)	119.7(5)
C(4) C(10) C(16)	114.2(5)	C(5) C(6) C(1)	119.6(5)
C(5) C(11) C(17)	115.9(5)		

It can be seen from Figures 3.4 and 3.5 that the molecular structures of $\text{Ru}(\eta^6\text{-C}_6\text{Et}_6)(\text{CO})\text{Cl}_2$ and $\text{Ru}(\eta^6\text{-C}_6\text{Et}_6)(\text{Bu}^t\text{NC})\text{Cl}_2$ as determined by single crystal X-ray crystallography are very similar. The CO and Bu^tNC ligands are end on C-bonded and essentially linear, with Ru-C distances of 1.904(9) and 1.970(7) Å respectively. The arene ring is orientated in both such that, when viewed along the arene ruthenium bond axis, the three the arene carbon atoms bearing distal ethyl groups eclipse the tripodal ligand substituents. While *t*-butyl is usually considered a bulky group, it can be seen, even if only in a qualitative manner, that in the isocyanide complex, where the central carbon atom of the Bu^t groups are *ca.* 5 Å from the ruthenium atom, that interactions between the ethyl groups and the *t*-butyl moiety are limited. Thus the *t*-butylisocyanide can be considered to behave sterically like carbon monoxide ligand, at least as far as its effect on the conformation of the hexaethylbenzene is concerned. In these two cases the limited steric interference of three small, essentially cylindrical ligands allows the hexaethylbenzene to adopt the same conformation as observed in solid state for the free ligand, i.e. the ethyl groups are staggered proximal/distal to minimize steric interaction between them. Tables of pertinent bond lengths and angles are listed in Table 3.5 and 3.6 below. A discussion of CO and isocyanide metrical parameters is given below in the section devoted to cationic ruthenium (II) complexes.

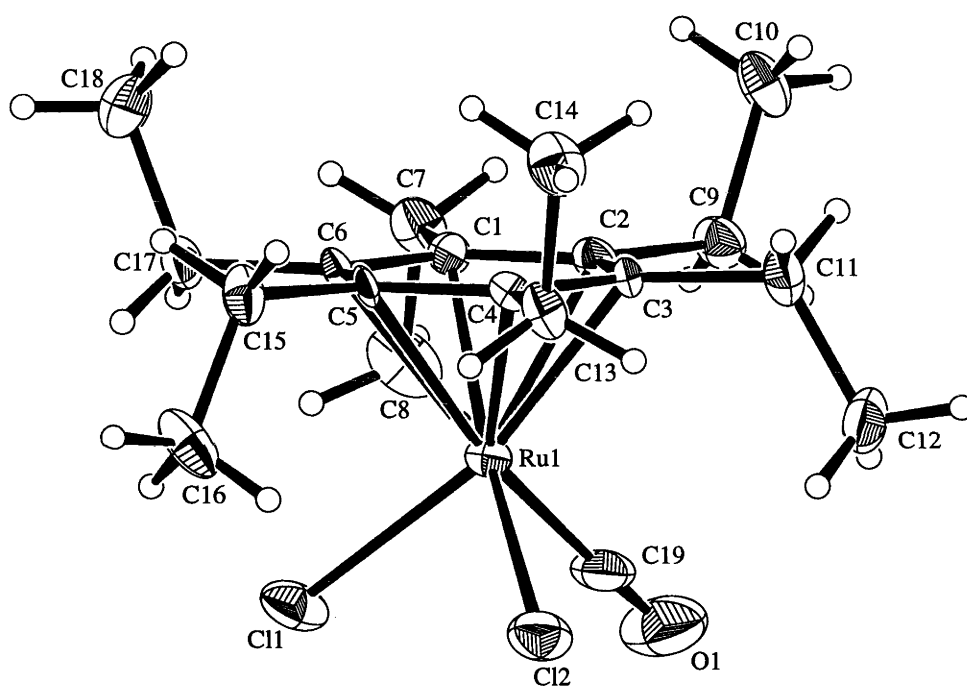


Figure 3.4. ORTEP diagram showing solid state structure of $\text{Ru}(\eta^6\text{-C}_6\text{Et}_6)(\text{CO})\text{Cl}_2$

Table 3.5. Selected bond lengths and angles for Ru(C₆Et₆)(CO)Cl₂

Ru(1)-Cl(1)	2.381(2)	Ru(1)-Cl(2)	2.383(2)
Ru(1)-C(1)	2.237(6)	Ru(1)-C(2)	2.201(7)
Ru(1)-C(3)	2.239(7)	Ru(1)-C(4)	2.261(6)
Ru(1)-C(5)	2.272(6)	Ru(1)-C(6)	2.240(7)
Ru(1)-C(19)	1.904(9)	O(1)-C(19)	1.012(9)
C(1)-C(2)	1.431(9)	C(1)-C(6)	1.402(9)
C(1)-C(7)	1.532(9)	C(2)-C(3)	1.423(9)
C(2)-C(9)	1.532(9)	C(3)-C(4)	1.436(9)
C(3)-C(11)	1.518(9)	C(4)-C(5)	1.420(8)
C(4)-C(13)	1.505(8)	C(5)-C(6)	1.401(8)
C(5)-C(15)	1.522(9)	C(6)-C(17)	1.510(8)
C(7)-C(8)	1.53(1)	C(9)-C(10)	1.520(9)
C(11)-C(12)	1.53(1)	C(13)-C(14)	1.538(9)
C(15)-C(16)	1.51(1)	C(17)-C(18)	1.535(9)
		Ru-ring centroid	1.736(3)
Cl(1) Ru(1) Cl(2)	86.97(7)	C(2) C(9) C(10)	115.1(6)
Cl(1) Ru(1) C(19)	85.1(3)	C(3) C(11) C(12)	116.6(7)
Cl(2) Ru(1) C(19)	86.0(3)	C(5) C(15) C(16)	116.3(6)
Ru(1) C(19) O(1)	177(1)	C(6) C(17) C(18)	110.5(6)
C(1) C(7) C(8)	115.1(6)		

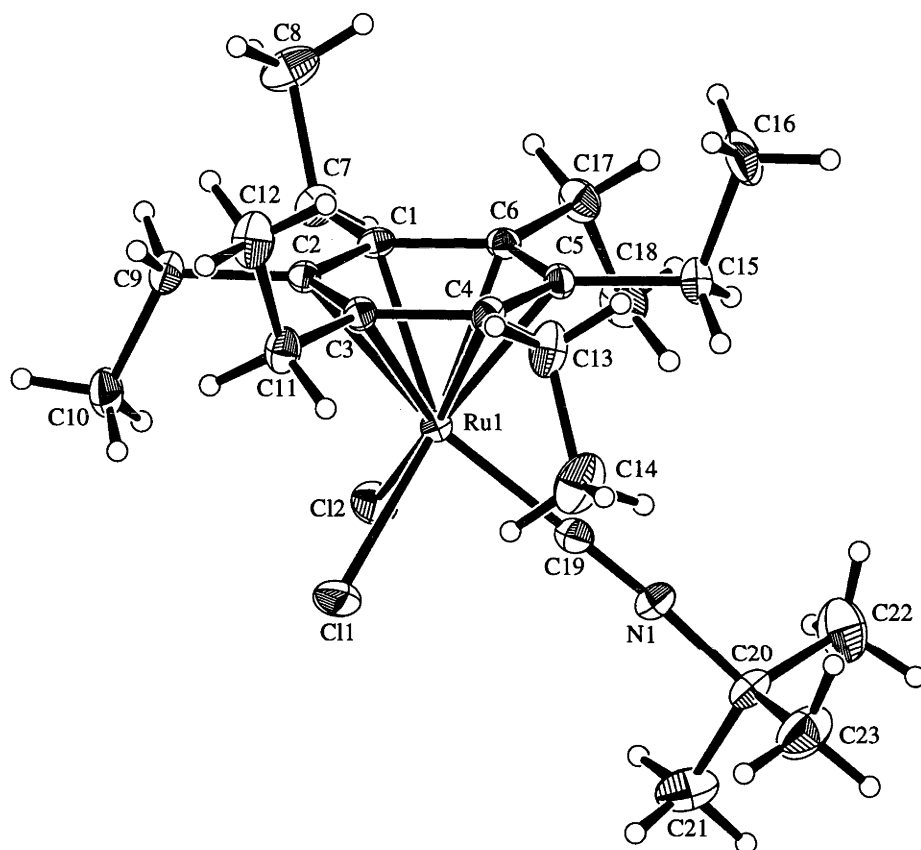


Figure 3.5. ORTEP plot of solid state structure of $\text{Ru}(\eta^6\text{-C}_6\text{Et}_6)(\text{Bu}^t\text{NC})\text{Cl}_2$

Table 3.6. Selected bond lengths (Å) and angles for (°)

 $\text{Ru}(\eta^6\text{-C}_6\text{Et}_6)(\text{Bu}^t\text{NC})\text{Cl}_2$

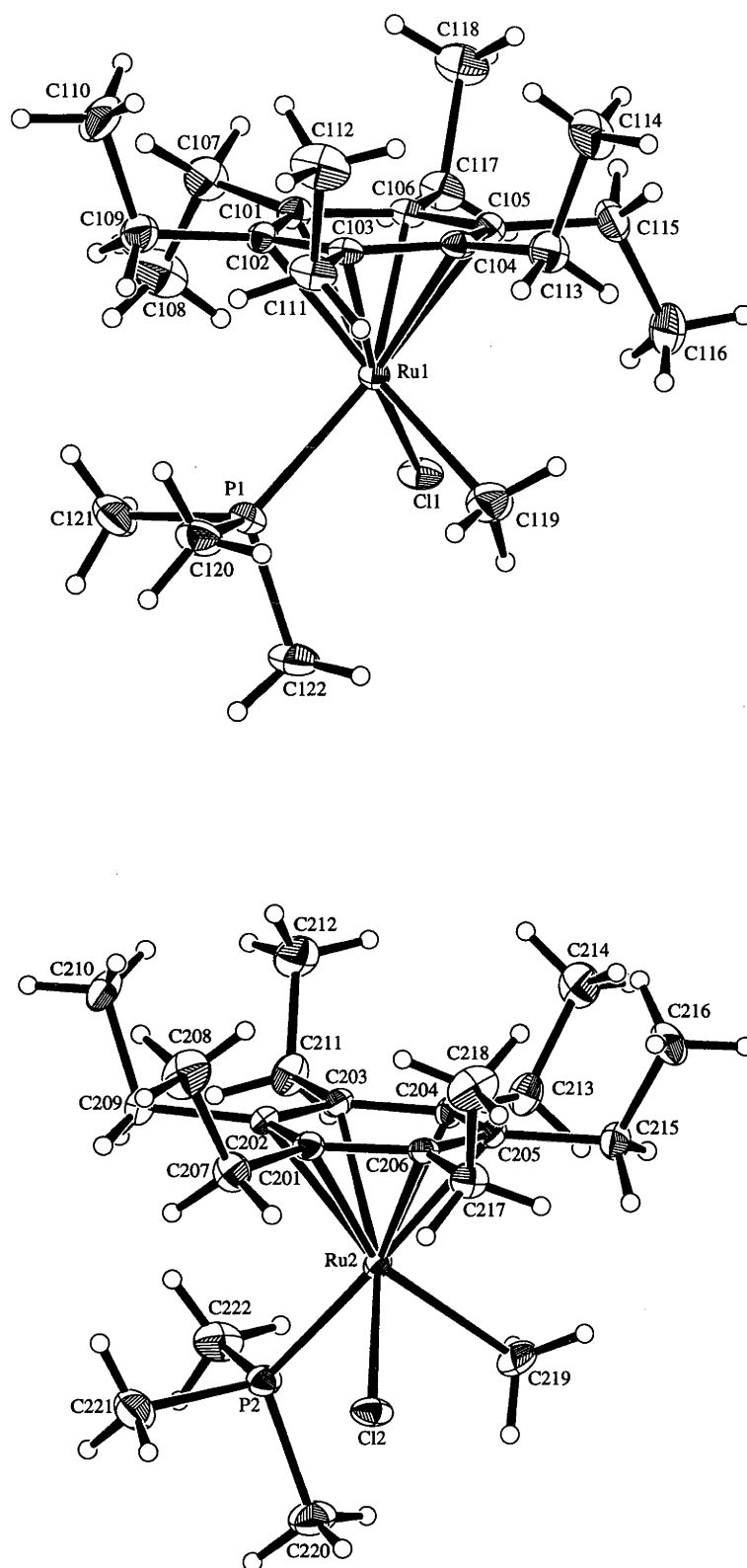
Ru(1)-Cl(1)	2.410(2)	Ru(1)-Cl(2)	2.409(2)
Ru(1)-C(1)	2.226(6)	Ru(1)-C(2)	2.243(6)
Ru(1)-C(3)	2.225(6)	Ru(1)-C(4)	2.210(6)
Ru(1)-C(5)	2.185(6)	Ru(1)-C(6)	2.220(6)
Ru(1)-C(19)	1.970(7)	N(1)-C(19)	1.155(7)
N(1)-C(20)	1.452(8)	C(1)-C(2)	1.423(8)
C(1)-C(6)	1.421(8)	C(1)-C(7)	1.518(8)
C(2)-C(3)	1.426(8)	C(2)-C(9)	1.528(8)
C(3)-C(4)	1.433(8)	C(3)-C(11)	1.535(8)
C(4)-C(5)	1.430(8)	C(4)-C(13)	1.530(8)
C(5)-C(6)	1.422(8)	C(5)-C(15)	1.510(8)
C(6)-C(17)	1.510(8)	C(7)-C(8)	1.524(9)
C(9)-C(10)	1.52(1)	C(11)-C(12)	1.52(1)
C(13)-C(14)	1.53(1)	C(15)-C(16)	1.52(1)
C(17)-C(18)	1.53(1)	C(20)-C(21)	1.50(1)
C(20)-C(22)	1.50(1)	C(20)-C(23)	1.50(1)
		Ru-ring centroid	1.699(3)
Cl(1) Ru(1) Cl(2)	87.52(8)	C(2) C(9) C(10)	115.4(6)
Cl(1) Ru(1) C(19)	85.7(2)	C(3) C(11) C(12)	116.6(6)
Cl(2) Ru(1) C(19)	83.8(2)	C(4) C(13) C(14)	115.9(6)
Ru(1) C(19) N(1)	179.4(6)	C(5) C(15) C(16)	111.7(6)
C(19) N(1) C(20)	172.8(7)	C(6) C(17) C(18)	115.4(6)
C(1) C(7) C(8)	112.6(6)		

X-ray structures of complexes of the type **$\text{Ru}(\eta^6\text{-arene})(\text{PMe}_3)(\text{X})_m\text{Cl}_{(2-m)}$ (where $m=2$, $\text{X}=\text{Me}$, H ; $m=1$, $\text{X}=\text{Me}$)**

All of these complexes have a rotational ring orientation such that when viewed along the arene-ruthenium bond axis the ligands do not eclipse the carbon atoms of the aromatic ring.

The ruthenium centre of $\text{Ru}(\eta^6\text{-C}_6\text{Et}_6)(\text{PMe}_3)(\text{Me})\text{Cl}$ is chiral because it is surrounded in a pseudo-tetrahedral arrangement by four different ligands (arene, Me, Cl, PMe_3). Thus, if the conformation of the C_6Et_6 ligand is ignored, there are two enantiomers. Figure 3.6 shows the two different isomers possible. Figure 3.7 shows that in each unit cell one molecule of each 'enantiomer' is present. Table 3.7 gives metrical parameters for this complex.

The conformation of the ethyl 'arms' of the hexaethylbenzene ligand is not the same for every molecule in the crystal. There is disorder such that both the 1,3-proximal-2,4,5,6-distal and the all distal conformations are present in about a 1:1 ratio. There are four different forms of the molecule present in the solid state, consisting of the two 'enantiomers', each having two possible ethyl group conformations. Clearly in the solid state, the difference in energy between these two conformations is quite small.

Figure 3.6. Ortep diagrams of $\text{Ru}(\eta^6\text{-C}_6\text{Et}_6)(\text{PMe}_3)(\text{Me})\text{Cl}$

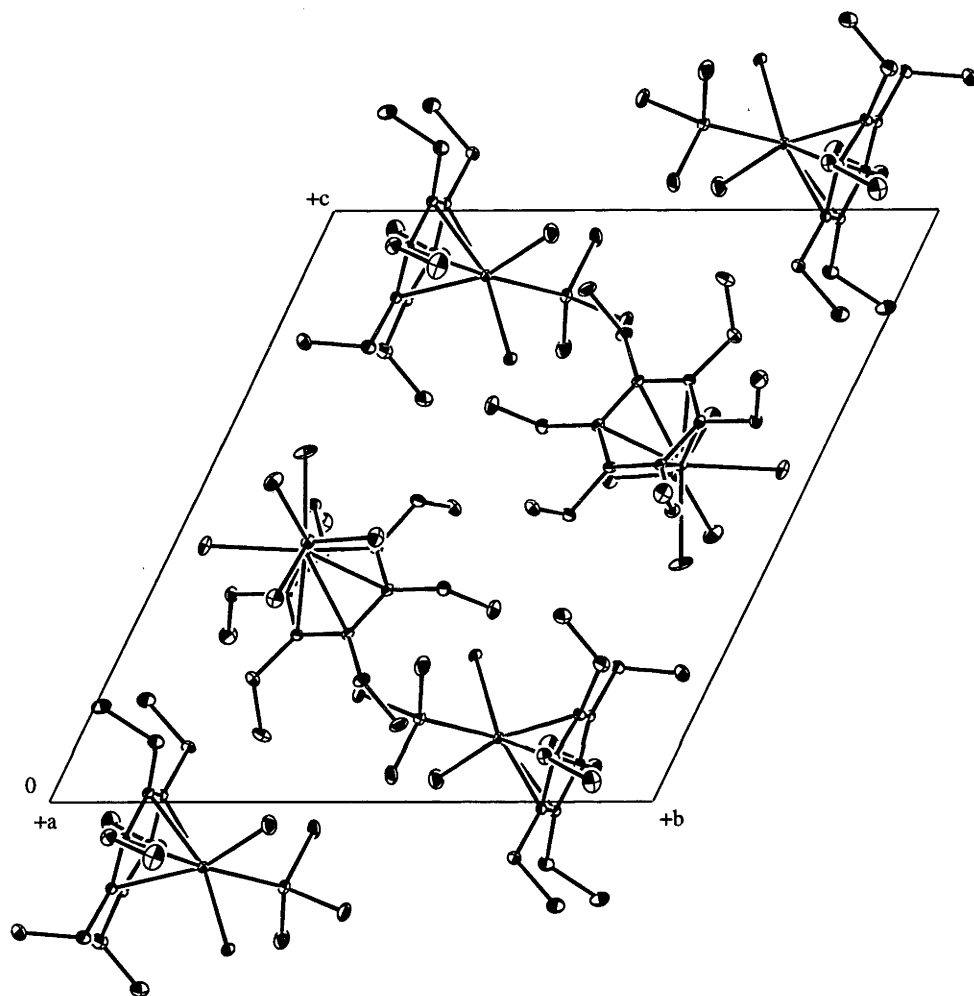


Figure 3.7. ORTEP diagram of the unit cell of $\text{Ru}(\eta^6\text{-C}_6\text{Et}_6)(\text{PMe}_3)(\text{Me})\text{Cl}$

Table 3.7. Selected bond lengths (Å) and angles (°) for
 $\text{Ru}(\eta^6\text{-C}_6\text{Et}_6)(\text{PMe}_3)(\text{Me})\text{Cl}$

Ru(1)-Cl(1)	2.400(2)	Ru(1)-P(1)	2.317(2)
Ru(1)-C(101)	2.282(5)	Ru(1)-C(102)	2.200(5)
Ru(1)-C(103)	2.215(5)	Ru(1)-C(104)	2.246(5)
Ru(1)-C(105)	2.259(5)	Ru(1)-C(106)	2.258(5)
Ru(1)-C(119)	2.295(4)	Ru(2)-Cl(2)	2.426(2)
Ru(2)-P(2)	2.306(2)	Ru(2)-C(201)	2.243(5)
Ru(2)-C(202)	2.255(5)	Ru(2)-C(203)	2.243(5)
Ru(2)-C(204)	2.210(5)	Ru(2)-C(205)	2.231(5)
Ru(2)-C(206)	2.244(5)	Ru(2)-C(219)	2.333(3)
P(1)-C(120)	1.814(6)	P(1)-C(121)	1.804(7)
P(1)-C(122)	1.814(6)	P(2)-C(220)	1.814(6)
P(2)-C(221)	1.813(7)	P(2)-C(222)	1.820(6)
C(101)-C(102)	1.429(7)	C(101)-C(106)	1.419(7)
C(101)-C(107)	1.549(8)	C(102)-C(103)	1.434(7)
C(102)-C(109)	1.509(7)	C(103)-C(104)	1.426(7)
C(103)-C(111)	1.513(7)	C(104)-C(105)	1.435(7)
C(104)-C(113)	1.510(7)	C(105)-C(106)	1.418(7)
C(105)-C(115)	1.531(7)	C(106)-C(117)	1.521(7)
C(107)-C(108)	1.492(9)	C(109)-C(110)	1.517(8)
C(111)-C(112)	1.552(8)	C(113)-C(114)	1.545(8)
C(115)-C(116)	1.510(9)	C(117)-C(118)	1.548(8)
C(201)-C(202)	1.420(7)	C(201)-C(206)	1.438(7)
C(201)-C(207)	1.531(7)	C(202)-C(203)	1.446(7)
C(202)-C(209)	1.536(7)	C(203)-C(204)	1.414(7)
C(203)-C(211)	1.550(7)	C(204)-C(205)	1.435(7)
C(204)-C(213)	1.526(7)	C(205)-C(206)	1.396(7)
C(205)-C(215)	1.532(7)	C(206)-C(217)	1.523(7)
C(207)-C(208)	1.512(8)	C(209)-C(210)	1.513(8)
C(211)-C(212)	1.523(8)	C(213)-C(214)	1.514(8)
C(215)-C(216)	1.512(8)	C(217)-C(218)	1.516(8)
ring centroid Ru(1)	1.731(3)	ring centroid Ru(2)	1.725(3)
C(119)Ru(1)Cl(1)	84.1(1)	C(104)C(105)C(106)	119.1(5)
C(219)Ru(2)Cl(2)	87.6(1)	C(105)C(106)C(101)	120.7(5)
P(1)Ru(1)Cl(1)	85.03(7)	C(106)C(101)C(102)	119.7(5)
P(2)Ru(2)Cl(2)	81.44(7)	C(201)C(202)C(203)	119.8(5)
P(1)Ru(1)C(119)	81.4(1)	C(202)C(203)C(204)	119.9(5)
P(2)Ru(2)C(219)	85.2(1)	C(203)C(204)C(205)	119.7(5)
C(101)C(102)C(103)	120.4(5)	C(204)C(205)C(206)	120.6(5)
C(102)C(103)C(104)	118.7(5)	C(205)C(206)C(201)	120.4(5)
C(103)C(104)C(105)	121.0(5)	C(206)C(201)C(202)	119.5(5)

For $\text{Ru}(\eta^6\text{-C}_6\text{Et}_6)(\text{PMe}_3)(\text{Me})_2$ there is substantial disorder in the ligand tripod for both the positions of the coordinated methyl groups and the rotational orientation of the trimethylphosphine ligand, so a detailed comparison of bond lengths and angles is not appropriate. One explanation for the disorder is that the PMe_3 ligand has two different rotational orientations and that steric interactions between one of the methyls of the trimethylphosphine and one of the two methyl groups coordinated to the ruthenium force the methyl groups around to one side of the molecule, giving a tripod without the expected C_2 symmetry. If the trimethylphosphine is rotated the other way the methyl groups are forced around to the other side of the molecule. These two orientations of the tripod give rise to two non-superimposable mirror image forms. Only one of the two forms is given in Figure 3.8 and in Table 3.8 of bond lengths and angles. The hexaethylbenzene ligand has the same conformation as it exhibits in the two phosphine adducts, $\text{Ru}(\eta^6\text{-C}_6\text{Et}_6)(\text{PR}_3)\text{Cl}$ ($\text{R} = \text{Me}, \text{Ph}$), that is, an entirely distal ethyl group arrangement, which is presumably determined by the steric bulk of the tertiary phosphine and the two chloro ligands. Replacing the two chloro groups with bulkier methyl groups should give an even greater preference to the entirely distal conformation. Figure 3.8 gives an ORTEP diagram of the molecular structure of $\text{Ru}(\eta^6\text{-C}_6\text{Et}_6)(\text{PMe}_3)(\text{Me})_2$ and Table 3.8 contains selected metrical parameters.

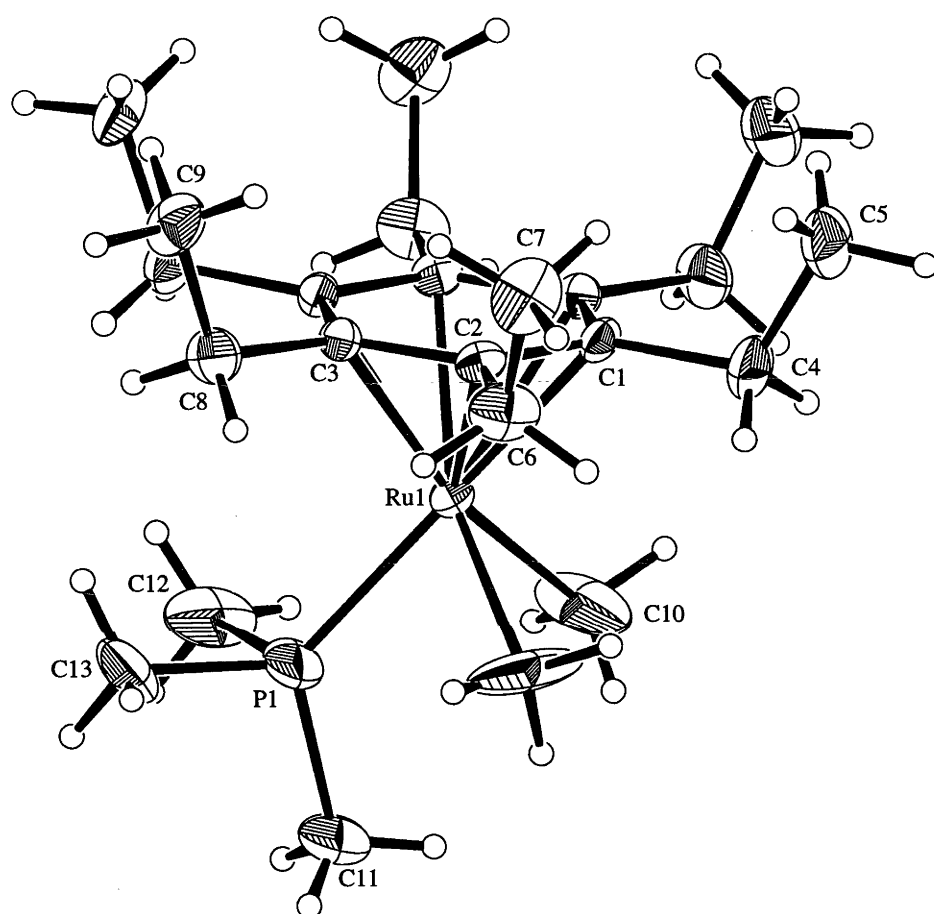


Figure 3.8. ORTEP plot of the solid state structure of $\text{Ru}(\eta^6\text{-C}_6\text{Et}_6)(\text{PMe}_3)(\text{Me})_2$

Table 3.8. Selected bond lengths (Å) and angles (°) for Ru(η^6 -C₆Et₆)(PMe₃)(Me)₂

Ru(1) P(1)	2.204(2)	Ru(1) C(1)	2.246(4)
Ru(1) C(1)	2.246(4)	Ru(1) C(2)	2.249(4)
Ru(1) C(2)	2.249(4)	Ru(1) C(3)	2.263(4)
Ru(1) C(3)	2.263(4)	Ru(1) C(10)	2.07(1)
Ru(1) C(10)	2.07(1)	Ru(1) C(10')	2.20(1)
Ru(1) C(10')	2.20(1)	P(1) C(11)	1.793(8)
P(1) C(12)	2.20(1)	P(1) C(12)	2.20(1)
P(1) C(13)	1.67(1)	P(1) C(13)	1.67(1)
C(1) C(1')	1.411(8)	C(1) C(2)	1.430(5)
C(1) C(4)	1.522(6)	C(2) C(3)	1.417(5)
C(2) C(6)	1.534(6)	C(3) C(3')	1.434(8)
C(3) C(8)	1.514(5)	C(4) C(5)	1.489(7)
C(6) C(7)	1.490(8)	C(8) C(9)	1.500(7)
C(13) C(13)	0.80(5)	Ru-ring centroid	1.7463(16)
C(10) Ru(1) C(10')	80.0(8)	C(1) C(2) C(3)	120.1(4)
C(10) Ru(1) P(1)	88.7(3)	C(2) C(3) C(3')	119.8(2)
C(10') Ru(1) P(1)	74.2(4)	C(1') C(1) C(2)	120.1(2)

For Ru(η^6 -C₆Et₆)(PMe₃)(H)₂ the two hydride ligands were located in the difference map and refined isotropically. A comparison of the Ru-H bond length in this complex of 1.45(3) Å with Ru-H distance in [Ru(η^6 -C₆Me₆)(PPh₃)(η^2 -C₂H₄)H]⁺PF₆⁻ of 1.5 Å¹²⁵, and of 1.55(5) Å in Ru(η^5 -C₅H₅)(dppp)H¹²⁶ shows no significant difference. Metrical parameters for this hexaethylbenzene complex are listed in Table 3.9.

It can be seen from the ORTEP plot of the solid state structure of this complex shown in Figure 3.9 that the hexaethylbenzene has taken on a 1,4-proximal-2,3,5,6-distal conformation. Again this observation can be rationalized entirely in terms of the steric bulk of the other ligands present in the coordination sphere, because the two hydrides are less bulky than the two chloride ligands in Ru(η^6 -C₆Et₆)(PMe₃)Cl₂. Thus there is less pressure for the ethyl groups to be distal.

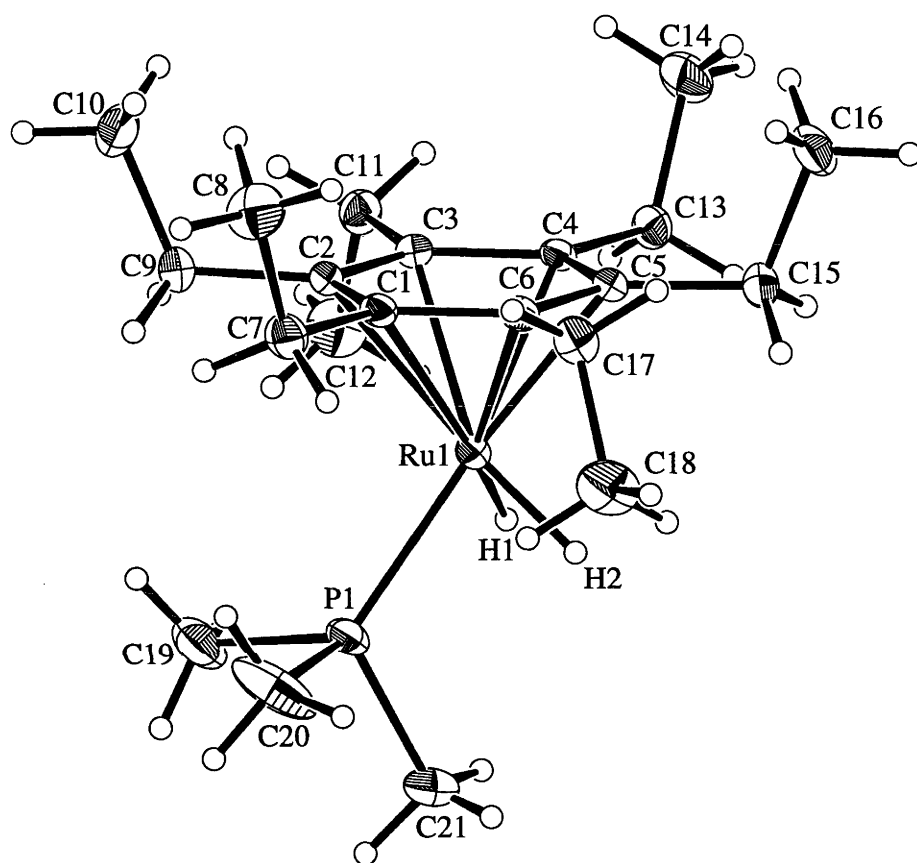


Figure 3.9. ORTEP diagram showing the solid state structure of $\text{Ru}(\eta^6\text{-C}_6\text{Et}_6)(\text{PMe}_3)(\text{H})_2$

Table 3.9. Selected bond lengths and angles for Ru(η^6 -C₆Et₆)(PMe₃)(H)₂

Ru(1)-P(1)	2.238(1)	Ru(1)-C(1)	2.255(3)
Ru(1)-C(2)	2.267(3)	Ru(1)-C(3)	2.255(3)
Ru(1)-C(4)	2.238(3)	Ru(1)-C(5)	2.246(3)
Ru(1)-C(6)	2.243(3)	P(1)-C(19)	1.821(4)
P(1)-C(20)	1.819(4)	P(1)-C(21)	1.802(4)
C(1)-C(2)	1.432(4)	C(1)-C(6)	1.413(4)
C(1)-C(7)	1.520(4)	C(2)-C(3)	1.411(4)
C(2)-C(9)	1.513(4)	C(3)-C(4)	1.447(4)
C(3)-C(11)	1.528(4)	C(4)-C(5)	1.425(4)
C(4)-C(13)	1.523(4)	C(5)-C(6)	1.438(4)
C(5)-C(15)	1.511(4)	C(6)-C(17)	1.523(4)
C(7)-C(8)	1.531(5)	C(9)-C(10)	1.527(5)
C(11)-C(12)	1.516(5)	C(13)-C(14)	1.530(4)
C(15)-C(16)	1.532(5)	C(17)-(18)	1.527(5)
Ru(1)-H(1)	1.45(3)	Ru(1)-H(2)	1.45(3)
		ring centroid-Ru	1.7398(4)
P(1)Ru(1)H(1)	77(1)	C(3)C(4)C(5)	119.7(3)
P(1)Ru(1)H(2)	79(1)	C(4)C(5)C(6)	119.4(3)
H(1)Ru(1)H(2)	71(1)	C(5)C(6)C(1)	120.4(3)
C(1)C(2)C(3)	119.9(3)	C(6)C(1)C(2)	120.3(3)
C(2)C(3)C(4)	120.2(3)		

X-ray structures of monomeric cationic ruthenium(II) complexes

The X-ray structures have been determined for three of these cationic species; $[\text{Ru}(\eta^6\text{-C}_6\text{Et}_6)(\text{CO})_2\text{Cl}]^+\text{PF}_6^-$, $[\text{Ru}(\eta^6\text{-C}_6\text{Et}_6)(\text{CO})(\text{Bu}^t\text{NC})\text{Cl}]^+\text{PF}_6^-$ and $[\text{Ru}(\eta^6\text{-C}_6\text{Et}_6)(\text{Bu}^t\text{NC})_2\text{Cl}]^+\text{PF}_6^-$. Figures 3.10, 3.12 and 3.13 give ORTEP diagrams showing their solid state structures and Tables 3.10, 3.11 and 3.12 give selected bond lengths and angles. In all these structures, when the complex is viewed along the arene ruthenium bond axis, three of the arene carbons eclipse the ligands. All three have small cylindrical sterically undemanding ligands in the tripod but only in $[\text{Ru}(\eta^6\text{-C}_6\text{Et}_6)(\text{CO})(\text{Bu}^t\text{NC})\text{Cl}]^+\text{PF}_6^-$ and $[\text{Ru}(\eta^6\text{-C}_6\text{Et}_6)(\text{CO})_2\text{Cl}]^+\text{PF}_6^-$ does the arene have just the expected 1,3,5-proximal-2,4,6-distal conformation. The complex $[\text{Ru}(\eta^6\text{-C}_6\text{Et}_6)(\text{Bu}^t\text{NC})_2\text{Cl}]^+\text{PF}_6^-$ has two different hexaethylbenzene conformations present in the solid state, the proximal-distal staggered conformation and the 1,3-proximal-2,4,5,6-distal conformation.

The complex $[\text{Ru}(\eta^6\text{-C}_6\text{Et}_6)(\text{CO})(\text{Bu}^t\text{NC})\text{Cl}]^+\text{PF}_6^-$, having three different ligands in its tripod, is chiral about the ruthenium in the same way as $\text{Ru}(\eta^6\text{-C}_6\text{Et}_6)(\text{PMe}_3)(\text{Me})(\text{Cl})$. Both enantiomers are present in the unit cell. The *t*-butyl group of the isocyanide ligand in this complex is substantially disordered. It takes on one of two different rotationally different forms. This can be seen in the unit cell diagram in Figure 3.11 below. For clarity only the most populated of the two isomeric forms is portrayed in the diagram in Figure 3.10.

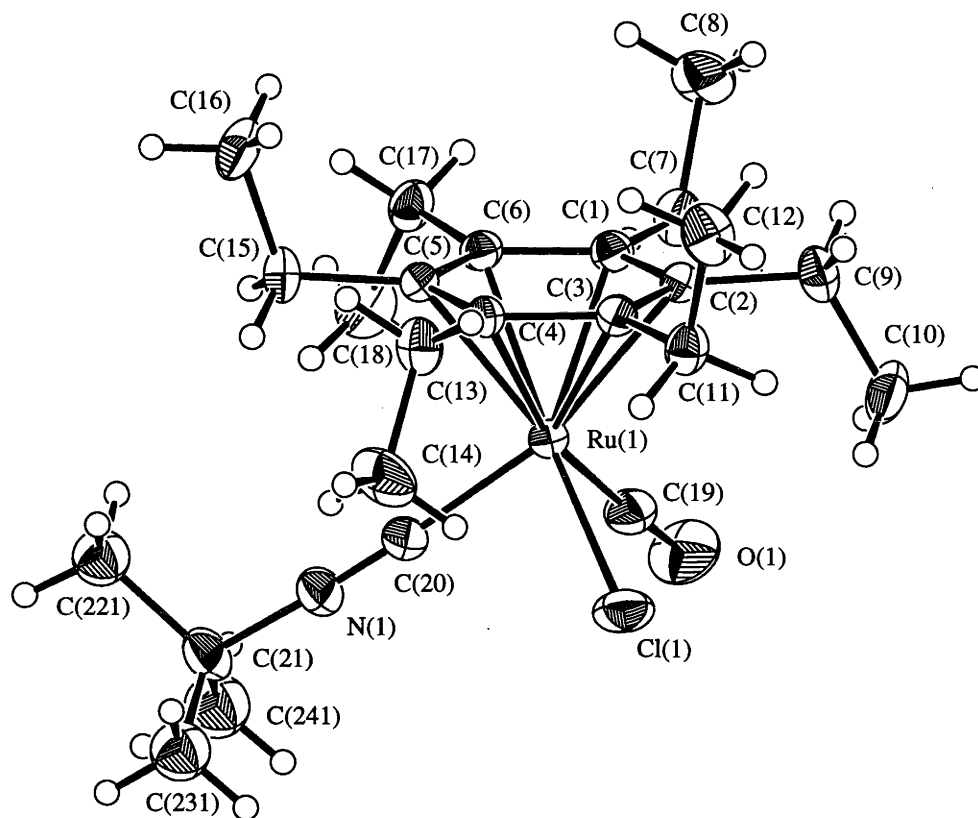


Figure 3.10. ORTEP diagram showing solid state structure of $[\text{Ru}(\eta^6\text{-C}_6\text{Et}_6)(\text{CO})(\text{Bu}^i\text{NC})\text{Cl}]^+\text{PF}_6^-$

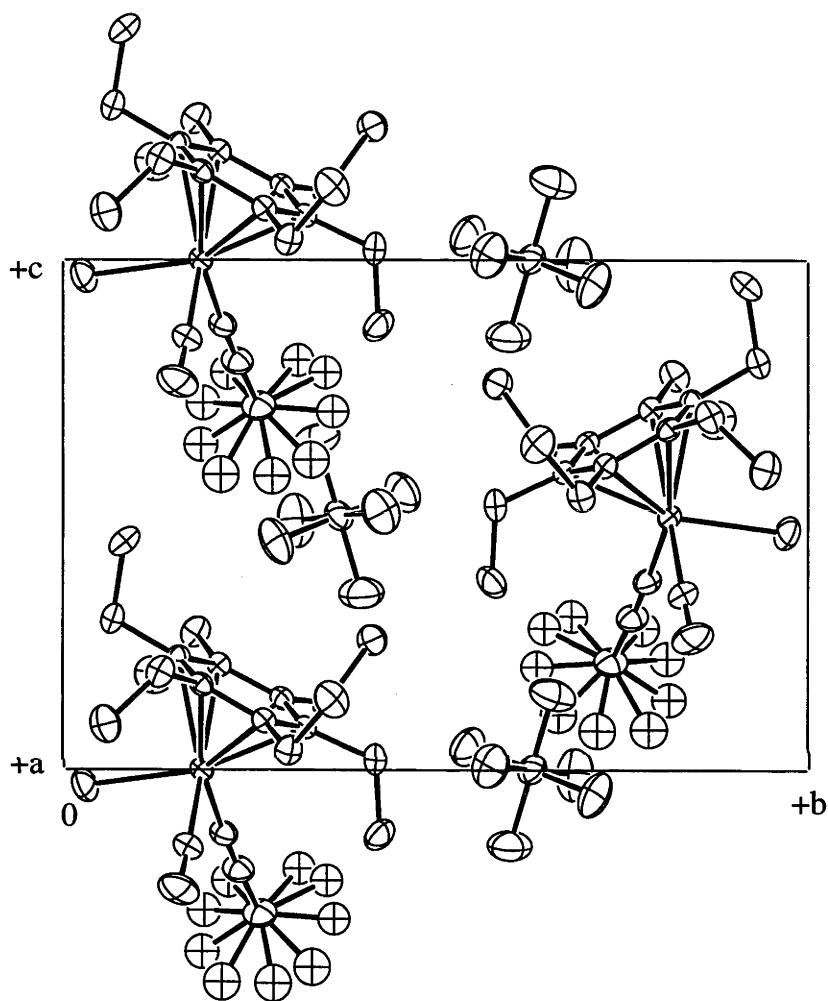


Figure 3.11. ORTEP diagram of the unit cell of $[\text{Ru}(\eta^6\text{-C}_6\text{Et}_6)(\text{Bu}^i\text{NC})(\text{CO})\text{Cl}]^+\text{PF}_6^-$

Table 3.10. Table of bond lengths (Å) and angles (°) for
 $[\text{Ru}(\eta^6\text{-C}_6\text{Et}_6)(\text{CO})(\text{Bu}^t\text{NC})\text{Cl}]\text{PF}_6^-$

Ru(1)-Cl(1)	2.385(2)	Ru(1)-C(1)	2.255(5)
Ru(1)-C(2)	2.299(5)	Ru(1)-C(3)	2.309(5)
Ru(1)-C(4)	2.309(5)	Ru(1)-C(5)	2.306(5)
Ru(1)-C(6)	2.267(5)	Ru(1)-C(19)	1.907(6)
Ru(1)-C(20)	1.973(6)	O(1)-C(19)	1.113(7)
N(1)-C(20)	1.138(7)	N(1)-C(21)	1.455(7)
C(1)-C(2)	1.431(7)	C(1)-C(6)	1.434(7)
C(1)-C(7)	1.510(7)	C(2)-C(3)	1.413(7)
C(2)-C(9)	1.507(7)	C(3)-C(4)	1.442(7)
C(3)-C(11)	1.507(7)	C(4)-C(5)	1.413(7)
C(4)-C(13)	1.525(7)	C(5)-C(6)	1.429(7)
C(5)-C(15)	1.510(7)	C(6)-C(17)	1.518(7)
C(7)-C(8)	1.546(9)	C(9)-C(10)	1.525(9)
C(11)-C(12)	1.527(9)	C(13)-C(14)	1.501(9)
C(15)-C(16)	1.533(9)	C(17)-C(18)	1.54(1)
C(21)-C(221)	1.59(2)	C(21)-C(222)	1.47(1)*
C(21)-C(223)	1.52(1)*	C(21)-C(231)	1.60(2)
C(21)-C(232)	1.55(1)*	C(21)-C(233)	1.50(1)*
C(21)-C(241)	1.47(2)	C(21)-C(242)	1.55(1)*
C(21)-C(243)	1.59(1)*	C(221)-C(222)	0.95(3)
C(221)-C(223)	0.69(3)	C(222)-C(223)	1.51(3)
C(222)-C(241)	1.82(3)	C(222)-C(243)	1.22(4)
C(223)-C(232)	1.44(4)	C(231)-C(232)	0.77(3)
C(231)-C(233)	0.97(3)	C(232)-C(233)	1.63(3)
C(233)-C(242)	1.09(3)	C(241)-C(242)	1.05(3)
C(241)-C(243)	0.84(3)	C(242)-C(243)	1.84(3)
		Ru(1)-ring centroid	1.793(2)
C(1) C(2) C(3)	119.7(5)	Ru(1) C(19) O(1)	176.6(7)
C(2) C(3) C(4)	120.6(5)	Ru(1) C(20) N(1)	177.7(6)
C(3) C(4) C(5)	119.5(4)	C(20) N(1) C(21)	177.4(6)
C(4) C(5) C(6)	120.5(5)	C(19) Ru(1) Cl(1)	84.1(2)
C(5) C(6) C(1)	119.6(5)	C(19) Ru(1) C(20)	88.0(3)
C(6) C(1) C(2)	120.1(5)	Cl(1) Ru(1) C(20)	87.5(2)

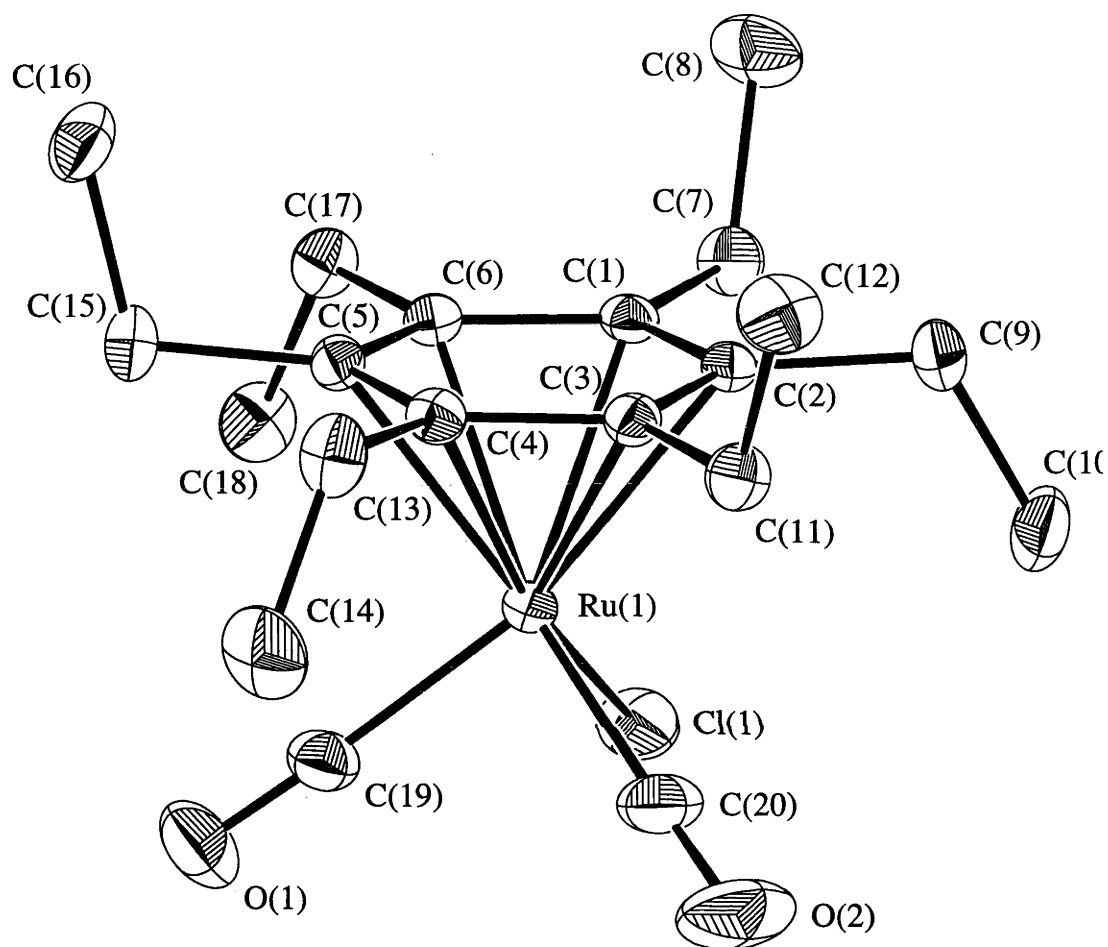
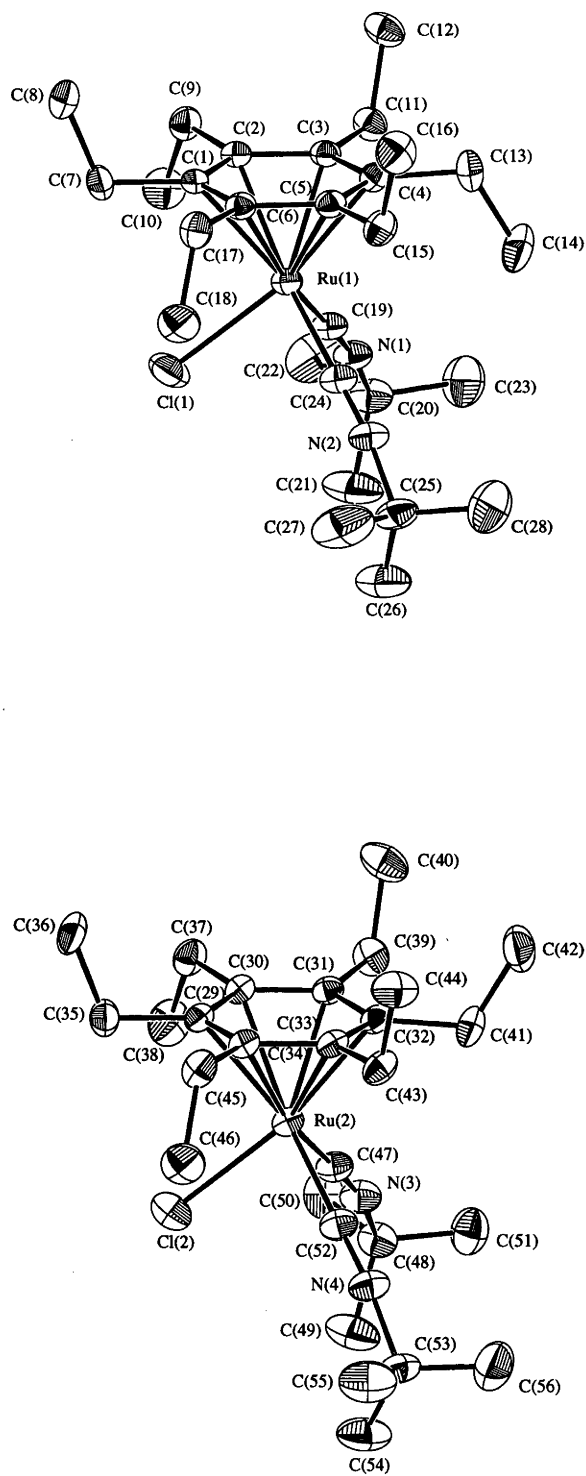
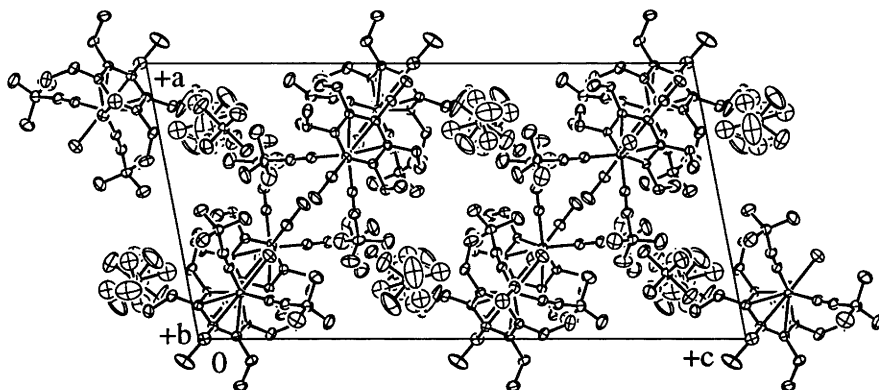


Figure 3.12. ORTEP diagram of $[\text{Ru}(\eta^6\text{-C}_6\text{Et}_6)(\text{CO})_2\text{Cl}]^+\text{PF}_6^-$

Table 3.11. Bond lengths (Å) and angles (°) for $[\text{Ru}(\eta^6\text{-C}_6\text{Et}_6)(\text{CO})_2\text{Cl}]^+\text{PF}_6^-$

Ru(1)-Cl(1)	2.3755(8)	Ru(1)-C(1)	2.322(2)
Ru(1)-C(2)	2.318(2)	Ru(1)-C(3)	2.264(2)
Ru(1)-C(4)	2.282(3)	Ru(1)-C(5)	2.318(3)
Ru(1)-C(6)	2.311(2)	Ru(1)-C(19)	1.907(3)
Ru(1)-C(20)	1.905(4)	O(1)-C(19)	1.100(4)
O(2)-C(20)	1.115(4)	C(1)-C(2)	1.418(4)
C(1)-C(6)	1.424(4)	C(1)-C(7)	1.512(4)
C(2)-C(3)	1.430(4)	C(2)-C(9)	1.520(4)
C(3)-C(4)	1.425(4)	C(3)-C(11)	1.518(4)
C(4)-C(5)	1.435(4)	C(4)-C(13)	1.515(4)
C(5)-C(6)	1.423(4)	C(5)-C(15)	1.508(4)
C(6)-C(17)	1.519(4)	C(7)-C(8)	1.533(4)
C(9)-C(10)	1.532(4)	C(11)-C(12)	1.530(4)
C(13)-C(14)	1.532(5)	C(15)-C(16)	1.538(4)
C(17)-C(18)	1.523(4)	Ru-Ring centroid	1.8082(8)
C(1)-C(2)-C(3)	119.3(2)	Ru(1)-C(19)-O(1)	177.6(3)
C(2)-C(3)-C(4)	120.5(2)	Ru(1)-C(20)-O(2)	176.5(3)
C(3)-C(4)-C(5)	119.3(2)	C(19)-Ru(1)-Cl(1)	87.1(1)
C(4)-C(5)-C(6)	120.4(2)	C(19)-Ru(1)-C(20)	89.1(1)
C(5)-C(6)-C(1)	119.3(2)	C(20)-Ru(1)-Cl(1)	86.9(1)
C(6)-C(1)-C(2)	121.0(2)		

Figure 3.13. ORTEP diagrams of $[\text{Ru}(\eta^6\text{-C}_6\text{Et}_6)(\text{Bu}^t\text{NC})_2\text{Cl}]^+\text{PF}_6^-$

Figure 3.14. ORTEP diagram of the unit cell of $[\text{Ru}(\eta^6\text{-C}_6\text{Et}_6)(\text{Bu}^t\text{NC})_2\text{Cl}]^+\text{PF}_6^-$ Table 3.12. Selected bond lengths (Å) and angles (°) for $[\text{Ru}(\eta^6\text{-C}_6\text{Et}_6)(\text{Bu}^t\text{NC})_2\text{Cl}]^+\text{PF}_6^-$

Ru(1) Cl(1)	2.397(1)	Ru(1) C(1)	2.272(4)
Ru(1) C(2)	2.275(4)	Ru(1) C(3)	2.237(4)
Ru(1) C(4)	2.248(4)	Ru(1) C(5)	2.252(4)
Ru(1) C(6)	2.279(4)	Ru(1) C(19)	1.959(4)
Ru(1) C(24)	1.950(4)	Ru(2) Cl(2)	2.405(1)
Ru(2) C(29)	2.265(4)	Ru(2) C(30)	2.289(4)
Ru(2) C(31)	2.249(4)	Ru(2) C(32)	2.212(4)
Ru(2) C(33)	2.246(4)	Ru(2) C(34)	2.287(4)
Ru(2) C(47)	1.952(4)	Ru(2) C(52)	1.968(4)
N(1) C(19)	1.140(5)	N(1) C(20)	1.470(5)
N(2) C(24)	1.146(5)	N(2) C(25)	1.462(5)
N(3) C(47)	1.138(5)	N(3) C(48)	1.463(5)
N(4) C(52)	1.141(5)	N(4) C(53)	1.457(5)
C(1) C(2)	1.428(5)	C(1) C(6)	1.425(5)
C(1) C(7)	1.505(5)	C(2) C(3)	1.421(5)
C(2) C(9)	1.521(5)	C(3) C(4)	1.430(5)
C(3) C(11)	1.509(5)	C(4) C(5)	1.430(5)
C(4) C(13)	1.520(5)	C(5) C(6)	1.431(5)
C(5) C(15)	1.513(5)	C(6) C(17)	1.520(5)
C(7) C(8)	1.525(6)	C(9) C(10)	1.524(6)
C(11) C(12)	1.533(6)	C(13) C(14)	1.519(6)
C(15) C(16)	1.538(6)	C(17) C(18)	1.536(6)
C(20) C(21)	1.515(7)	C(20) C(22)	1.519(7)
C(20) C(23)	1.510(7)	C(25) C(26)	1.515(7)
C(25) C(27)	1.503(7)	C(25) C(28)	1.504(7)
C(29) C(30)	1.418(5)	C(29) C(34)	1.429(5)
C(29) C(35)	1.520(5)	C(30) C(31)	1.423(5)
C(30) C(37)	1.525(5)	C(31) C(32)	1.429(5)

Table 3.12. continued

C(31) C(39)	1.514(5)	C(32) C(33)	1.430(5)
C(32) C(41)	1.534(5)	C(33) C(34)	1.429(5)
C(33) C(43)	1.513(5)	C(34) C(45)	1.515(5)
C(35) C(36)	1.530(6)	C(37) C(38)	1.529(6)
C(39) C(40)	1.524(6)	C(41) C(42)	1.513(6)
C(43) C(44)	1.531(6)	C(45) C(46)	1.526(6)
C(48) C(49)	1.513(6)	C(48) C(50)	1.526(6)
C(48) C(51)	1.515(6)	C(53) C(54)	1.519(6)
C(53) C(55)	1.505(7)	C(53) C(56)	1.510(7)
Ru(2)-ring centroid	1.7532(14)	Ru(1)-ring centroid	1.7506(14)
Cl(1)Ru(1)C(24)	85.8(1)	Cl(2)Ru(2)C(52)	85.5(1)
Cl(1)Ru(1)C(19)	83.8(1)	Cl(1)Ru(2)C(47)	85.2(1)
C(19)Ru(1)C(24)	85.6(2)	C(52)Ru(2)C(47)	83.2(2)
Ru(1)C(24)N(2)	179.2(4)	Ru(2)C(52)N(4)	176.5(4)
Ru(1)C(19)N(1)	177.0(4)	Ru(2)C(47)N(3)	176.5(4)
C(24)N(2)C(25)	172.9(5)	C(52)N(4)C(53)	173.7(5)
C(19)N(1)C(20)	172.5(5)	C(47)N(3)C(48)	169.0(5)
C(1)C(2)C(3)	118.9(4)	C(29)C(30)C(31)	119.0(4)
C(2)C(3)C(4)	121.0(4)	C(30)C(31)C(32)	120.9(4)
C(3)C(4)C(5)	119.0(4)	C(31)C(32)C(33)	118.9(4)
C(4)C(5)C(6)	120.9(4)	C(32)C(33)C(34)	121.2(4)
C(5)C(6)C(1)	118.7(4)	C(33)C(34)C(29)	118.1(4)
C(6)C(1)C(2)	121.4(4)	C(34)C(29)C(30)	121.8(4)

While the molecular structures of compounds of the type $\text{Ru}(\eta^6\text{-arene})(\text{L})\text{Cl}_2$ ($\text{L} = \text{CO}$, Bu^tNC , arene not equal to C_6Et_6) do not appear to have been determined by X-ray crystallography, there are many $\eta^5\text{-C}_5\text{H}_5$ complexes of ruthenium containing CO and Bu^tNC as ligands. Table 3.13 contains a list of complexes and the Ru-C, C-O, and C-N bond lengths for a range of ruthenium (II) cyclopentadienyl complexes.

Table 3.13. Selected bond lengths for a range of CO and Bu^tNC containing ruthenium complexes

Complex	Ref	Ru-CO Å	C-O Å	Ru-CN Å	C-N Å
Ru(η^5 -C ₅ Me ₄ CH ₂ Cl)(CO) ₂ Cl	127	1.882(8)	1.132(10)		
[Ru(η^5 -C ₅ Me ₄ CH ₂ OEt)(PPh ₃)(CO) ₂] ⁺ OTf ⁻	127	1.904(10) 1.892(10)	1.121(13) 1.127(12)		
[Ru(η^5 -C ₅ H ₅)(PPh ₃) ₂ CO] ⁺ BPh ₄ ⁻	128	1.869(2)	1.144(3)		
[Ru(η^5 -C ₅ H ₅)(CO)(Bu ^t NC)(PPh ₃)] ⁺ PF ₆ ⁻	129	1.901(6)	1.121(8)	1.961(4)	1.152(7)
Ru[η^5 -C ₅ H ₄ CH ₂ (C ₆ H ₃ -2,4-Me ₂)](CO) ₂ Cl	130	1.884(5)			
Ru(η^5 -C ₅ H ₅)(CO) ₂ Br	131	1.895(16)	1.114(20)		
Ru(η^5 -C ₅ Me ₅)(CO) ₂ Br	132	1.892(14)	1.116(17)		
[Ru(η^5 -C ₅ H ₅)(Bu ^t NC)(PPh ₃ (NH ₃))] ⁺ PF ₆ ⁻	133			1.934(5)	1.152(7)

Table 3.14. Selected bond lengths for hexaethylbenzene complexes containing CO or Bu^tNC

Complex	Ru-CN Bu ^t (Å)	Ru-CO (Å)	Ru-Arene (Å)
Ru(η ⁶ -C ₆ Et ₆)(CO)Cl ₂		1.904(9)	1.699(3)
Ru(η ⁶ -C ₆ Et ₆)(Bu ^t NC)Cl ₂	1.970(7)		1.736(3)
[Ru(η ⁶ -C ₆ Et ₆)(CO) ₂ Cl] ⁺ PF ₆ ⁻		1.905(4) ^a 1.907(3)	1.8082(8)
[Ru(η ⁶ -C ₆ Et ₆)(Bu ^t NC) ₂ Cl] ⁺ PF ₆ ⁻	1.959(4) 1.952(4)		1.7506(14)
[Ru(η ⁶ -C ₆ Et ₆)(CO)(Bu ^t NC)Cl] ⁺ PF ₆ ⁻	1.973(6)	1.907(6)	1.793(2)

^aTwo Ru-CO ligand distances are given as the two CO ligands are not exactly the same

It appears that all the Ru-CO (1.904(9)-1.907(6) Å) and Ru-CN (1.952(4)-1.970(7) Å) bond lengths fall within the same range as that in the compounds taken from the literature (Ru-CO = 1.869(2)-1.904(10) Å and Ru-CN = 1.934(5) -1.961(4)Å). The Ru-CO distance is insensitive to the change in ligand environment (CO, Bu^tNC, Cl) about the ruthenium centre and to the presence or absence of a net positive charge on the metal atom. The Ru-CN Bu^t distance does not appear to change significantly with the change in environment . There is a tendency for the ruthenium-arene separation to be shorter in the neutral species (1.699(3)-1.736(3) Å as against 1.7506(14)-1.8082(8) Å).

There are changes in the C-O (1.012(9)-1.115(4) Å) and C-N (1.155(7)-1.138(7) Å) bond lengths in the ligands in different complexes, with the cationic complexes having shorter (almost 3σ) C-N distances for the isocyanide ligand and substantially longer C-O bond lengths (see Table 3.15). One would expect that in the cationic metal complexes amount of back donation to the π* orbital of the CO ligand would be less than in the neutral complexes and thus the bond length would be shorter. However the opposite is observed. The changes in the observed infrared C-O stretching bands also do not correlate with the observed bond lengths.

The limited differences observed for the isocyanide complexes do, however, appear consistent both with reduced back donation causing in increase both in C-N bond order and C-N stretching frequency with the move from neutral to cationic complexes.

This analysis of the Ru-ligand, C-O and C-N distances and the observed infrared bands does not take into account several factors. Firstly, the complexes do not have exactly the

same ligands in the move from neutral to cationic, there is only one electronegative chloride ligand for the cationic species and two for the neutral species. Secondly, the infrared $\text{C}\equiv\text{O}$ stretching bands are from solid state infrared measurements whereas, ideally, comparisons should be based on spectra measured in solution.

Table 3.15. C-O and C-N distances and infrared stretching frequencies for ruthenium hexaethylbenzene complexes containing Bu^tNC and CO ligands

Complex	$\nu(\text{CN})^a \text{ cm}^{-1}$	$\nu(\text{CO})^a \text{ cm}^{-1}$	C-N or C-O (Å)
$\text{Ru}(\eta^6\text{-C}_6\text{Et}_6)(\text{CO})\text{Cl}_2$		2010	1.012(9)
$[\text{Ru}(\eta^6\text{-C}_6\text{Et}_6)(\text{CO})_2\text{Cl}]^+\text{PF}_6^-$		2064 2000	1.115(4) 1.100(4)
$\text{Ru}(\eta^6\text{-C}_6\text{Et}_6)(\text{Bu}^t\text{NC})\text{Cl}_2$	2168		1.155(7)
$[\text{Ru}(\eta^6\text{-C}_6\text{Et}_6)(\text{Bu}^t\text{NC})_2\text{Cl}]^+\text{PF}_6^-$	2186 2202		1.146(5) ^b 1.138(5) 1.140(5) 1.141(5)
$[\text{Ru}(\eta^6\text{-C}_6\text{Et}_6)(\text{CO})(\text{Bu}^t\text{NC})\text{Cl}]^+\text{PF}_6^-$	2207	2035	1.113(7) (C-O) 1.138(7) (C-N)

^a All infrared spectra were measured as KBr disks, except for that of $\text{Ru}(\eta^6\text{-C}_6\text{Et}_6)(\text{CO})\text{Cl}_2$ which was measured as a nujol mull.

^b The two molecules present, differing only in C_6Et_6 conformation, have different metrical parameters

The X-ray structures in general

The conformation adopted by the ethyl groups of the coordinated hexaethylbenzene in the solid state structures of ruthenium (II) complexes seems to be controlled mainly by steric effects. As one would expect, the relatively bulky ligands such as PPh_3 and PMe_3 favour distal ethyl groups, thus reducing the steric interactions between the ethyl groups and the ligands. When smaller ligands are present, the hexaethylbenzene ligand prefers to take on the conformation that minimizes steric interactions within the ligand itself, that is, the 1,3,5-proximal-2,4,6-distal conformation. For ligands of intermediate bulk intermediate conformations are observed in which a balance is reached between the steric demands of the other ligands and the steric demands of the hexaethylbenzene itself, such behaviour being observed in $\text{Ru}(\eta^6\text{-C}_6\text{Et}_6)(\text{PMe}_3)(\text{H})_2$. It also appears that the energy differences between the various conformations in the solid state is small. In $\text{Ru}(\eta^6\text{-C}_6\text{Et}_6)(\text{PMe}_3)(\text{Me})\text{Cl}$ and $[\text{Ru}(\eta^6\text{-C}_6\text{Et}_6)(\text{Bu}^t\text{NC})_2\text{Cl}]^+\text{PF}_6^-$, for example, two different ethyl group conformations occur in each of their respective unit cells.

The steric bulk of the ligands apparently also affects the rotational orientation of the arene ring with respect to the ligands. When the ligands are small and cylindrical, such as CO and Bu^tNC , the arene is orientated such that when the molecule is viewed along the arene-ruthenium bond axis three of the arene carbons eclipse the ligands. When the ligands of the tripod are larger this is no longer the case; the ligands do not eclipse the arene carbons in the tertiary phosphine complexes.

There is a general, although not linear correlation between arene-ruthenium distances and the $^{13}\text{C}\{^1\text{H}\}$ NMR chemical shifts for the coordinated arene carbons (Table 3.16). As the arene ring to ruthenium distance increases the chemical shift increases. This is as one would expect, because carbon atoms in the less strongly bonded arene rings should exhibit a chemical shift closer to that of the free arene, while the carbon atoms in more strongly bound arenes are more shielded. There is one notable exception, namely, $[\text{Ru}(\eta^6\text{-C}_6\text{Et}_6)(\text{CO})_2]^+\text{PF}_6^-$, which shows an exceptionally shielded ^{13}C resonance but an unusually large Ru-arene separation. It is not certain whether the same species is present in solutions of this complex as in the solid state, especially in consideration of its anomalous variable temperature NMR behaviour (see Chapter 4).

Table 3.16. Ruthenium arene distances and arene carbon atom $^{13}\text{C}\{^1\text{H}\}$ NMR chemical shifts^a

Compound	Ru-arene distance (Å)	$\delta^{13}\text{C}$ NMR C _{aromatic} (ppm)
$[\text{Ru}(\eta^6\text{-C}_6\text{Et}_6)(\text{CO})_2\text{Cl}]^+\text{PF}_6^-$	1.808(2)	93.2
$\text{Ru}(\eta^6\text{-C}_6\text{Et}_6)(\text{PMe}_3)\text{Cl}_2$	1.696(1)	100.5
$\text{Ru}(\eta^6\text{-C}_6\text{Et}_6)(\text{PMe}_3)(\text{Me})_2$	1.745(16)	101.1
$\text{Ru}(\eta^6\text{-C}_6\text{Et}_6)(\text{PPh}_3)\text{Cl}_2$	1.720(2)	101.9
$\text{Ru}(\eta^6\text{-C}_6\text{Et}_6)(\text{PMe}_3)(\text{H})_2$	1.7398(4)	102.6
$\text{Ru}(\eta^6\text{-C}_6\text{Et}_6)(\text{Bu}^t\text{NC})\text{Cl}_2$	1.699(3)	103.1
$\text{Ru}(\eta^6\text{-C}_6\text{Et}_6)(\text{PMe}_3)(\text{Me})\text{Cl}$	1.731(3), 1.725(3)	103.2
$[\text{Ru}(\eta^6\text{-C}_6\text{Et}_6)(\text{Bu}^t\text{NC})_2\text{Cl}]^+\text{PF}_6^-$	1.7532(14)	109.8
$\text{Ru}(\eta^6\text{-C}_6\text{Et}_6)(\text{CO})\text{Cl}_2$	1.736(3)	110.1
$[\text{Ru}(\eta^6\text{-C}_6\text{Et}_6)(\text{Bu}^t\text{NC})(\text{CO})\text{Cl}]^+\text{PF}_6^-$	1.793(2)	118.9

It is not possible to correlate the steric and electronic properties of ligands of the tripod with the arene-ruthenium distance. While there is a big range of distances, 1.696-1.808 Å, the only trend apparent is that the cationic complexes have longer arene ruthenium bond lengths than the neutral complexes. Nor is it possible to correlate the arene ruthenium bond lengths with the C-C bond distances of the ring, since the latter do not appear to differ significantly between the complexes studied and are the least accurately determined distances in the molecules.

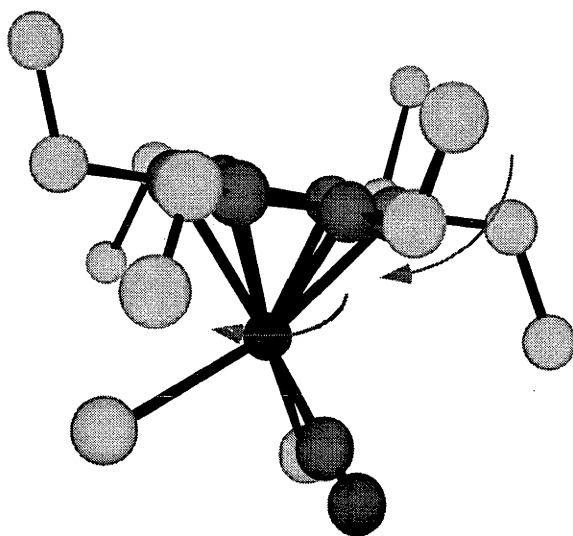
There are substantial differences in Ru-P bond lengths within the series of complexes containing the Ru-PMe₃ unit, which range from 2.343(1) Å for $\text{Ru}(\eta^6\text{-C}_6\text{Et}_6)(\text{PMe}_3)\text{Cl}_2$ to 2.204(2) Å for $\text{Ru}(\eta^6\text{-C}_6\text{Et}_6)(\text{PMe}_3)(\text{Me})_2$, but no systematic trend could be perceived.

The Ru-Cl distances in complexes containing Cl ligands differed significantly in the group (2.4181(9) Å for $\text{Ru}(\eta^6\text{-C}_6\text{Et}_6)(\text{PMe}_3)\text{Cl}_2$ to 2.3775(8) Å for $[\text{Ru}(\eta^6\text{-C}_6\text{Et}_6)(\text{CO})_2\text{Cl}]^+\text{PF}_6^-$) but again there were no trends apparent.

^a cf. free arene C_{aromatic} = δ 137 ppm in CDCl₃

While the conformational properties of the complexes are well defined in the solid state, the dynamic nature of these species in solution is not as well defined. The relationship between the molecular structures of these complexes in the solid state and their dynamic behaviour in solution is investigated by variable temperature NMR spectroscopy in Chapter 4.

Chapter 4: *Variable temperature NMR Spectroscopy*



Chem 3D representation of the two motions thought to occur in
 $\text{Ru}(\eta^6\text{-C}_6\text{Et}_6)(\text{CO})\text{Cl}_2$ at room temperature in solution

Room temperature NMR spectra of hexaethylbenzene complexes	134
Low temperature NMR spectra.....	137
Complexes with one sort of ethyl group at the limiting temperature	141
The complexes $[\text{Ru}(\eta^6\text{-C}_6\text{Et}_6)\text{Cl}_2]_2$ and $[\text{Ru}_2(\eta^6\text{-C}_6\text{Et}_6)_2\text{Cl}_3]^+\text{PF}_6^-$	143
Complexes with three small cylindrical ligands making up the tripod	151
$\text{Ru}(\eta^6\text{-C}_6\text{Et}_6)(\text{PMe}_3)(\text{H})_2$	168
Other arenes	173
Summary	173

Room temperature NMR spectra of hexaethylbenzene complexes

As mentioned in Chapter 3, the room temperature ^1H and $^{13}\text{C}\{^1\text{H}\}$ NMR spectra of the coordinated hexaethylbenzene in all the ruthenium complexes studied show similar features. These are summarized in Table 4.1.

Table 4.1. Room temperature ^1H and ^{13}C resonances for hexaethylbenzene in its ruthenium complexes (in CD_2Cl_2 unless otherwise stated)

Compound	$\delta\text{H}_{\text{CH}_2}$ (ppm)	$\delta\text{H}_{\text{CH}_3}$ (ppm)	$\delta\text{C}_{\text{Ar}}$ (ppm)	$\delta\text{C}_{\text{CH}_2}$ (ppm)	$\delta\text{C}_{\text{CH}_3}$ (ppm)
$\text{C}_6\text{Et}_6^{\text{a}}$	2.67	1.22	137.4	22.2	15.7
$\text{Ru}(\eta^6\text{-C}_6\text{Et}_6)(\text{COD})^{\text{b}}$	2.10	1.82	103.4	21.1	18.9
$[\text{Ru}(\eta^6\text{-C}_6\text{Et}_6)\text{Cl}_2]_2$	2.40	1.30	94-95	21.1	14.7
$[\text{Ru}_2(\eta^6\text{-C}_6\text{Et}_6)_2\text{Cl}_3]^+\text{PF}_6^-$	2.50	1.33	93-98	21.5	15.0
$\text{Ru}(\eta^6\text{-C}_6\text{Et}_6)(\text{PPh}_3)\text{Cl}_2$	2.26	1.19	101.9	22.2	15.0
$\text{Ru}(\eta^6\text{-C}_6\text{Et}_6)(\text{PMe}_3)\text{Cl}_2$	2.40	1.26	100.5	22.6	14.9
$\text{Ru}(\eta^6\text{-C}_6\text{Et}_6)(\text{PMe}_3)\text{MeCl}$	2.42	1.26	103.2	22.6	15.7
$\text{Ru}(\eta^6\text{-C}_6\text{Et}_6)(\text{PMe}_3)(\text{Me})_2^{\text{b}}$	2.26	1.16	101.1	22.4	16.3
$\text{Ru}(\eta^6\text{-C}_6\text{Et}_6)(\text{PMe}_3)(\text{H})_2^{\text{c}}$	2.34	1.23	102.6	22.9	19.7
$\text{Ru}(\eta^6\text{-C}_6\text{Et}_6)(\text{CO})\text{Cl}_2$	2.52	1.36	110.1	21.8	14.6
$\text{Ru}(\eta^6\text{-C}_6\text{Et}_6)(\text{Bu}^t\text{NC})\text{Cl}_2$	2.45	1.53	103.1	22.0	15.0
$[\text{Ru}(\eta^6\text{-C}_6\text{Et}_6)(\text{CH}_3\text{CN})_2\text{Cl}]+\text{PF}_6^-^{\text{d}}$	2.46	1.31	100.3	21.4	14.3
$[\text{Ru}(\eta^6\text{-C}_6\text{Et}_6)(\text{CH}_3\text{CN})_3]^{2+}(\text{CF}_3\text{SO}_3^-)_2^{\text{d}}$	2.50	1.32	116.9	21.4	14.2
$[\text{Ru}(\eta^6\text{-C}_6\text{Et}_6)(\text{CO})(\text{Bu}^t\text{NC})\text{Cl}]+\text{PF}_6^-$	2.59	1.37	118.9	30.2	22.3
$[\text{Ru}(\eta^6\text{-C}_6\text{Et}_6)(\text{Bu}^t\text{NC})_2\text{Cl}]+\text{PF}_6^-$	2.49	1.32	109.8	22.3	16.2
$[\text{Ru}(\eta^6\text{-C}_6\text{Et}_6)(\text{CO})_2\text{Cl}]+\text{PF}_6^-$	2.67	1.43	93.2	21.4	13.5

^a In CDCl_3

^b In C_6D_6

^c In $\text{d}^8\text{-THF}$

^d In CD_2Cl_2

The $^{13}\text{C}\{^1\text{H}\}$ and ^1H NMR room temperature spectra of $[\text{Ru}_2(\eta^6\text{-C}_6\text{Et}_6)_2\text{Cl}_3]^+\text{PF}_6^-$ are given in Figure 4.1 as a representative example of the spectra of coordinated hexaethylbenzene. In the ^1H NMR spectrum there is a quartet centered at δ 2.50 ppm and a triplet at δ 1.33 ppm, corresponding to the methylene and methyl protons respectively.

In the $^{13}\text{C}\{^1\text{H}\}$ NMR spectrum there are three resonances assignable to the coordinated hexaethylbenzene at δ 93-98, 21.5 and 15.0 ppm, corresponding to the coordinated arene, the methylene and the methyl carbons atoms respectively. The resonance for the coordinated arene carbon is quite broad and was difficult to observe at room temperature unless a long delay time was used. The ranges over which these ^1H and $^{13}\text{C}\{^1\text{H}\}$ NMR resonances fall for the different complexes are outlined in Chapter 3.

As there is only one set of resonances for the ethyl groups in both the ^1H and $^{13}\text{C}\{^1\text{H}\}$ NMR spectra for each of the complexes studied, there must be some dynamic process or processes occurring at room temperature in solution that make the ethyl groups equivalent on an NMR timescale. Taking $[\text{Ru}_2(\eta^6\text{-C}_6\text{Et}_6)_2\text{Cl}_3]^+\text{PF}_6^-$ as a representative example; if no intramolecular motions occur and the complex has the same conformation as observed in the solid state, one would expect at least two different sorts of ethyl group: the distal ethyl groups bonded to arene carbons atoms that, when viewed along the arene-ruthenium bond axis, eclipse the chloro ligands and the proximal ethyl groups that are bonded to arene carbon atoms which do not eclipse the chloro ligands. These two sorts of ethyl group are in magnetically different environments and thus should have different chemical shifts. Although the number of different ethyl groups might not be the same in all cases, a similar argument can be extended to all the complexes studied.

Presumably the dynamic processes are the same as those believed to occur in $\text{Cr}(\eta^6\text{-C}_6\text{Et}_6)(\text{CO})_3$ and its derivatives, namely, free rotation about the arene methylene bond and about the arene ruthenium bond (Figure 4.2). If these two processes are rapid on an NMR timescale at a given temperature then only one set of ethyl group resonances will be observed in the NMR spectra.

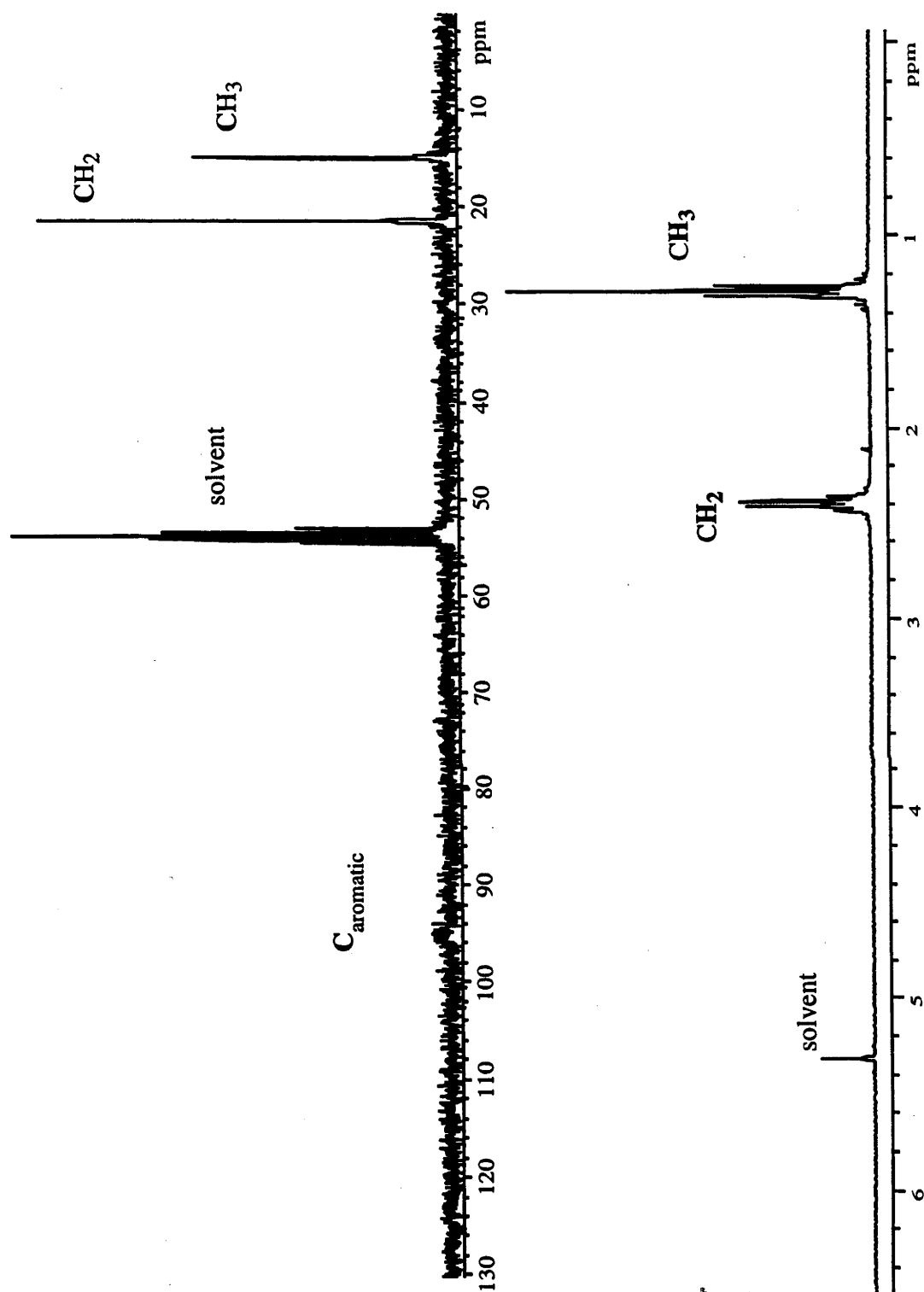


Figure 4.1 ^1H and $^{13}\text{C}\{^1\text{H}\}$ NMR (CD_2Cl_2 , 300 and 75.42 MHz) of $[\text{Ru}_2(\eta^6\text{-C}_6\text{Et}_6)_2\text{Cl}_3]^+\text{PF}_6^-$

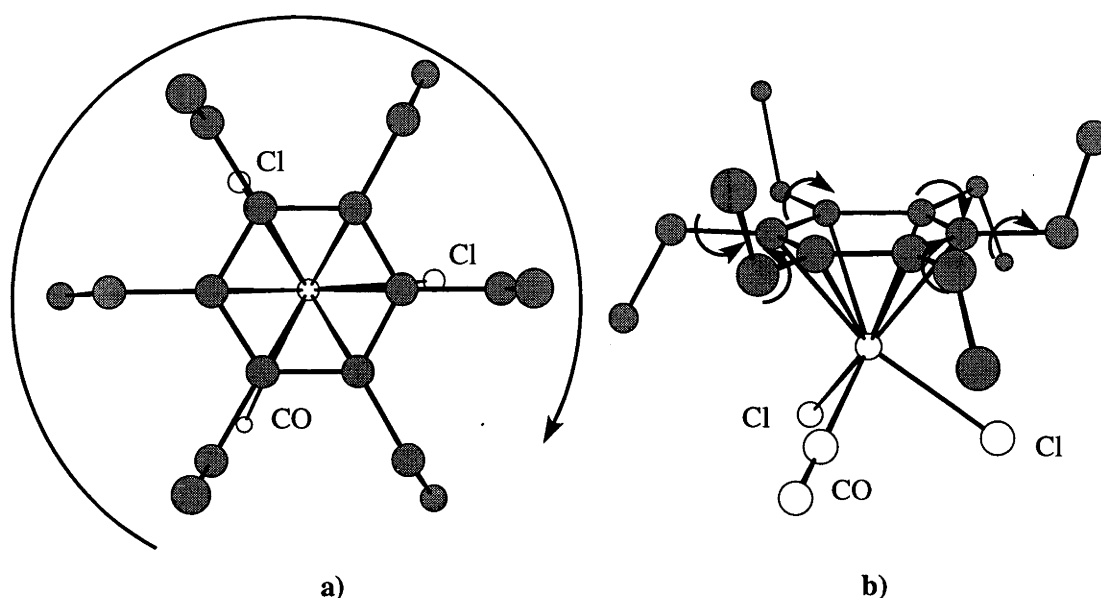


Figure 4.2. Rotation about **a)** the arene-ruthenium bond and **b)** the arene-methylene bond shown for $\text{Ru}(\eta^6\text{-C}_6\text{Et}_6)(\text{CO})\text{Cl}_2$

Low temperature NMR spectra

At low temperature in solution many of the ruthenium hexaethylbenzene complexes no longer show just the single ethyl resonance. Table 4.2 reports the low temperature $^{13}\text{C}\{^1\text{H}\}$ NMR chemical shifts for the hexaethylbenzene complexes for which the NMR spectra varied with temperature. The aim of this work has been to determine, if possible, the low temperature limiting spectra and to correlate them with the structures determined by X-ray crystallography in the solid state. No effort has been made to determine the activation parameters characteristic of the observed changes by line shape analysis, which would require measurement at temperatures differing by *ca.* 5°C between room temperature and the lowest accessible temperature.

In the series of hexaethylbenzene chromium tricarbonyl complexes discussed in Chapter 1 temperature dependant NMR behaviour is also observed, and there is some dispute as to which dynamic process is responsible for it. In summary, while it was generally accepted that rotation about the arene-methylene bond could slow on an NMR timescale, the issue of whether rotation could slow on an NMR timescale about the arene-metal bond axis was contentious.⁷⁵

In order to bring some structure to the discussion, the ruthenium hexaethylbenzene complexes have been divided into categories according to their low temperature NMR behaviour and their solid state conformation. This classification is outlined in Table 4.3. The first class of compounds includes those whose spectra are temperature invariant. All of these complexes have an entirely distal ethyl group conformation in the solid state (see Chapter 3). The complex $\text{Ru}(\eta^6\text{-C}_6\text{Et}_6)(\text{PMe}_3)(\text{Me})\text{Cl}$ also has the 1,3-proximal-2,4,6-distal conformation in about half the molecules present in the solid state.

Table 4.2. Low temperature $^{13}\text{C}\{^1\text{H}\}$ NMR chemical shifts (measured in CD_2Cl_2 unless otherwise stated)

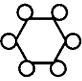
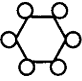
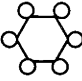
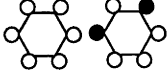
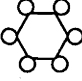
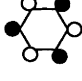

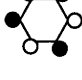
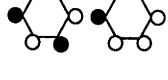
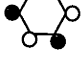
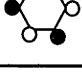
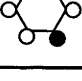
Complex	δ_{Carene} (ppm) (intensity)	δ_{Cethyl} (ppm)	Limiting Temp ($^{\circ}\text{C}$)
$[\text{Ru}(\eta^6\text{-C}_6\text{Et}_6)\text{Cl}_2]_2$	101.7(1), 87.6(1)	22.7, 20.0, 17.3, 11.3	-59
$[\text{Ru}_2(\eta^6\text{-C}_6\text{Et}_6)_2\text{Cl}_3]^+\text{PF}_6^-$	101.1(1), 87.1(1)	22.1, 19.4, 16.7, 12.7	-59
$\text{Ru}(\eta^6\text{-C}_6\text{Et}_6)(\text{CO})\text{Cl}_2$	124(2), 108(1), 103(1), 96(2)	22.8, 22.2, 20.6, 18.7, 17.7, 13.5, 12.5, 11.6	-97
$\text{Ru}(\eta^6\text{-C}_6\text{Et}_6)(\text{Bu}^t\text{NC})\text{Cl}_2$	115.7(2), 104.4(1), 98.4(1), 89.9(2)	23.9, 23.1, 21.3, 19.7, 17.8, 14.5, 14.3, 13.0	-97
$[\text{Ru}(\eta^6\text{-C}_6\text{Et}_6)(\text{Bu}^t\text{NC})_2\text{Cl}]+ \text{PF}_6^-$	126.9(1), 117.3(2), 104.3(2), 97.5(1)	23.1, 22.7, 20.9, 20.1, 18.5, 17.1, 13.6, 12.3	-97
$[\text{Ru}(\eta^6\text{-C}_6\text{Et}_6)(\text{CO})_2\text{Cl}]+ \text{PF}_6^-$	99.2(1), 83.4(1)	21.3, 19.0, 13.8, 11.7	-97
$[\text{Ru}(\eta^6\text{-C}_6\text{Et}_6)(\text{Bu}^t\text{NC})(\text{CO})\text{Cl}]+ \text{PF}_6^-$	133.8(1), 126.1(1), 121.1(1), 111.2(1), 110.5(1), 106.0(1)	24.0, 23.1, 21.3, 20.8, 19.2, 19.0, 17.5, 16.9, 14.4, 13.9, 13.5, 12.6	-97
$\text{Ru}(\eta^6\text{-C}_6\text{Et}_6)(\text{PMe}_3)\text{H}_2^1$	Not fully resolved at the limiting temperature of THF		

¹measured in d^8 -THF

The second class of complexes has two members, $[\text{Ru}(\eta^6\text{-C}_6\text{Et}_6)\text{Cl}_2]_2$ and $[\text{Ru}_2(\eta^6\text{-C}_6\text{Et}_6)_2\text{Cl}_3]^+\text{PF}_6^-$, which are grouped together because of the similar nature of their variable temperature NMR behaviour and the possible relationship between them in solution (see chapter 2). The third class contains complexes that have three small, sterically undemanding ligands in their tripod. All the members of this group have a 1,3,5-proximal-2,4,6-distal arrangement for the ethyl groups in the solid state. The complex $[\text{Ru}(\eta^6\text{-C}_6\text{Et}_6)(\text{Bu}^t\text{NC})_2\text{Cl}]+ \text{PF}_6^-$ also has the 1,3-proximal-2,4,5,6-distal conformation in half the molecules present. It is this class of molecules that bears the closest similarity to the $\text{Cr}(\eta^6\text{-C}_6\text{Et}_6)(\text{CO})_3$ complexes and derivatives discussed in Chapter 1. The complex $\text{Ru}(\eta^6\text{-C}_6\text{Et}_6)(\text{PMe}_3)(\text{H})_2$ cannot be classified as its ^{13}C NMR spectrum was not fully resolved at -110°C , the lowest accessible temperature. The variable temperature NMR spectra of $[\text{Ru}(\eta^6\text{-C}_6\text{Et}_6)(\text{CH}_3\text{CN})_2\text{Cl}]+ \text{PF}_6^-$ and $[\text{Ru}(\eta^6\text{-C}_6\text{Et}_6)(\text{CH}_3\text{CN})_3]^{2+}(\text{CF}_3\text{SO}_3^-)_2$ were not investigated as their solid state structures were

not obtained and the lability of the CH_3CN ligands makes it difficult to determine the species present in solution.

Table 4.3. Number of ethyl groups at the limiting temperature

Complex	Solid state conformation of arene	^{13}C resonances observed at limiting temperature
$\text{Ru}(\eta^6\text{-C}_6\text{Et}_6)(\text{PMe}_3)\text{Cl}_2$		1
$\text{Ru}(\eta^6\text{-C}_6\text{Et}_6)(\text{PMe}_3)(\text{Me})_2$		1
$\text{Ru}(\eta^6\text{-C}_6\text{Et}_6)(\text{PPh}_3)\text{Cl}_2$		1
$\text{Ru}(\eta^6\text{-C}_6\text{Et}_6)(\text{PMe}_3)(\text{Me})\text{Cl}$		1
$[\text{Ru}(\eta^6\text{-C}_6\text{Et}_6)\text{Cl}_2]_2$		2 (1:1)
$[\text{Ru}_2(\eta^6\text{-C}_6\text{Et}_6)_2\text{Cl}_3]^+\text{PF}_6^-$		2 (1:1)
$\text{Ru}(\eta^6\text{-C}_6\text{Et}_6)(\text{CO})\text{Cl}_2$		4 (2:1:1:2)
$\text{Ru}(\eta^6\text{-C}_6\text{Et}_6)(\text{Bu}^t\text{NC})\text{Cl}_2$		4 (2:1:1:2)
$[\text{Ru}(\eta^6\text{-C}_6\text{Et}_6)(\text{Bu}^t\text{NC})_2\text{Cl}]^+\text{PF}_6^-$		4 (1:2:2:1)
$[\text{Ru}(\eta^6\text{-C}_6\text{Et}_6)(\text{CO})_2\text{Cl}]^+\text{PF}_6^-$		2 (1:1)
$[\text{Ru}(\eta^6\text{-C}_6\text{Et}_6)(\text{CO})(\text{Bu}^t\text{NC})\text{Cl}]^+\text{PF}_6^-$		6 (1:1:1:1:1:1)
$\text{Ru}(\eta^6\text{-C}_6\text{Et}_6)(\text{PMe}_3)(\text{H})_2$		unresolved

Complexes with one sort of ethyl group at the limiting temperature

The ^1H and $^{13}\text{C}\{^1\text{H}\}$ NMR spectra in CD_2Cl_2 of $\text{Ru}(\eta^6\text{-C}_6\text{Et}_6)(\text{PMe}_3)\text{Cl}_2$, $\text{Ru}(\eta^6\text{-C}_6\text{Et}_6)(\text{PMe}_3)(\text{Me})_2$, $\text{Ru}(\eta^6\text{-C}_6\text{Et}_6)(\text{PPh}_3)\text{Cl}_2$ and $\text{Ru}(\eta^6\text{-C}_6\text{Et}_6)(\text{PMe}_3)(\text{Me})\text{Cl}$ are temperature invariant, as shown in Figure 4.2 for $\text{Ru}(\eta^6\text{-C}_6\text{Et}_6)(\text{PMe}_3)(\text{Me})_2$. The broadening at -97°C can be attributed to the increased viscosity of the solvent. Since the ethyl groups in the solid state structure are not in equivalent environments there must be dynamic processes that give rise to averaging, as discussed on above. Presumably, the energy barriers to be overcome are too low for separate resonances to be observed at the accessible temperatures.

Two possible fluxional behaviours for these complexes at low temperature in solution that are consistent with the observed spectra are: a) both rotation about the arene-methylene bond and arene-ruthenium bond axis continue unhindered or b) rotation has slowed on an NMR timescale about the arene-methylene bonds giving an all distal conformation and rotation continues unhindered about the arene-ruthenium bond axis. It is impossible to distinguish between these two dynamic processes on the basis of the NMR spectra available.

One common feature of all these complexes is the entirely distal conformation of the hexaethylbenzene observed in the solid state. The complex $\text{Ru}(\eta^6\text{-C}_6\text{Et}_6)(\text{PMe}_3)(\text{Me})\text{Cl}$ is exceptional, since both the all-distal and the 1,3-proximal-2,4,5,6-distal conformation are observed in the solid state.

Three tertiary phosphine complexes of chromium of the type $\text{Cr}(\eta^6\text{-C}_6\text{Et}_6)(\text{CO})_2(\text{PR}_3)$ ($\text{R} = \text{Me}^{99}, \text{Et}^{97}, \text{Ph}^{90}$) have previously been investigated for their variable temperature behaviour. In the solid state all three have two different hexaethylbenzene conformations (see Table 1.1, Chapter 1). For $\text{R} = \text{Me}, \text{Et}$ more than one ^{31}P resonance was observed at low temperature (-100°C). This was ascribed to the presence of different coordinated hexaethylbenzene conformers; in agreement the aromatic region of the ^{13}C NMR spectrum of these complexes showed a complex array of resonances. In the PPh_3 complex, however, only one arene carbon resonance was observed at low temperature in solution. In these three chromium complexes it was assumed that rotation about the arene-metal bond axis continues rapidly on an NMR timescale. In none of the tertiary phosphine complexes of ruthenium discussed so far was there any evidence for the presence of different conformers at low temperature in solution. In the case of $\text{Ru}(\eta^6\text{-C}_6\text{Et}_6)(\text{PMe}_3)\text{Cl}_2$ the low temperature ^{31}P NMR spectrum was measured to *ca.* -60°C and no broadening was observed of the single resonance present.

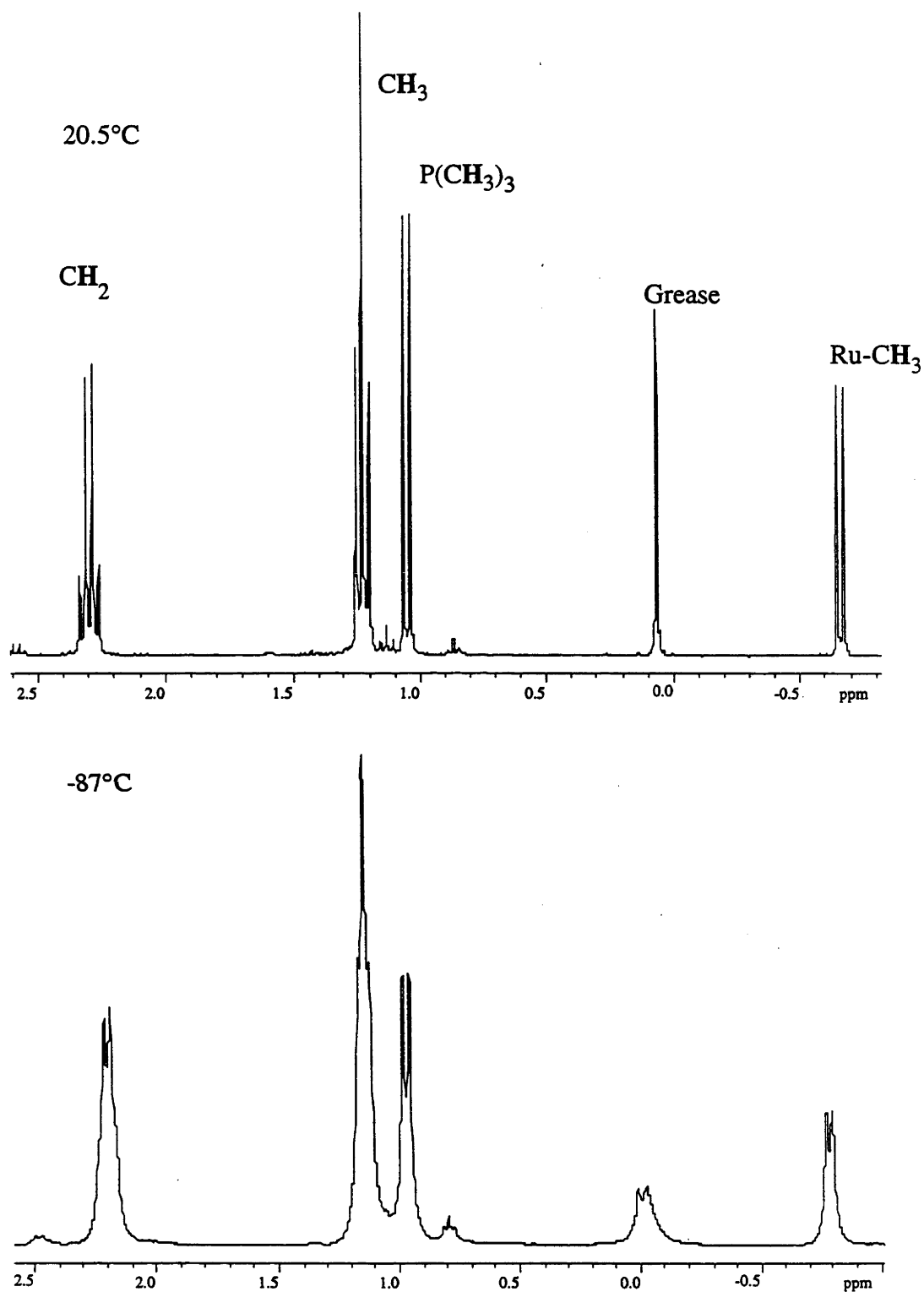


Figure 4.3. Variable temperature ^1H NMR (CD_2Cl_2 , 300 MHz) of $\text{Ru}(\eta^6\text{-C}_6\text{Et}_6)(\text{PMe}_3)(\text{Me})_2$

The complexes $[\text{Ru}(\eta^6\text{-C}_6\text{Et}_6)\text{Cl}_2]_2$ and $[\text{Ru}_2(\eta^6\text{-C}_6\text{Et}_6)_2\text{Cl}_3]^+\text{PF}_6^-$

The variable temperature ^1H NMR spectra of $[\text{Ru}(\eta^6\text{-C}_6\text{Et}_6)\text{Cl}_2]_2$ and the tri- μ -chloro salt, $[\text{Ru}_2(\eta^6\text{-C}_6\text{Et}_6)_2\text{Cl}_3]^+\text{PF}_6^-$, (Figures 4.4 and 4.5 respectively) are similar, as are the corresponding $^{13}\text{C}\{^1\text{H}\}$ NMR spectra (Figure 4.6 and 4.7). In the variable temperature ^1H NMR spectra for these complexes the ethyl resonances at *ca.* δ 2.4 and 1.3 ppm broaden at around -5°C and then eventually collapse into the baseline, with the methylene resonance undergoing this behaviour at a slightly lower temperature than the methyl resonance. They then start to reappear at around -30°C and at -59°C there are two triplets for the methyl protons and two quartets for the methylene protons in a one to one ratio. The average positions of the two new resonances for the methyl and methylene protons are centred approximately on the room temperature resonances.

Similar behaviour is observed in the $^{13}\text{C}\{^1\text{H}\}$ NMR variable temperature spectra. As the temperature is lowered from room temperature, the single methyl, methylene and aromatic carbon atom resonances (*ca.* δ 15, 21 and 93 ppm respectively), collapse and reappear out of the baseline at -30°C as a pair of resonances for each, being fully resolved at -59°C . The temperature range over which these changes occur is closely comparable to that of $\text{Cr}(\eta^6\text{-C}_6\text{Et}_6)(\text{CO})_3$ ⁹⁰ suggesting that the activation barrier is of the same order (*ca.* 48 kJmol^{-1}), although it should be noted that the chemical shift difference between inequivalent arene carbons is somewhat greater in the ruthenium compounds.

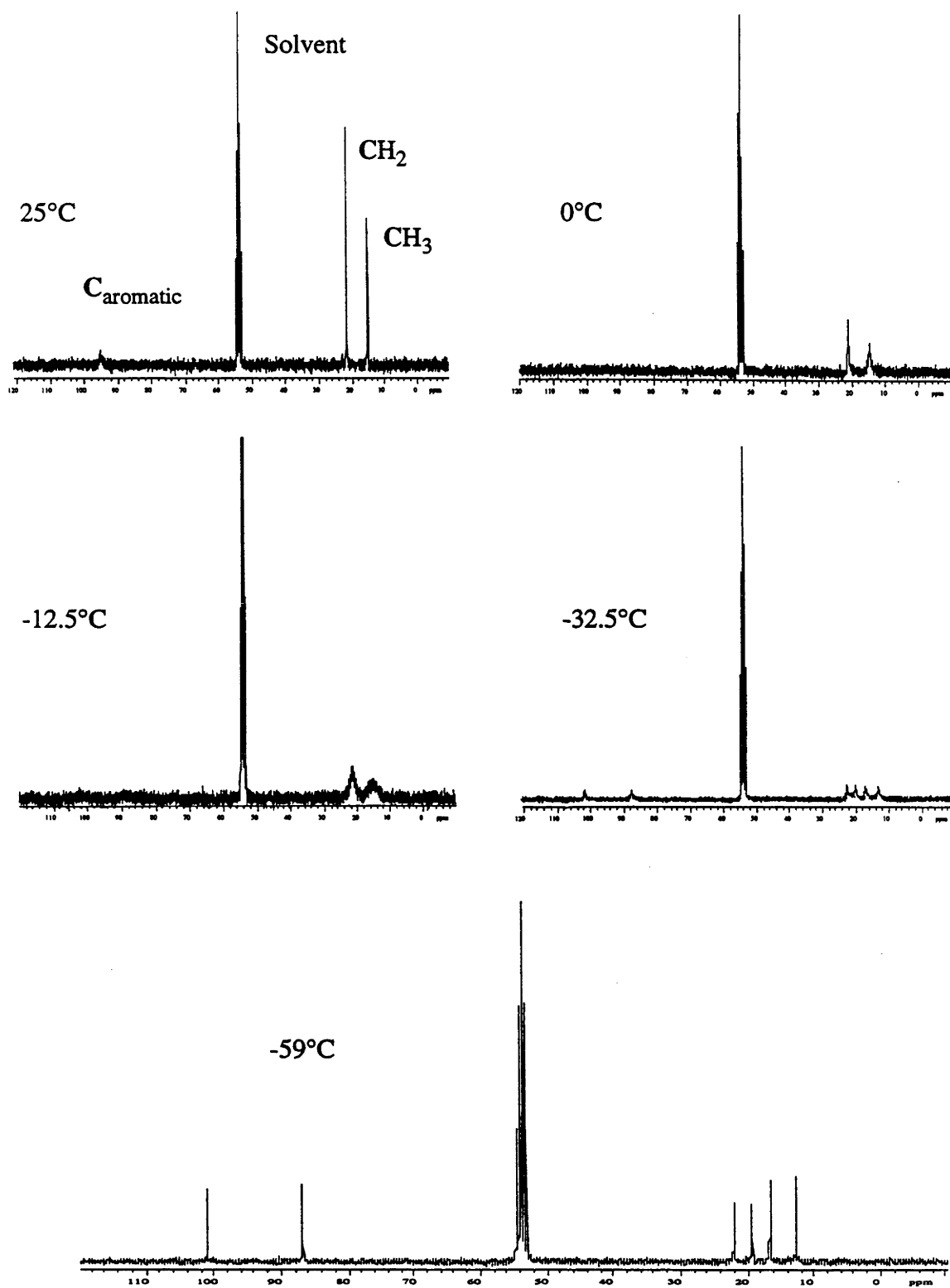


Figure 4.4. Variable temperature $^{13}\text{C}\{^1\text{H}\}$ NMR (CD_2Cl_2 , 75.42 MHz) of $[\text{Ru}(\eta^6\text{-C}_6\text{Et}_6)\text{Cl}_2]_2$

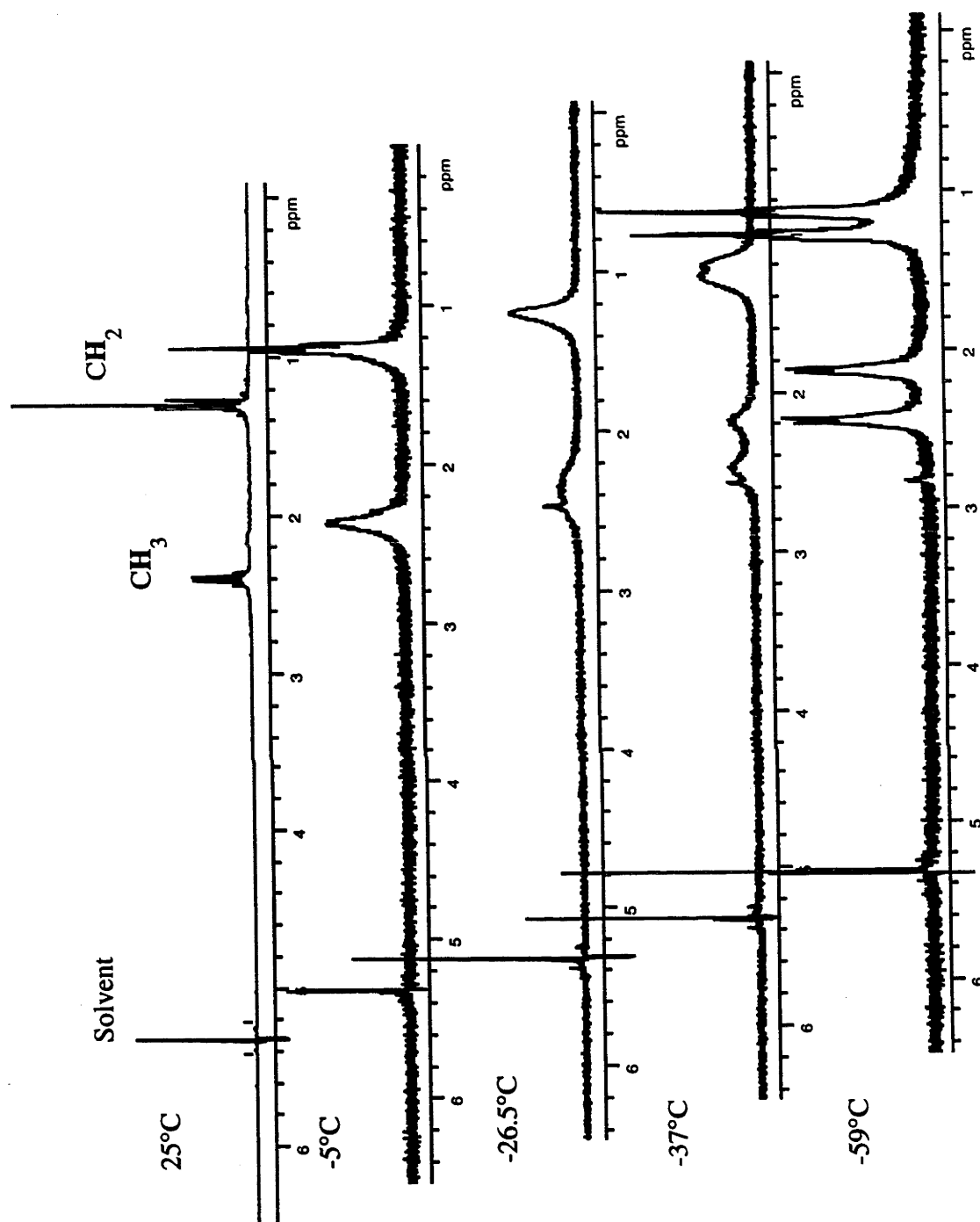


Figure 4.5 Variable temperature ^1H NMR (CD_2Cl_2 , 300MHz) of $[\text{Ru}(\eta^6\text{-C}_6\text{Et}_6)\text{Cl}_2]_2$

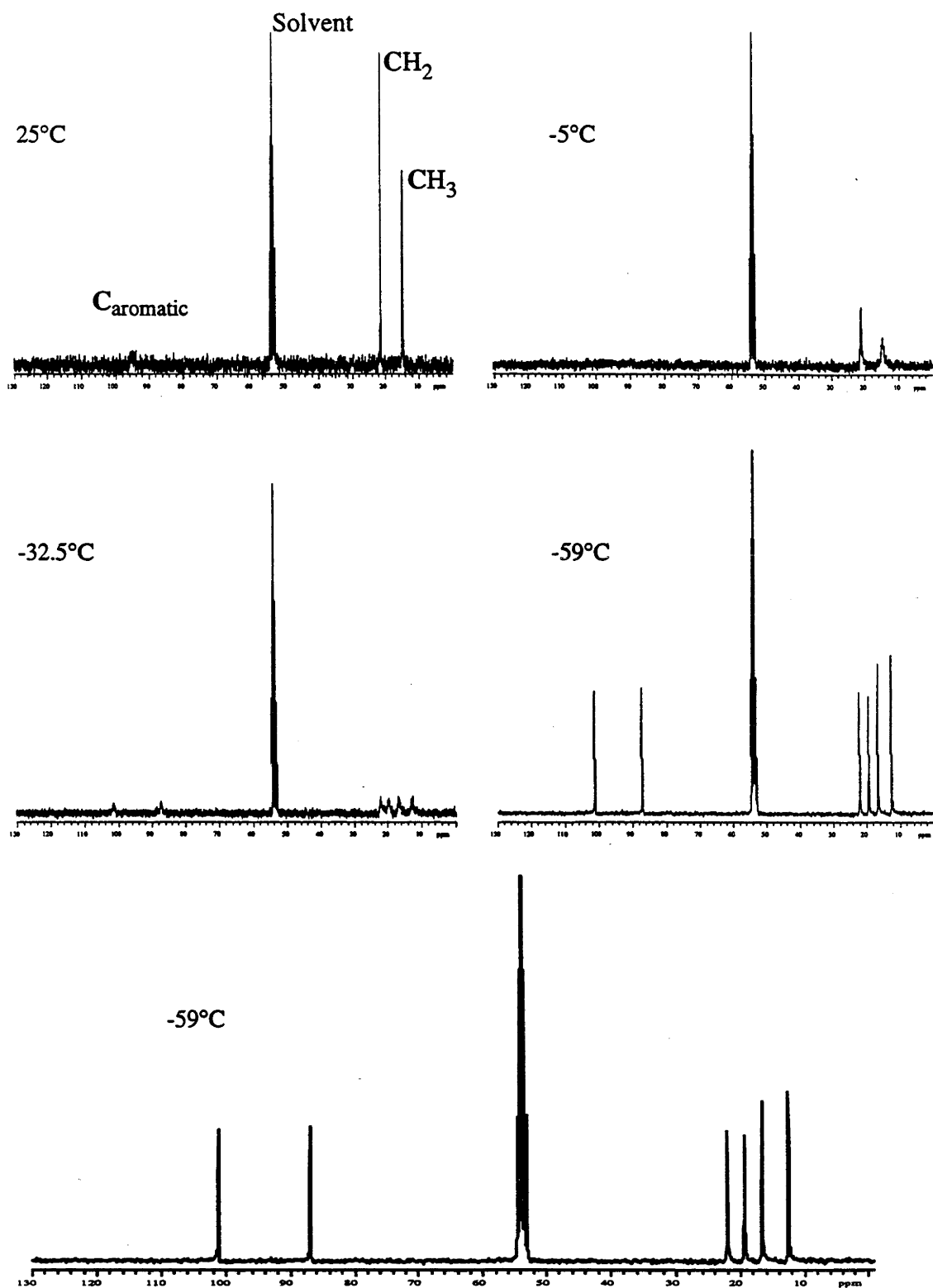


Figure 4.6. Variable temperature $^{13}\text{C}\{^1\text{H}\}$ NMR (CD_2Cl_2 , 75.42 MHz) of $[\text{Ru}_2(\eta^6\text{-C}_6\text{Et}_6)_2\text{Cl}_3]^+\text{PF}_6^-$

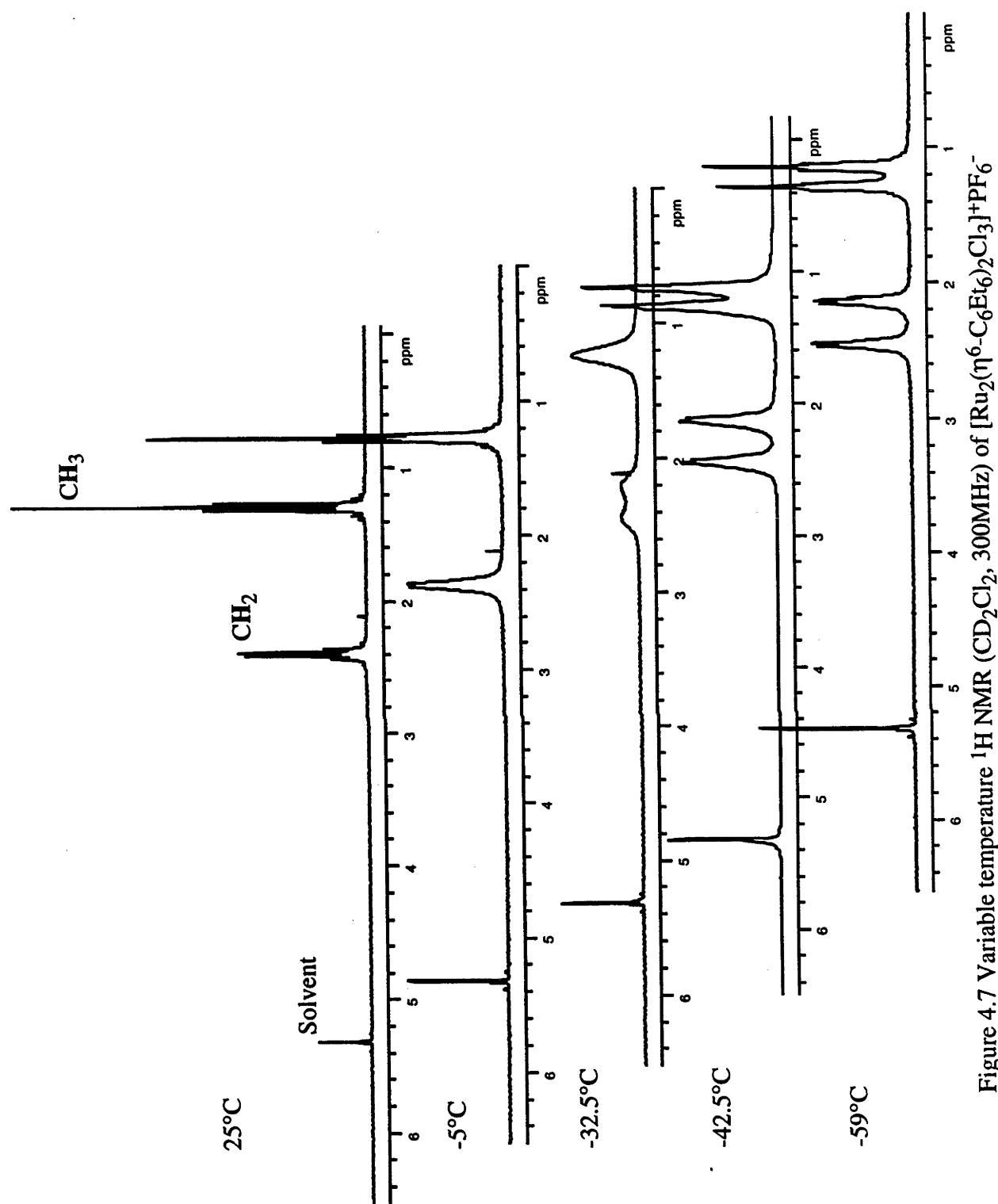


Figure 4.7 Variable temperature ^1H NMR (CD_2Cl_2 , 300MHz) of $[\text{Ru}_2(\eta^6\text{-C}_6\text{Et}_6)_2\text{Cl}_3]^+\text{PF}_6^-$

The molecule $[\text{Ru}_2(\eta^6\text{-C}_6\text{Et}_6)_2\text{Cl}_3]^+\text{PF}_6^-$ resembles $\text{Cr}(\eta^6\text{-C}_6\text{Et}_6)(\text{CO})_3$ in having a 1,3,5-proximal-2,4,6-distal conformation of the ethyl groups and in having three identical ligands in the local tripod about each metal atom. It also has similar variable temperature NMR behaviour.⁷⁶ If the assumption is made that the ruthenium complex has the same identity in solution as it does in the solid state, then the variable temperature NMR behaviour of $[\text{Ru}_2(\eta^6\text{-C}_6\text{Et}_6)_2\text{Cl}_3]^+\text{PF}_6^-$ is consistent either with a) slowing of ethyl group rotation leaving the arene in the same 1,3,5-proximal-2,4,6-distal conformation as observed in the solid state, while continuing to freely rotate on an NMR timescale about the arene-ruthenium bond or b) slowing down of both motions, with the ligands of the tripod eclipsing the distal ethyl groups, as found in the solid state. In both cases, two different ethyl groups would be observed in a 1:1 ratio at low temperature (Figure 4.8.).

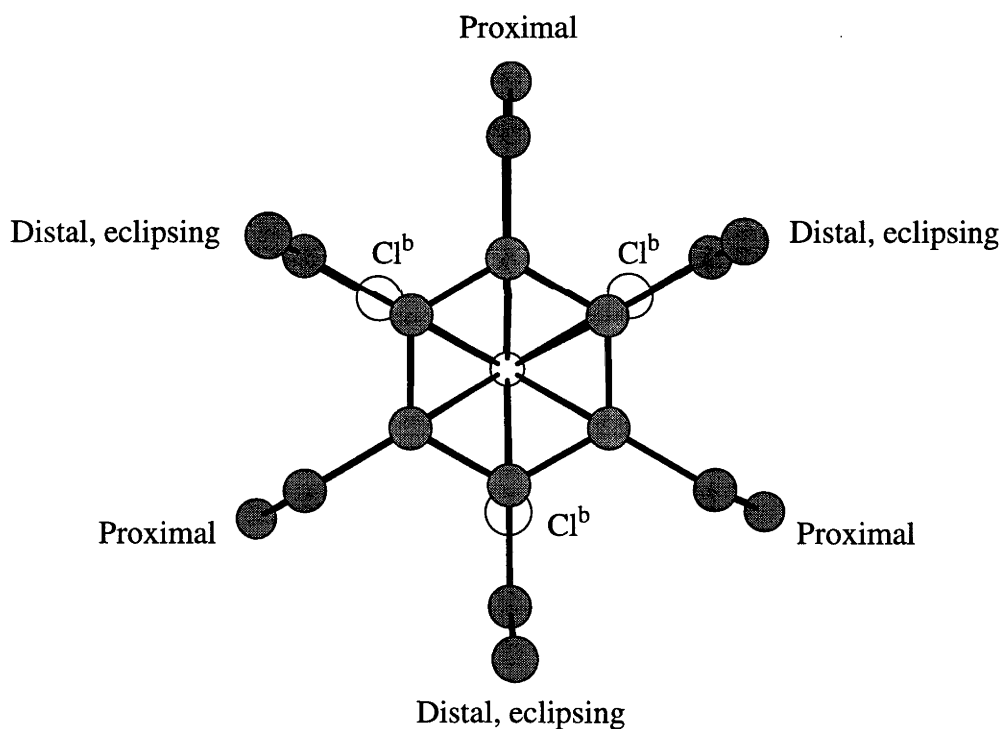


Figure 4.8. Chem 3D view of the solid state structure of $\text{Ru}_2(\eta^6\text{-C}_6\text{Et}_6)_2\text{Cl}_3]^+\text{PF}_6^-$, viewed along the Ru-Ru bond showing the two different ethyl groups with distal ethyl groups eclipsing the bridging chlorine atoms and proximal ethyl groups located between the bridging chlorine atoms.

It is not possible to distinguish between these explanations on the basis of the NMR data available, that is, it is not possible to tell whether the hexaethylbenzene rotation about the arene ruthenium bond slows on an NMR timescale in this complex.

The variable temperature NMR behaviour of $[\text{Ru}(\eta^6\text{-C}_6\text{Et}_6)\text{Cl}_2]_2$ is apparently not consistent with the solid state structure of the molecule, in which an all distal ethyl group arrangement is observed. Cessation on an NMR timescale of any combination of the arene-methylene rotation or arene-ruthenium rotation, freezing out to the solid state conformation cannot give rise to two different ethyl groups. Indeed, if the molecule at low temperature in solution, has the same conformation as it has in the solid state, there should be three different sorts of ethyl groups in a 2:2:2 ratio. (Figure 4.9).

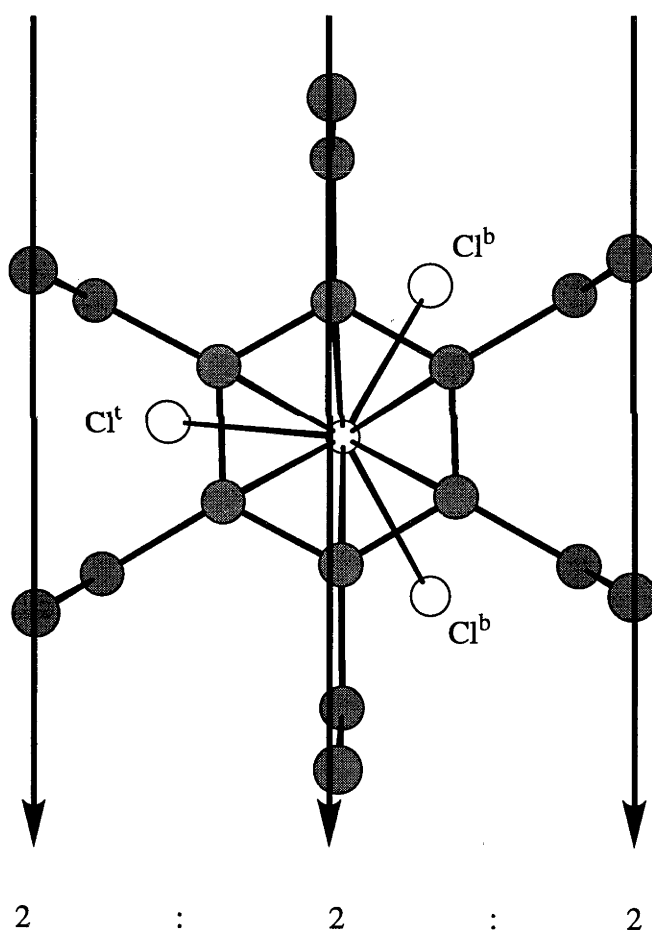


Figure 4.9. Chem 3D view of the solid state structure of $[\text{Ru}(\eta^6\text{-C}_6\text{Et}_6)\text{Cl}_2]_2$, viewed along the arene-centroid ruthenium axis, showing the three different sorts of ethyl groups; two distal groups are either side of the terminal chloride ligand, two are between the terminal chloride and the bridging chloride ligands, and two are between the bridging chloride ligands.

One possible explanation for the observed variable temperature NMR behaviour is that the species responsible is the cation $[\text{Ru}_2(\eta^6\text{-C}_6\text{Et}_6)_2\text{Cl}_3]^+\text{Cl}^-$. If the ethyl groups in the cation have the 1,3,5-proximal-2,4,6-distal conformation observed in the PF_6 salt, and the same process were occurring as in the PF_6 salt, this would give rise to a 1:1 ratio of ethyl groups at low temperature. However, as shown in Chapter 2, $[\text{Ru}(\eta^6\text{-C}_6\text{Et}_6)\text{Cl}_2]_2$ appears to dissociate only to a limited extent in CH_2Cl_2 . Unless there is almost complete dissociation, this explanation is not valid.

An alternative possibility is that the complex does not have the same hexaethylbenzene conformation at low temperature in solution as in the solid state. If rotations about the arene methylene bonds in the complex have slowed at low temperature on an NMR timescale to give the 1,3,5-proximal-2,4,6-distal conformation and the arene has continued to spin about the arene-ruthenium bond axis, then one would expect the 1:1 ratio of two distinct ethyl groups observed in the low temperature NMR spectra.

The variable temperature NMR behaviour of the complex $[\text{Ru}(\eta^6\text{-C}_6\text{H}_4\text{-1,2-Et}_2)\text{Cl}_2]_2$ was examined in the hope that it would be a simpler model for the behaviour of $[\text{Ru}(\eta^6\text{-C}_6\text{Et}_6)\text{Cl}_2]_2$, but this was not realized. At room temperature in CD_2Cl_2 only a quartet and triplet are observed in the ^1H NMR spectrum for the methyl and methylene resonances. At -75°C the methylene protons give rise to a complex multiplet consistent with an ABX_3 system; the methyl resonance remains unchanged with change in temperature. This is consistent with a chemical shift change with change in temperature, the chemical shifts of the two inequivalent methylene protons being accidentally coincident at room temperature in CD_2Cl_2 but changing as the temperature is lowered. At room temperature in CD_3CN , in which solvent the species present is probably the monomeric solvent adduct $\text{Ru}(\eta^6\text{-C}_6\text{H}_4\text{-1,2-Et}_2)(\text{CH}_3\text{CN})\text{Cl}_2$, the expected complex ABX_3 multiplet for the methylene protons is observed. The same spin system was observed in the corresponding tri- μ -chloro salt, $[\text{Ru}_2(\eta^6\text{-C}_6\text{H}_4\text{-1,2-Et}_2)_2\text{Cl}_3]^+\text{PF}_6^-$ (Chapter 2). No evidence of hindered rotation about the arene methylene bond was obtained.

Complexes with three small cylindrical ligands making up the tripod

There are five complexes in this class; $[\text{Ru}(\eta^6\text{-C}_6\text{Et}_6)(\text{Bu}^t\text{NC})_2\text{Cl}]^+\text{PF}_6^-$, $\text{Ru}(\eta^6\text{-C}_6\text{Et}_6)(\text{CO})\text{Cl}_2$, $\text{Ru}(\eta^6\text{-C}_6\text{Et}_6)(\text{Bu}^t\text{NC})\text{Cl}_2$, $[\text{Ru}(\eta^6\text{-C}_6\text{Et}_6)(\text{CO})_2\text{Cl}]^+\text{PF}_6^-$ and $[\text{Ru}(\eta^6\text{-C}_6\text{Et}_6)(\text{CO})(\text{Bu}^t\text{NC})\text{Cl}]^+\text{PF}_6^-$. All of the complexes have a 1,3,5-proximal-2,4,6-distal ethyl group conformation in the solid state. The complex $[\text{Ru}(\eta^6\text{-C}_6\text{Et}_6)(\text{Bu}^t\text{NC})_2\text{Cl}]^+\text{PF}_6^-$ has as well the 1,3-proximal-2,4,5,6-distal conformation for half the molecules present. The first three complexes to be discussed are those for which the behaviour is the simplest to reconcile with their solid state structure: $\text{Ru}(\eta^6\text{-C}_6\text{Et}_6)(\text{CO})\text{Cl}_2$ and $\text{Ru}(\eta^6\text{-C}_6\text{Et}_6)(\text{Bu}^t\text{NC})\text{Cl}_2$ and $[\text{Ru}(\eta^6\text{-C}_6\text{Et}_6)(\text{Bu}^t\text{NC})_2\text{Cl}]^+\text{PF}_6^-$. In these three molecules there is a single mirror plane of symmetry through the tripod. The variable temperature ^{13}C NMR spectra of these three complexes is given in Figures 4.1, 4.11 and 4.12.

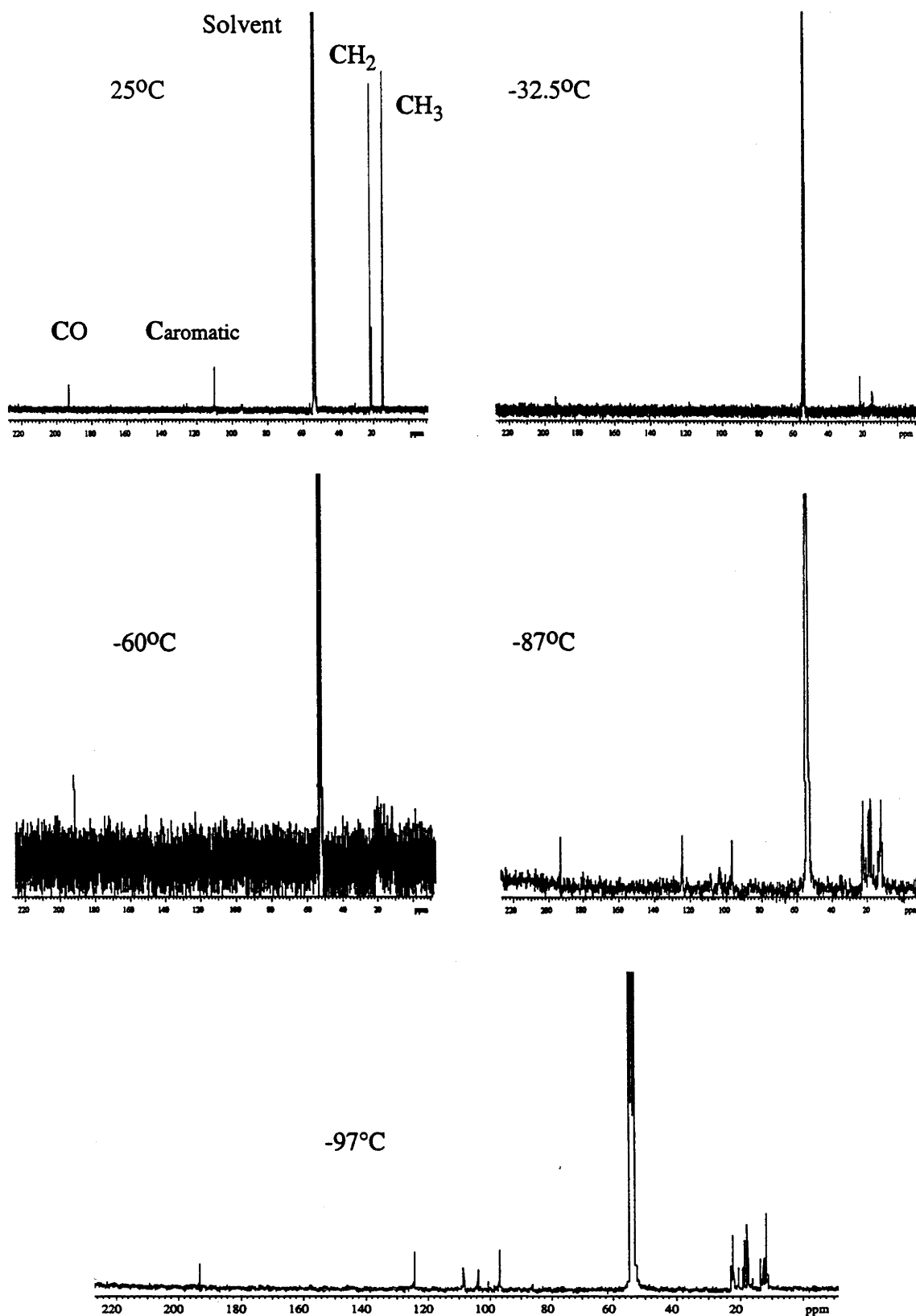


Figure 4.10. Variable temperature $^{13}\text{C}\{^1\text{H}\}$ NMR spectra for $\text{Ru}(\eta^6\text{-C}_6\text{Et}_6)(\text{CO})\text{Cl}_2$ (CD_2Cl_2 , 75.43MHz)

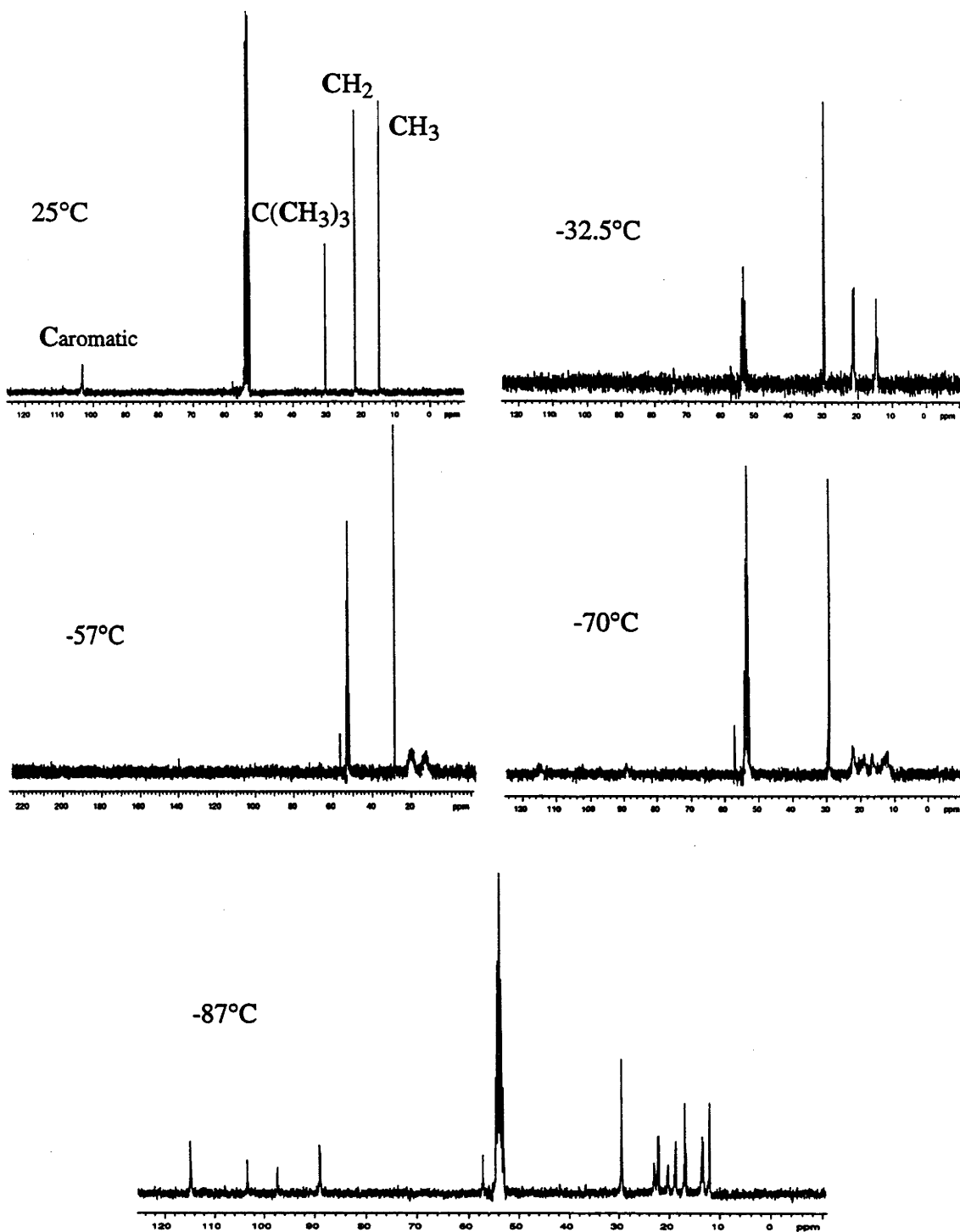


Figure 4.11. Variable temperature ^{13}C { ^1H } NMR spectra for $\text{Ru}(\eta^6\text{-C}_6\text{Et}_6)(\text{Bu}^t\text{NC})\text{Cl}_2$ (CD_2Cl_2 , 75.43MHz)

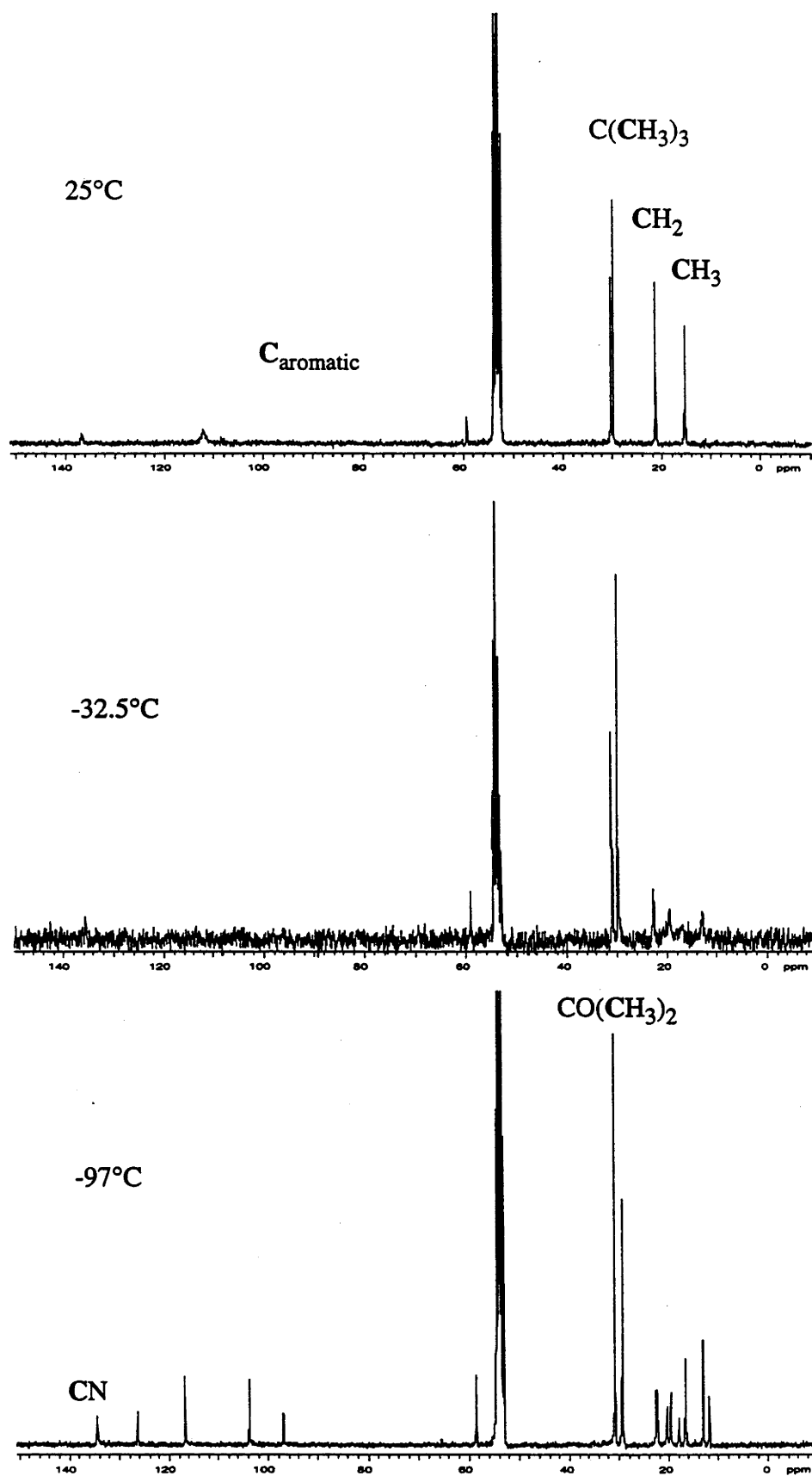


Figure 4.12. Variable temperature ^{13}C $\{^1\text{H}\}$ NMR spectra for $[\text{Ru}(\eta^6\text{-C}_6\text{Et}_6)(\text{BuNC})_2\text{Cl}]^+\text{PF}_6^-$ (CD_2Cl_2 , 75.43MHz)

The three variable temperature $^{13}\text{C}\{^1\text{H}\}$ NMR spectra shown above all display the same features, namely, four different aromatic carbon resonances in a 2:2:1:1 ratio at the limiting temperature. Unfortunately in the solution used for the variable temperature NMR measurements for $[\text{Ru}(\eta^6\text{-C}_6\text{Et}_6)(\text{Bu}^t\text{NC})_2\text{Cl}]\text{PF}_6^-$ there was acetone present as an impurity, which gives rise to a singlet at 31.0 ppm close to the Bu^t resonance of the isocyanide at 30.7 ppm. Taking this complex as representative example, the best region of the spectrum to follow the behaviour is the aromatic carbon signal. As expected, at room temperature, the aromatic carbon atoms give rise to only one resonance (δ 109.8 ppm) and thus there is one sort of ethyl group present. This resonance collapses at *ca.* 0°C and new resonances grow out of the baseline at *ca.* -40°C to give four different arene carbon atom resonances in a 1:2:2:1 ratio (δ 126.9, 117.3, 104.3, and 97.5 ppm) in the fully resolved spectrum at -97°C. The solid state hexaethylbenzene conformation and tripod symmetry as well as the variable temperature NMR behaviour of these three molecules are similar to those observed for $\text{Cr}(\eta^6\text{-C}_6\text{Et}_6)(\text{CO})_2(\text{CS})$.¹⁰⁰

For $\text{Ru}(\eta^6\text{-C}_6\text{Et}_6)(\text{CO})\text{Cl}_2$ ($\text{C}_{\text{aromatic}}$ at low temp, δ 124, 108, 103, 96 ppm) and $\text{Ru}(\eta^6\text{-C}_6\text{Et}_6)(\text{Bu}^t\text{NC})\text{Cl}_2$ ($\text{C}_{\text{aromatic}}$ at low temp δ 115.7, 104.4, 98.4, 89.9 ppm) there are at least two different motions that are consistent with the observed low temperature $^{13}\text{C}\{^1\text{H}\}$ NMR spectra. Firstly, if the arene methylene bond rotation has ceased on an NMR timescale and the arene has taken on a 1,3-proximal-2,4,5,6-distal conformation, or indeed any hexaethylbenzene conformation with a single mirror plane that runs through an arene carbon atom (1-proximal-2,3,4,5,6-distal or 1,2,3-proximal-4,5,6-distal), a 2:2:1:1 ratio is expected. In this case it is not necessary to invoke hindered arene ruthenium rotation. (Figure 4.13)

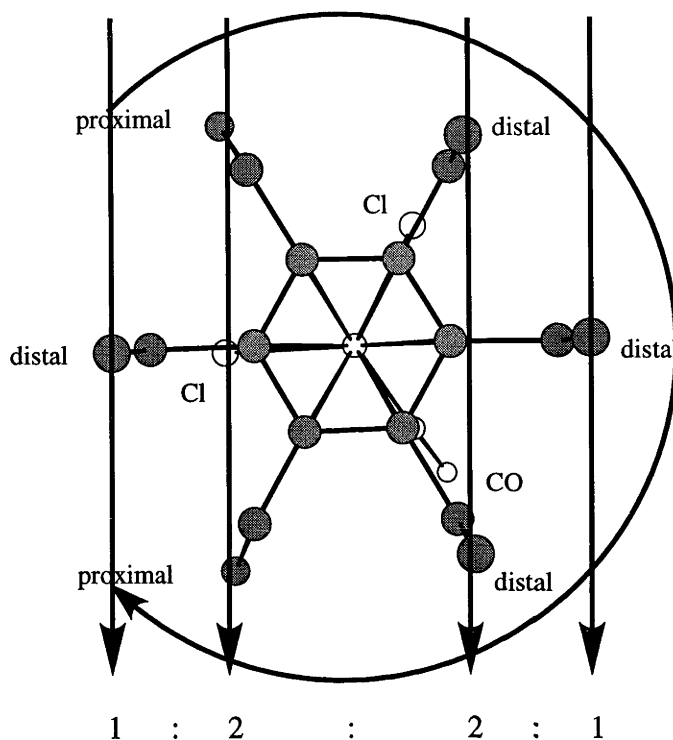


Figure 4.13. Chem 3D diagram of $\text{Ru}(\eta^6\text{-C}_6\text{Et}_6)(\text{CO})\text{Cl}_2$ viewed along arene ruthenium bond axis with 1,3-proximal-2,4,5,6-distal conformation of ethyl groups showing the presence of four different ethyl groups in a 1:2:2:1 ratio. As rotation about the arene-ruthenium bond axis continues unhindered the ligands of the tripod do not change the ethyl environment.

Secondly, if both the arene ruthenium and arene methylene rotations have ceased on an NMR timescale and the rotational orientations of both the hexaethylbenzene about the arene-ruthenium bond and the arene methylene bonds are the same as in the solid state, then the four arene carbon resonances in a 2:2:1:1 ratio are expected. (Figure 4.14).

It is to be noted that for these arguments to hold, the hexaethylbenzene must be frozen into exactly the same rotational conformer as found in the solid state. If the ligands do not eclipse the arene carbons, but are located between the carbon atoms the observed 2:2:1:1 ratio of ethyl groups is not expected but, rather, every ethyl group becomes inequivalent. (Figure 4.15).

In some of the complexes of hexaethylbenzene previously studied it has been found that more than one conformer of coordinated hexaethylbenzene is present at low temperature in solution (see Chapter 1). There are two pieces of evidence that make this unlikely in the three complexes discussed above. Firstly, there would have to be an accidentally coincident chemical shift for the carbon resonances of the CO and Bu^tNC ligands for the different conformers. Secondly, they would have to be present in exactly the right ratio to

give the 2:2:1:1 ratio observed, which seems unlikely. For example, it is conceivable, though improbable, that the 2:2:1:1 ratio arises from the presence of the 1,4-proximal-2,3,4,6- distal, the 1,3,5-proximal-2,4,6-distal and the all distal conformation in a 3:2:1, ratio with accidental coincidence of the chemical shift of the single all distal resonance and one of the two resonances of the proximal-distal staggered conformation, and with free rotation about the arene ruthenium bond axis in all three conformers.

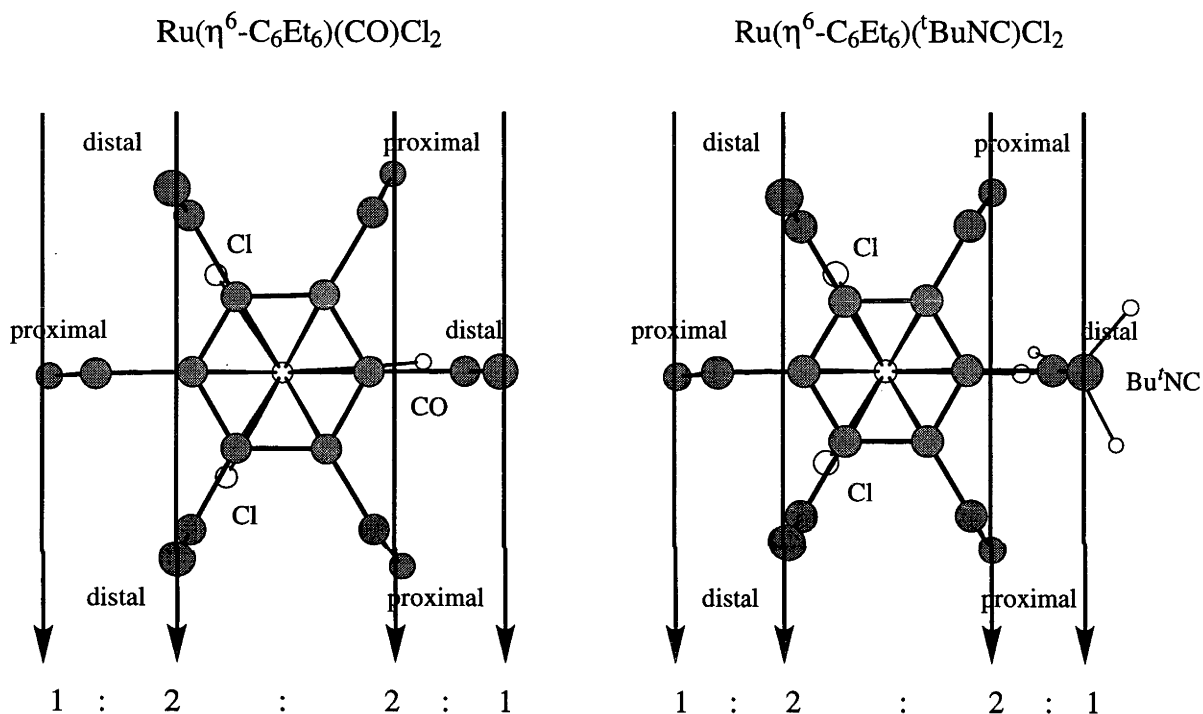


Figure 4.14. Chem 3D portrayal of the solid state conformations of $\text{Ru}(\eta^6\text{-C}_6\text{Et}_6)(\text{CO})\text{Cl}_2$ and $\text{Ru}(\eta^6\text{-C}_6\text{Et}_6)(\text{tBuNC})\text{Cl}_2$ viewed from above along the ruthenium arene bond axis showing the four different ethyl groups present in each of these complexes.

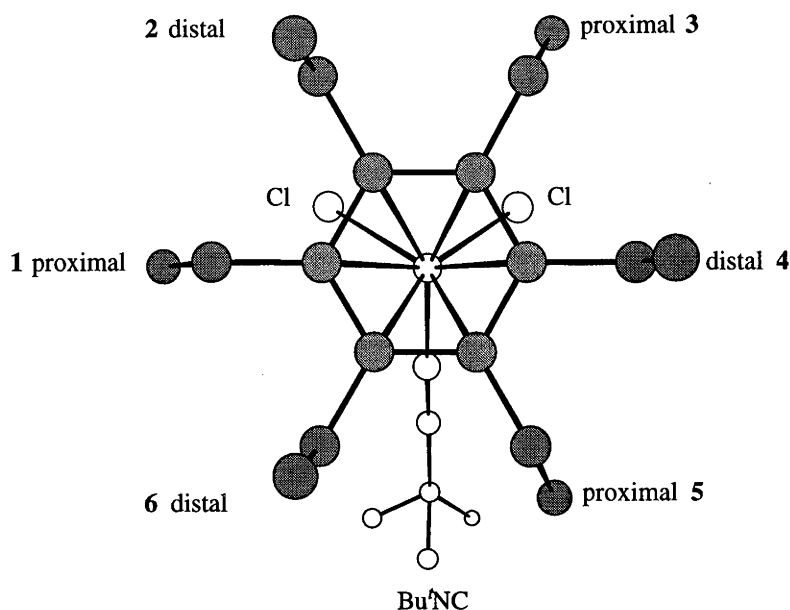


Figure 4.15. Chem 3D portrayal of $\text{Ru}(\eta^6\text{-C}_6\text{Et}_6)(\text{Bu}'\text{NC})\text{Cl}_2$ viewed along the arene-ruthenium bond axis in a 'staggered' conformation showing six inequivalent ethyl groups.

In the unit cell of $[\text{Ru}(\eta^6\text{-C}_6\text{Et}_6)(\text{Bu}'\text{NC})_2\text{Cl}]^+\text{PF}_6^-$ equal proportions of the 1,3,5-proximal-2,4,6-distal and the 1,3-proximal-2,4,5,6-distal conformation of hexaethylbenzene are observed which must be of comparable energy. If rotation about the arene ruthenium bond axis has ceased on an NMR timescale, and if the hexaethylbenzene takes either of these two conformations, the same 1:2:2:1 ratio of ethyl groups should be observed (Figure 4.16). Alternatively, the rotation about the arene ruthenium bond axis could continue and the arene could have taken on a conformation in which a single mirror plane through an arene carbon atom exists; the same ratio of ethyl group resonances would be expected.

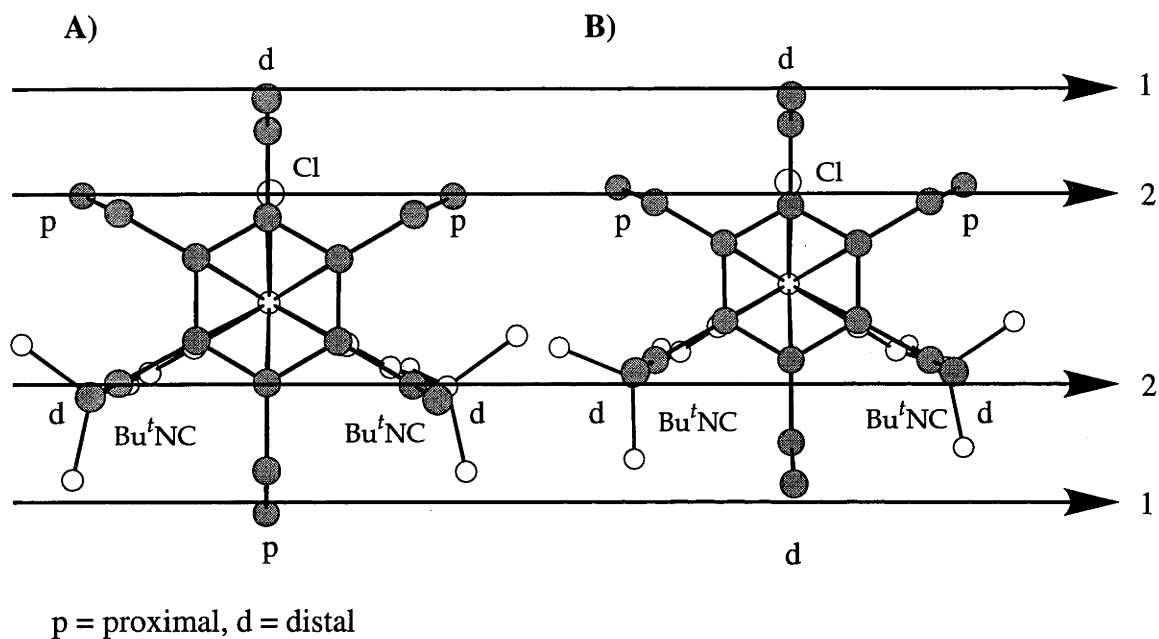


Figure 4.16. Chem 3D portrayal along arene-ruthenium bond axis of **A)** 1,3,5-proximal-2,4,6-distal conformation of $[\text{Ru}(\eta^6\text{-C}_6\text{Et}_6)(\text{Bu}^t\text{NC})_2\text{Cl}]\text{PF}_6^-$, **B)** 1,3-proximal-2,4,5,6-distal conformation of $[\text{Ru}(\eta^6\text{-C}_6\text{Et}_6)(\text{Bu}^t\text{NC})_2\text{Cl}]\text{PF}_6^-$ showing 1:2:2:1 ratio of ethyl groups

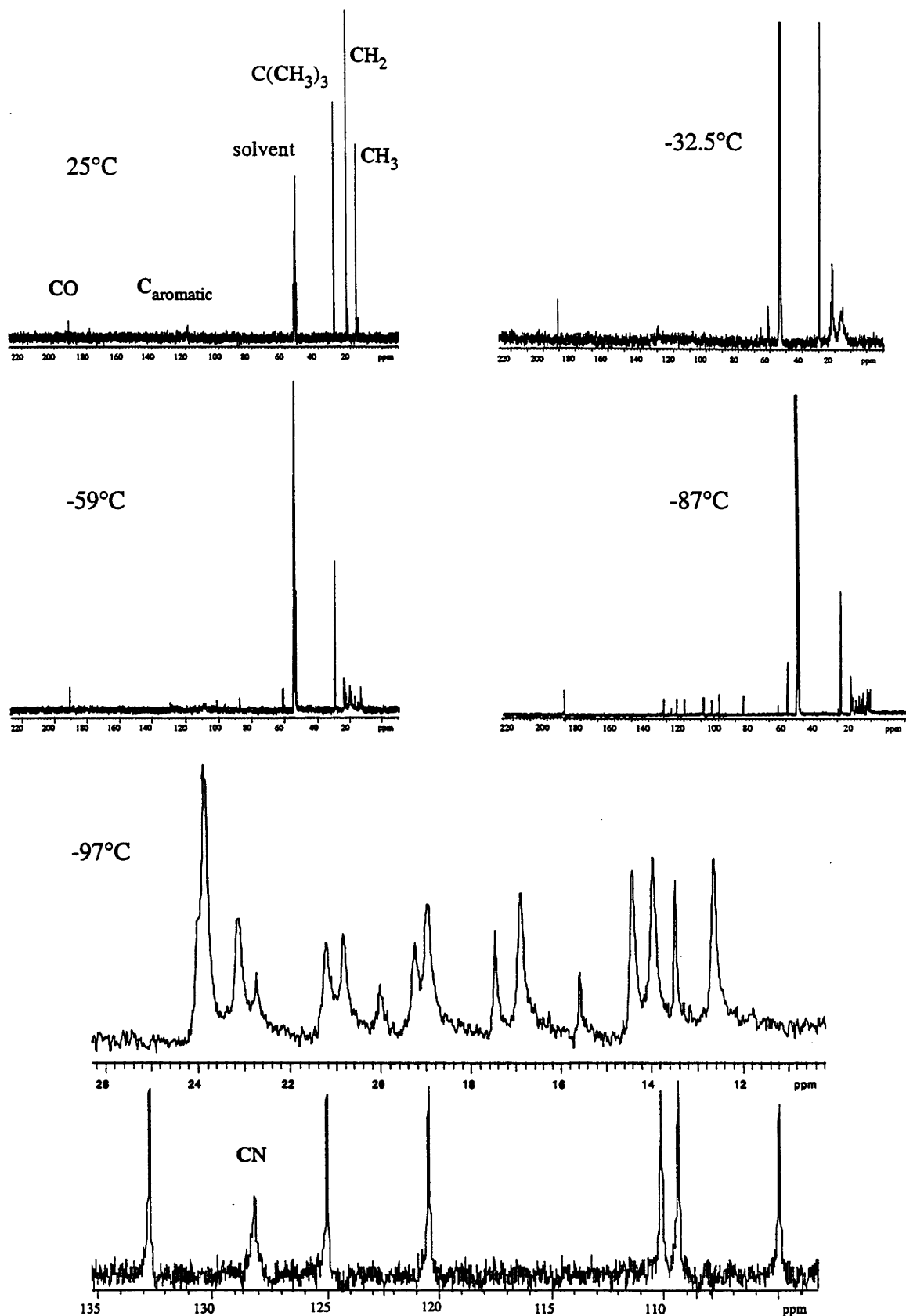


Figure 4.17. Variable temperature $^{13}\text{C}\{^1\text{H}\}$ NMR spectra for $[\text{Ru}(\eta^6\text{-C}_6\text{Et}_6)(\text{BuNC})(\text{CO})\text{Cl}]^+\text{PF}_6^-$ (CD_2Cl_2 , 75.43 MHz)

The cation $[\text{Ru}(\eta^6\text{-C}_6\text{Et}_6)(\text{Bu}^t\text{NC})(\text{CO})\text{Cl}]^+\text{PF}_6^-$ was synthesized (Chapter 2) and its variable temperature NMR behaviour was examined because it was thought that this complex, containing three different rod-like ligands in the tripod would probe arene-Ru rotation. The cation $[\text{Cr}(\eta^6\text{-C}_6\text{Et}_6)(\text{CO})(\text{CS})(\text{NO})]^+$ has been used for the same purpose in the series of compounds derived from $\text{Cr}(\eta^6\text{-C}_6\text{Et}_6)(\text{CO})_3$. The variable temperature $^{13}\text{C}\{^1\text{H}\}$ NMR spectra for $[\text{Ru}(\eta^6\text{-C}_6\text{Et}_6)(\text{Bu}^t\text{NC})(\text{CO})\text{Cl}]^+\text{PF}_6^-$ are given in Figure 4.17. If the behaviour of the complex is again followed from the resonances of the coordinated arene carbon atoms, it can be seen that there is one resonance at room temperature, which collapses as the temperature is reduced to approximately 0°C , then reappears as six distinct resonances of equal intensity as the temperature is reduced to -97°C . This behaviour is also observed with each of the methyl and methylene resonances. There is a small amount of $[\text{Ru}_2(\eta^6\text{-C}_6\text{Et}_6)_2\text{Cl}_3]^+\text{PF}_6^-$ present as an impurity (δ 101 and 87 ppm for the coordinated aromatic carbon atoms). The seventh broader and less intense resonance at *ca.* δ 128 ppm in the coordinated aromatic region of the $^{13}\text{C}\{^1\text{H}\}$ NMR spectrum (see bottom of Figure 4.17) can be assigned to the coordinated carbon atom of the isocyanide, on the basis of its temperature invariance (*cf.* δ 157 to 138 ppm for various arene ruthenium isocyanide complexes⁴⁵). This resonance becomes more intense relative to the coordinated arene carbon atom resonances at low temperature and has an almost triplet like appearance, as expected from coupling to ^{14}N ($I=1$).

The variable temperature NMR behaviour is consistent with slowing of both rotational motions on an NMR timescale, leaving the complex in its solid state conformation, leading to inequivalence of all six ethyl groups. (Figure 4.18)

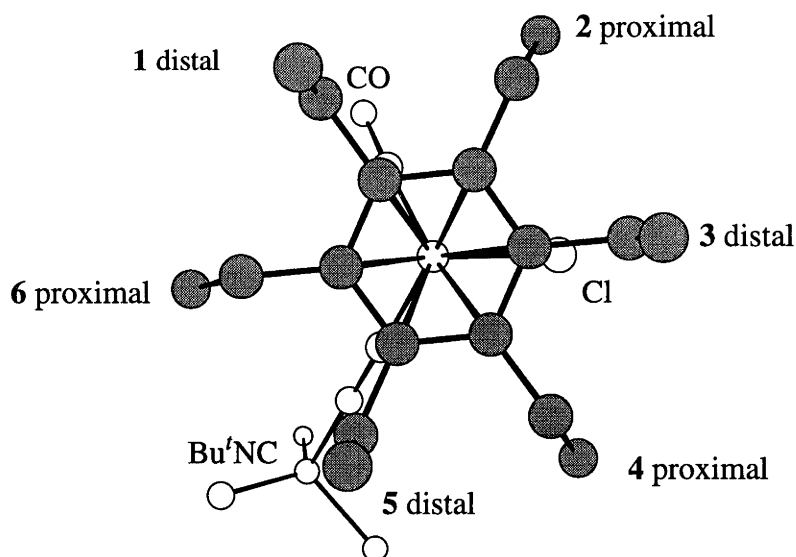


Figure 4.18. Chem3D portrayal of $[\text{Ru}(\eta^6\text{-C}_6\text{Et}_6)(\text{Bu}^i\text{NC})(\text{CO})\text{Cl}]^+\text{PF}_6^-$ along the arene-ruthenium bond axis showing six different ethyl groups. (1 distal, eclipsing CO; 2 proximal, between CO and Cl; 3 distal, eclipsing Cl; 4 proximal, between Cl and Bu^iNC ; 5 distal, eclipsing Bu^iNC ; 6 proximal, between CO and Bu^iNC)

Unfortunately, this is still not decisive evidence for slowing of rotation about the arene-ruthenium bond. If rotation has only slowed about the arene methylene bonds, leaving the hexaethylbenzene in a conformation with a single mirror plane of symmetry which runs through an arene carbon atom, the 1,3-proximal-2,4,5,6-distal conformation for example, then each of the eighteen carbons in the hexaethylbenzene ligand is magnetically inequivalent, regardless of whether rotation about the arene ruthenium bond has slowed.

This can be seen from Figure 4.19. When the ethyl group designated P_1 is between the CO and the Cl ligands ethyl group P_2 is between the CO and Bu^iNC ligands. For ethyl groups P_1 and P_2 to be equivalent, as indeed they are when the arene is not bonded to a tripod with three different substituents, then when P_1 rotates around to the position between the CO and Bu^iNC ligands P_2 should lie between the CO and Cl ligands. It can be seen that this is not the case; P_2 now lies between the Bu^iNC ligand and the Cl ligand. Thus all the ethyl groups are inequivalent regardless of the rotational motion of the arene about the arene ruthenium bond.

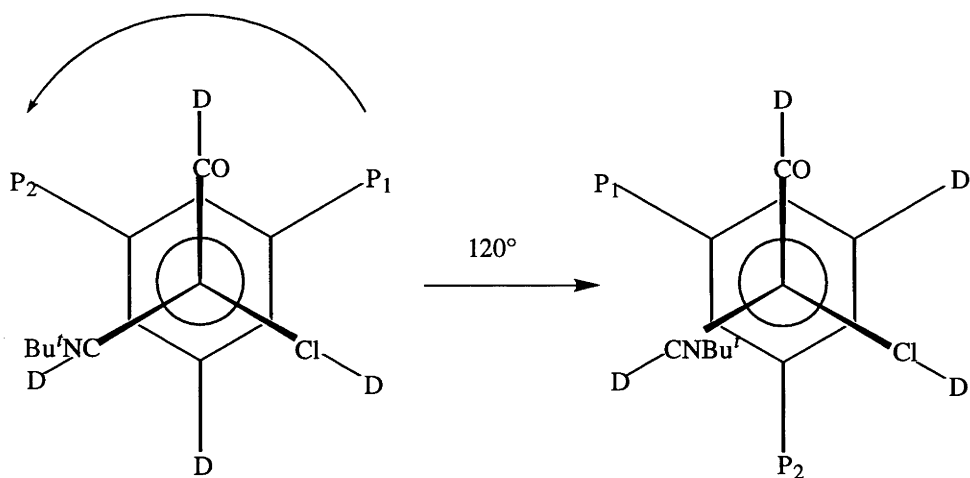


Figure 4.19. View of $[\text{Ru}(\eta^6\text{-C}_6\text{Et}_6)((\text{Bu}^{\text{T}}\text{NC})(\text{CO})\text{Cl})]^+\text{PF}_6^-$ looking from top along ruthenium-ring centroid axis. Ring substituents P_1 and P_2 are proximal ethyl groups while those designated D are distal ethyl groups.

Thus, in the examples discussed so far, the variable temperature behaviour can be explained in one of two ways: either rotations about both the arene ruthenium bond and the arene methylene bonds have ceased on an NMR timescale, or ethyl groups rotation has ceased, freezing the hexaethylbenzene into a particular conformation, while rotation about the arene-ruthenium bond continues freely.

What needs to be known in all these cases is what proportion of ethyl groups are proximally orientated and what proportion of ethyl groups are distally orientated. If it were known that three were distal and three were proximal, then the possibility that the arene had taken on a conformation with a single mirror plane of symmetry could be almost discounted; the only possibility would be that the arene had taken on the sterically unfavourable 1,2,3-proximal-4,5,6-distal conformation, which has never been observed for any complexes of hexaethylbenzene. If this were known then the case for hindered rotation in hexaethylbenzene complexes of ruthenium would be a strong one.

The variable temperature NMR behaviour of $[\text{Cr}(\eta^6\text{-C}_6\text{Et}_6)(\text{CO})(\text{CS})(\text{NO})]^+\text{BF}_4^-$, which has both the same solid state conformation of hexaethylbenzene and molecular symmetry as $[\text{Ru}(\eta^6\text{-C}_6\text{Et}_6)(\text{Bu}^{\text{T}}\text{NC})(\text{CO})\text{Cl}]^+\text{PF}_6^-$ has identical behaviour in the variable temperature $^{13}\text{C}\{^1\text{H}\}$ NMR spectra. However, in this particular complex, it was found possible to assign the proximal and distal ethyl groups on the basis of assignments made on previously characterised complexes of hexaethylbenzene¹⁰² and $\text{Cr}(\eta^6\text{-C}_6\text{H}_5\text{COCH}_3)(\text{CO})_3$ for which the ethyl conformations were known in solution. On this

basis, it was stated unequivocally that rotation about the arene ruthenium bond had ceased in this complex.⁹²

It has been observed at -60°C in the $^{13}\text{C}\{^1\text{H}\}$ NMR spectrum of $\text{Ru}(\eta^6\text{-C}_6\text{H}_4\text{-1,4-Bu}^t_2)(^{13}\text{CO})(\text{SiCl}_3)_2$, a complex in which rotation about the arene ruthenium bond axis ceases on an NMR timescale at low temperature, that the resonance for the arene carbon atom trans to the ^{13}CO ligand is a doublet due to ^{13}C - ^{13}C coupling, while the other aromatic carbon resonances were singlets. This enabled the assignment of the spectrum and was conclusive evidence for cessation of rotation about the arene ruthenium bond on an NMR timescale.⁸⁵

The complex $\text{Ru}(\eta^6\text{-C}_6\text{Et}_6)(^{13}\text{CO})\text{Cl}_2$ was prepared in a similar manner to the unlabelled analogue. It was hoped that it would be possible to observe coupling between the ^{13}CO and the aromatic ring carbons. The coordinated aromatic carbon region of the $^{13}\text{C}\{^1\text{H}\}$ NMR spectrum at -97°C is given in Figure 4.20. At room temperature no coupling between the aromatic ring carbon atoms and the ^{13}CO was observed, which is to be expected given the broad nature of the aromatic ring carbon atom resonance under these conditions. At the limiting temperature, however, the same four resonances in the 2:1:1:2 ratio are observed (δ 124, 108, 103 and 96 ppm) as for the unlabelled complex, only two resonances now appear to be split into doublets [δ 124 and 103 ppm $J(^{13}\text{C}\text{-}^{13}\text{C}) = ca. 1 \text{ Hz}$ cf. $\text{Ru}(\eta^6\text{-C}_6\text{H}_4\text{-1,2-Bu}^t_2)(^{13}\text{CO})(\text{SiCl}_3)_2$ $J(^{13}\text{C}\text{-}^{13}\text{C}) = 0.7 \text{ Hz}$ ⁸⁵]. It is proposed that the less intense of these two resonances (δ 103 ppm) corresponds to the carbon of the aromatic ring that is trans to the carbonyl group while the resonance of greater intensity (δ 124 ppm) can be assigned to the carbon atoms that, when viewed along the arene ruthenium bond axis, eclipse the chloro ligands. Unfortunately, the resolution of the spectrum is not good enough to say for certain that the other resonances are not also coupled to ^{13}CO . A second complicating factor is the peak from an impurity at *ca.* 101 ppm, which is thought to be one of the two resonances for the aromatic carbons of $[\text{Ru}(\eta^6\text{-C}_6\text{Et}_6)\text{Cl}_2]_2$ observed at low temperature. If indeed only two of the resonances are coupled, this would be good evidence that rotation about the arene-ruthenium bond axis has slowed on an NMR timescale.

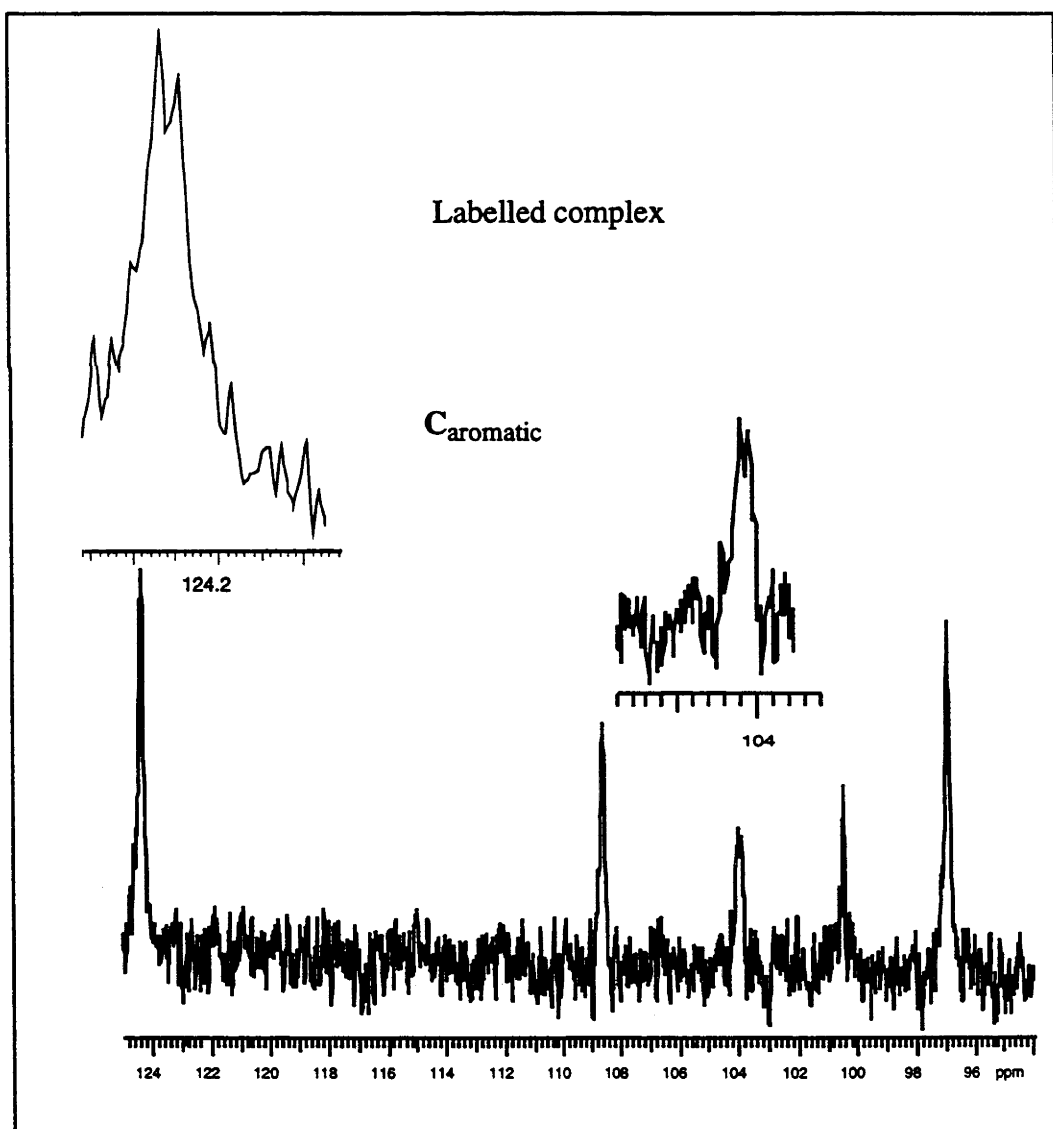
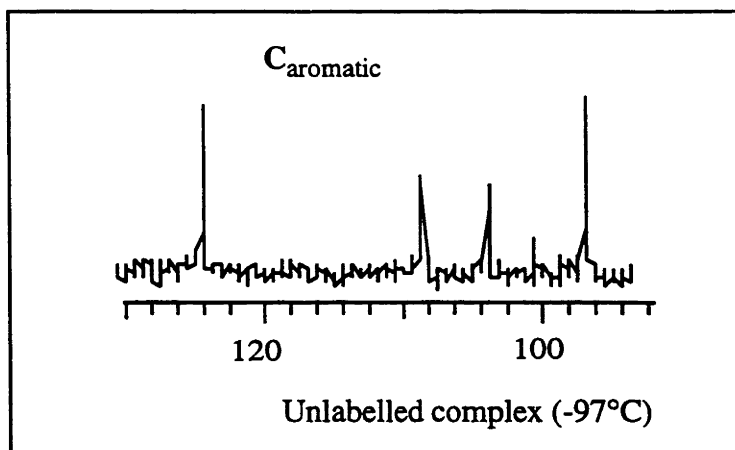


Figure 4.20. $^{13}\text{C}\{^1\text{H}\}$ NMR (CD_2Cl_2 , 75.43 MHz, -97°C) of $\text{Ru}(\eta^6\text{-C}_6\text{Et}_6)(^{13}\text{CO})\text{Cl}_2$

The complex $[\text{Ru}(\eta^6\text{-C}_6\text{Et}_6)(\text{CO})_2\text{Cl}]\text{PF}_6^-$ is the one anomalous member of this group of complexes with three small cylindrical ligands making up the tripod. If the assumption is made that the molecule maintains its identity in solution, then its behaviour at low temperature in solution is not consistent with rotation about the arene-ruthenium bond axis having ceased. Figure 4.21 gives the room temperature and low temperature $^{13}\text{C}\{^1\text{H}\}$ NMR spectra of this molecule in CD_2Cl_2 . At -97°C in solution, two different sorts of ethyl groups are present in a 1:1 ratio. The symmetry of this complex is such that it is impossible for the rotation to cease about the arene ruthenium bond axis and obtain the observed spectrum. Instead the low temperature NMR spectrum is only consistent with rotation about the arene methylene bond having ceased, the ethyl groups freezing out in the 1,3,5-proximal-2,4,6-distal conformation and rotation about the arene-ruthenium bond axis continuing rapidly on an NMR timescale.

One possible explanation for the observed behaviour to be considered is that the complex has decomposed to $[\text{Ru}_2(\eta^6\text{-C}_6\text{Et}_6)_2\text{Cl}_3]\text{PF}_6^-$ in CD_2Cl_2 , since the low temperature ^{13}C NMR spectra are very similar. However, the chemical shifts of the aromatic ring carbons at low temperature are significantly different (δ 101.1, 87.6 ppm for the tri- μ -chloro salt and δ 99.2 and 83.4 ppm for the bis(carbonyl) complex), and the infrared spectrum of the solid left after evaporating the NMR sample still had strong bands for CO stretching at around 2000 and 2064 cm^{-1} , which are the same as in the starting compound, suggesting that the complex does not give up CO in CD_2Cl_2 . Moreover, the crystals from which the X-ray structure was obtained were grown from a dichloromethane solution. As noted in Chapter 3, the room temperature chemical shift of the arene carbon atoms is anomalous and does not follow the general trend observed between neutral and cationic species in this series of complexes with a tripod of cylindrical ligands. While the other cationic species prepared have chemical shifts of *ca.* δ 110 ppm or higher, the dicarbonyl cation has an anomalously low chemical shift of *ca.* δ 93 ppm, which is the lowest chemical shift for any of the hexaethylbenzene complexes prepared. At present the anomalous ^{13}C NMR behaviour of $[\text{Ru}(\eta^6\text{-C}_6\text{Et}_6)(\text{CO})_2\text{Cl}]\text{PF}_6$ has no satisfactory explanation.

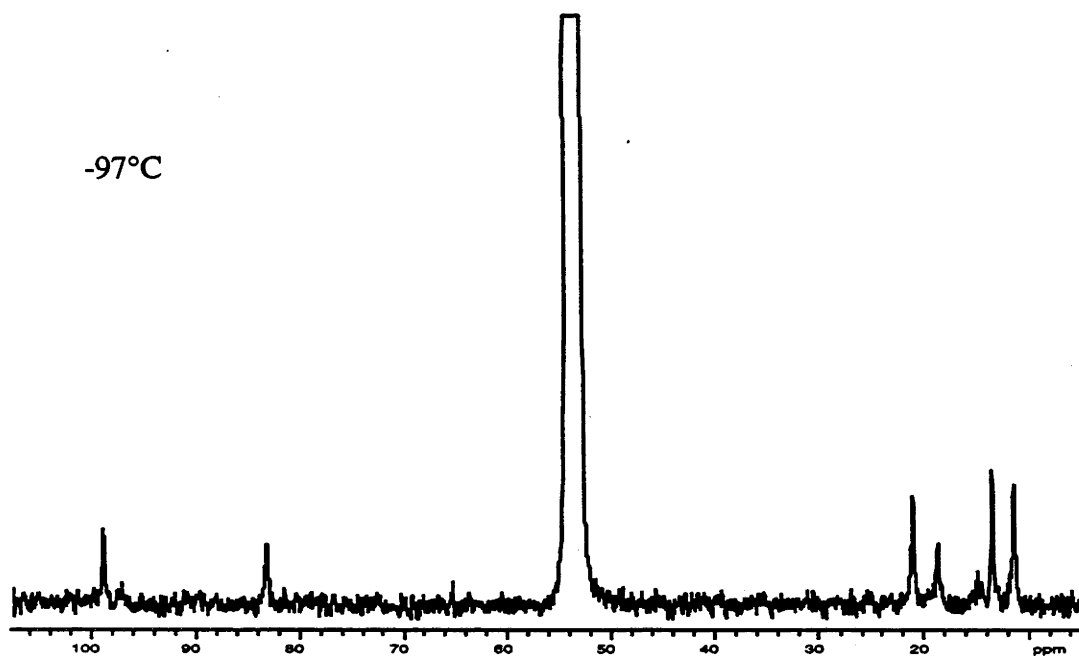
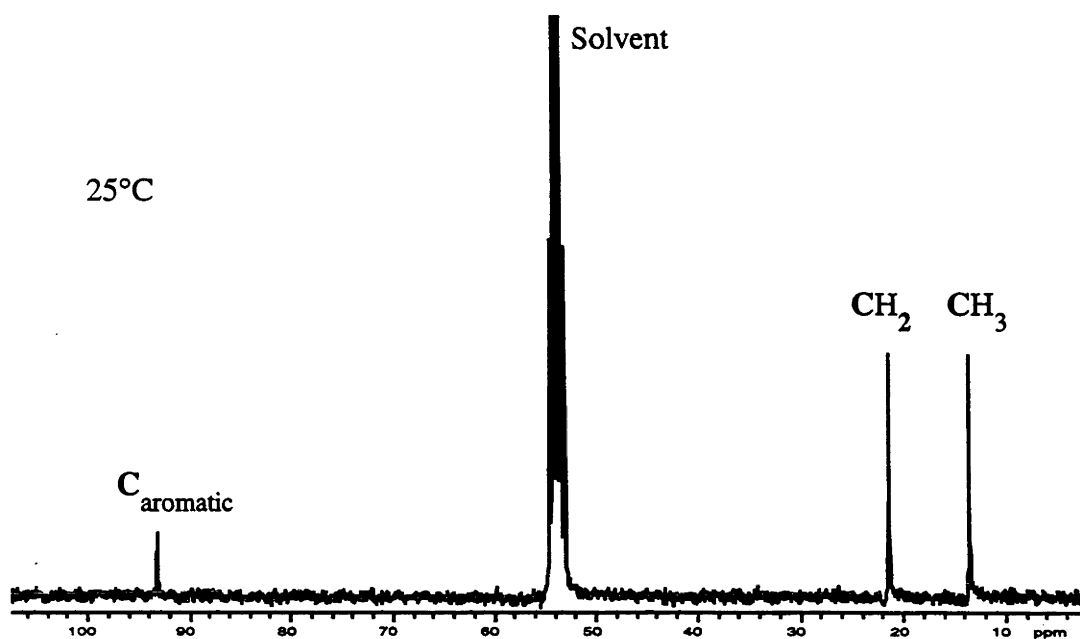


Figure 4.21. Variable temperature ^{13}C $\{^1\text{H}\}$ NMR spectra for $[\text{Ru}(\eta^6\text{-C}_6\text{Et}_6)(\text{CO})_2\text{Cl}]^+\text{PF}_6^-$ (CD_2Cl_2 , 75.43MHz)

$\text{Ru}(\eta^6\text{-C}_6\text{Et}_6)(\text{PMe}_3)(\text{H})_2$

The variable temperature ^1H NMR spectrum of this complex in $\text{d}^8\text{-THF}$ is given in Figure 4.24. At room temperature the hydride resonance appears as a doublet at δ -10.7 ppm, coupled to ^{31}P . As the temperature is lowered, this doublet broadens until at the limiting temperature of the solvent, -110°C , this resonance appears as a poorly resolved doublet of doublets, suggesting that two inequivalent hydrides are present. This is not consistent with the solid state structure of the molecule in which the hexaethylbenzene has the 1,4-proximal-2,3,5,6-distal conformation and is rotationally orientated such that the hydride ligands are equivalent. It also appears that there are two inequivalent ethyl groups at this temperature, although this region of the spectrum is poorly resolved. The concentration of the complex in solution at this temperature is reduced, presumably owing to precipitation from solution; the intensity of peaks due to impurities (*ca.* δ 2.4 and 4.1 ppm) increases relative to the peaks assignable to the complex. The ^{31}P NMR spectrum consisting of a singlet at δ 4.4 ppm is temperature-invariant.

The variable temperature $^{13}\text{C}\{^1\text{H}\}$ NMR spectrum sheds little light on the behaviour of this complex at low temperature in solution (Figure 4.25). At room temperature there is one aromatic carbon resonance (δ 102.6 ppm) and a methyl and methylene resonance (δ 19.7 and 22.9 ppm respectively). These resonances collapse and then the aromatic carbon resonance grows out of the baseline until at -110°C , between δ 118 and 106 ppm, there are at least six discernible but poorly resolved resonances of different intensities. At this temperature the methyl and methylene resonances remain broad and even less well resolved than the aromatic carbon resonances. If the molecule in solution has adopted the solid state structure there should be three aromatic carbon atom resonances in a 2:2:2 ratio (Figure 4.22).

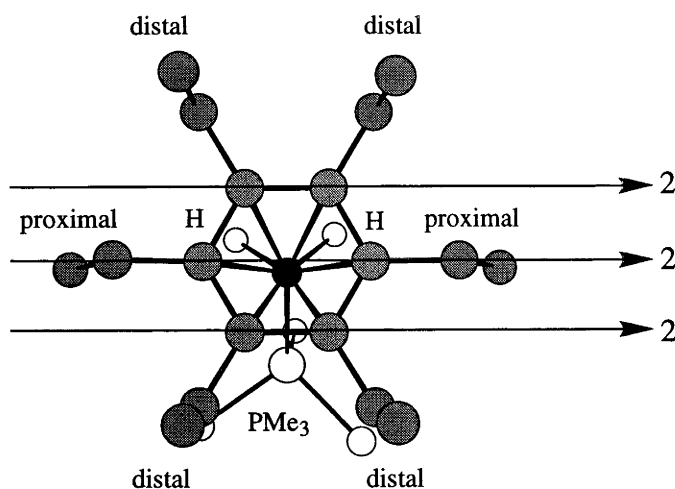


Figure 4.22. Chem 3D view of $\text{Ru}(\eta^6\text{-C}_6\text{Et}_6)(\text{PMe}_3)(\text{H}_2)$ along the arene ruthenium axis showing the expected 2:2:2 ratio of arene carbon atoms in the solid state

One possible explanation for the greater than expected number of aromatic carbon resonances could be coupling of some of the aromatic ring carbon atoms to the phosphorus atom of the PMe_3 ligand. At room temperature, when the line broadening on the resonance for the aromatic carbons is reduced and the region is expanded the aromatic carbon atom resonance is a doublet with a coupling of *ca.* 1 Hz. The separation of resonances at low temperature is greater than this (> 25 Hz), hence the extra peaks are unlikely to be due to ^{31}P - ^{13}C coupling. A second possibility is that more than one species is present in solution. This would account for the observation of the two inequivalent hydride resonances, but is inconsistent with the single ^{31}P NMR resonance.

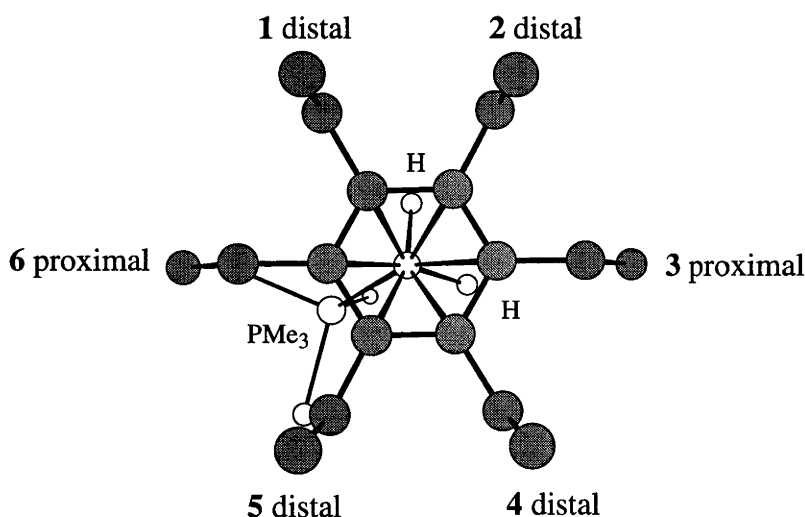


Figure 4.23. Chem 3D portrayal of $\text{Ru}(\eta^6\text{-C}_6\text{Et}_6)(\text{PMe}_3)(\text{H})_2$ with a 1,4-proximal-2,3,5,6-distal ethyl group conformation along the ruthenium-arene bond axis with an arene rotational orientation such that there are six different ethyl groups and two different hydride ligands

Alternatively, it is possible that at low temperature in solution, both rotation about the arene ruthenium axis and arene methylene bond have slowed and that the coordinated hexaethylbenzene has adopted the 1,4-proximal-2,3,5,6-distal conformation, but with the arene is rotated 60° from the solid state structure (Figure 4.23). Under these conditions six inequivalent arene carbon atoms and two inequivalent hydrides are expected. However, this is not consistent with the unequal intensities observed for the arene carbon resonances at the lowest temperature spectrum obtained.

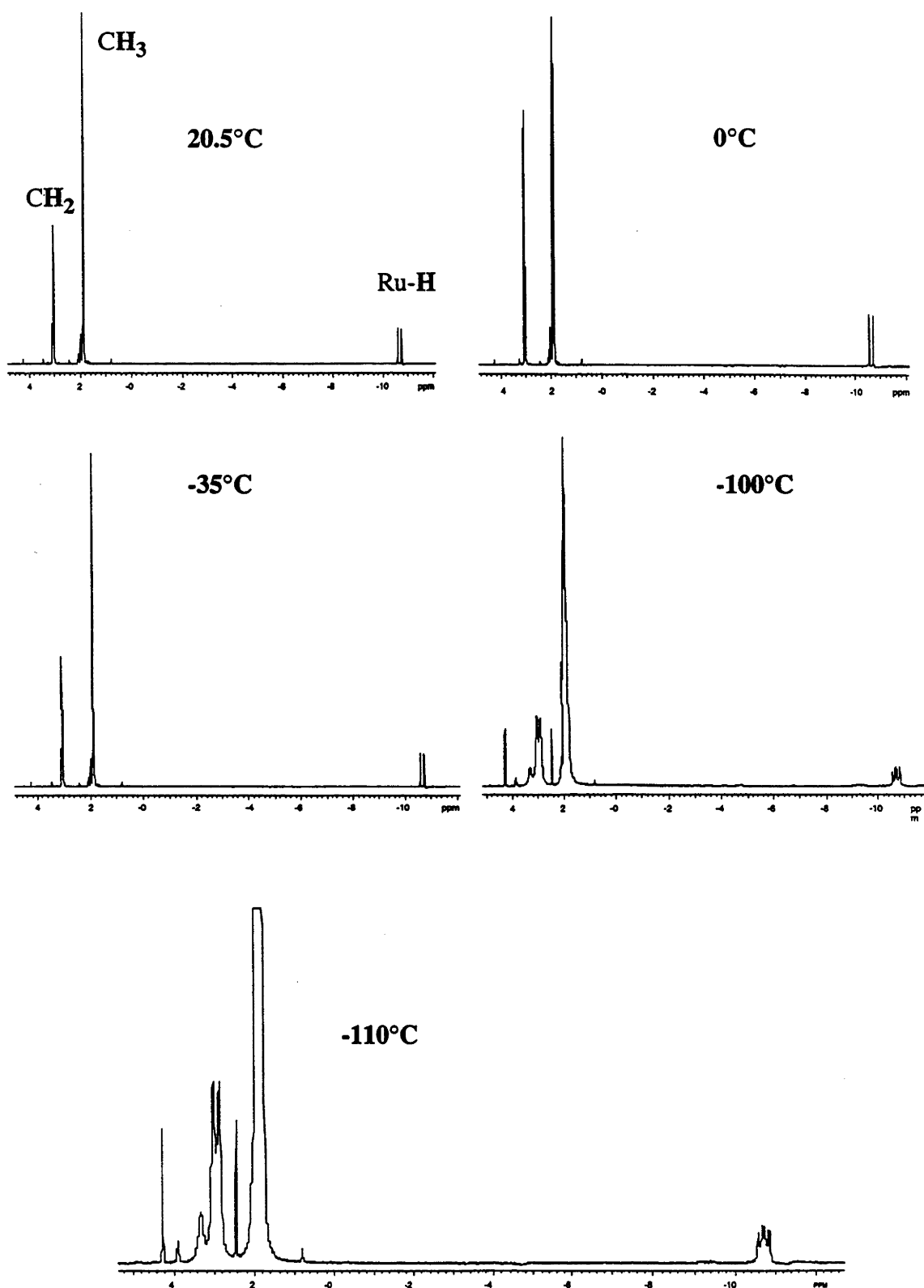


Figure 4.24. Variable temperature ^1H NMR spectrum ($\text{d}^8\text{-THF}$, 300 MHz) of $\text{Ru}(\eta^6\text{-C}_6\text{Et}_6)(\text{PMe}_3)(\text{H})_2$

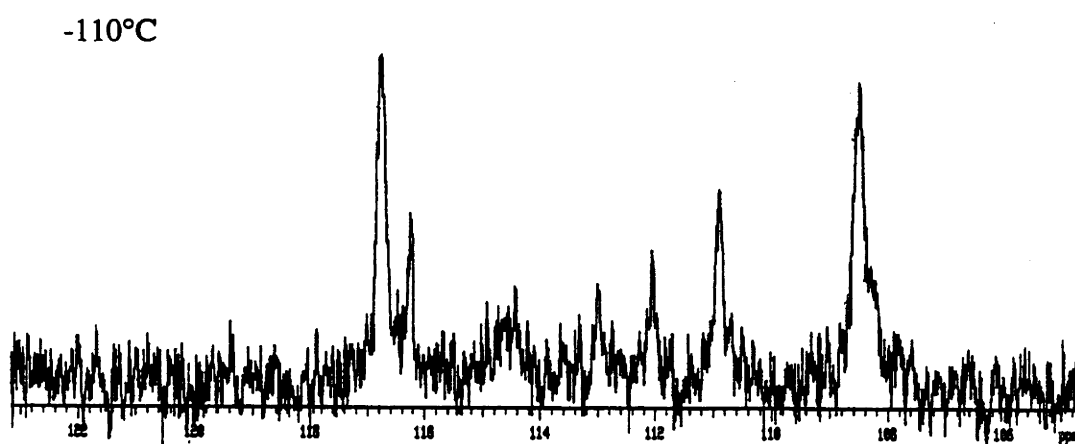
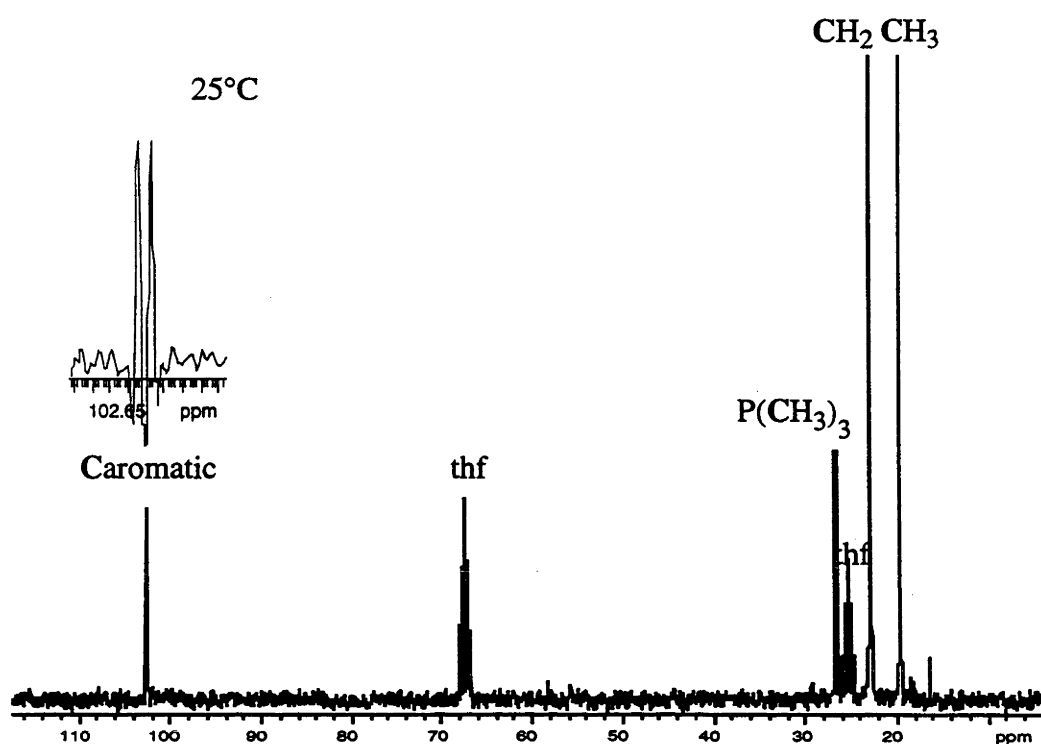


Figure 4.25. Variable temperature $^{13}\text{C}\{^1\text{H}\}$ NMR spectrum ($\text{d}^8\text{-THF}$, 75.42 MHz) of $\text{Ru}(\eta^6\text{-C}_6\text{Et}_6)(\text{PMe}_3)(\text{H})_2$

Other arenes

The variable temperature ^1H and $^{13}\text{C}\{^1\text{H}\}$ NMR spectra of $[\text{Ru}(\eta^6\text{-C}_6\text{Me}_6)\text{Cl}_2]_2$, $\text{Ru}(\eta^6\text{-C}_6\text{Me}_6)(\text{CO})\text{Cl}_2$, $[\text{Ru}\{\eta^6\text{-benzotris(cyclooctene)}\}\text{Cl}_2]_2$, $\text{Ru}\{\eta^6\text{-benzotris(cyclooctene)}\}(\text{CO})\text{Cl}_2$, and $\text{Ru}(\eta^6\text{-C}_6\text{H}_3\text{-1,3,5-Pr}^i_3)(\text{CO})\text{Cl}_2$ were also measured in CD_2Cl_2 down to -75°C but no change was observed. This is particularly surprising in the case of the last compound, considering that 1,3,5-tri-isopropylbenzene and hexaethylbenzene are similar in gross steric bulk.

Summary

In this series of ruthenium complexes of hexaethylbenzene the question of hindered rotation about the arene ruthenium bond axis has been left at the same stage as for the hexaethylbenzene chromium series. Without knowing the conformation of the coordinated hexaethylbenzene at low temperature in solution (and in some case the identity of the species in solution), it is impossible on the basis of NMR experiments on unlabelled compounds to determine whether rotation about the arene ruthenium bond axis has ceased on an NMR timescale.

The variable temperature NMR behaviour of the complexes discussed in this chapter can be divided into two categories: (1) those whose NMR behaviour can be rationalized on the basis of their solid state hexaethylbenzene conformations assuming that a combination of rotation about the arene-ruthenium and arene methylene-bond axes occurs and (2) those whose behaviour cannot be rationalized in these terms

In the first class come $[\text{Ru}_2(\eta^6\text{-C}_6\text{Et}_6)_2\text{Cl}_3]^+\text{PF}_6^-$, $\text{Ru}(\eta^6\text{-C}_6\text{Et}_6)(\text{CO})\text{Cl}_2$, $\text{Ru}(\eta^6\text{-C}_6\text{Et}_6)(\text{Bu}^t\text{NC})\text{Cl}_2$, $[\text{Ru}(\eta^6\text{-C}_6\text{Et}_6)(\text{Bu}^t\text{NC})_2\text{Cl}]^+\text{PF}_6^-$ and $[\text{Ru}(\eta^6\text{-C}_6\text{Et}_6)(\text{CO})(\text{Bu}^t\text{NC})\text{Cl}]^+\text{PF}_6^-$ and $[\text{Ru}(\eta^6\text{-C}_6\text{Et}_6)(\text{CO})_2\text{Cl}]^+\text{PF}_6^-$, as well as all the complexes containing a tertiary phosphine ligand and all distal ethyl groups. For all these complexes the low temperature NMR behaviour can be explained without invoking slowed rotation about the arene ruthenium bond axis, but in terms of just slowed rotation about the arene methylene bonds. This is the only explanation that is valid for the complexes with entirely distal ethyl groups. The complexes $[\text{Ru}_2(\eta^6\text{-C}_6\text{Et}_6)_2\text{Cl}_3]^+\text{PF}_6^-$, $\text{Ru}(\eta^6\text{-C}_6\text{Et}_6)(\text{CO})\text{Cl}_2$, $\text{Ru}(\eta^6\text{-C}_6\text{Et}_6)(\text{Bu}^t\text{NC})\text{Cl}_2$, $[\text{Ru}(\eta^6\text{-C}_6\text{Et}_6)(\text{Bu}^t\text{NC})_2\text{Cl}]^+\text{PF}_6^-$ and $[\text{Ru}(\eta^6\text{-C}_6\text{Et}_6)(\text{CO})(\text{Bu}^t\text{NC})\text{Cl}]^+\text{PF}_6^-$, all had the 1,3,5-proximal-2,4,6-distal conformation in the solid state, except for $[\text{Ru}(\eta^6\text{-C}_6\text{Et}_6)(\text{Bu}^t\text{NC})_2\text{Cl}]^+\text{PF}_6^-$ which also displayed the 1,3-proximal 2,4,5,6-distal conformation. All these complexes, except for $\text{Ru}(\eta^6\text{-C}_6\text{Et}_6)(\text{CO})_2\text{Cl}]^+\text{PF}_6^-$, have low temperature NMR spectra at the limiting

temperature that are exactly consistent with both rotational motions having ceased on an NMR timescale and the complexes having the same arene rotational orientation as observed in the solid state. The complex $[\text{Ru}(\eta^6\text{-C}_6\text{Et}_6)(\text{CO})_2\text{Cl}]^+\text{PF}_6^-$ does not have behaviour consistent with slowed rotation about the arene ruthenium bond axis, despite displaying the same 1,3,5-proximal-2,4,6-distal conformation of these complexes in the solid state. It is unclear as to why this molecule displays this anomalous behaviour.

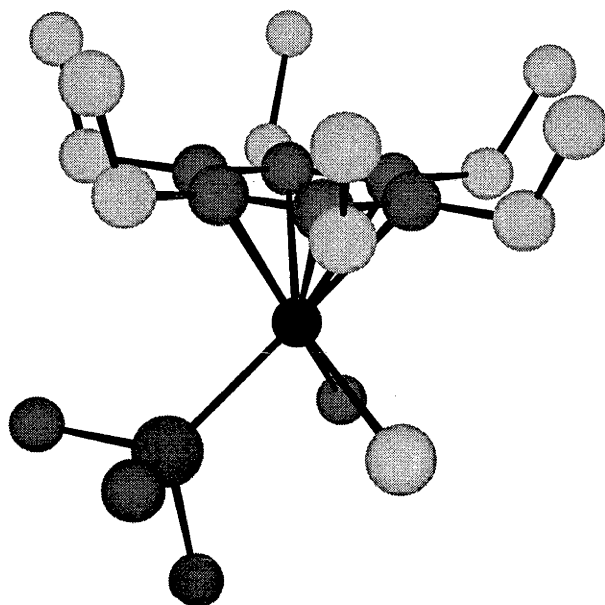
In the second class are included $[\text{Ru}(\eta^6\text{-C}_6\text{Et}_6)\text{Cl}_2]_2$ and $\text{Ru}(\eta^6\text{-C}_6\text{Et}_6)(\text{PMe}_3)(\text{H})_2$, whose low temperature NMR spectra are inconsistent with expectation based on the solid state conformation of hexaethylbenzene in the molecule. For $[\text{Ru}(\eta^6\text{-C}_6\text{Et}_6)\text{Cl}_2]_2$ at low temperature in solution, it must be assumed that the hexaethylbenzene has a 1,3,5-proximal-2,4,6-distal conformation, in contrast to the all distal solid state conformation. The behaviour of $\text{Ru}(\eta^6\text{-C}_6\text{Et}_6)(\text{PMe}_3)(\text{H})_2$ cannot be explained at this stage.

These results are discussed further in Chapter 6 in relation to those for other arene complexes, especially the arene chromium tricarbonyls.

Chapter 5: *Experimental*

"Science" means simply the aggregate of all the recipes that are always successful. All the rest is just literature.

(Vance, Moralités, 1932)



Chem 3D representation of $\text{Ru}(\eta^6\text{-C}_6\text{Et}_6)(\text{PMe}_3)(\text{Me})\text{Cl}$

Preparation of $\text{Ru}(\eta^6\text{-C}_6\text{Et}_6)(\eta^4\text{-COD})$	178
Preparation of $\text{Ru}[\eta^6\text{-benzo (1,2:3,4:5,6)}$ $1,2,3,4,5,6\text{-hexahydrocyclooctene}](\eta^4\text{-COD})$	179
Preparation of $\text{Ru}(\eta^6\text{-tri-isopropylbenzene})(\eta^4\text{-COD})$	180
Preparation of $\text{Ru}[\eta^6\text{-tris(trimethylsilyl)benzene}](\eta^4\text{-COD})$	181
Preparation of $\text{Ru}(\eta^6\text{-C}_6\text{H}_3\text{Bu}^t_3)(\eta^4\text{-COD})$	182
Preparation of $[\text{Ru}(\eta^6\text{-C}_6\text{Et}_6)\text{Cl}_2]_2$	183
Preparation of $[\text{Ru}\{\eta^6\text{-benzotris(cyclooctene)}\}\text{Cl}_2]_2$	184
Preparation of $[\text{Ru}_2(\eta^6\text{-C}_6\text{Et}_6)_2\text{Cl}_3]^+\text{PF}_6^-$	185
Preparation of $[\text{Ru}_2(\eta^6\text{-C}_6\text{H}_4\text{-1,2-Pr}^i_2)_2\text{Cl}_3]^+\text{PF}_6^-$ and $[\text{Ru}_2(\eta^6\text{-C}_6\text{H}_4\text{-1,2-Et}_2)_2\text{Cl}_3]^+\text{PF}_6^-$	186
Preparation of $\text{Ru}(\eta^6\text{-C}_6\text{Et}_6)(\text{PPh}_3)\text{Cl}_2$	187
Preparation of $\text{Ru}(\eta^6\text{-C}_6\text{Et}_6)(\text{PMe}_3)\text{Cl}_2$	188
Preparation of $\text{Ru}[\eta^6\text{-benzotris(cyclooctene)}](\text{PMe}_3)\text{Cl}_2$	189

Preparation of $\text{Ru}(\eta^6\text{-C}_6\text{Et}_6)(\text{PMe}_3)(\text{Me})\text{Cl}$	190
Preparation of $\text{Ru}(\eta^6\text{-C}_6\text{Et}_6)(\text{PMe}_3)(\text{Me})_2$	191
Preparation of $\text{Ru}(\eta^6\text{-C}_6\text{Et}_6)(\text{PMe}_3)(\text{H})_2$	192
Preparation of $\text{Ru}(\eta^6\text{-C}_6\text{Et}_6)(\text{CO})\text{Cl}_2$	193
Preparation of $\text{Ru}[\eta^6\text{-benzotris(cyclooctene)}](\text{CO})\text{Cl}_2$	194
Preparation of $\text{Ru}(\eta^6\text{-tri-isopropylbenzene})(\text{CO})\text{Cl}_2$	195
Preparation of $\text{Ru}(\eta^6\text{-C}_6\text{Et}_6)(\text{Bu}^t\text{NC})\text{Cl}_2$	196
Preparation of $[\text{Ru}(\eta^6\text{-C}_6\text{Et}_6)(\text{CH}_3\text{CN})_2\text{Cl}]^+\text{PF}_6^-$	197
Preparation of $[\text{Ru}(\eta^6\text{-C}_6\text{Et}_6)(\text{CH}_3\text{CN})_3]_2^+(\text{CF}_3\text{SO}_3^-)_2$	198
Preparation of $[\text{Ru}(\eta^6\text{-C}_6\text{Et}_6)(\text{Bu}^t\text{NC})_2\text{Cl}]^+\text{PF}_6^-$	199
Preparation of $[\text{Ru}(\eta^6\text{-C}_6\text{Et}_6)(\text{CO})_2\text{Cl}]^+\text{PF}_6^-$	200
Preparation of $[\text{Ru}(\eta^6\text{-C}_6\text{Et}_6)(\text{Bu}^t\text{NC})(\text{CO})\text{Cl}]^+\text{PF}_6^-$	201
Experimental details for the collection of X-ray data and solution of structures	203

All solvents were purified before use using standard methods. Pentane, hexane, THF, ether, benzene and toluene were pre-dried over sodium wire and distilled from sodium/benzophenone under nitrogen. Isopropanol was distilled from magnesium turnings under nitrogen. Dichloromethane was distilled from calcium hydride. Acetone was dried over 3 Å molecular sieves.

NMR spectra were recorded on Varian XL200, Varian VXR 300, Varian Gemini 300 BB or Varian VXR 500 spectrometers. All NMR spectra reported in this chapter were measured at 25°C.

The ^{35}Cl NMR spectra were measured on a Varian VXR 300 machine at an operating frequency of 29.396 MHz with a spectral window of 100000 Hz. Times to collect enough scans for a spectrum ranged from five minutes for $[\text{NEt}_4]\text{Cl}$ in CD_2Cl_2 to a couple of hours for $[(\eta^6\text{-C}_6\text{Et}_6)\text{RuCl}_2]_2$ in CD_2Cl_2 . Approximately 15 mg of each of the complexes was dissolved in 0.5 cm³ of solvent.

Mass spectra were measured on a VG ZAB2-SEQ spectrometer (FAB) or a VG Micromass 7070 spectrometer (EI).

Infrared spectra were measured on Perkin-Elmer 683 or Perkin Elmer FTIR 1800 spectrometers. Far infrared spectra were measured on the latter instrument, either as polythene disks or as CH_2Cl_2 solutions in a polythene cell of 0.1 mm path length.

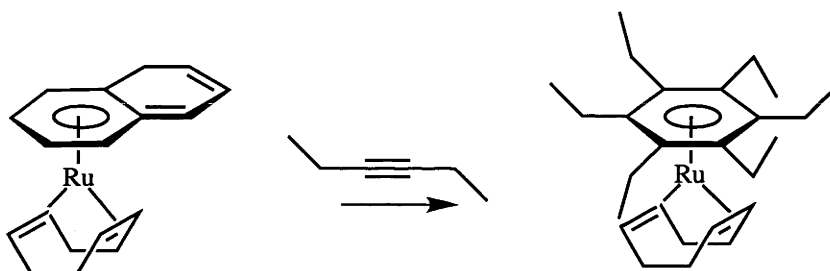
Microanalysis and vapour pressure osmometry measurements were conducted by the staff of the Australian National University Analytical Services Unit, Canberra. Vapour pressure osmometry of a solution of $[\text{Ru}(\eta^6\text{-C}_6\text{Et}_6)\text{Cl}_2]_2$ (1.6198 mg in 1 cm³ of CH_2Cl_2) was carried out on a Knauer vapour pressure osmometer at 37°C.

Conductivities were measured on a digital conductivity meter LF DIGI 550 from Wissenschaft-Technische Werkstätten using a CDC 344 platinum electrode from Radiometer. The cell constant was determined by calibration with a standard solution of KCl in H_2O . The dichloromethane used was purified by distillation from calcium hydride. Methanol was dried over molecular sieves. Λ_0 values were determined from a plot of Λ_m against the square root of concentration for a series of solutions of different concentrations. The linear portion of the graph was extrapolated and Λ_0 was taken as the intercept with the axis where the concentration was equal to zero.

X-ray structural determinations of the complexes $[\text{Ru}(\eta^6\text{-C}_6\text{Et}_6)(\text{Bu}'\text{NC})_2\text{Cl}]^+\text{PF}_6^-$, $[\text{Ru}(\eta^6\text{-C}_6\text{Et}_6)(\text{CO})_2\text{Cl}]^+\text{PF}_6^-$, $[\text{Ru}(\eta^6\text{-C}_6\text{Et}_6)(\text{CO})(\text{Bu}'\text{NC})\text{Cl}_2]^+\text{PF}_6^-$ and $[\text{Ru}\{\eta^6\text{-benzotris(cyclooctene)}\}\text{Cl}_2]_2$ were solved by A. Willis and the remainder by D. Hockless.

It is to be noted that many of the compounds and techniques used have inherent hazards. Before undertaking any synthetic chemistry of the nature described here one should be aware of the possible dangers associated. Reference to the MSDS information for the various reagents should be made before their use. The toxicological properties of the new complexes made are unknown and thus these complexes should be treated with caution. For the procedures to be followed to ensure safety of operations such as drying of solvent over alkali metals reference can be made to any one of a number of laboratory safety texts

Preparation of $\text{Ru}(\eta^6\text{-C}_6\text{Et}_6)(\eta^4\text{-COD})$



3-Hexyne (0.4 cm^3 , 3.52 mmol) was added to a solution of $\text{Ru}(\eta^6\text{-naphth})(\eta^4\text{-COD})$ (0.2 g , 0.53 mmol) in THF (10 cm^3) and the reaction mixture was stirred at room temperature for 3 h. The solvent was evaporated *in vacuo* and the resulting residue was dissolved in n-pentane (10 cm^3). The dark brown solution was chromatographed on an alumina column at ($20 \times 1.5 \text{ cm}$, activity III). Pentane eluted a yellow fraction which was concentrated under reduced pressure to *ca.* 5 cm^3 . This was cooled to -78°C and light yellow air-sensitive crystals of $\text{Ru}(\eta^6\text{-C}_6\text{Et}_6)(\eta^4\text{-COD})$ were obtained (0.25 g , 100%).

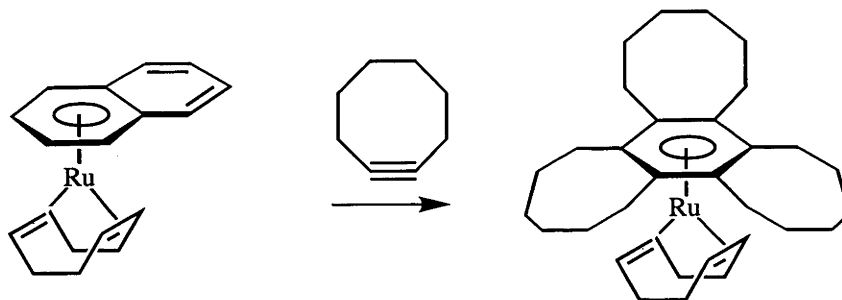
$^1\text{H NMR}$ (C_6D_6 , 200 MHz) δ 2.76 [br s, 4H, $\text{CH}(\text{COD})$], 2.36 [br s, 8H, $\text{CH}_2(\text{COD})$], 2.1 (q, 12H, $^3J(\text{HH})$ 7.5 Hz, CH_2), 1.82 ppm (t, $^3J(\text{HH})$ 7.5 Hz, CH_3)

$^{13}\text{C}\{^1\text{H}\} \text{NMR}$ (C_6D_6 , 75.42 MHz) δ 103.4 (s, $\text{C}_{\text{aromatic}}$), 64.3 [s, $\text{CH}(\text{COD})$], 34.6 [s, $\text{CH}_2(\text{COD})$], 21.1 (s, CH_2), 18.8 ppm (s, CH_3)

Mass spectrum (EI 70 eV), $m/z = 456$ (M^+)

Anal. calcd. for $\text{C}_{26}\text{H}_{42}\text{Ru}$: C 68.56; H, 9.23. Found: C 68.72; H 8.97.

**Preparation of Ru[η^6 -benzo(1,2:3,4:5,6)
1,2,3,4,5,6-hexahydrocyclooctene](η^4 -COD)**



Ru(η^6 -naphth)(η^4 -COD) (134 mg, 0.40 mmol) was dissolved in 10 cm³ of THF. Cyclooctyne (1.5 cm³, 1.5 mmol) was added and the resulting solution was stirred overnight. THF and excess cyclooctyne were removed *in vacuo* and the resulting brown waxy solid was dissolved in a minimum amount of hexane and loaded onto an Al₂O₃ column (10 x 1.5 cm activity III, neutral). The complex was eluted with *ca.* 200 cm³ of hexane. The hexane was removed *in vacuo* and excess naphthalene was sublimed on a liquid nitrogen-cooled probe. The product was isolated as a pale yellow, air-sensitive solid (48 mg, 22 %).

¹H NMR (C₆D₆, 300 MHz) δ 1-3 ppm (m, 48H, COD and benzotris(cyclooctene))^a

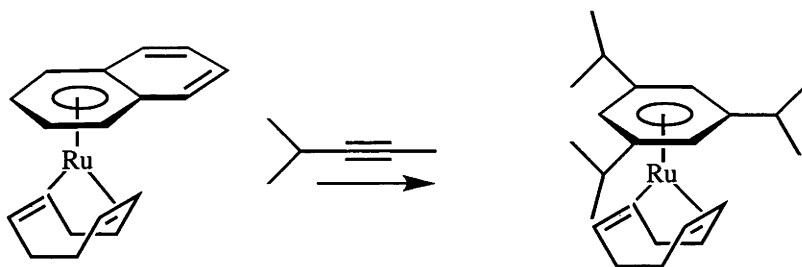
¹³C{¹H} NMR (C₆D₆, 75.42 MHz) δ 101.4 (s, C_{aromatic}), 64.1 [s, CH(COD)], 34.5 [s, CH₂(COD)], 32.0 [s, CH₂{benzotris(cyclooctene)}], 27.6 [s, CH₂{benzotris(cyclooctene)}], 27.3 ppm [s, CH₂{benzotris(cyclooctene)}]

Mass spectrum (EI 70 eV) m/z = 533 (M⁺)

Anal. calcd. for C₃₂H₆₀Ru: C 72.00; H 9.06. Found: C 71.67; H 8.60.

^a benzotris(cyclooctene) = benzo (1,2:3,4:5,6) 1,2,3,4,5,6-hexahydrocyclooctene](η^4 -COD)

Preparation of Ru(η^6 -tri-isopropylbenzene)(η^4 -COD)



A mixture of Ru(η^6 -naphth)(η^4 -COD) (100 mg, 0.29 mmol) and isopropylacetylene (0.5 cm³, 10.7 mmol) was stirred for 15 h in *ca.* 5 cm³ of THF to give a brown solution. The THF and excess acetylene were then removed *in vacuo*. The resulting brown oil was dissolved in a minimum amount of hexane and loaded onto an Al₂O₃ column (activity III, neutral, 1.5 x 15 cm). A yellow solution was obtained on elution with 250 cm³ of hexane. A bright yellow, air-sensitive oil was obtained on removal of hexane *in vacuo* (34 mg, 28 %).

A 7.6:1 ratio of symmetrical to unsymmetrical isomers was obtained, determined by ¹H NMR spectroscopy from the integration of the coordinated arene proton resonances for the two isomers.

¹H NMR [C₆D₆, 300 MHz (for a mixture of both isomers)] δ 1.25 [d, ³J(HH) 6.8Hz, 9H, CH₃ (symmetrical isopropyl)], 1.8-2.2 [m, 8H, CH₂ (η^4 -COD)], 2.38 (septet, 3H, ³J(HH) 6.8 Hz, CH(symmetrical isopropyl)], 2.9-3.0 [m, 4H, CH (η^4 -COD)], 4.60-4.75 [m, 3H, CH_{aromatic}(unsymmetrical)]^b, 5.10 ppm [s, 3H, CH_{aromatic}(symmetrical)]^b

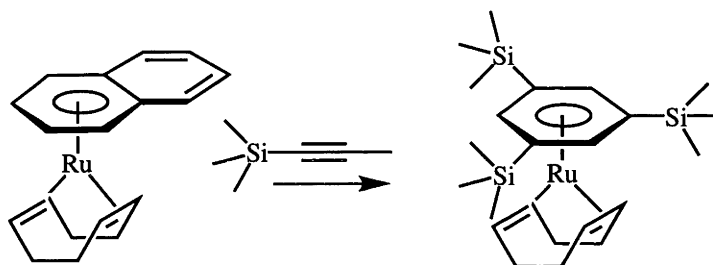
¹³C{¹H} NMR [C₆D₆, 75.42 MHz (data for symmetrical isomer)] δ 109.8 (s, CH_{aromatic}), 84.6 [CH(COD)], 61.5 [s, CH₂(COD)], 34.0 [s, CH(isopropyl)], 23.8 ppm [s, CH₃(isopropyl)]^c

^b resonances integrated to determine ratio of isomers

^c tertiary aromatic carbons not seen

High resolution FAB⁺ mass spectrum gave a peak at 412.185914 which differs by less than 0.1 ppm from the mass calculated for $^{101}\text{Ru}^{12}\text{C}_{23}\text{H}_{36}$ of 412.185919 amu

Preparation of Ru[η^6 -tris(trimethylsilyl)benzene](η^4 -COD)



A mixture of Ru(η^6 -naphth)(η^4 -COD) (86 mg, 0.26 mmol) and trimethylsilylacetylene (250 μl , 1.91 mmol) was stirred for 3.5 h in 10 cm^3 of hexane. The hexane and excess acetylene were removed *in vacuo*. The resulting brown oil was dissolved in a minimum amount of hexane and eluted from an Al_2O_3 column (activity III, neutral, 1.5 x 10 cm) with *ca.* 200 cm^3 of hexane. The hexane was removed *in vacuo* to give a pale yellow air-sensitive oil (30 mg, 23 %).

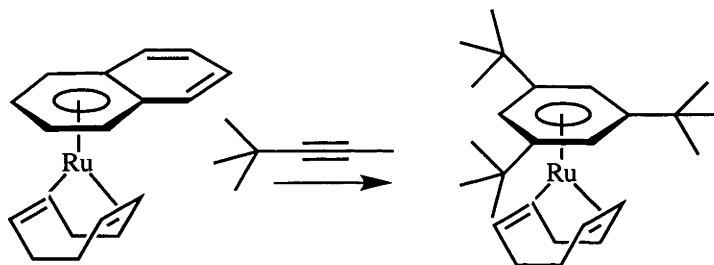
A 4:6 ratio of symmetrical to unsymmetrical isomers was obtained, as calculated from the integration of the coordinated arene protons for the two isomers in the ^1H NMR spectrum.

^1H NMR [CD_2Cl_2 , 300 MHz (symmetrical and unsymmetrical isomers)] δ 0.22 [s, 27H, TMS(symmetrical)], 0.22 [s, 9H, TMS(unsymmetrical)], 0.33 [s, 9H, TMS(unsymmetrical)], 0.425 [s, 9H, TMS(unsymmetrical)], 2.33-2.14 [m, 8H, $\text{CH}_2(\text{COD}$, both isomers)], 3.54-3.46 [m, 4H $\text{CH}(\text{COD}$, both isomers)], 4.48 [m, H, $\text{CH}_{\text{aromatic}}(\text{unsymmetrical})$]^b, 4.75 (m, H, $\text{CH}_{\text{aromatic}}(\text{unsymmetrical})$]^b, 4.82 [m, H, $\text{CH}_{\text{aromatic}}(\text{unsymmetrical})$]^b, 5.36 ppm [s, 3H, $\text{CH}(\text{symmetrical})$]^b

^b resonances integrated to determine ratio of isomers

The EI high resolution mass spectrum gave an M^+ peak at 504.1643 amu which is within 1 ppm of that calculated for $^{102}\text{Ru}^{12}\text{C}_{23}^1\text{H}_{42}^{28}\text{Si}_3$, 504.1638 amu.

Preparation of $\text{Ru}(\eta^6\text{-C}_6\text{H}_3\text{Bu}^t_3)(\eta^4\text{-COD})$



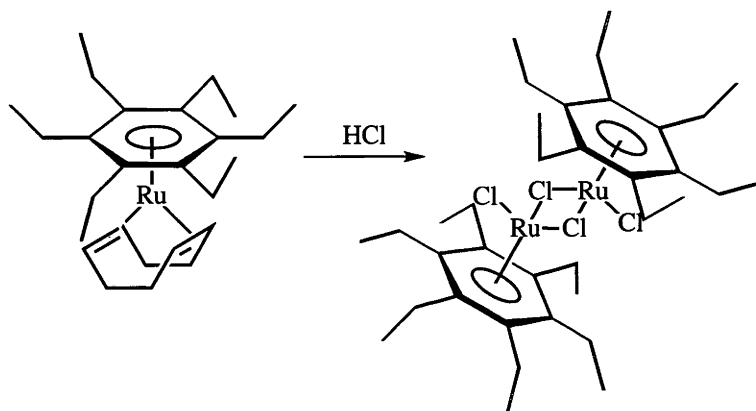
$\text{Ru}(\eta^6\text{-naphth})(\eta^4\text{-COD})$ (90 mg, 0.27 mmol) was stirred with *t*-butylacetylene (500 μl , 8.3 mmol) in 10 cm^3 of THF for 15h. The solution changed colour from yellow/brown to very dark brown. The THF and excess acetylene were removed *in vacuo* to leave a black oil. This was dissolved in a minimum amount of hexane and loaded onto an Al_2O_3 column (activity III, neutral, 2 x 10 cm) and eluted with *ca.* 200 cm^3 of hexane. The hexane was removed from the resulting dark yellow solution *in vacuo* to leave a dark yellow air-sensitive oil (40 mg, 33 %). It was found by ^1H NMR spectroscopy that although the unsymmetrical isomer was formed, the amount present in comparison to the symmetrical isomer was insignificant.

^1H NMR [CD_2Cl_2 , 300 MHz (symmetrical isomer)] δ 1.29 [s, 9H, $\text{CH}_3(\text{Bu}^t)$], 1.8-2.1 [m, 8H, $\text{CH}_2(\text{COD})$], 3.15-3.25 [m, 4H, $\text{CH}(\text{COD})$], 5.46 ppm (s, 3H, $\text{CH}_{\text{aromatic}}$)

$^{13}\text{C}\{^1\text{H}\}$ NMR [CD_2Cl_2 , 75.42 MHz (symmetrical isomer)] δ 113.2 (s, $\text{CH}_{\text{aromatic}}$), 81.6 [s, $\text{CH}(\text{COD})$], 58.6 [s, $\text{CH}_2(\text{COD})$], 33.2 [s, $\text{C}(\text{Bu}^t)$], 31.5 ppm [s, $\text{CH}_3(\text{Bu}^t)$]

FAB $^+$ Mass spectrum gave a M^+ peak at 455 amu. High resolution FAB $^+$ mass spectrum gave a peak at 455.234426 amu which is within 0.4 ppm of that calculated for $^{102}\text{Ru}^{12}\text{C}_{26}^1\text{H}_{42}$, 455.234232 amu.

Preparation of $[\text{Ru}(\eta^6\text{-C}_6\text{Et}_6)\text{Cl}_2]_2$



To a stirred solution of $\text{Ru}(\eta^6\text{-C}_6\text{Et}_6)(\eta^4\text{-COD})$ (50 mg, 0.11 mmol) in *ca.* 100 cm³ of *n*-hexane was added concentrated HCl dropwise from a Pasteur pipette until an orange cloudy precipitate was observed.^d After 2 h of stirring, the solution was allowed to settle and the *n*-hexane was decanted. The resulting orange, air-stable solid was dried *in vacuo*. Single crystals for X-ray analysis were grown from a solution of the dimer in CH_2Cl_2 to which Et_2O was added until cloudiness was observed. *n*-Hexane was then layered on top of the solution. Over three days, red cubic crystals formed which lost solvent when exposed to air (38 mg, 87 %).

¹H NMR (CD_2Cl_2 , 300 MHz): δ 2.40 (q, 12H, ³*J*(HH) 8Hz, CH₂), 1.30 ppm (t, 18H, ³*J*(HH) 8Hz, CH₃)

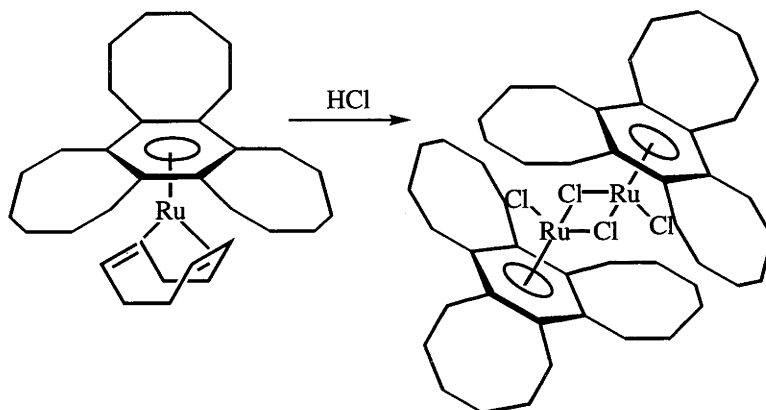
¹³C{¹H}NMR (CD_2Cl_2 , 75.42 MHz): δ 94-95 (s, C_{aromatic}), 21.1 (s, CH₂), 14.7 ppm (s, CH₃).

Anal. calcd. for $\text{C}_{36}\text{H}_{60}\text{Cl}_4\text{Ru}_2$: C 51.67; H 7.23. Found: C, 50.01; H, 7.1.

MS (EI) *m/z* = 800 ($\text{M}^+ - \text{Cl}$).

^d The $\text{Ru}(\eta^6\text{-C}_6\text{Et}_6)(\eta^4\text{-COD})$ solution was usually used immediately after elution from a column because of the inherent instability of this complex

Preparation of $[\text{Ru}\{\eta^6\text{-benzotris(cyclooctene)}\}\text{Cl}_2]_2$



A chromatographed solution of $\text{Ru}(\eta^6\text{-benzotris(cyclooctene)})(\eta^4\text{-COD})$ in hexane was treated with *ca.* 0.5 cm^3 of concentrated HCl with vigorous stirring. The *n*-hexane was removed *in vacuo* and the naphthalene was sublimed onto a liquid nitrogen cooled probe. The resulting orange powder was dissolved in a minimum amount of CH_2Cl_2 and the solution layered with ether to give a dark red microcrystalline solid which was collected by vacuum filtration. (60 mg, 28 %, based on 153 mg of $\text{Ru}(\eta^6\text{-naphth})(\eta^6\text{-COD})$).

^1H NMR (CD_2Cl_2 , 500 MHz) δ 2.6 - 2.9 [m, benzotris(cyclooctene)], 1.9 - 2.0 [m, benzotris(cyclooctene)] 1.5 - 1.3 ppm [m, benzotris(cyclooctene)]

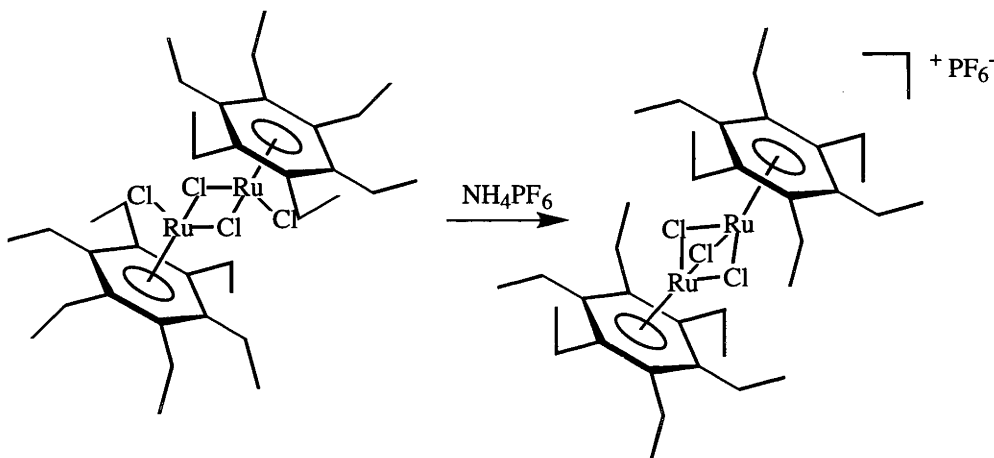
$^{13}\text{C}\{^1\text{H}\}$ NMR (CD_2Cl_2 , 75.42 MHz) δ 93.7 (s, $\text{C}_{\text{aromatic}}$), 30.6 [s, $\text{CH}_2\{\text{benzotris(cyclooctene)}\}$], 28.5 [s, $\text{CH}_2\{\text{benzotris(cyclooctene)}\}$], 27.3 ppm [s, $\text{CH}_2\{\text{benzotris(cyclooctene)}\}$]

Mass spectrum (FAB^+) $m/z = 957$ ($\text{M}^+ - \text{Cl}$)

Anal. calcd. for $\text{C}_{48}\text{H}_{72}\text{Cl}_4\text{Ru}_2$: C 58.06; H 7.67. Found C 57.67; H 7.64.

$\text{Ru}(\eta^6\text{-C}_6\text{H}_3\text{Pr}_3)(\eta^4\text{-COD})$ could also be converted into a dichloride dimer using the method above but the product was not characterized.

Preparation of $[\text{Ru}_2(\eta^6\text{-C}_6\text{Et}_6)_2\text{Cl}_3]^+\text{PF}_6^-$



Solid NH_4PF_6 was slowly added to a stirred solution of $[\text{Ru}(\eta^6\text{-C}_6\text{Et}_6)\text{Cl}_2]_2$ (50 mg, 0.06 mmol) in 3 cm^3 of ethanol or methanol until saturation. The solution was then allowed to stand without stirring for three days whereupon red cubic crystals formed. These were suitable for X-ray analysis. The solvent was decanted and the crystals were washed with n-hexane and cold ethanol (44 mg, 78 %).

^1H NMR (CD_3OD , 200 MHz) δ 2.50 (q, 12H, $^3J(\text{HH})$ 7.6 Hz, CH_2), 1.33 ppm (t, 18H, $^3J(\text{HH})$ 7.6 Hz, CH_3)

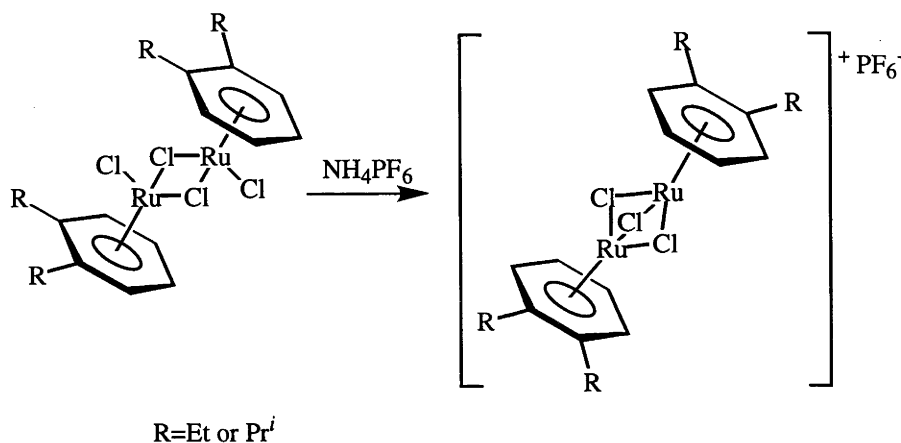
$^{13}\text{C}\{^1\text{H}\}$ NMR (CD_2Cl_2 , 75.42 MHz) δ 93–95 (br, $\text{C}_{\text{aromatic}}$), 21.5 (s, CH_2), 15.0 ppm (s, CH_3)

$^{31}\text{P}\{^1\text{H}\}$ NMR (CD_3OD , 81 MHz) δ -142.7 ppm (sept, $^1J(\text{PF})$ 708 Hz, PF_6)

Anal. calcd. for $\text{C}_{36}\text{H}_{60}\text{Cl}_3\text{F}_6\text{PRu}_2$: C 45.69; H 6.31. Found: C 44.31; H 6.50.

Mass spectrum (EI) $m/z = 383$ ($\text{RuCl}(\text{C}_6\text{Et}_6)^+$)

**Preparation of $[\text{Ru}_2(\eta^6\text{-C}_6\text{H}_4\text{-1,2-Pr}^i_2)_2\text{Cl}_3]^+\text{PF}_6^-$ and
 $[\text{Ru}_2(\eta^6\text{-C}_6\text{H}_4\text{-1,2-Et}_2)_2\text{Cl}_3]^+\text{PF}_6^-$**



The tri- μ -chloro salts could be prepared from *o*-di-isopropylbenzene dichloride dimer and the *o*-diethylbenzene dichloride dimer as described for the hexaethylbenzene analogue.^c

For $[\text{Ru}_2(\eta^6\text{-C}_6\text{H}_4\text{-1,2-Et}_2)_2\text{Cl}_3]^+\text{PF}_6^-$:

^1H NMR (CD_2Cl_2 , 300 MHz) δ 5.63 [m(AA'BB'), 8H, $\text{H}_{\text{aromatic}}$], 2.54 [m(ABX₃), 8H, CH_2], 1.27 ppm (t, 12H, CH_3)

$^{13}\text{C}\{^1\text{H}\}$ NMR (CD_2Cl_2 , 75.42 MHz) δ 98.0 (s, $\text{C}_{\text{aromatic}}$), 78.7 (s, $\text{C}_{\text{aromatic}}$), 78.3 (s, $\text{C}_{\text{aromatic}}$), 23.5 (s, CH_2), 12.8 ppm (s, CH_3)

Anal. calcd. for $\text{C}_{20}\text{H}_{28}\text{Cl}_3\text{F}_6\text{PRu}_2$: C 33.28; H 3.91. Found: C 32.56; H 3.41.

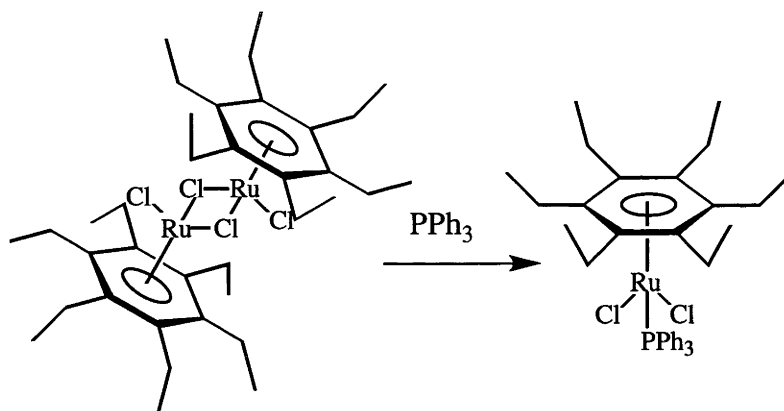
For $[\text{Ru}_2(\eta^6\text{-C}_6\text{H}_4\text{-1,2-Pr}^i_2)_2\text{Cl}_3]^+\text{PF}_6^-$ (most abundant species):

^1H NMR (CD_2Cl_2 , 300 MHz) δ 5.64 [m(AA'BB'), 8H, $\text{H}_{\text{aromatic}}$], 3.42 [m(A₃B₃X), 4H, CH], 1.39 (d, 12H, CH_3), 1.22 ppm (d, 12H, CH_3)

$^{13}\text{C}\{^1\text{H}\}$ NMR (CD_2Cl_2 , 75.42 MHz) δ 103.6 (s, $\text{C}_{\text{aromatic}}$), 79.8 (s, $\text{C}_{\text{aromatic}}$), 75.5 (s, $\text{C}_{\text{aromatic}}$), 27.74 (s, CH), 24.8 (s, CH_3), 21.3 ppm (s, CH_3)

^c The dichloride dimer starting materials for these two complexes were supplied by Dr Mark Bown.

Preparation of $\text{Ru}(\eta^6\text{-C}_6\text{Et}_6)(\text{PPh}_3)\text{Cl}_2$



A solution of $[\text{Ru}(\eta^6\text{-C}_6\text{Et}_6)\text{Cl}_2]_2$ (110 mg, 0.13 mmol) in CH_2Cl_2 was heated at reflux for 2 h with an excess of PPh_3 (0.15 g, 1.4 mmol). The solution was filtered through a glass sinter and then reduced in volume to *ca.* 1 cm³ *in vacuo*. The solution was layered with *n*-hexane to give dark red air-stable needle-like crystals overnight. The solution was decanted and the crystals were washed three times with 10 cm³ portions of *n*-hexane to remove excess triphenylphosphine. The yield was 83 mg (60 %).

^1H NMR (CD_2Cl_2 , 300 MHz) δ 7.3–8.1 (m, 15H, PPh_3), 2.26 (q, 12H, $^3J(\text{HH})$ 7.5 Hz, CH_2), 1.19 ppm (t, 18H, $^3J(\text{HH})$ 7.5 Hz, CH_3).

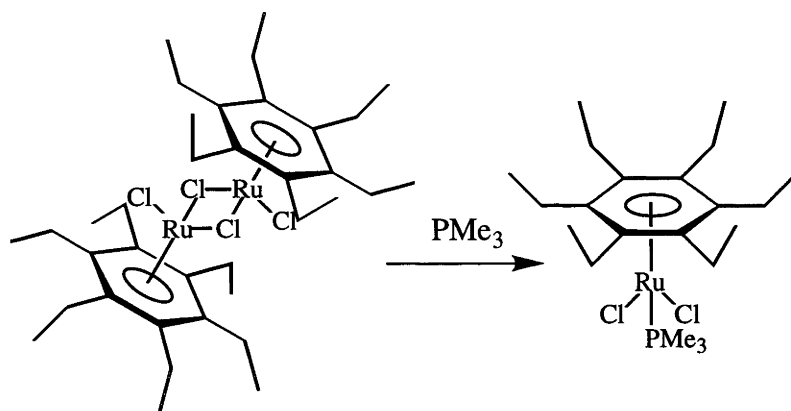
$^{13}\text{C}\{^1\text{H}\}$ NMR (CD_2Cl_2 , 75.42 MHz) δ 136–128 (m, PPh_3), 101.9 (s, coord C), 22.2 (s, CH_2), 15.0 ppm (s, CH_3)

$^{31}\text{P}\{^1\text{H}\}$ NMR (CD_2Cl_2 , 121.4 MHz) δ 24.0 ppm (s, PPh_3)

Anal. calcd. for $\text{C}_{36}\text{H}_{45}\text{Cl}_2\text{PRu}$: C 63.52; H 6.66. Found: C 61.97; H 6.67.

Mass spectrum (FAB) M^+ m/z = 680; ($\text{M}^+ - \text{Cl}$) m/z = 645, ($\text{M}^+ - \text{PPh}_3$)

Preparation of $\text{Ru}(\eta^6\text{-C}_6\text{Et}_6)(\text{PMe}_3)\text{Cl}_2$



$[\text{Ru}(\eta^6\text{-C}_6\text{Et}_6)\text{Cl}_2]_2$ (36 mg, 0.43 mmol) was suspended in 10 cm³ of toluene. To this was added PMe_3 (0.087 cm³, 0.86 mmol). The resulting mixture was stirred at 60°C for 2 h, after which most of the solid had dissolved to give a deep red solution. This solution was filtered and dried *in vacuo* to give an orange red solid. The solid was dissolved in a minimum of CH_2Cl_2 and layered with *n*-hexane to yield over night a crop of red air-stable needle-like crystals suitable for X-ray analysis (32 mg, 78 %).

^1H NMR (CD_2Cl_2 , 200 MHz) δ 2.40 (q, 12H, $^3J(\text{HH})$ 7.6 Hz, CH_2), 1.26 (d, 9H, $^2J(\text{PH})$ 10.4 Hz, PMe_3), 1.08 ppm (t, 18H, $^3J(\text{HH})$ 7.6 Hz, CH_3)

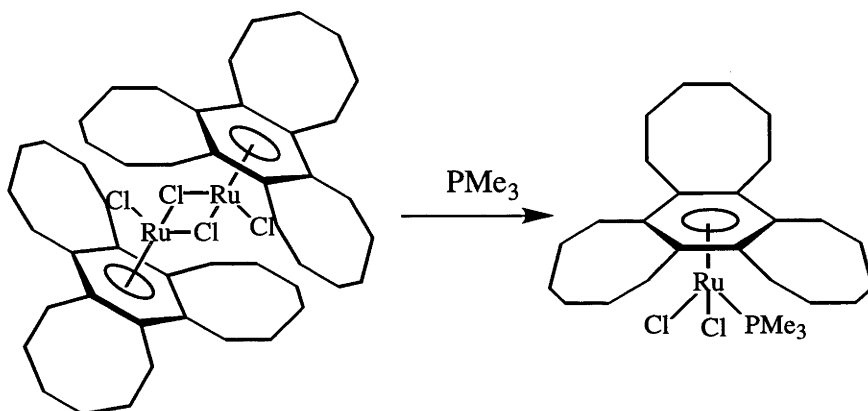
$^{13}\text{C}\{^1\text{H}\}$ NMR (CD_2Cl_2 , 75.42 MHz) δ 100.5 (s, $\text{C}_{\text{aromatic}}$), 22.6 (s, CH_2), 15.2 (d, $^1J(\text{PC})$ 34 Hz, PMe_3), 14.9 ppm (s, CH_3)

$^{31}\text{P}\{^1\text{H}\}$ NMR (CD_2Cl_2 , 81.0 MHz) δ 3.1 ppm (s, PMe_3).

Anal. calcd. for $\text{C}_{21}\text{H}_{39}\text{Cl}_2\text{PRu}$: C, 51.01; H, 7.95. Found: C 50.98; H 7.80.

Mass spectrum (FAB⁺) M^+ m/z = 494 (M^+); m/z = 459 ($\text{M}^+ - \text{Cl}$)

Preparation of $\text{Ru}[\eta^6\text{-benzotris(cyclooctene)}](\text{PMe}_3)\text{Cl}_2$



This compound was prepared the same way as the corresponding C_6Et_6 compound (see above).

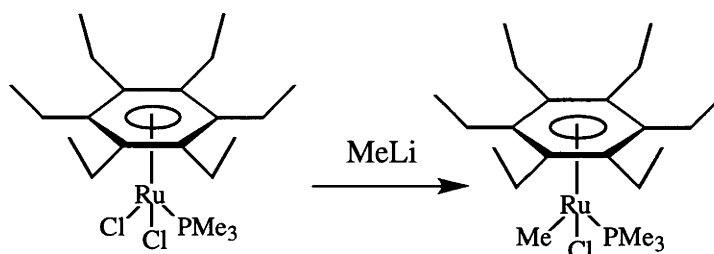
^1H NMR (C_6D_6 , 300 MHz) δ 2.8-2.4 [m, benzotris(cyclooctene)], 1.7-1.1 [m, benzotris(cyclooctene)], 1.31 ppm (d, $^2J(\text{HP})$ 10.5 Hz, PMe_3)

$^{13}\text{P}\{^1\text{H}\}$ NMR (C_6D_6 , 121.4 MHz) δ -1.7 (s, PMe_3)

Mass Spectrum (EI 70 eV) $m/z = 572$ (M^+)

Anal. calcd. for $\text{C}_{27}\text{H}_{45}\text{Cl}_2\text{PRu}$: C 56.64; H 7.92; Cl 12.38. Found: C 56.74; H 7.83; Cl 12.56.

Preparation of $\text{Ru}(\eta^6\text{-C}_6\text{Et}_6)(\text{PMe}_3)(\text{Me})\text{Cl}$



To a stirred suspension of $\text{Ru}(\eta^6\text{-C}_6\text{Et}_6)(\text{PMe}_3)\text{Cl}_2$ (100 mg, 0.21 mmol) in 10 cm³ of toluene was added 0.155 cm³ of 1.4 M ethereal MeLi solution (0.21 mmol). The solution was stirred for 2 h, then reduced in volume *in vacuo* to 2 cm³, and loaded on an Al_2O_3 column (activity III, neutral, 1.5 x 6 cm). The column was washed with 300 cm³ of toluene to remove $\text{Ru}(\eta^6\text{-C}_6\text{Et}_6)(\text{PMe}_3)\text{Me}_2$, which was formed as a side product. The desired product was then eluted with CH_2Cl_2 . A bright yellow solution was obtained which was reduced *in vacuo* to give an air-sensitive yellow solid. The solid was dissolved in a minimum amount of pentane and cooled to -5°C overnight. Yellow crystals suitable for X-ray analysis were obtained (30 mg, 27 %).

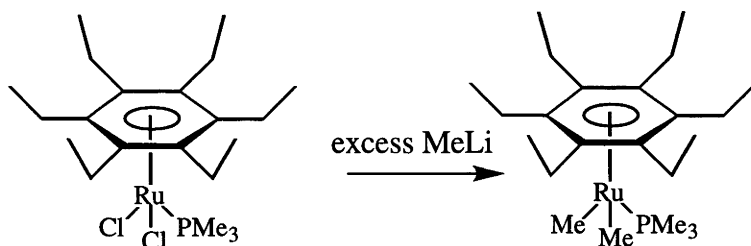
^1H NMR (CD_2Cl_2 , 300 MHz) δ 2.42 (q, 12H, $^3J(\text{HH})$ 7.5 Hz, CH_2), 1.26 (t, 18H, $^3J(\text{HH})$ 7.5 Hz, CH_3), 1.23 (d, $^2J(\text{HP})$ 9.2 Hz, PMe_3), 0.27 ppm [d, $^2J(\text{HP})$ 9.2 Hz, $\text{CH}_3(\text{coordinated methyl group})$]

$^{13}\text{C}\{^1\text{H}\}$ NMR (CD_2Cl_2 , 75.42 MHz) δ 103.2 (s, $\text{C}_{\text{aromatic}}$), 22.6 (s, CH_2), 15.9 (d, $^3J(\text{PC})$ 48 Hz, PMe_3), 15.7 (s, CH_3), 10.0 ppm [d, $^3J(\text{PC})$ 35 Hz, $\text{Ru-CH}_3(\text{coordinated methyl group})$]

$^{31}\text{P}\{^1\text{H}\}$ NMR (CD_2Cl_2 , 121.24 MHz) δ 2.9 ppm (s, PMe_3)

Mass spectrum (EI, accurate mass with apparent resolution 10^4) Calcd. for $^{12}\text{C}_{22}^{1}\text{H}_{42}^{31}\text{P}^{37}\text{Cl}^{102}\text{Ru}$: 474.175615; Found: 474.176254 amu (1.3 ppm deviation)

Preparation of $\text{Ru}(\eta^6\text{-C}_6\text{Et}_6)(\text{PMe}_3)(\text{Me})_2$



$\text{Ru}(\eta^6\text{-C}_6\text{Et}_6)(\text{PMe}_3)\text{Cl}_2$ (88 mg, 0.17 mmol) was stirred in 10 cm³ of toluene. On addition of 0.5 cm³ of 1 M ethereal MeLi, solution the solution changed colour from bright red to dirty green over 1 h. Solvent was removed under vacuum. The residue was dissolved in a minimum amount of toluene and loaded onto an Al_2O_3 column (activity III, neutral, 1.5 x 6 cm). The complex was eluted with toluene and the solvent removed *in vacuo* to give a pale yellow solid. This solid was dissolved in a minimum amount of pentane and cooled in a dry ice bath to give pale yellow crystals suitable for X-ray analysis (14 mg, 17 %).

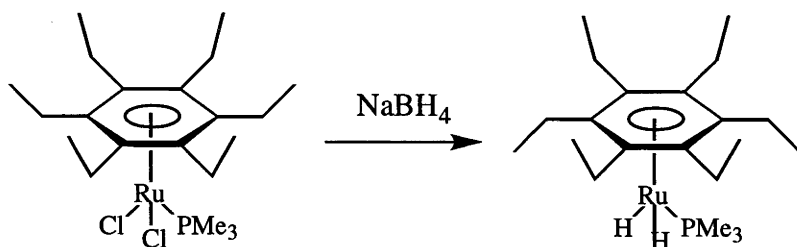
¹H NMR (C_6D_6 , 300 MHz) δ 2.26 (q, 12H, ³*J*(HH) 7.5 Hz, CH₂), 1.16 (t, 18H ³*J*(HH) 7.5 Hz, CH₃), 0.99 (d, 9H, ²*J*(HP) 8.0 Hz, PMe_3), -0.04 ppm [d, 3H, ²*J*(HP) 7.6 Hz, Ru-CH₃(coordinated methyl group)]

³¹P{¹H} NMR (C_6D_6 , 121.42 MHz) δ 6.0 ppm (s, PMe_3)

¹³C {¹H} NMR (C_6D_6 , 75.42 MHz) δ 101.1 (s, C_{aromatic}), 22.4 (s, CH₂), 16.93 (d, ¹*J*(CP) 41 Hz, PMe_3), 16.3 (s, CH₃), -4.4 ppm (d, ²*J*(CP) 33 Hz, Ru-CH₃)

Mass spectrum (FAB⁺, accurate mass with apparent resolution 10⁴) Calc. for ¹²C_{23¹H₄₅³¹P¹⁰²Ru: 454.230225; Found: 454.230238 (<1 ppm deviation)}

Preparation of Ru (η^6 -C₆Et₆)(PMe₃)(H)₂



Ru(η^6 -C₆Et₆)(PMe₃)Cl₂ (140 mg, 0.28 mmol) was stirred in 10 cm³ of 2-propanol with NaBH₄ (50 mg, 1.33 mmol). The solution was then heated to reflux under nitrogen for 1 h, during which the clear deep-red solution gave way to a yellow-grey suspension and finally to a grey suspension. The 2-propanol was removed *in vacuo* to give a grey solid. A sublimation probe was inserted into the flask and cooled to -15°C. The flask was then heated to 100°C in a water bath and vacuum applied. A white solid collected on the probe. The probe was transferred in a dry box to another flask. The solid was washed off the probe with a minimum amount of pentane and the resulting solution was cooled to dry ice temperature. The pentane was slowly removed with a gentle stream of nitrogen to give small colourless crystals (68 mg, 59 %).

¹H NMR (C₆D₆, 300 MHz) δ 2.34 (q, 12H, ³J(HH) 7.5 Hz, CH₂), 1.23 (t, 18H, ³J(HH) 7.5 Hz, CH₃), 1.20 (d, 9H, ²J(HP) 8.0 Hz, PMe₃), -10.84 ppm (d, 2H, ²J(PH) 50 Hz, Ru-H)

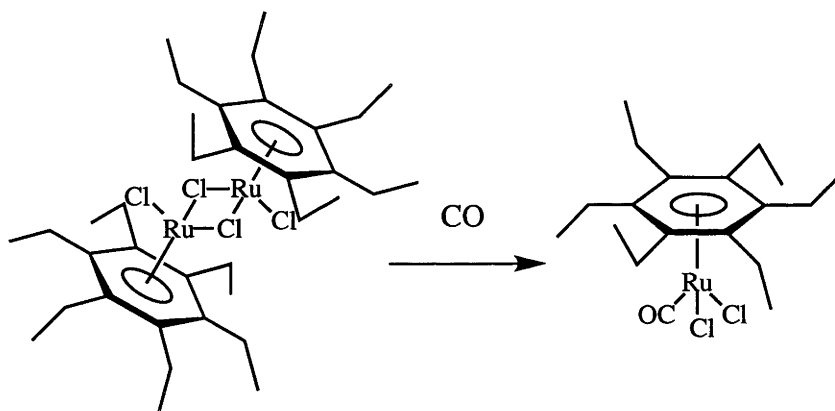
³¹P{¹H} NMR (C₆D₆, 12.42 MHz) δ 4.4 ppm (s, PMe₃)

¹³C{¹H} (C₆D₆, 75.42 MHz) δ 102.6 (s, arene C), 26.6 (d, ¹J(CP) 48.5 Hz, PMe₃), 22.9 (s, CH₂), 19.7 ppm (s, CH₃)

Mass spectrum (EI) m/z = 424 (M⁺)

Anal. calcd. for C₂₁H₄₁RuP: C 59.26; H 9.71. Found: C 59.08; H 9.50.

Preparation of $\text{Ru}(\eta^6\text{-C}_6\text{Et}_6)(\text{CO})\text{Cl}_2$



A solution of $[\text{Ru}(\eta^6\text{-C}_6\text{Et}_6)\text{Cl}_2]_2$ (44 mg, 0.052 mmol) in 30 cm³ of CH_2Cl_2 was stirred under an atmosphere of CO for 1 h. The solution changed colour from yellow/orange to red. The solution was reduced in volume to *ca.* 5 cm³ and filtered through a celite plug in a Pasteur pipette. The volume was again reduced and the remaining solution layered with ether. Small dark-red crystals were obtained (32 mg, 70 %). If CO was bubbled through the solution for 2 h, $\text{Ru}_3(\text{CO})_{12}$ was also formed (as shown by mass spectrometry).

^1H NMR (CD_2Cl_2 , 300 MHz) δ 2.52 (q, 12H, $^3J(\text{HH})$ 7.5 Hz, CH_2), 1.36 ppm (t, 18H, $^3J(\text{HH})$ 7.5 Hz, CH_3)

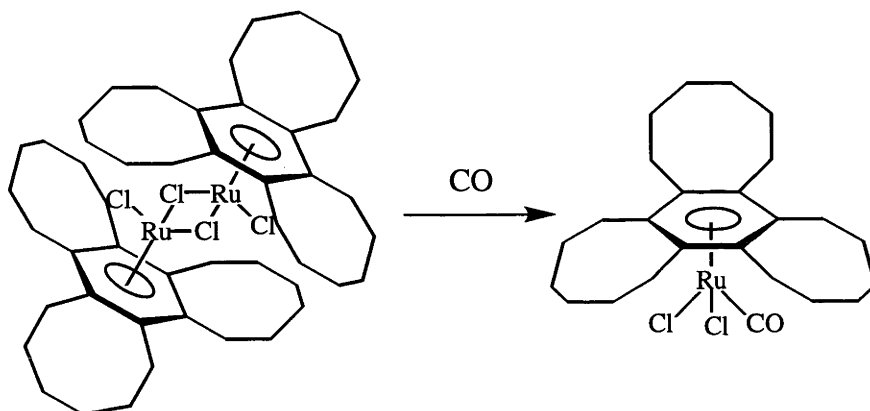
$^{13}\text{C}\{^1\text{H}\}$ NMR (CD_2Cl_2 , 75.42 MHz) δ 193.4 (s, CO), 110.1 (s, $\text{C}_{\text{aromatic}}$), 21.8 (s, CH_2), 14.6 ppm (s, CH_3)

IR (nujol mull) 2010 cm⁻¹ (s, CO)

Mass spectrum (EI) $m/z = 418$ ($\text{M}^+ - \text{CO}$)

Anal. calcd. for $\text{C}_{19}\text{H}_{30}\text{Cl}_2\text{ORu}$: C 51.12; H 6.77. Found: C 51.08; H 7.02.

Preparation of $\text{Ru}[\eta^6\text{-benzotris(cyclooctene)}](\text{CO})\text{Cl}_2$



The same method was used as for $\text{Ru}(\eta^6\text{-C}_6\text{Et}_6)(\text{CO})\text{Cl}_2$ above.

^1H NMR (CD_2Cl_2 , 300 MHz) δ 3.0-2.6 [m, benzotris(cyclooctene)], 2.1-1.9 [m, benzotris(cyclooctene)], 1.8-1.3 ppm [m, benzotris(cyclooctene)].

$^{13}\text{C}\{^1\text{H}\}$ NMR (CD_2Cl_2 , 75.42 MHz) δ 109.1 (s, $\text{C}_{\text{aromatic}}$), 31.1 [s, $\text{CH}_2(\text{benzotris(cyclooctene)})$], 28.8 [s, $\text{CH}_2(\text{benzotris(cyclooctene)})$], 27.19 ppm [s, $\text{CH}_2(\text{benzotris(cyclooctene)})$]^e

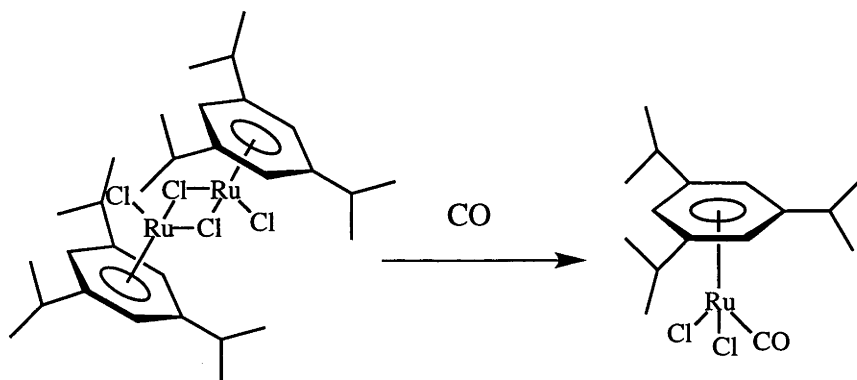
Mass spectrum (FAB^+) (m/z) = 524 (M^+)

IR (nujol mull) 2005cm^{-1} (s, m, CO)

Anal. calcd. for $\text{C}_{16}\text{H}_{24}\text{Cl}_2\text{ORu}$: C 57.25; H 5.94. Found: C 56.67; H 6.04.

^e the quaternary carbon of the coordinated CO was not found

Preparation of $\text{Ru}(\eta^6\text{-tri-isopropylbenzene})(\text{CO})\text{Cl}_2$



The same method was used as for $\text{Ru}(\eta^6\text{-C}_6\text{Et}_6)(\text{CO})\text{Cl}_2$ above. Only the symmetrical isomer, containing 1,3,5-tri-isopropylbenzene, was present after recrystallization from $\text{CH}_2\text{Cl}_2/\text{Et}_2\text{O}$.

^1H NMR (CD_2Cl_2 , 300 MHz) δ 5.57 (s, $\text{CH}_{\text{aromatic}}$), 2.92 (d, $^3J(\text{HH})$ 7.2 Hz, $\text{CH}(\text{Pr}^i)$), 1.31 ppm [d, $^3J(\text{HH})$ 7.2 Hz, $\text{CH}_3(\text{Pr}^i)$]

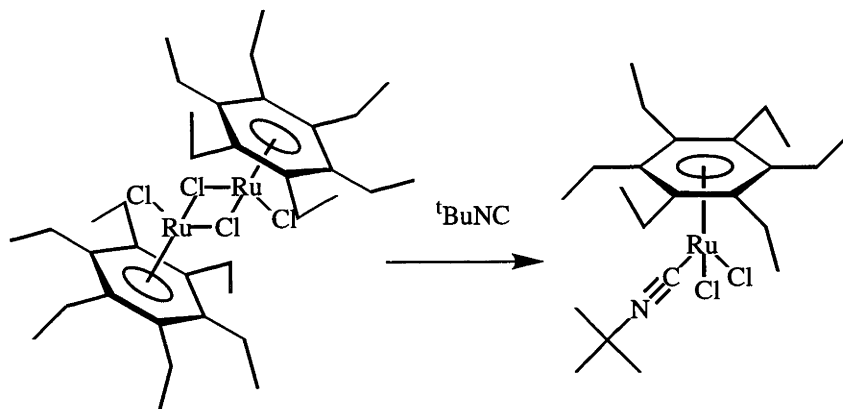
$^{13}\text{C}\{^1\text{H}\}$ NMR (CD_2Cl_2 , 125.74 MHz) δ 191.6 (s, CO), 121.5 (s, $\text{C}_{\text{aromatic}}$), d 86.7 (s, $\text{CH}_{\text{aromatic}}$), 31.8 [s, $\text{CH}(\text{Pr}^i)$], 21.8 ppm [s, $\text{CH}_3(\text{Pr}^i)$]

M^+ was not found in the FAB^+ mass spectrum

IR (nujol mull) 2007 cm^{-1} (s, m, CO)

Anal. calcd. for $\text{C}_{16}\text{H}_{24}\text{Cl}_2\text{ORu}$: C 47.53; H 5.98. Found: C 47.25; H 5.66.

Preparation of $\text{Ru}(\eta^6\text{-C}_6\text{Et}_6)(\text{Bu}^t\text{NC})\text{Cl}_2$



$[\text{Ru}(\eta^6\text{-C}_6\text{Et}_6)\text{Cl}_2]_2$ (50 mg, 0.059 mmol) was stirred in 5 cm³ of toluene with 20 μl of *t*-butylisocyanide. After 3 h the solution was filtered through celite and most of the toluene was removed to give an orange oil. Addition of pentane afforded an orange crystalline solid which was collected by vacuum filtration (37 mg, 37 % yield). Ether was allowed to diffuse into a dichloromethane solution of the product to give red block-like crystals suitable for X-ray analysis.

¹H NMR (CD_2Cl_2 , 300 MHz) δ 2.45 (q, 12H, ³*J*(HH) 7.5 Hz, CH₂), 1.53 (s, 9H, Bu^t), 1.34 ppm (t, 18H, ³*J*(HH) 7.5 Hz, CH₃)

¹³C{¹H} NMR (CD_2Cl_2 , 74.43 MHz) δ 103.1 (s, C_{aromatic}), 30.7 [s, CH₃ (Bu^t)], 22.0 (s, CH₃), 15.0 ppm (s, CH₂).^f

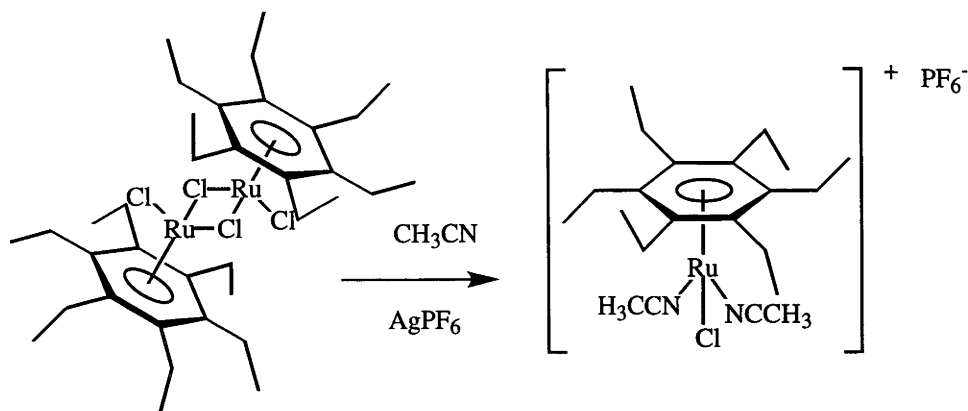
Mass spectrum (EI 70 eV) *m/z* = 501 (M⁺)

Anal. calcd. for C₂₂H₃₉Cl₂NRu: C 53.98; H 8.03; N 2.86. Found C 54.87; H 7.69; N 2.45.

IR (KCl disk) 2168 cm⁻¹ (s, sharp, CN)

^f Tertiary carbon of the Bu^t group and the coordinated carbon of the isocyanide not visible.

Preparation of $[\text{Ru}(\eta^6\text{-C}_6\text{Et}_6)(\text{CH}_3\text{CN})_2\text{Cl}]^+\text{PF}_6^-$



$[\text{Ru}(\eta^6\text{-C}_6\text{Et}_6)\text{Cl}_2]_2$ (50 mg, 0.059 mmol) was stirred with 21 mg of NH_4PF_6 in 5 cm^3 of acetonitrile. The solution changed colour from a clear yellow/orange to a pale yellow with a white precipitate. The precipitate was removed by filtration through celite. The volume of CH_3CN was reduced *in vacuo* to 2 cm^3 and ether was added to give a pale orange microcrystalline solid, which was collected by vacuum filtration (55 mg, 90%). It was found that this complex decomposed to $[\text{Ru}(\eta^6\text{-C}_6\text{Et}_6)\text{Cl}_2]_2$ in CH_2Cl_2 and to an unknown species in acetone unless there was excess free acetonitrile present.

^1H NMR ($\text{CD}_2\text{Cl}_2/\text{CH}_3\text{CN}$, 300 MHz) δ 2.46 (q, 12H, $^3J(\text{HH})$ 7.6 Hz, CH_2), 1.90 [br s, 3H, $\text{CH}_3(\text{acetonitrile})$], 1.31 ppm (t, 18H, $^3J(\text{HH})$ 7.5 Hz, CH_3)

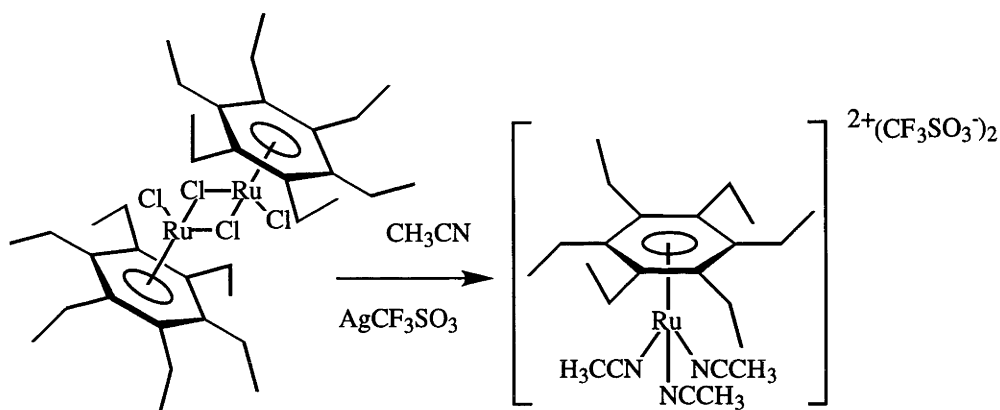
$^{13}\text{C}\{^1\text{H}\}$ NMR ($\text{CD}_2\text{Cl}_2/\text{CH}_3\text{CN}$, 75.42 MHz) δ 117.0 (s, CN), 100.3 (s, $\text{C}_{\text{aromatic}}$), 21.4 (s, CH_2), 14.3 (s, CH_3), 1.0 ppm [m, $\text{CH}_3(\text{acetonitrile})]$ [§]

Mass spectrum (FAB⁺) (m/z) = 424 ($\text{M}^+ - \text{CH}_3\text{CN}$)

Anal. calcd. for $\text{C}_{22}\text{H}_{36}\text{ClF}_6\text{N}_2\text{PRu}$: C 43.32; H 5.95; N 4.59. Found: C 42.88; H 5.57; N 5.01.

[§] the coordinated acetonitrile signal in both the ^1H NMR and ^{13}C NMR spectra was obscured by the large resonances due to the partially deuterated acetonitrile.

Preparation of $[\text{Ru}(\eta^6\text{-C}_6\text{Et}_6)(\text{CH}_3\text{CN})_3]^{2+}(\text{CF}_3\text{SO}_3^-)_2$



$[\text{Ru}(\eta^6\text{-C}_6\text{Et}_6)\text{Cl}_2]_2$ (50 mg, 0.059 mmol) and 70 mg of AgSO_3CF_3 were mixed and dissolved in CH_2Cl_2 . The initially yellow/orange solution became progressively lighter over a period of 15 h and a grey precipitate of AgCl became apparent. The solution was centrifuged to remove the precipitate and the resulting light-orange solution was carefully decanted. The solvent was removed *in vacuo* to give a very moisture-sensitive orange solid which was recrystallised from dichloromethane/hexane, to give a yellow microcrystalline solid, presumably $\text{Ru}(\eta^6\text{-C}_6\text{Et}_6)(\text{CF}_3\text{SO}_3)_2$. Dry CH_3CN , 5 cm^3 , was added to this solid and the resulting solution changed colour from orange to yellow over a period of 5 min. The volume of the solution was reduced and 10 cm^3 of pentane was added to give a pale yellow microcrystalline precipitate which was collected by vacuum filtration (36 mg, 47 %).

^1H NMR (CD_3CN , 300 MHz) δ 2.66 [br s, 9H, $\text{CH}_3(\text{acetonitrile})$], 2.50 (q, 12H, $^3J(\text{HH})$ 7.7 Hz, CH_2), 1.32 ppm (t, 18H, $^3J(\text{HH})$ 7.6 Hz, CH_3)

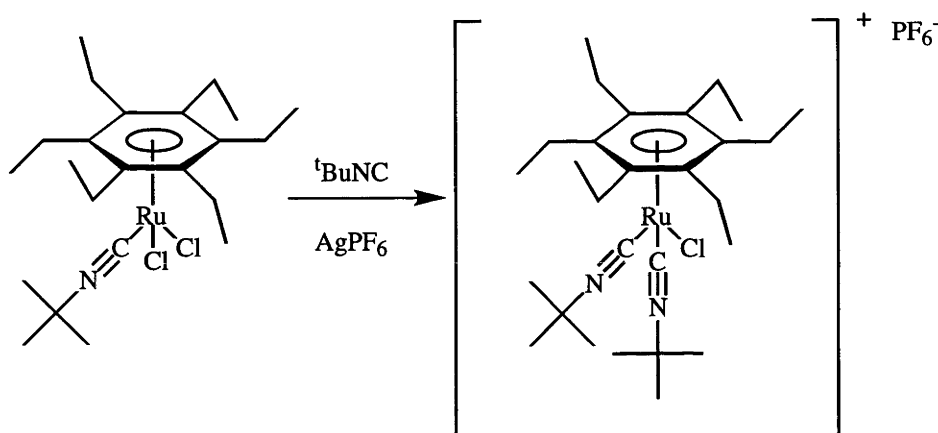
$^{13}\text{C}\{^1\text{H}\}$ NMR ($\text{CD}_2\text{Cl}_2/\text{CD}_3\text{CN}$, 75.42 MHz) δ 116.9 (s, $\text{C}_{\text{aromatic}}$), 21.4 (s, CH_2), 14.2 ppm (s, CH_3)^h

^h coordinated acetonitrile and triflate CF_3 not visible.

Mass spectrum (FAB⁺) $m/z = 620$ ($M^+ - CF_3SO_3$)

Anal. calcd. for $C_{26}H_{39}F_6N_3O_6RuS_2$: C 40.6; H 5.08; N 5.46. Found: C 40.51; H 4.87; N 5.60.

Preparation of $[Ru(\eta^6-C_6Et_6)(Bu^tNC)_2Cl]^+PF_6^-$



A stirred solution of $[Ru(\eta^6-C_6Et_6)Cl_2]_2$ (73 mg, 0.087 mmol) in CH_2Cl_2 was treated with 20 μ l (0.174 mmol) of Bu^tNC . After 1 h the solvent and any remaining isocyanide was removed *in vacuo* to give $Ru(\eta^6-C_6Et_6)(Bu^tNC)Cl_2$. To this was added a stoichiometric amount of $AgPF_6$ (44 mg, 0.174 mmol) and 10 cm^3 of CH_2Cl_2 , and the resulting suspension was stirred in the dark. Subsequently, the solution was observed to have changed colour from deep red to yellow-brown and to contain a grey suspended solid, presumably $AgCl$. To this suspension was added a second 20 μ l portion of Bu^tNC whereupon the colour changed to pale yellow and a white precipitate formed. The precipitate of $AgCl$ was removed by centrifugation and careful decantation. The solvent was removed from the resulting pale yellow solution *in vacuo* to give a yellow powder. Recrystallization by vapour diffusion from CH_2Cl_2/Et_2O gave yellow needle-like crystals suitable for single crystal X-ray analysis (60 mg, 63 %)

1H NMR (CD_2Cl_2 , 200 MHz) δ 2.49 (q, 12H, $^3J(HH)$ 7.4 Hz, CH_2), 2.12 [s, 18H, $CH_3(Bu^t)$], 1.32 ppm (t, 18H, $^3J(HH)$ 7.4 Hz, CH_3)

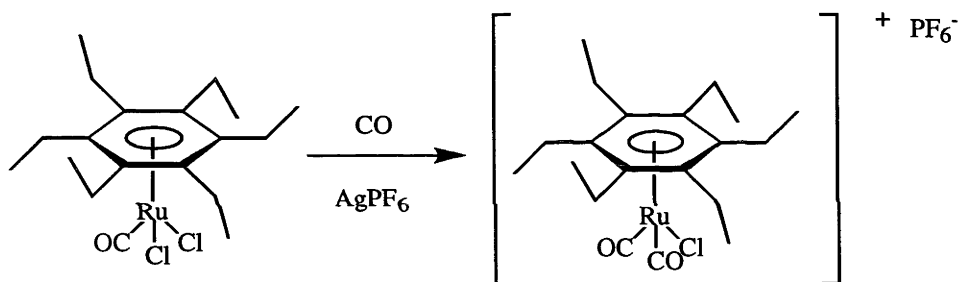
$^{13}\text{C}\{^1\text{H}\}$ NMR (CD_2Cl_2 , 75.42 MHz) δ 138.3 (s, CN), 109.8 (s, $\text{C}_{\text{aromatic}}$), 30.2 [s, $\text{CH}_3(\text{Bu}^i\text{NC})$], 22.3 (s, CH_2), 16.2 ppm (s, CH_3)

IR (KBr disk) ν 2202 (s, CN) 2186 cm^{-1} (s, CN)

Mass spectrum (FAB $^+$) m/z = 549 ($\text{M}^+ - \text{PF}_6^-$)

Anal. calcd. for $\text{C}_{28}\text{H}_{48}\text{ClF}_6\text{N}_2\text{PRu}$: C 48.45; H 6.97; N 4.04. Found: C 47.73; H 6.77; N 4.28.

Preparation of $[\text{Ru}(\eta^6\text{-C}_6\text{Et}_6)(\text{CO})_2\text{Cl}]^+\text{PF}_6^-$



The compound $[\text{Ru}(\eta^6\text{-C}_6\text{Et}_6)\text{Cl}_2]_2$ (65 mg, 0.078 mmol) was stirred under CO in CH_2Cl_2 (10cm^3) for two hours until the solution had changed from orange-red to the deep red colour of $\text{Ru}(\eta^6\text{-C}_6\text{Et}_6)(\text{CO})\text{Cl}_2$. The solvent was removed and a stoichiometric amount of AgPF_6 added, followed by 10cm^3 of CH_2Cl_2 ; the reaction mixture was stirred in the dark. After 5 min the solution had become a greenish yellow colour and a grey precipitate had formed. This solution was then placed under an atmosphere of CO for a further 2 h, whereupon the solution became more orange/yellow with a white precipitate. The precipitate was removed by centrifugation of the mixture and the clear yellow solution was decanted and pumped down to give an orange oily solid. This was recrystallized from $\text{CH}_2\text{Cl}_2/\text{Et}_2\text{O}$ to give pale yellow, square, plate-like crystals that were suitable for X-ray crystallography. This solid also contained a small amount of material which had crystallized as red cubic blocks, which were found to be $[\text{Ru}_2(\eta^6\text{-C}_6\text{Et}_6)\text{Cl}_3]^+\text{PF}_6^-$.

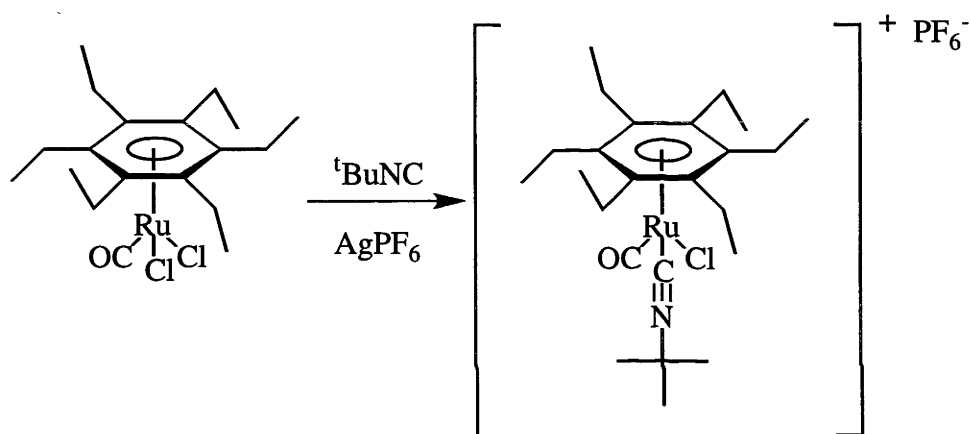
^1H NMR (CD_2Cl_2 , 300 MHz) δ 2.67 (q, 12H, $^3J(\text{HH})$ 7.4 Hz, CH_2), 1.42 ppm (t, 18H, $^3J(\text{HH})$ 7.4 Hz, CH_3)

$^{13}\text{C}\{^1\text{H}\}$ NMR (CD_2Cl_2 , 75.42 MHz) δ 160.1 (s, CO), 95.3 (s, $\text{C}_{\text{aromatic}}$), 21.4 (s, CH_2), 15.0 ppm (s, CH_3)

IR (KBr disk) ν 2064 (s, sharp, CO stretching) 2000 cm^{-1} (s, sharp, CO stretching)

Anal calcd. for $\text{C}_{20}\text{H}_{30}\text{ClF}_6\text{O}_2\text{PRu}$: C 41.14; H 5.18. Found: C 40.83; H 4.89.

Preparation of $[\text{Ru}(\eta^6\text{-C}_6\text{Et}_6)(\text{Bu}^t\text{NC})(\text{CO})\text{Cl}]^+\text{PF}_6^-$



$\text{Ru}(\eta^6\text{-C}_6\text{Et}_6)(\text{Bu}^t\text{NC})\text{Cl}_2$ (82 mg, 0.168 mmol) and 42 mg of AgPF_6 were placed under nitrogen in a Schlenk flask wrapped in aluminium foil to exclude light. To this was added 10 cm^3 of CH_2Cl_2 and the resulting solution was stirred for 15 min, whereupon a change from a red solution to a brown suspension was observed. This suspension was then stirred vigorously in the dark under a CO atmosphere supplied from a balloon attached to the flask. After two hours the suspension was centrifuged, after which a yellow solution was observed over a grey precipitate. The solution was carefully decanted and reduced in volume to 1 cm^3 *in vacuo*, layered with Et_2O and placed in the refrigerator for several days. Fluffy yellow crystals (67 mg) were collected by vacuum filtration and washed with dry Et_2O .

The ^1H NMR spectrum showed two complexes containing C_6Et_6 to be present in a 3:1 ratio (from integration of the two methylene resonances present). The impurity was found to be $[\text{Ru}_2(\eta^6\text{-C}_6\text{Et}_6)_2\text{Cl}_3]^+\text{PF}_6^-$. The yellow crystals were redissolved in CH_2Cl_2 and

recrystallized by diffusion of ether into the dichloromethane solution. Yellow plate-like crystals suitable for X-ray analysis were obtained (51 mg, 61 %).

^1H NMR (CD_2Cl_2 , 300 MHz) δ 2.59 (q, 12H, $^3J(\text{HH})$ 7.65 Hz, CH_2), 1.59 [s, $\text{CH}_3(\text{Bu}^t\text{NC})$], 1.37 ppm (t, 18H, $^3J(\text{HH})$ 7.65 Hz, CH_3)

$^{13}\text{C}\{^1\text{H}\}$ NMR (CD_2Cl_2 , 75.42 MHz) δ 191.1 (s, CO), 118.9 (s, $\text{C}_{\text{aromatic}}$), 30.2 (s, CH_2), 22.3 (s, CH_3), 16.2 ppm [s, $\text{CH}_3(\text{Bu}^t\text{NC})$]

IR (KBr disk) 2207 (s, CN), 2035 cm^{-1} (s, CO)

Mass spectrum (FAB) $m/z = 494$ ($\text{M}^+ - \text{PF}_6$)

Anal. calcd. for $\text{C}_{24}\text{H}_{39}\text{ClF}_6\text{NOPRu}$: C 45.11; H 6.15; N 2.19. Found: C 44.65; H 6.14; N 2.11.

Experimental details for the collection of X-ray data and solution of structures

Compound	$\text{Ru}(\eta^6\text{-C}_6\text{Et}_6)(\text{COD})$	$[\text{Ru}(\eta^6\text{-C}_6\text{Et}_6)\text{Cl}_2]_2$	$[\text{Ru}\{\eta^6\text{-benzotris(cyclooctene)}\}\text{Cl}_2]_2$
<i>(a) Crystal data</i>			
Chemical formula	$\text{C}_{26}\text{H}_{42}\text{Ru}$	$\text{C}_{36}\text{H}_{60}\text{Cl}_4\text{Ru}_2$	$\text{C}_{26}\text{H}_{40}\text{Cl}_6\text{Ru}$
FW	455.66	836.82	666.39
Crystal system	triclinic	monoclinic	triclinic
Unit cell dimensions			
a (Å)	9.578(3)	10.900(3)	11.061(8)
b (Å)	10.712(3)	9.566(3)	11.273(7)
c (Å)	13.336(4)	18.439(3)	13.142(7)
α (°)	68.61(3)		70.47(4)
β (°)	84.16(3)	101.99(2)	79.10(5)
γ (°)	64.32(3)		71.48(5)
V (Å ³)	1145.6(6)	1880.7(7)	1457(1)
Space group	$P\bar{1}(\#2)$	$P21/n(\#14)$	$P\bar{1}(\#2)$
Dc (g cm ⁻³)	1.32	1.49	1.52
Z	2	2	2
F(000)	484	864	684
Colour, habit	yellow/prism	orange/plate	orange/block
Crystal dimensions	0.32 x 0.64 x 0.17 mm	0.28 x 0.08 x 0.20 mm	0.15 x 0.17 x 0.27 mm
$\mu(\text{cm}^{-1})$	6.92	92.85 (Mo K α)	11.01 (Mo K α)
<i>(b) Data collection and processing</i>			
Diffractometer	Ital Structures	Rigaku AFC6S	Rigaku AFC6S
X-Radiation	Mo K α	Mo K α	Mo K α
Scan mode		ω -2 θ	ω -2 θ
ω -scan width		$(1.20 + 0.30\tan\theta)^\circ$	$(1.00 + 0.34\tan\theta)^\circ$
2 θ max (°)	50.00	50.1	50.1
No. of reflections			
Total	4243	3179	5310
Unique	3981	3004	5032
Observed	3979	1953	4241
	$[I > 2\sigma(I)]$	$[I > 3\sigma(I)]$	$(I > 3.\sigma(I))$
Min, max correction	-	0.39-1.00	0.85-1.00
<i>(c) Structure analysis and refinement</i>			
Structure solution	Patterson methods (SHELX86 SHELX93)	Patterson methods (DIRDIF92 PATTY)	direct methods (SIR92)
Refinement	full-matrix least-squares	full-matrix least-squares	full-matrix least-squares
No. of parameters	260	190	289
Weighting scheme (w=)	$\frac{1}{\left[\sigma^2(F_0^2) + (0.0519P)^2 + 0.85P\right]}$ where $P = \frac{\left[\text{MAX}(F_0^2, 0) + 2F_c^3\right]}{3}$	$[\sigma^2(F_0) + (0.25p^2F_0)^2]^{-1}$ $p=0.012$	$[\sigma^2(F_0) + (0.25p^2F_0)^2]^{-1}$ $p=0.0009$
R(observed data)	0.040	0.039	0.051
Rw(observed data)	0.099	0.040	0.074

Compound	[Ru ₂ (η ⁶ -C ₆ Et ₆) ₂ Cl ₃] ⁺ PF ₆ ⁻	[Ru ₂ (η ⁶ -C ₆ H ₄ -1,2-Et ₂) ₂ Cl ₃] ⁺ PF ₆ ⁻	Ru(η ⁶ -C ₆ H ₄ -1,2-Pr ⁱ ₂) ₂ Cl ₃] ⁺ PF ₆ ⁻
<i>(a) Crystal data</i>			
Chemical formula	C ₃₆ H ₆₀ Cl ₃ F ₆ PRu ₂	C ₂₀ H ₂₈ Cl ₃ F ₆ PRu ₂	C ₂₄ H ₃₆ Cl ₃ F ₆ PRu ₂
FW	946.33	721.90	778.01
Crystal system	triclinic	monoclinic	trigonal
Unit cell dimensions			
a (Å)	13.913(3)	12.107(2)	22.166(4)
b (Å)	14.132(3)	15.675(7)	
c (Å)	21.625(3)	13.585(3)	32.245(6)
α (°)	90.97(1)		
β (°)	90.56(1)	98.90(2)	
γ (°)	100.89(2)		
V (Å ³)	4174(1)	2547(1)	1448.9(5)
Space group	<i>P</i> $\bar{1}$ (#2)	<i>P</i> 2 ₁ / <i>c</i> (#14)	<i>P</i> 3 ₁ 12 (#151)
D _c (g cm ⁻³)	1.51	1.88	1.70
Z	4	4	18
F(000)	1936	1424	6984
Colour, habit	orange/ block	orange/ plate	red/ needle
Crystal dimensions	0.12x0.16x0.24 mm	0.48x0.24x0.06mm	0.74x0.27x0.17mm
μ(cm ⁻¹)	10.05 (MoKα)	139.24 (CuKα)	13.55 (MoKα)
<i>(b) Data collection and processing</i>			
Diffractometer	Rigaku AFC6S	RigakuAFC6R	Philips PW1100/20
X-Radiation	MoKα	CuKα	MoKα
Scan mode	ω-2θ	ω-2θ	ω
ω-scan width	(1.31+0.34tanθ)°	(1.40+0.30tanθ)°	(1.20+0.35tanθ)°
2θ max (°)	50.1	120.3	50.0
No. of reflections			
Total	15431	4146	9165
Unique	14767	3962	8476
Observed	10182	2884	4236
	[I > 3σ(I)]	(I > 3σ(I))	(I > 3σ(I))
Min, max correction	0.93-1.00	0.2560-1.0000	0.724-0.808
<i>(c) Structure analysis and refinement</i>			
Structure solution	Patterson methods (DIRDIF92 PATTY)	Patterson methods (DIRDIF92 PATTY)	Patterson methods (DIRDIF92 PATTY)
Refinement	full-matrix least-squares	full-matrix least-squares	full-matrix least-squares
No. of parameters	865	317	520
Weighting scheme (w=)	[σ ² (F _o)+(0.25p ² F _o) ²] ⁻¹	[σ ² (F _o)+(0.25p ² F _o) ²] ⁻¹	[σ ² (F _o)+(0.25p ² F _o) ²] ⁻¹
	p=0.003	p=0.0120	p=0.012
R(observed data)	0.037	0.088	0.070
Rw(observed data)	0.030	0.097	0.063

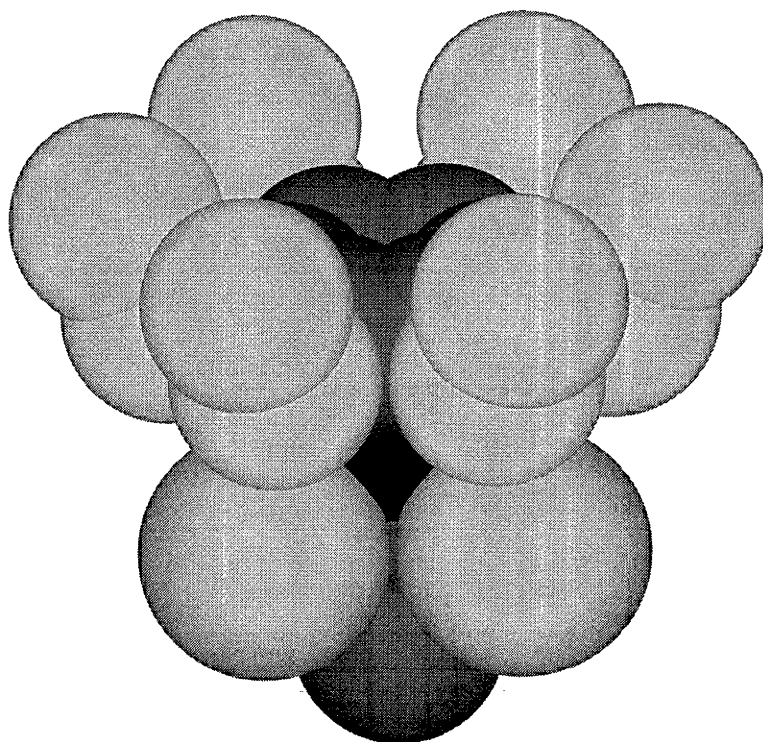
Compound	$\text{Ru}(\eta^6\text{-C}_6\text{Et}_6)(\text{PPh}_3)\text{Cl}_2$	$\text{Ru}(\eta^6\text{-C}_6\text{Et}_6)(\text{PMe}_3)\text{Cl}_2$
<i>(a) Crystal data</i>		
Chemical formula	$\text{C}_{42}\text{H}_{51}\text{Cl}_2\text{PRu}$	$\text{C}_{21}\text{H}_{41}\text{Cl}_2\text{PRuO}$
FW	758.81	512.50
Crystal system	orthorhombic	monoclinic
Unit cell dimensions		
a (Å)	9.358(2)	8.698(2)
b (Å)	19.226(1)	14.618(4)
c (Å)	20.478(2)	9.613(2)
α (°)		
β (°)		99.01(2)
γ (°)		
V (Å ³)	3685.2(6)	1207.1(4)
Space group	$P212121$ (#19)	$P21/m$ (#11)
Dc (g cm ⁻³)	1.368	1.410
Z	4	2
F(000)	1584	536
Colour, habit	orange/prism	orange/ block
Crystal dimensions	0.18x0.06x0.12mm	0.36x0.28x0.32mm
$\mu(\text{cm}^{-1})$	53.97 (Cu K α)	9.45 (Mo K α)
<i>(b) Data collection and processing</i>		
Diffractometer	Rigaku AFC6R	Rigaku AFC6S
X-Radiation	Cu K α	Mo K α
Scan mode	$\omega/2\theta$	$\omega/2\theta$
ω -scan width	$(1.30 + 0.34\tan\theta)^\circ$	$(0.9 + 0.34\tan\theta)^\circ$
2 θ max (°)	120.1	50.1
No. of reflections		
Total	3131	2399
Unique		2246
Observed	2857	2008
	[I > 3 σ (I)]	[I > 3 σ (I)]
Min, max correction	0.7906-0.9983	0.96-1.00
<i>(c) Structure analysis and refinement</i>		
Structure solution	direct methods (SIR88)	Patterson methods (DIRDIF92 PATTY)
Refinement	full-matrix least-squares	full-matrix least-squares
No. of parameters	415	133
Weighting scheme (w=)	$[\sigma_c^2(F_0) + (0.25p^2F_0)^2]^{-1}$	$[\sigma_c^2(F_0) + (0.25p^2F_0)^2]^{-1}$
	p=0.015	p=0.002
R(observed data)	0.025	0.028
Rw(observed data)	0.027	0.024

Compound	Ru(η^6 -C ₆ Et ₆)(PMe ₃)(Me)Cl	Ru(η^6 -C ₆ Et ₆)(PMe ₃)(Me) ₂	Ru(η^6 -C ₆ Et ₆)(PMe ₃)(H) ₂
<i>(a) Crystal data</i>			
Chemical formula	C ₂₂ H ₄₂ ClPRu	C ₂₃ H ₄₅ RuP	C ₂₁ H ₄₁ PRu
FW	474.07	453.65	425.60
Crystal system	triclinic	monoclinic	triclinic
Unit cell dimensions			
a (Å)	11.593(6)	8.833(2)	9.185(5)
b (Å)	15.492(5)	14.816(4)	10.454(5)
c (Å)	16.014(4)	9.503(2)	12.910(7)
α (°)	62.17(2)		90.45(5)
β (°)	79.11(3)	101.96(2)	105.48(6)
γ (°)	68.27(3)		108.97(3)
V (Å ³)	2362(2)	1216.7(5)	1124(1)
Space group	$P\bar{1}$ (#2)	$P21/m$ (#11)	$P\bar{1}$ (#2)
Dc (g cm ⁻³)	1.33	1.24	1.26
Z	4	2	2
F(000)	1000	484	452
Colour, habit	orange/ prism	yellow/ needle	colorless/ block
Crystal dimensions	0.37x0.32x0.18 mm	0.56x0.12x0.08 mm	0.42x0.37x0.18 mm
μ (cm ⁻¹)	8.48 (MoK α)	71.4 (MoK α)	7.54 (MoK α)
<i>(b) Data collection and processing</i>			
Diffractionmeter	Rigaku AFC6S	Rigaku AFC6S	Rigaku AFC6S
X-Radiation	MoK α	MoK α	MoK α
Scan mode	ω -2 θ	ω -2 θ	ω -2 θ
ω -scan width	(1.00+0.34tan θ)°	(0.80+0.34tan θ)°	(0.80+0.34tan θ)°
2 θ max (°)	50.1	50.1	50.2
No. of reflections			
Total	8828	2404	4261
Unique	8375	2254	3994
Observed	6387	1640	3256
	(I>3 σ (I))	(I>3 σ (I))	(I>3 σ (I))
Min, max correction	0.86-1.00	0.85-1.00	0.85-1.00
<i>(c) Structure analysis and refinement</i>			
Structure solution	direct methods (SIR92)	direct methods (SIR92)	direct methods (SIR92)
Refinement	full-matrix least squares	full-matrix least-squares	full-matrix least-squares
No. of parameters	452	136	216
Weighting scheme (w=)	$[\sigma^2(F_0)+(0.25p^2F_0)^2]^{-1}$ p=0.005	$[\sigma^2(F_0)+(0.25p^2F_0)^2]^{-1}$ p=0.020	$[\sigma^2(F_0)+(0.25p^2F_0)^2]^{-1}$ p=0.0030
R(observed data)	0.036	0.040	0.027
Rw(observed data)	0.040	0.043	0.022

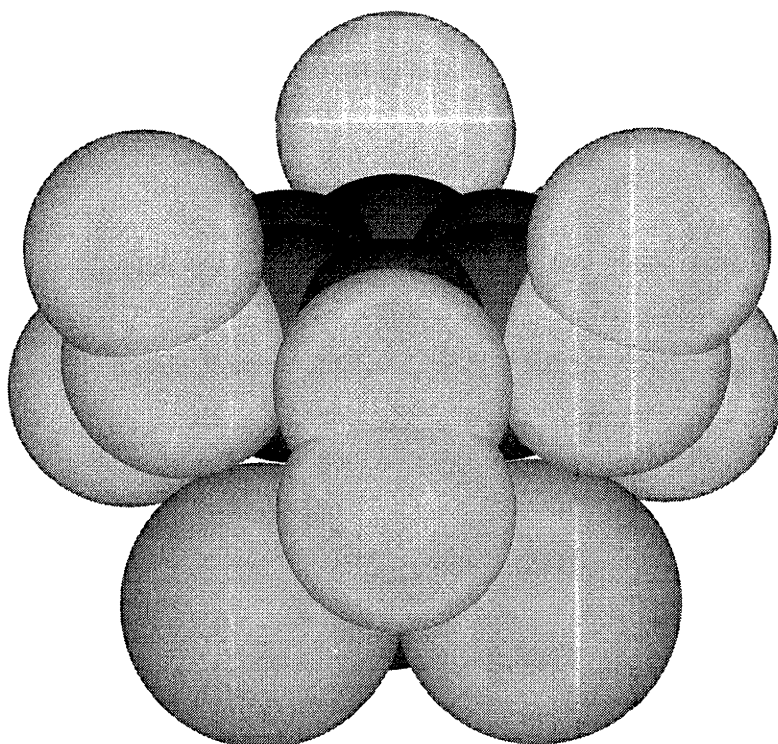
Compound	$\text{Ru}(\eta^6\text{-C}_6\text{Et}_6)(\text{CO})\text{Cl}_2$	$\text{Ru}(\eta^6\text{-C}_6\text{Et}_6)(\text{Bu}^t\text{NC})\text{Cl}$ 2	$[\text{Ru}(\eta^6\text{-C}_6\text{Et}_6)(\text{Bu}^t\text{NC})_2\text{Cl}]^+\text{PF}_6^-$
<i>(a) Crystal data</i>			
Chemical formula	$\text{C}_{19}\text{H}_{30}\text{Cl}_2\text{ORu}$	$\text{C}_{23}\text{H}_{39}\text{Cl}_2\text{NRu}$	$\text{C}_{28}\text{H}_{48}\text{ClF}_6\text{N}_2\text{PRu}$
FW	446.42	501.54	694.19
Crystal system	monoclinic	monoclinic	monoclinic
Unit cell dimensions			
a (Å)	9.835(3)	9.883(3)	13.957(2)
b (Å)	15.593(6)	16.377(6)	18.058(2)
c (Å)	13.653(5)	15.351(2)	27.370(2)
α (°)			
β (°)	99.59(2)	94.76(2)	100.70(1)
γ (°)			
V (Å ³)	2065(1)	2476(1)	6778(1)
Space group	$P2_1/n$ (#14)	$P2_1/n$ (#14)	$P2_1/c$ (#14)
Dc (g cm ⁻³)	1.436	1.345	1.360
Z	4	4	8
F(000)	920	1048	2888
Colour, habit	red/prism	red/prism	yellow/prism
Crystal dimensions	0.28x0.28x0.10 mm	0.44x0.38x0.36 mm	0.41x0.23x0.16 mm
$\mu(\text{cm}^{-1})$	10.8 (MoK α)	8.46 (MoK α)	6.41 (MoK α)
<i>(b) Data collection and processing</i>			
Diffractometer	Rigaku AFC6S	Rigaku AFC6S	Philips PW1100/20
X-Radiation	MoK α	MoK α	MoK α
Scan mode	ω -2 θ	ω -2 θ	ω -2 θ
ω -scan width	(0.90+0.34tan θ)°	(0.80+0.34tan θ)°	(0.90+0.34tan θ)°
2 θ max (°)	45.1	50.1	55.1
No. of reflections			
Total	2517	4730	16498
Unique	2328	4451	16108
Observed	1558	3088	8210
	(I>3 σ (I))	(I>3 σ (I))	(I>3 σ (I))
Min, max correction	0.85-1.00	0.96-1.00	0.869-0.915
<i>(c) Structure analysis and refinement</i>			
Structure solution	direct methods (SIR92)	direct methods (SIR92)	direct methods (SIR92)
Refinement	full-matrix least-squares	full-matrix least-squares	full-matrix least-squares
No. of parameters	208	245	723
Weighting scheme (w=)	$[\sigma^2(\text{F}_0) + (0.25\text{p}^2\text{F}_0)^2]^{-1}$ p=0.0020	$[\sigma^2(\text{F}_0) + (0.25\text{p}^2\text{F}_0)^2]^{-1}$ p=0.0030	$[\sigma^2(\text{F}_0) + (0.25\text{p}^2\text{F}_0)^2]^{-1}$ p=0.020
R(observed data)	0.034	0.030	0.041
Rw(observed data)	0.025	0.025	0.036

Compound	[Ru(η^6 -C ₆ Et ₆)(CO) ₂ Cl] ⁺ PF ₆ ⁻	Ru(η^6 -C ₆ Et ₆)(Bu ^t NC)(CO)Cl] ⁺ PF ₆ ⁻
<i>(a) Crystal data</i>		
Chemical formula	C ₂₀ H ₃₀ ClF ₆ O ₂ PRu	C ₂₄ H ₃₉ ClF ₆ NOPRu
FW	583.94	639.07
Crystal system	monoclinic	monoclinic
Unit cell dimensions		
a (Å)	16.760(2)	9.918(3)
b (Å)	8.747(1)	14.659(3)
c (Å)	16.940(2)	10.028(2)
α (°)		
β (°)	105.770(6)	96.39(2)
γ (°)		
V (Å ³)	2389.9(5)	1448.9(5)
Space group	<i>P</i> 2 ₁ / <i>n</i> (#14)	<i>Pn</i> (#7)
D _c (g cm ⁻³)	1.62	1.47
Z	4	2
F(000)	1184	656
Colour, habit	yellow/needle	yellow/plate
Crystal dimensions	0.52x0.31x0.14 mm	0.44x0.30x0.09 mm
μ (cm ⁻¹)	8.95 (MoK α)	7.31 (MoK α)
<i>(b) Data collection and processing</i>		
Diffractometer	Philips PW1100/20	Rigaku AFC6S
X-Radiation	MoK α	MoK α
Scan mode	ω -2 θ	ω -2 θ
ω -scan width	(1.20+0.34tan θ)°	(1.30+0.34tan θ)°
2 θ max (°)	55.1	60.1
No. of reflections		
Total	6035	4619
Unique	5864	4397
Observed	4628	3308
	(I>2 σ (I))	(I>2 σ (I))
Min, max correction	0.780-0.887	0.78-0.93
<i>(c) Structure analysis and refinement</i>		
Structure solution	direct methods (SIR92)	direct methods (SIR92)
Refinement	full-matrix least-squares	full-matrix least-squares
No. of parameters	305	318
Weighting scheme	[$\sigma_c^2(F_0)+(0.25p^2F_0)^2$] ⁻¹	[$\sigma_c^2(F_0)+(0.25p^2F_0)^2$] ⁻¹
(w=)	p=0.020	p=0.020
R(observed data)	0.034	0.0357
Rw(observed data)	0.036	0.0380

Chapter 6: *Conclusions*



A)



B)

Figure 6.1. Chem 3D representation of a space filling model of
A) $\text{Ru}(\eta^6\text{-C}_6\text{Et}_6)(\text{PMe}_3)\text{Cl}_2$ and B) $\text{Ru}(\eta^6\text{-C}_6\text{Et}_6)(\text{CO})\text{Cl}_2$

This project has achieved a number of goals. A new group of ruthenium complexes containing bulky arenes has been prepared via cyclotrimerization of acetylenes on $\text{Ru}(\eta^6\text{-naphth})(\eta^4\text{-COD})$. The product of the cyclotrimerization of 3-hexyne, $\text{Ru}(\eta^6\text{-arene})(\eta^4\text{-COD})$, has been used in further reactions to give a range of complexes containing the bulky arene hexaethylbenzene, nearly all of which have been characterized crystallographically. The solution and solid state conformational properties of coordinated hexaethylbenzene have been investigated.

The reaction of $\text{Ru}(\eta^6\text{-naphth})(\eta^4\text{-COD})$ with acetylenes gives complexes of the type $\text{Ru}(\eta^6\text{-arene})(\eta^4\text{-COD})$ which can be treated with HCl to give versatile starting materials of the type $[\text{Ru}(\eta^6\text{-arene})\text{Cl}_2]_2$. While the range of arenes is necessarily limited to those with hexa-, 1,3,5- or 1,2,4-substitution patterns by the nature of the cyclotrimerization reaction, many of these complexes would be difficult or impossible to obtain by previously existing methodologies. For instance, it was found impossible to coordinate hexaethylbenzene to ruthenium by such routes as the displacement of *p*-cymene in $[\text{Ru}(\eta^6\text{-}p\text{-cymene})\text{Cl}_2]_2$ in a manner analogous to that used to obtain $[\text{Ru}(\eta^6\text{-C}_6\text{Me}_6)\text{Cl}_2]_2$ ²⁵, displacement of naphthalene in $\text{Ru}(\eta^6\text{-naphth})(\eta^4\text{-COD})$ in the presence of CH_3CN ²⁹, and the direct reaction of the corresponding cyclohexadiene with $\text{RuCl}_3 \cdot x\text{H}_2\text{O}$ in EtOH,²⁰⁻²⁵ as the appropriate cyclohexadiene could not be obtained from Birch reduction of C_6Et_6 .

In this work, a large number of derivatives of the hexaethylbenzene ruthenium complex have been prepared and structurally characterized in the solid state by X-ray crystallography. This appears to be the largest series of structurally characterized arene ruthenium complexes where the arene has been kept constant and the auxiliary ligands varied. In general, the solid state structures were similar to those of previously determined for half-sandwich arene ruthenium complexes. In all the complexes the arene is essentially planar and the aromatic carbon atoms are equidistant from the ruthenium atom.

This series of derivatives has allowed a number of different comparisons to be made within the group. For example, arene-ruthenium distances could be correlated with the ^{13}C NMR chemical shift of the aromatic carbon atoms (Chapter 3). In general, as expected, the longer the arene-ruthenium distance, the closer the shielding was to the uncoordinated arene. The complex $[\text{Ru}(\eta^6\text{-C}_6\text{Et}_6)(\text{CO})_2\text{Cl}]^+\text{PF}_6^-$ does not follow this trend, however, and its variable temperature NMR behaviour is also anomalous (Chapter 4).

The series of derivatives has also allowed comparisons between hexaethylbenzene complexes of ruthenium and complexes of other arenes. For instance, the complexes of hexaethylbenzene are generally similar to those of hexamethylbenzene. Three distinctions can be made. As previously mentioned, hexaethylbenzene does not exchange with *p*-cymene in $[\text{Ru}(\eta^6\text{-}p\text{-cymene})\text{Cl}_2]_2$, probably because of the increased steric bulk of the hexaethylbenzene relative to hexamethylbenzene. Secondly, in attempts to form the monomeric ligand adducts of the type $\text{Ru}(\eta^6\text{-arene})(\text{L})\text{Cl}_2$ ($\text{L} = \text{CO}$, pyridine), from the dichloride dimer and the ligand, the hexaethylbenzene is readily displaced by the incoming ligand, whereas this has not appeared to be a problem in the hexamethylbenzene complexes. Thus it appears that hexaethylbenzene is a more labile ligand than hexamethylbenzene. Thirdly, some of the complexes of hexaethylbenzene have temperature-dependent NMR behaviour while those of hexamethylbenzene did not.

The nature of the dichloride dimer $[\text{Ru}(\eta^6\text{-C}_6\text{Et}_6)\text{Cl}_2]_2$ has been investigated both in the solid state and solutions of non-coordinating solvents, a study that was aided by the enhanced solubility obtained from hexaalkyl substitution. In the solid state the structure was well defined, in contrast to complexes such as $[\text{Ru}(\eta^6\text{-C}_6\text{H}_6)\text{Cl}_2]_2$ ⁷¹, and found to be the same face-sharing bioctahedron as that of previously crystallographically characterized dichloride dimers.⁶⁷⁻⁷⁰ In dichloromethane and methanol solution, it appears that some dissociation to $[\text{Ru}_2(\eta^6\text{-C}_6\text{Et}_6)_2\text{Cl}_3]^+\text{Cl}^-$ occurs, although most of the complex appears to retain its identity since infrared spectroscopy shows strong terminal Ru-Cl stretching bands in solution. The temperature-dependence of the ³⁵Cl NMR spectrum of $[\text{Ru}(\eta^6\text{-C}_6\text{Et}_6)\text{Cl}_2]_2$ reaffirms the lability of the chloro ligands in these arene complexes. From the results obtained in the present study, it is difficult to estimate the degree of dissociation in CH_2Cl_2 and MeOH. Conductance measurements in these solvents show that both the complex $\text{Ru}(\eta^6\text{-C}_6\text{Et}_6)\text{Cl}_2$ and $[\text{Ru}_2(\eta^6\text{-C}_6\text{Et}_6)_2\text{Cl}_3]^+\text{PF}_6^-$ behave as weak rather than strong electrolytes and the bridging chloride species is not observed in the room temperature infrared spectra. This seems to set an upper limit of *ca.* 20 % for the degree of dissociation.

Dissociation of a neutral dichloride dimer to a cationic tri- μ -chloro species has recently been proposed by McGlinchey *et al.*⁶⁹ to explain the observation of separate species in the NMR spectra at room and low temperature of the analogous complex, $[\text{Ru}(\eta^6\text{-trindane})\text{Cl}_2]_2$, but this may not be correct. From NMR spectroscopy, the dissociation is thought to be about 50% complete at room temperature in CD_2Cl_2 , and greater than 90% in nitromethane. By no stretch of the imagination can the degree of dissociation of the hexaethylbenzene complex be 50% in dichloromethane at room temperature. Moreover, the ³⁵Cl NMR spectra show that the dissociation of Cl is rapid on an NMR timescale at room temperature. An alternative explanation of McGlinchey *et al.*'s results is that in solution some of the complex has isomerized to a species in which the trindane ligands

are *syn* rather than *anti* with respect to each other as they are in the solid state. A *syn*-isomer would have a higher dipole moment than the *anti*-isomer and this could explain the increased abundance of the second species in more polar solvents. However, it must be admitted that there is no precedent for the existence of *syn*-isomers in $[\text{Ru}(\eta^6\text{-arene})\text{Cl}_2]_2$ complexes.

The large number of structurally characterized hexaethylbenzene complexes of ruthenium has enabled a study of the conformational variability of the hexaethylbenzene ligand in the solid state and solution. Previously the only existing study of this nature was on the complex $\text{Cr}(\eta^6\text{-C}_6\text{Et}_6)(\text{CO})_3$ and its derivatives.

Within the ruthenium series, there are various rotational orientations of the arene in the solid state with respect to the ligand tripod. When there are small sterically undemanding co-ligands, the arene is orientated such that, when viewed along the the arene ruthenium axis the carbon atoms of the arene eclipse the ligands, while when there are larger ligands this was not the case. The rotational orientation of arenes in $(\eta^6\text{-arene})\text{Cr}(\text{CO})_3$ complexes in the solid state has previously been rationalized in terms of the electronic properties of the arene substituents.⁷⁵ In these complexes the arene is orientated such that the electron rich arene carbon atoms eclipse the ligands of the tripod, thus ensuring the greatest electron donation from the arene to the pseudo-octahedral coordination environment of the metal. Presumably these effects still operate in the hexaethylbenzene ruthenium complexes studied, but it appears that steric effects between the ligands and the alkyl substituents play a greater role. When proximal ethyl groups are present they appear to neatly arrange themselves so as to fit the space left by the auxiliary ligands. One counter-intuitive effect observed is that the complexes with all distal ethyl groups in the solid state do not have the eclipsed conformation. One would expect this conformation in the absence of steric effects, as it would maximize the electron donation from the arene to the octahedral metal environment.

In the solid state, the conformation of the ethyl groups of the hexaethylbenzene ligand is easy to correlate with the bulk of the auxiliary ligands. Not surprisingly, large ligands such as tertiary phosphines favour distal ethyl groups, while small sterically undemanding ligands allow intramolecular steric effects within the arene itself to play a larger role in determining the arene conformation, leading to a 1,3,5-proximal-2,4,6-distal conformation. Much the same behaviour has been observed in the chromium complexes (see Table 1.1). However, five out of the eleven ruthenium hexaethylbenzene complexes studied have an all distal ethyl group conformation in the solid state, whereas of the fifteen published structures of η^6 -hexaethylbenzene, only two complexes, $\text{Cr}(\eta^6\text{-C}_6\text{Et}_6)(\text{PEt}_3)(\text{CO})_2$ ⁹⁷ and $\text{Cr}(\eta^6\text{-C}_6\text{Et}_6)(\text{PPh}_3)(\text{CO})_2$,⁹⁰ have an entirely distal conformation, and that in only some of the molecules present in the solid state.

This difference in behaviour is difficult to rationalize. In the hexaethylbenzene ruthenium complexes the metal-ring centroid distance ranges between 1.808(2) and 1.638(1) Å and averages 1.742 Å, while in the literature available on chromium complexes the hexaethylbenzene chromium distances are between 1.713 and 1.804 Å with an average also of 1.742 Å.^{72,89,90,92,97-99} Thus, there is no obvious difference in steric repulsions between the ethyl substituents of the arene and auxiliary ligands in the two series.

As discussed in Chapter 1, the contentious issue in hexaethylbenzene complexes is whether their variable temperature NMR behaviour can be explained entirely in terms of hindered rotation about the arene methylene bond or whether hindered rotation about the arene metal bond axis needs to be invoked.⁷⁵ Eventually, as described in Chapter 1 and Chapter 4, for both the ruthenium(II) and the chromium series, the question comes down to whether it is possible to assign the proximal and distal ethyl groups in the low temperature ¹³C NMR spectrum of a complex with three different substituents forming the tripod of auxiliary ligands. This was achieved in the chromium series for the cation [Cr(η⁶-C₆Et₆)(CO)(CS)(NO)]⁺⁹² by: (a) a comparison of chemical shifts in solution of complexes whose hexaethylbenzene conformation in the solid state is known (either by X-ray crystallography or solid state NMR)¹⁰², a somewhat dubious process given the conformation variability even in the solid state, and (b) comparison of chemical shifts with those of Cr(η⁶-C₆Et₅COMe)(CO)₃,¹⁰¹ whose ethyl groups adopt a 2,4,6-distal-3,5-proximal conformation in the solid state. In the second comparison, however, it could be difficult to distinguish between possible electronic effects arising from the carbonyl group of the arene and the relative proximity of the ethyl groups to the arene. The difficulty in making such assignments can easily be seen when the large range of chemical shifts for the nuclei of hexaethylbenzene observed in the ruthenium complexes is considered. No relationship in this series could be seen between the solid state conformation of ethyl groups and the chemical shifts of the associated nuclei. A possible resolution to the problem has been investigated in the ruthenium series, namely, the introduction of the spin active ¹³CO moiety into the ligand tripod in the hope of observing ¹³C(CO)-¹³C(arene) coupling. This coupling has been observed in the low temperature ¹³C{¹H}NMR spectrum of the complex Ru(η⁶-C₆H₄-1,4-Bu^t₂)(SiCl₃)(¹³CO),⁸⁵ in which rotation about the arene ruthenium bond axis certainly slows on an NMR timescale. While the conclusions that could be drawn from the preliminary experiments conducted with the hexaethylbenzene complex Ru(η⁶-C₆Et₆)(¹³CO)Cl₂ are limited, the promise of such an approach can be seen.

In the ruthenium complexes of hexaethylbenzene the properties of a given complex that lead to behaviour that is consistent with hindered rotation about the arene-ruthenium bond, appear in the first instance, to be counter intuitive. It is necessary for the complex

to have small cylindrical co-ligands with little steric demand, so that the ethyl groups of the hexaethylbenzene are not orientated in an entirely distal manner. Complexes with the relatively bulky ligands PMe_3 and PPh_3 do not undergo the variable temperature behaviour. Once there are proximal ethyl groups in the solid state structure, it appears that the ethyl groups then interfere with the auxiliary ligands at low temperature and act to slow down the rotation of the hexaethylbenzene. The reason for this is evident from a comparison of space-filling models of $\text{Ru}(\eta^6\text{-C}_6\text{Et}_6)(\text{CO})\text{Cl}_2$ and $\text{Ru}(\eta^6\text{-C}_6\text{Et}_6)(\text{PMe}_3)\text{Cl}_2$, which have 1,3,5-proximal-2,4,6-distal and all distal conformations, respectively (Figure 6.1). In the former, the 1,3,5-ethyl groups swing down between the auxiliary ligands, locking the arene such that it appears impossible for it to spin. If, however, the ethyl groups are entirely distal, as in $\text{Ru}(\eta^6\text{-C}_6\text{Et}_6)(\text{PMe}_3)\text{Cl}_2$, then there is limited or no interference with the auxiliary ligands and the arene can be expected to spin freely.

A major difference in the variable temperature NMR between the hexaethylbenzene ruthenium(II) and chromium(0) complexes is that in the latter there are a number of complexes whose low temperature NMR spectra were consistent with the presence of more than one conformer of coordinated arene, whereas there is no firm evidence for this in former. Again no rationalization could be found for this in the comparison of the metrical parameters between the two classes of compounds.

It has become apparent in this investigation that synergy between the properties of coligands present in the coordination sphere of arene complexes and the arene itself determines the dynamic behaviour of the arene and this is not easily quantified. This is consistent with the arguments put forward for the differences in behaviour of variously substituted $\text{C}_6\text{H}_x\text{Bu}^t_{(6-x)}$ ($x = 3,4$) and $\text{C}_6\text{H}_4\text{Pr}^i_2$ complexes of iron, ruthenium and osmium⁸³⁻⁸⁵ (see Chapter 1). In these complexes it was found that the specific steric interactions within each molecule have to be carefully considered individually to determine their effects on arene-metal rotation. This was observed in the complexes of other arenes investigated for variable temperature NMR behaviour in the course of the present study. None of these displayed any signs of NMR temperature dependence, despite similarities in the gross structure. Thus it appears that it is the special properties of the three dimensional shape of both the ancillary ligands and the hexaethylbenzene that allows the ethyl groups to drop down and lock the molecule into a particular rotational conformer, raising the barrier to rotation about the arene ruthenium bond to such an extent that it becomes observable by NMR line broadening techniques.

There are a number of areas of this project that warrant further investigation. For example, there are many acetylenes whose reaction with $\text{Ru}(\eta^6\text{-naphth})(\eta^4\text{-COD})$ should give rise to ruthenium complexes of new arenes. According to the preliminary

experiments described in Chapter 2, one promising candidate is di-isopropyl acetylene, which would give the first example of η^6 -coordinated hexaisopropylbenzene. Obviously preparation and characterization of further hexaethylbenzene ruthenium complexes containing spin active nuclei in their co-ligands may help to resolve the question of rotation about the arene-ruthenium bond axis. It is unfortunate that almost none of the tertiary-phosphine complexes investigated in this series displayed any variable temperature NMR behaviour, and that the complex that did, $\text{Ru}(\eta^6\text{-C}_6\text{Et}_6)(\text{PMe}_3)(\text{H})_2$, did not have a fully resolved spectrum at the lowest temperature accessible. Further studies on the nature of species present in solutions of some of these complexes may also help bring some insight.

Bibliography

- (1) Bozec, H. L.; Touchard, D.; Dixneuf, P. H. *Advances in Organometallic Chemistry* **1988**, 29, 163.
- (2) Bennett, M. A. In *Comprehensive Organometallic Chemistry*; 2nd ed.; Abel, E. W.; Stone, F. G. A.; Wilkinson, G., Eds.; Pergamon: New York, 1995; Vol. 7; p 549.
- (3) Hein, F. *Berichte* **1919**, 52, 195.
- (4) Zeiss, H. H.; Tsutsui, M. *J. Am. Chem. Soc.* **1957**, 79, 3062.
- (5) Weiss, E.; Fischer, E. O. *Z. anorg. allgem. Chem.* **1956**, 286, 142.
- (6) Fischer, E. O.; Hafner, W. *Z. Naturforsch.* **1955**, 10B, 655.
- (7) Fischer, E. O.; Hafner, W. *Z. anorg. allgem. Chem.* **1956**, 286, 246.
- (8) Silverthorn, W. E. *Adv. Organomet. Chem.* **1975**, 13, 47.
- (9) Klabunde, K. J. *Acc. Chem. Res.* **1975**, 8, 393.
- (10) Timms, P. L. *Angew. Chem. Int. Ed.* **1975**, 14, 273.
- (11) Natta, G.; Calderazzo, F.; Santambrogio, E. *Chim. Ind. (Milan)* **1958**, 40, 1003.
- (12) Nicholls, B.; Whiting, M. C. *J. Chem. Soc.* **1959**, 551.
- (13) Nicholls, B.; Whiting, M. C. *Proc. Chem. Soc.* **1958**, 152.
- (14) Fischer, E. O.; Öfele, K. *Z. Naturforsch.* **1956**, 11b, 758.
- (15) Sneed, R. P. A. *Organochromium Complexes* p. 255; Academic Press: New York, 1975.
- (16) Huttner, G.; Lange, S. *Acta. Cryst., Sect B.* **1972**, 28, 2049.
- (17) Huttner, G.; Lange, S.; Fischer, E. O. *Angew. Chem.* **1971**, 10, 556.
- (18) Finke, R. G.; Voegeli, R. H.; Laganis, E. D.; Boekelheide, V. *Organometallics* **1983**, 2, 347.
- (19) Collman, J. P.; Hegedus, L. S.; Norton, J. R.; Finke, R. G. *Principles and Applications of Organotransition Metal Chemistry*; University Science Books: Mill Valley, 1987.
- (20) Winkhaus, G.; Singer, H. *J. Organomet. Chem.* **1967**, 7, 487.
- (21) Zelonka, R. A.; Baird, M. C. *J. Organomet. Chem.* **1972**, 35, C43.
- (22) Zelonka, R. A.; Baird, M. C. *J. Organomet. Chem.* **1972**, 44, 383.

- (23) Bennett, M. A.; Robertson, G. B.; Smith, A. K. *J. Organomet. Chem.* **1972**, *43*, C41.
- (24) Bennett, M. A.; Smith, A. K. *J. Chem. Soc., Dalton Trans.* **1974**, 233.
- (25) Bennett, M. A.; Huang, T. N.; Matheson, T. W.; Smith, A. K. *Inorganic Synthesis* **1982**, *21*, 74.
- (26) J. W. Hull, Jr.; Gladfelter, W. L. *Organometallics* **1984**, *3*, 605.
- (27) Pertici, P.; Vitulli, G.; Paci, M.; Porri, L. *J. Chem. Soc., Dalton Trans.* **1980**, 1961.
- (28) Pertici, P.; Vitulli, G.; Lazzaroni, R.; Salvadori, P.; Barili, P. L. *J. Chem. Soc. Dalton Trans.* **1982**, 1019.
- (29) Vitulli, G.; Pertici, P.; Salvadori, P. *J. Chem. Soc., Dalton Trans.* **1984**, 2255.
- (30) Bennett, M. A.; Neumann, H.; Thomas, M.; Wang, X.-q.; Pertici, P.; Salvadori, P.; Vitulli, G. *Organometallics* **1991**, *10*, 3237.
- (31) Lucherini, A.; Porri, L. *J. Organomet. Chem.* **1978**, *155*, C45.
- (32) Crocker, M.; Green, M.; Orpen, A. G.; Thomas, D. M. *J. Chem. Soc., Chem. Comm.* **1984**, 1141.
- (33) Crocker, M.; Froom, S. F. T.; Green, M.; Nagle, K. R.; Orpen, A. G.; Thomas, D. M. *J. Chem. Soc., Dalton Trans.* **1987**, 2803.
- (34) Masuda, K.; Ohkita, H.; Kurumatani, S.; Itoh, K. *Organometallics* **1993**, 2221.
- (35) Pertici, P.; Verazzani, A.; Vitulli, G.; Baldwin, R.; Bennett, M. A. *J. Organomet. Chem.* **1997**, *551*, 37.
- (36) Werner, H.; Kletzin, H. *J. Organomet. Chem.* **1984**, *276*, 231.
- (37) Robertson, D. R.; Stephenson, T. A.; Arthur, T. *J. Organomet. Chem.* **1978**, *162*, 121.
- (38) Robertson, D. R.; Stephenson, T. A. *J. Organomet. Chem.* **1976**, *116*, C29.
- (39) Arthur, T.; Stephenson, T. A. *J. Organomet. Chem.* **1981**, *208*, 369.
- (40) Arthur, T.; Stephenson, T. A. *J. Organomet. Chem.* **1979**, *168*, C39.
- (41) McCormick, F. B.; Gleason, W. B. *Acta Cryst., Sect. C* **1993**, *49*, 1493.
- (42) Tocher, D. A.; Walkinshaw, M. D. *Acta Cryst., Sect. B* **1982**, *38*, 3083.
- (43) Struchkov, Y. T.; Batanov, A. S. *Metalloorg. Khim.* **1988**, *1*, 1143.
- (44) Grepioni, F.; Braga, D.; Dyson, P. J.; Johnson, B. F. G.; Sanderson, F. M.; Calhorda, M. J.; Veiros, L. F. *Organometallics* **1995**, *14*, 121.
- (45) Dussel, R.; Pilette, D.; Dixneuf, P. H. *Organometallics* **1991**, *10*, 3287.

- (46) Werner, H.; Kletzin, H. *J. Organomet. Chem.* **1982**, 228, 289.
- (47) Werner, H.; Stahl, S.; Kohlmann, W. *J. Organomet. Chem.* **1991**, 409, 285.
- (48) Werner, H.; Roder, K. *J. Organomet. Chem.* **1985**, 355, 401.
- (49) Werner, H.; Kletzin, H.; Roder, K. *J. Organomet. Chem.* **1988**, 355, 401.
- (50) Roder, K.; Werner, H. *J. Organomet. Chem.* **1989**, 367, 321.
- (51) Bennett, M. A.; Weerasuria, A. M. M. *J. Organomet. Chem.* **1990**, 394, 481.
- (52) Bennett, M. A.; Huang, T.-N.; Latten, J. L. *J. Organomet. Chem.* **1984**, 272, 189.
- (53) Bennett, M. A.; Latten, J. *Aust. J. Chem.* **1987**, 40, 841.
- (54) Isobe, K.; Bailey, P. M.; Maitlis, P. M. *J. Chem. Soc., Dalton Trans* **1981**, 2003.
- (55) Morris, R. H.; Shiralian, M. *J. Organomet. Chem.* **1984**, 260, C47.
- (56) Werner, H.; Kletzin, H.; Hohn, A.; Paul, W.; Knaup, W.; Ziegler, M. L.; Serhadli, O. *J. Organomet. Chem.* **1986**, 306, 227.
- (57) M. A. Bennett *et al.* *Organometallics* **1992**, 11, 3069.
- (58) Stebler-Rothlisberger, M.; Ludi, A. *Polyhedron* **1986**, 5, 1217.
- (59) McCormick, F. B.; Cox, D. D.; Gleason, W. B. *Organometallics* **1993**, 12, 610.
- (60) Bennett, M. A.; Matheson, T. W. *J. Organomet. Chem.* **1979**, 175, 87.
- (61) Rybinskaya, M. I.; Kaganovich, V. S.; Kudinov, A. R. *J. Organomet. Chem.* **1982**, 235, 215.
- (62) Robertson, I. W.; Stephenson, T. A.; Tocher, D. A. *J. Organomet. Chem.* **1982**, 228, 171.
- (63) Oshima, N.; Suzuki, H.; Moro-oka, Y. *Inorg. Chem.* **1986**, 25, 3407.
- (64) Stumpf, A. W.; Saive, E.; Demonceau, A.; Noels, A. F. *J. Chem. Soc., Chem. Comm.* **1995**, 1127.
- (65) Fujii, A.; Hashiguchi, S.; Uematsu, N.; Ikariya, T.; Nyori, R. *J. Am. Chem. Soc.* **1996**, 118, 2521.
- (66) Mashima, K.; Kusano, K.-b.; Sato, N.; Matsumura, Y.-i.; Nozaki, K.; Kumobayashi, H.; Sayo, N.; Hori, Y.; Ishizaki, T.; Akutagawa, S.; Takaya, H. *J. Org. Chem.* **1994**, 59, 1064.
- (67) McCormick, F. B.; Gleason, W. B. *Acta Cryst., Sect. C* **1988**, 44, 603.
- (68) Watkins, S. F.; Fronczek, F. R. *Acta Cryst., Sect. B* **1982**, 38, 270.

- (69) Gupta, H. K.; Lock, P. E.; Hughes, D. W.; McGlinchey, M. J. *Organometallics* **1997**, *16*, 4335.
- (70) Therrien, B.; Ward, T.; Pilkington, M.; Hoffmann, C.; Gilardoni, F.; Weber, J. *Organometallics* **1998**, *17*, 330.
- (71) Iwata, R.; Ogata, I. *Tetrahedron* **1973**, *29*, 2753.
- (72) Iverson, D. J.; Hunter, G.; Blount, J. F.; J. R. Damewood, J.; Mislow, K. J. *Am. Chem. Soc.* **1981**, *103*, 6073.
- (73) Pal, H. K.; Guha, A. C. Z. *Kristallogr. Kristallgeom. Kristallphys. Kristallchem* **1935**, *92*, 392.
- (74) Hunter, G.; Weakley, T. J. R.; Mislow, K.; Wong, M. G. *J. Chem. Soc., Dalton. Trans.* **1986**, 577.
- (75) McGlinchey, M. J. *Adv. Organomet. Chem.* **1992**, *34*, 285.
- (76) Hunter, G.; Mislow, D. K.; Iverson, J.; Mislow, K.; Blount, J. F. *J. Am. Chem. Soc.* **1980**, *103*, 6073.
- (77) Chhor, K.; Sourisseau, C.; Lucazeau, G. *J. Mol. Struct.* **1982**, *82*, 485.
- (78) Howard, J.; Robson, K.; Waddington, T. C. *J. Chem. Soc., Dalton Trans.* **1982**, 967.
- (79) Gilson, D. F. R.; Gomez, G.; Butler, I. S.; Fitzpatrick, P. J. *Can. J. Chem.* **1983**, *61*, 737.
- (80) Braga, D.; Grepioni, F. *Polyhedron* **1990**, *9*, 53.
- (81) Chudek, J. A.; Hunter, G.; Mackay, R. L.; Farber, G.; Weissensteiner, W. J. *J. Organomet. Chem.* **1989**, *377*, C69.
- (82) Howell, J. A.; Palin, M. G.; McArdle, P.; Cunningham, D.; Goldschmidt, Z.; Gottlieb, H. E.; Hezroni-Langerman, D. *Organometallics* **1993**, *12*, 1694.
- (83) Pomeroy, R. K.; Harrison, D. J. *J. Chem. Soc., Chem. Comm.* **1980**, 661.
- (84) Hansen, V. M.; Batchelor, R. J.; Einstein, F. W. B.; Male, J. L.; Pomeroy, R. K. *Organometallics* **1997**, *16*, 4875.
- (85) Hu, X.; Duchowski, J.; Pomeroy, R. K. *J. Chem. Soc., Chem. Comm.* **1988**, 363.
- (86) Nambu, M.; Mohler, D. L.; Hardcastle, H.; Baldrige, K. K.; Siegel, J. S. *J. Am. Chem. Soc.* **1993**, *115*, 6138.
- (87) Acampora, M.; Ceccon, A.; Farra, M. D.; Giacometti, G.; Rigatti, G. *J. Chem. Soc., Perkin Trans.* **1977**, *2*, 483.
- (88) Sanger, M. J.; Angelici, R. J. *Organometallics* **1994**, *13*, 1821.

- (89) Denholm, S.; Hunter, G.; Weakley, T. J. R. *J. Chem. Soc., Dalton. Trans.* **1987**, 2789.
- (90) Hunter, G.; Iverson, D. J.; Mislow, K.; Blount, J. F. *J. Am. Chem. Soc.* **1980**, *102*, 5943.
- (91) Herrmann, W. A.; Thiel, W. R.; Herdtweck, E. *Polyhedron* **1988**, *7*, 2027.
- (92) Mailvaganam, B.; Frampton, C. S.; Top, S.; Sayer, B. G.; McGlinchey, M. J. *J. Am. Chem. Soc.* **1991**, *113*, 1177.
- (93) Muller, J.; Qiao, K.; Schubert, R.; Tschampel, M. *Z. Naturforsch., Teil. B* **1993**, *48*, 1558.
- (94) Wexler, P. A.; Wigley, D. E.; Koerner, J. B.; Albright, T. A. *Organometallics* **1991**, *10*, 2319.
- (95) Dubois, R. H.; Zarawotko, M. J.; White, P. S. *J. Organomet. Chem.* **1989**, *362*, 155.
- (96) Hamon, J.-R.; Saillard, J.-Y.; LeBeuze, A.; McGlinchey, M. J.; Astruc, D. *J. Am. Chem. Soc.* **1982**, *104*, 7549.
- (97) Hunter, G.; Blount, J. F.; Damewood, J. R.; Iverson, D. J.; Mislow, K. *Organometallics* **1982**, *1*, 448.
- (98) McGlinchey, M. J.; Fletcher, J. L.; Sayer, B. G.; Bougeard, P.; Faggiani, R.; Lock, C. J. L.; Bain, A. D.; Rodger, C.; Kündig, E. P.; Astruc, D.; Hamon, J. R.; LeMaux, P.; Top, S.; Jaouen, G. *J. Chem. Soc., Chem. Comm.* **1983**, 634.
- (99) Blount, J. F.; Hunter, G.; Mislow, K. *J. Chem. Soc., Chem Comm.* **1984**, 170.
- (100) Hunter, G.; Mislow, K. *J. Chem. Soc., Chem Comm.* **1984**, 172.
- (101) Downton, P. A.; Mailvaganam, B.; Sayer, B. G.; McGlinchey, M. J.; Frampton, C. S. *J. Am. Chem. Soc.* **1990**, *112*, 27.
- (102) McGlinchey, M. J.; Bougeard, P.; Sayer, B. G.; Hofer, R.; Lock, C. J. L. *J. Chem. Soc., Chem. Comm.* **1984**, 789.
- (103) P. Pertici *et al.* unpublished results.
- (104) Meier, H.; Heiss, J.; Suhr, H.; Muller, E. *Tetrahedron* **1968**, *24*, 2307.
- (105) Meier, H.; Voigt, E. *Tetrahedron* **1972**, *28*, 187.
- (106) Sakurai, H.; Ebata, K.; Kabuto, C.; Sekiguchi, A. *J. Am. Chem. Soc.* **1990**, *112*, 1799.
- (107) Siegel, J.; Mislow, K. *J. Am. Chem. Soc.* **1983**, *105*, 7763.

- (108) Pertici, P.; Verrazzani, A.; Baretta, U.; Marchetti, F.; Salvadori, P.; Baldwin, R.; Bennett, M. A.; Hockless, D. C. R. *Unpublished*
- (109) Schmid, H.; Ziegler, M. L. *Chem. Ber.* **1976**, *109*, 132.
- (110) Lu, Z. *PhD thesis, ANU* **1998**,
- (111) Wang, X.-q. *PhD thesis, ANU* **1992**,
- (112) Yamazaki, H.; Wakasuki, Y. *J. Organomet. Chem.* **1984**, *272*, 251.
- (113) Van Meurs, F.; Van der Toorn, J. M.; Van Bekkum, H. *J. Organomet. Chem.* **1976**, *113*, 341.
- (114) Feltham, R. D.; Hayter, R. G. *J. Chem Soc.* **1964**, 4587.
- (115) Geary, W. J. *Coord. Chem. Rev.* **1971**, *7*, 81.
- (116) Rosenthal, M. S.; Drago, R. S. *Inorg. Chem.* **1965**, *4*, 841.
- (117) Uguagliati, P.; Deganello, G.; Busetto, L.; Belluco, U. *Inorg. Chem.* **1969**, *8*, 1625.
- (118) *Multinuclear NMR*; first ed.; Mason, J., Ed.; Plenum Press: New York, 1987.
- (119) Kiel, W. A.; Ball, R. G.; Graham, W. A. G. *J. Organomet. Chem.* **1990**, *383*, 481.
- (120) Bown, M.; Fontaine, X. L. R.; Greenwood, N. N.; Kennedy, J. D. *J. Organomet. Chem.* **1987**, *325*, 233.
- (121) Werner, H.; Kletzin, H. *J. Organomet. Chem.* **1981**, *228*, 289.
- (122) Werner, H.; Werner, R. *Chem. Ber.* **1982**, *115*, 3766.
- (123) Bennett, M. A.; Robertson, G. B.; Smith, A. K. *J. Organomet. Chem.* **1972**, *43*, C41.
- (124) Elsegood, M. R. J.; Tocher, D. A. *Polyhedron* **1995**, *14*, 3147.
- (125) Werner, H.; Kletzin, H.; Hohn, A.; Paul, W.; Knaup, W.; Ziegler, M. L.; Serhadli, O. *J. Organomet. Chem.* **1986**, *306*, 227.
- (126) Lister, S. A.; Redhouse, A. D.; Simpson, S. J. *Acta Cryst., Sect. C* **1992**, *48*, 1661.
- (127) Fan, L.; Turner, M. L.; Adams, H.; Bailey, N. A.; Maitlis, P. M. *Organometallics* **1995**, *14*, 676.
- (128) Wisner, J. M.; Bartczak, T. J.; Ibers, J. A. *Inorg. Chim. Acta* **1985**, *100*, 115.
- (129) Simson, S. J. *Acta Cryst., Sect. C* **1993**, *49*, 1333.
- (130) O'Leary, S. R.; Adams, H.; Bailey, N. A.; Maitlis, P. M. *J. Chem. Soc. Chem. Comm.* **1995**, 2019.

- (131) Adams, H.; Bailey, N. A.; White, C. *Inorg. Chem.* **1993**, 22, 1155.
- (132) Wilczewski, T.; Dauter, Z. *J. Organomet. Chem.* **1986**, 312, 349.
- (133) Conroy-Lewis, F. M.; Simpson, S. J. *J. Organomet. Chem.* **1990**, 296, 83.